



## **EIDESSTATTLICHE ERKLÄRUNG**

### ***AFFIDAVIT***

Ich erkläre an Eides statt, dass ich die vorliegende Arbeit selbstständig verfasst, andere als die angegebenen Quellen/Hilfsmittel nicht benutzt, und die den benutzten Quellen wörtlich und inhaltlich entnommenen Stellen als solche kenntlich gemacht habe. Das in TUGRAZonline hochgeladene Textdokument ist mit der vorliegenden Masterarbeit identisch.

*I declare that I have authored this thesis independently, that I have not used other than the declared sources/resources, and that I have explicitly indicated all material which has been quoted either literally or by content from the sources used. The text document uploaded to TUGRAZonline is identical to the present master's thesis.*

---

Datum / Date

---

Unterschrift / Signature

## Acknowledgements

I am very grateful to the head of the Institute *O. Univ.-Prof. Dr. Georg Gescheidt-Demner* for the provision of equipment and resources to make this work possible.

I would like to give special thanks to *Ao. Univ.-Prof. Dr. Franz A. Mautner* for his intensive and generous support and coordination of my master thesis and for interesting discussions.

I would also like to give great thanks to *Ao. Univ.-Prof. Dr. Karl Gatterer* for his help concerning all issues regarding spectroscopy.

I would like to thank, *Ao. Univ.-Prof. Dr. Christoph Marschner* and *Ass.-Prof. Dr. Roland Fischer*, for the X-ray measurements and data collection for all single crystals.

Another thank will be given to *BSc. Elisabeth Domian* for her engaged help in the laboratory.

I would also like to give great thanks to *MSc. Stefan Müller* for his help with the infrared spectroscopy measurements.

I would like to thank *Ing. Helmut Eisenkölbl* for technical- as well as *Mrs Hilde Freißmuth* and *Ms Ines Gössler* for laboratory support.

Last but not least I would like to thank my laboratory trainees *Barbara, Magdalena, Martin, Patricia* and *Saskia* for the excellent support in the laboratory.

Finally I want to thank Ute Bruckner for proofreading my master thesis.

**dedicated to my family**

## Table of Contents

<b>1) Introduction .....</b>	<b>1</b>
<b>2) Theoretical principles on the spectroscopy of inorganic solids .....</b>	<b>3</b>
2.1 Fundamentals .....	3
2.1.1 The electromagnetic spectrum .....	3
2.1.2 Interaction of the incoming beam with the solid sample .....	4
2.1.3 Different types of luminescence .....	5
2.2 Absorption of UV/VIS light .....	6
2.2.1 Electronic transitions in polyatomic molecules .....	6
2.3 Selection rules .....	8
2.3.1 Spin-forbidden transitions.....	8
2.3.2 Symmetry-forbidden transitions.....	8
2.4 The Frank-Condon principle .....	8
2.5 Characteristics of fluorescence emission .....	9
2.5.1 Radiative and non-radiative transitions .....	9
2.5.2 Internal conversion (IC) .....	10
2.5.3 Intersystem crossing (ISC) .....	11
2.5.4 Fluorescence .....	11
2.5.4.1 Spontaneous and stimulated emissions.....	11
2.5.5 Phosphorescence .....	12
2.6 Emission and excitation spectra .....	13
2.6.1 Emission spectra.....	13
2.6.2 Excitation spectra .....	13
2.6.3 Stokes-shift.....	13
2.7 Impact of the molecular structure on fluorescence.....	14
2.7.1 Extend of $\pi$ -electron system .....	14
2.7.2 Heterocyclic compounds.....	14
2.7.3 Electron-donating substituents.....	15
2.7.4 Electron-withdrawing substituents .....	15
2.8 Data analysis and quality parameters .....	15
2.9 Charge-transfer mechanisms .....	16
2.9.1 Ligand to metal charge-transfer.....	16
2.9.2 Metal to ligand charge-transfer .....	16
2.9.3 Effect on the emission spectra .....	16
2.10 Chemistry of pyridine-N-oxides.....	17

2.11 Pseudohalides.....	17
2.11.1 Azides .....	17
2.11.2 Thiocyanates .....	17
<b>3) Experimental .....</b>	<b>18</b>
3.1 Preparation.....	18
3.1.1 Preparation of HN <sub>3</sub> saturated water .....	18
3.2 Used devices.....	19
3.2.1 Single crystal diffraction.....	19
3.2.2 Luminescence spectroscopy.....	19
3.2.3 Diffuse reflection spectroscopy .....	19
3.2.4 Infrared spectroscopy (FT-IR) .....	20
<b>4) Cd(II) complexes .....</b>	<b>21</b>
4.1 [Cd(2-picoline-N-oxide)(NCS) <sub>2</sub> ] <sub>n</sub> <b>(1)</b> .....	21
4.2 [Cd(3-picoline-N-oxide)(NCS) <sub>2</sub> ] <sub>n</sub> <b>(2)</b> .....	23
4.3 [Cd(4-cyanopyridine-N-oxide) <sub>2</sub> (NCS) <sub>2</sub> (H <sub>2</sub> O)] <sub>2</sub> <b>(3)</b> .....	25
4.4 [Cd(4-nitropyridine-N-oxide) <sub>2</sub> (NCS) <sub>2</sub> ] <sub>n</sub> <b>(4)</b> .....	27
4.5 [Cd(4-quinoline-N-oxide)(NCS) <sub>2</sub> ] <sub>n</sub> <b>(5)</b> .....	29
4.6 [Cd(2,6-lutidine-N-oxide)(NCS) <sub>2</sub> ] <sub>n</sub> <b>(6)</b> .....	31
4.7 [Cd(N <sub>3</sub> ) <sub>2</sub> (H <sub>2</sub> O) <sub>2</sub> ] <sub>n</sub> (4-quinoline-N-oxide) <sub>2n</sub> <b>(7)</b> .....	33
4.8 [Cd(2,6-lutidine-N-oxide)(N <sub>3</sub> ) <sub>2</sub> ] <sub>n</sub> <b>(8)</b> .....	34
<b>5) Zn(II) complexes .....</b>	<b>36</b>
5.1 [Zn(2-picoline-N-oxide) <sub>2</sub> (NCS) <sub>2</sub> (H <sub>2</sub> O)] <sub>n</sub> <b>(9)</b> .....	36
5.2 [Zn(4-quinoline-N-oxide) <sub>6</sub> ] <sup>2+</sup> [Zn(NCS) <sub>4</sub> ] <sup>2-</sup> <b>(10)</b> .....	38
5.3 [Zn(4-cyanopyridine-N-oxide) <sub>2</sub> (NCS) <sub>2</sub> (H <sub>2</sub> O)] <sub>2</sub> <b>(11)</b> .....	41
5.4 [Zn(2,6-lutidine-N-oxide) <sub>2</sub> (NCS) <sub>2</sub> ] <b>(12)</b> .....	43
5.5 [Zn(4-quinoline-N-oxide)(N <sub>3</sub> ) <sub>2</sub> ] <sub>n</sub> <b>(13)</b> .....	45
5.6 [Zn(2,6-lutidine-N-oxide)(N <sub>3</sub> ) <sub>2</sub> ] <sub>n</sub> <b>(14)</b> .....	47
5.7 [Zn(4-picoline-N-oxide)(N <sub>3</sub> ) <sub>2</sub> ] <sub>n</sub> <b>(15)</b> .....	49
5.8 [Zn(2-O-pyridine-N-oxide)(N <sub>3</sub> )(H <sub>2</sub> O)] <sub>n</sub> <b>(16)</b> .....	51
<b>6) Co(II) complexes .....</b>	<b>53</b>
6.1 [Co(2,6-lutidine-N-oxide) <sub>2</sub> (NCS) <sub>2</sub> ] <sub>2</sub> <b>(17)</b> .....	53
6.2 [Co(4-cyanopyridine-N-oxide) <sub>2</sub> (NCS) <sub>2</sub> (H <sub>2</sub> O)] <sub>2</sub> <b>(18)</b> .....	55
6.3 [Co(N <sub>3</sub> ) <sub>2</sub> (H <sub>2</sub> O) <sub>2</sub> ] <sub>n</sub> (3-picoline-N-oxide) <sub>2n</sub> <b>(19)</b> .....	56
6.4 [Co(2,6-lutidine-N-oxide)(N <sub>3</sub> ) <sub>2</sub> ] <sub>n</sub> <b>(20)</b> .....	58

<b>7) Mn(II) complexes .....</b>	<b>60</b>
7.1 [Mn(2-picoline-N-oxide)(NCS) <sub>2</sub> ] <sub>n</sub> <b>(21)</b> .....	60
7.2 [Mn(3-picoline-N-oxide) <sub>2</sub> (NCS) <sub>2</sub> ] <sub>n</sub> <b>(22)</b> .....	62
7.3 [Mn(4-picoline-N-oxide) <sub>2</sub> (NCS) <sub>2</sub> (H <sub>2</sub> O) <sub>2</sub> ] <sub>n</sub> <b>(23)</b> .....	64
7.4 [Mn(4-cyanopyridine-N-oxide) <sub>2</sub> (NCS) <sub>2</sub> (H <sub>2</sub> O)] <sub>2</sub> <b>(24)</b> .....	66
7.5 [Mn(2-picoline-N-oxide)(N <sub>3</sub> ) <sub>2</sub> ] <sub>n</sub> <b>(25)</b> .....	68
7.6 [Mn(N <sub>3</sub> ) <sub>2</sub> (H <sub>2</sub> O) <sub>2</sub> ] <sub>n</sub> (3-picoline-N-oxide) <sub>2n</sub> <b>(26)</b> .....	70
7.7 [Mn <sub>3</sub> (N <sub>3</sub> ) <sub>6</sub> (4-picoline-N-oxide) <sub>2</sub> (H <sub>2</sub> O) <sub>2</sub> ] <sub>n</sub> <b>(27)</b> .....	72
<b>8) Luminescence data .....</b>	<b>75</b>
8.1 Introduction.....	75
8.1.1 Adjustment of the specimen carrier .....	75
8.2 The measurement procedure.....	75
8.3 Measurement settings.....	77
8.4 Luminescence properties .....	78
8.4.1 Ligands.....	78
8.4.2 Cd(II) complexes .....	79
8.4.3 Zn(II) complexes .....	82
8.5 Charge-transfer properties of the Cd(II) and Zn(II) compounds.....	85
<b>9) Diffuse reflection data .....</b>	<b>86</b>
9.1 Introduction into the crystal field spectroscopy .....	86
9.2 Parameters .....	86
9.2.1 Tanabe-Sugano diagram.....	86
9.3 Discussion of selected Co(II) compounds .....	86
<b>10) Discussion .....</b>	<b>88</b>
10.1 Comparison of the published thiocyanato complexes .....	88
10.2 Comparison of the published azido complexes .....	90
10.3 Comparison of the thiocyanato and azido complexes .....	92
10.4 Interpretation of the luminescence data .....	93
10.4.1 Ligands .....	93
10.4.2 Cd(II) complexes .....	94
10.4.3 Zn(II) complexes .....	94
<b>11) Summary .....</b>	<b>95</b>
<b>12) References.....</b>	<b>96</b>
<b>13) Attachment .....</b>	<b>102</b>

## 1) Introduction

The main focus of this master thesis lies in the synthesis and the investigation of the structural behavior of the complex azide and thiocyanate bridged ligands, whereby different substituted pyridine-N-oxides act as ligands. Divalent cations of cadmium, zinc, cobalt and manganese act as metal centers. Pyridine-N-oxide derivatives are used, because they are more nucleophilic and electrophilic than the pyridine itself. [1]

The chemistry and applications of different substituted pyridine N-oxides received much attention due to their usefulness as synthetic building blocks and as biologically important substances [2]. Heterocyclic N-oxides are useful as protecting groups, auxiliary agents, oxidants [2], catalysts [2] and ligands in metal complexes. [3]

There are big differences in the chemical behavior of the pyridine itself compared to the N-oxide. Besides the fact, that the molar mass changes the appearance changes from the liquid pyridine to a colorless solid of the pyridine-N-oxide. Differences in the melting and boiling point follows the same trend as the different solubilities in water. [4]

Furthermore there are less compounds structurally characterized compared to the pyridine derivatives.

At the beginning of this master thesis (June 2014), as far as I know only 21 azido structures of the above mentioned divalent metals with a substituted pyridine-N-oxide and 28 thiocyanato structures were published, according to the Cambridge Crystallographic Data Centre, CSD version 5.35 (Update May 2014).[5]

The use of the azide anion ( $N_3^-$ ) as bridging ligand, has its origin in the design of molecule-based magnets. The three-atomic pseudohalide  $N_3^-$  has the ability to act as bridging ligand between the paramagnetic metal ions. This is also the case with divalent Co(II) and Mn(II) compounds. A very important fact for the magnetochemistry is that the metal centers vary their magnetic behavior with a different configuration of the azido-bridge. Ferro-magnetic coupling is mainly achieved by the connection between an end-nitrogen atom of the azido group and the metal centers, whereas antiferro-magnetic coupling is preferred when both end-nitrogen atoms of the azido group connect to the metal centers. [6] The synthesized Co(II) and Mn(II) compounds will be investigated for their properties in magnetochemistry.

To introduce new coordination modes, an isoelectronic substance compared to  $N_3^-$  will be used. This substance is isothiocyanate ( $NCS^-$ ), because of its additional electronegative atom (sulfur). [7]

The structure of the synthesized complexes will be characterized with single crystal diffraction and the functional groups ( $N_3^-$  and  $NCS^-$ ) will be detected via infrared spectroscopy. These measurements will be performed in the facilities of the institute of inorganic chemistry at Graz, University of Technology.

A characterization of the crystal field of Co(II) compounds will be done by calculating the Racah parameter B and the crystal field splitting from the collected data of the diffuse reflective spectroscopy measurements. [8]

The observation of luminescence from a number of compounds with  $d^{10}$  metal centers such as Cd(II) and Zn(II) represents an important factor for developing luminescent polynuclear  $d^{10}$  metal complexes. [9]

Complexes with  $d^{10}$  ions often show efficient luminescence at room temperature. The emission transition has been assigned to a ligand to metal charge-transfer or a metal to ligand charge-transfer transition. This is mainly depending on the ligand. [10]

The Cd(II) and Zn(II) compounds, as well as the pure ligands will be investigated on their luminescence properties in solid state.

CHN analysis will be performed at the institute of inorganic chemistry at Graz, University of Technology.

## 2) Theoretical principles on the spectroscopy of inorganic solids

### 2.1 Fundamentals [11]

#### 2.1.1 The electromagnetic spectrum

There exists a wide range of electromagnetic radiation starting in a low-frequency regime e.g. radiation generated by an AC circuit (approximately 50 Hz) up to the highest photon energy radiation of gamma rays (frequencies up to  $1 \cdot 10^{22}$  Hz). The electromagnetic spectrum contains the different types of frequencies.

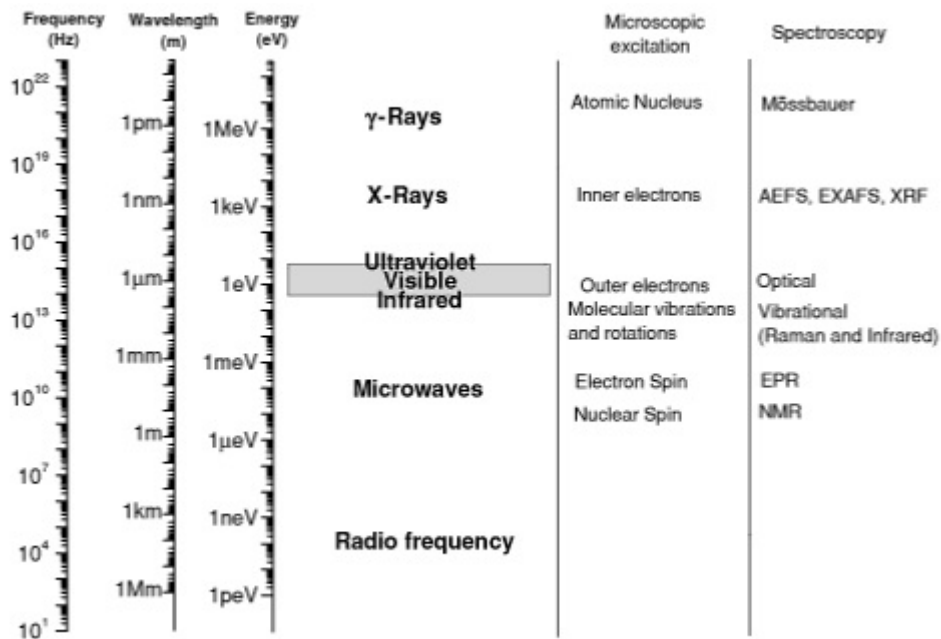


Figure 1: The electromagnetic spectrum with the different excitation sources and their spectral region [11]

Figure 1 shows that there are seven well known spectral regions which propagate radiation through the space as transverse electromagnetic wave at a speed of  $c \cong 3 \cdot 10^8 \text{ m s}^{-1}$  in a vacuum. The limits between the regions are fixed by convention rather than by sharp discontinuities of the physical phenomena involved. Each monochromatic electromagnetic radiation is labeled by its frequency  $\nu$ , wavelength  $\lambda$ , photon energy  $E$  or wavenumber  $\bar{\nu}$ . These magnitudes are interrelated in the following equation, where  $h$  is the Planck's constant ( $h = 6.22 \cdot 10^{-34} \text{ J s}$ ).

$$E = h\nu = \frac{hc}{\lambda} = hc\bar{\nu} \quad \text{Equ. (2.1)}$$

Atoms in solid state vibrate at frequencies from  $10^{12}$  to  $10^{13}$  Hz. Vibrational modes can be excited to higher energy states by radiation (Infrared radiation). Infrared spectroscopy and Raman scattering are the two major techniques of this vibrational spectroscopy. These techniques are mainly used to characterize the vibrational modes of molecules and solids.

The major task of these methods is the identification of different complexes and the characterization of structural changes in solids.

Electrons located in the outer energy levels are commonly called valence electrons. They can be excited via ultraviolet (UV), visible (VIS) and even near infrared (NIR) radiation. The wavelength range is covered from about 200 nm to 3000 nm. This field is called optical range.

### 2.1.2 Interaction of the incoming beam with the solid sample

A radiation beam hits the sample with the intensity  $I_0$  and leaves the sample with its attenuated intensity  $I_t$ . The intensity of the transmitted beam is lower than the intensity  $I_0$ , because there are several different effects in the specimen.

- Absorption is happening, if the beam frequency is resonant with a ground to excited state transition of the atoms in the solid. Most of the intensity is absorbed by a non-radiative way (heat). A very small part of the intensity (usually at lower frequencies) is emitted  $I_e$ .
- Reflection from the internal and external surfaces  $I_R$ .
- Scattering happens in an elastically way (the frequency of the incident beam is the same) or inelastic (the frequencies are lower or higher than that of the incident beam)  $I_S$ , which is called Raman scattering.

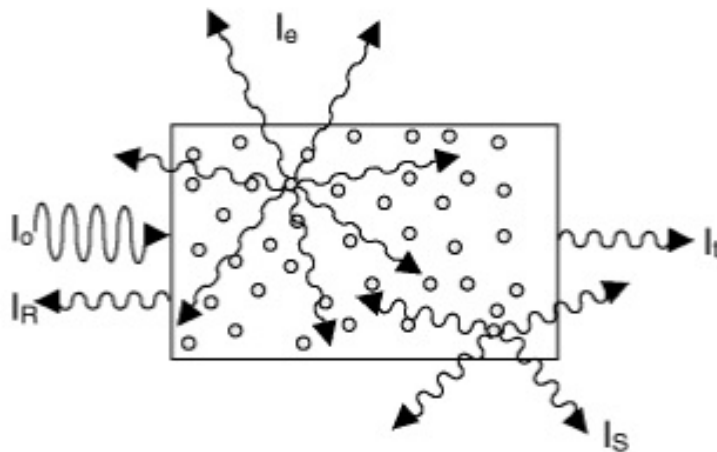


Figure 2: Interaction of the incoming beam with the sample [11]

Figure 2 shows the various beam intensities after the primary beam hits the sample with the intensity  $I_0$ . The emerging beam with the intensity  $I_t$  is attenuated because of absorption, reflection and scattering effects. At total reflection conditions the reflected beam  $I_R$  leaves the surface of the specimen at the same angle which it was appearing. Scattering and emission effects show uniform spreading in all directions.

Optical spectroscopy analyses the frequency and the intensity of the emitted beams. Thereby it is possible to understand the color of an object. This depends on the various emissions, reflection and transmission processes of the light and the sensitivity of the human eye. The spectral range of the visible light is given in Table 1.

Table 1: The spectral range associated with the different colors

Color	$\lambda$ [nm]	$\nu$ [Hz] · $10^{14}$	E [eV]
Violet	390-455	7.69-6.59	3.18-2.73
Blue	455-492	6.59-6.10	2.73-2.52
Green	492-577	6.10-5.20	2.52-2.15
Yellow	577-597	5.20-5.03	2.15-2.08
Orange	597-622	5.03-4.82	2.08-1.99
Red	622-780	4.82-3.84	1.99-1.59

This method is an excellent tool to obtain information about the electronic structure of the absorbing or emitting centers (atoms, ions), their lattice locations and the environment.

To take a closer look into the interaction between the incoming beam and the solid matter a classical approximation is used. This describes the radiation as classical electromagnetic wave and the solid as a continuous medium described by its dielectric constant  $\epsilon$  or its magnetic permeability  $\mu$ . The interaction will then be described as a classical oscillator (Lorentz oscillator).

### 2.1.3 Different types of luminescence

A simple two level atomic system promotes to an excited state, when photons of appropriate frequency are absorbed. This excited state can however return in to the ground state by spontaneous emission of photons. This de-excitation process is called luminescence. There are many different ways to elevate the system in an excited state. The most common ones are listed in Table 2.

Table 2: Different types of luminescence [11]

Name	Excitation mechanism
Photoluminescence	Light
Cathodoluminescence	Electrons
Radioluminescence	X-rays
Thermoluminescence	Heating
Electroluminescence	Electric field or current
Triboluminescence	Mechanical energy
Sonoluminescence	Sound waves in liquids
Chemiluminescence and Bioluminescence	Chemical reactions

Photoluminescence occurs after excitation with light (predominantly light in the optical range). This is very important in the field of the organic laundry detergents. Luminescence can also be produced under an electron beam. This technique is called cathodoluminescence. You can use this method to investigate trace impurities or lattice defects as well as crystal distortion. Excitation at high-energy electromagnetic radiation (X-rays) leads to a special type of photoluminescence, which is called Radioluminescence. One useful application is a so called scintillation counter, which detects x-rays by the common luminescence mechanism. The crystal is excited by the x-rays and produces luminescence which is detected by a photomultiplier. Thermoluminescence happens, when a substance emits light during the heating process. This method is used for dating minerals and ancient ceramics. By passing electric current through a sample, light emits by the mechanism of

electroluminescence. This technique is mainly used in nightlight panels. Triboluminescence is an optical phenomenon, where the breaking of bonds give away energy in the form of light. Sonoluminescence occurs when acoustic waves pass through the liquid sample. Chemoluminescence is a result of a chemical reaction. You can use it to determine NO or NO<sub>2</sub> in the atmosphere. Bioluminescence has the same basic principle than chemoluminescence with the main difference that it only occurs inside an organism. It is the predominant source of light in the deep ocean.

## 2.2 Absorption of UV/VIS light [12a]

### 2.2.1 Electronic transitions in polyatomic molecules

An electron transition happens, if an electron of a molecule in the ground state promotes to an unoccupied orbital by absorption of a photon. This molecule is then in an excited state.

To form a  $\sigma$  orbital you can either use two s orbitals or one s and one p orbital. It also works with two p atomic orbitals when they have a collinear axis of symmetry. A  $\pi$  orbital is formed by two overlapping p atomic orbitals.

For example ethylene (CH<sub>2</sub>=CH<sub>2</sub>), the two carbons are linked by one  $\sigma$  and one  $\pi$  bond. Absorption of a photon with the appropriate energy can promote one of the  $\pi$  electrons to an antibonding orbital  $\pi^*$ . This transition is called  $\pi \rightarrow \pi^*$ . The promotion of a  $\sigma$  electron requires a much higher energy. [13]

“It is also possible, that a molecule possess non-bonding electrons located on heteroatoms such as oxygen or nitrogen. The resulting molecular orbitals are called n orbitals. Promotion of a non-bonding electron to an antibonding orbital is possible ( $n \rightarrow \pi^*$ ).” [12b]

The energy of these transitions follow a straight order.

$$n \rightarrow \pi^* < \pi \rightarrow \pi^* < n \rightarrow \sigma^* < \sigma \rightarrow \pi^* < \sigma \rightarrow \sigma^*$$

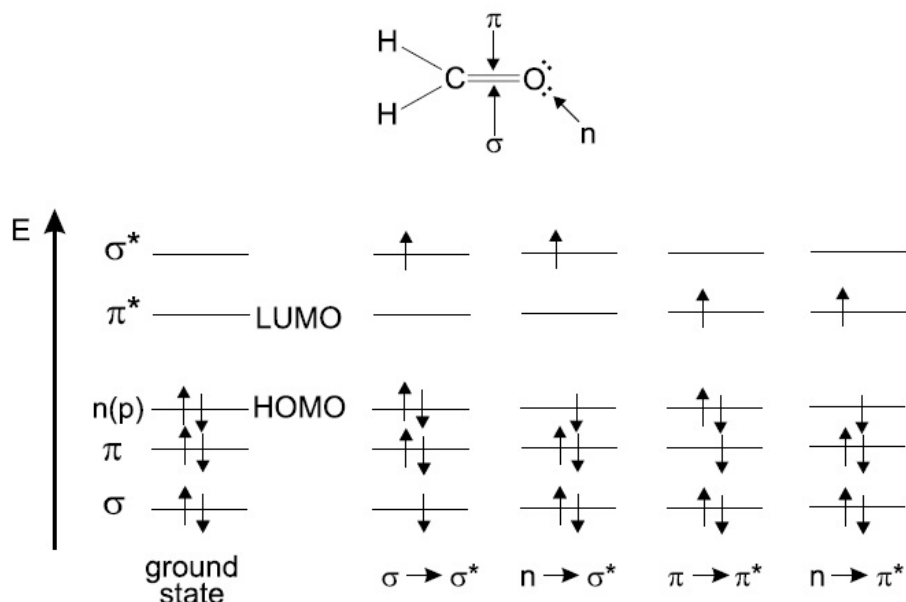


Figure 3: Energy levels of molecular orbitals in formaldehyde (HOMO: Highest Occupied Molecular Orbitals; LUMO: Lowest Unoccupied Molecular Orbitals) [12a]

Figure 3 illustrates the energy levels with the possible transitions for formaldehyde. The  $n \rightarrow \pi^*$  transition has a charge transfer character, because one electron is removed from the oxygen atom and translocated in the  $\pi^*$  orbital, which is localized half on carbon and half on the oxygen atom. Thereby a change of the dipole moment is measurable.

There are two important types of orbitals in spectroscopy, the Highest Occupied Molecular Orbitals (HOMO) and the Lowest Unoccupied Molecular Orbitals (LUMO). Both of them refer to the ground state and they are marked in Figure 3.

If one of the two electrons with opposite spin is promoted to a molecular orbital of higher energy, its spin is in principle unchanged, so that the total spin quantum number ( $S = \sum s_i$  with  $s_i = +\frac{1}{2}$  or  $-\frac{1}{2}$ ) remains equal to zero. The multiplicities of the ground and the excited states ( $M = 2S + 1$ ), are equal to one, because both are labelled singlet state ( $S_0$  is the ground state and  $S_1, \dots, S_n$  are the excited states). The corresponding transition is called singlet-singlet transition. A molecule in a singlet excited state can undergo conversion into a state, where the promoted electron has changed its spin. That implies the existence of two electrons with parallel spins, the total quantum number is one and the multiplicity is three. Such a state is called triplet state, because it corresponds to the three states of equal energy. According to the Hund'sche Rule, the triplet state has a lower energy than the singlet state of the same configuration.

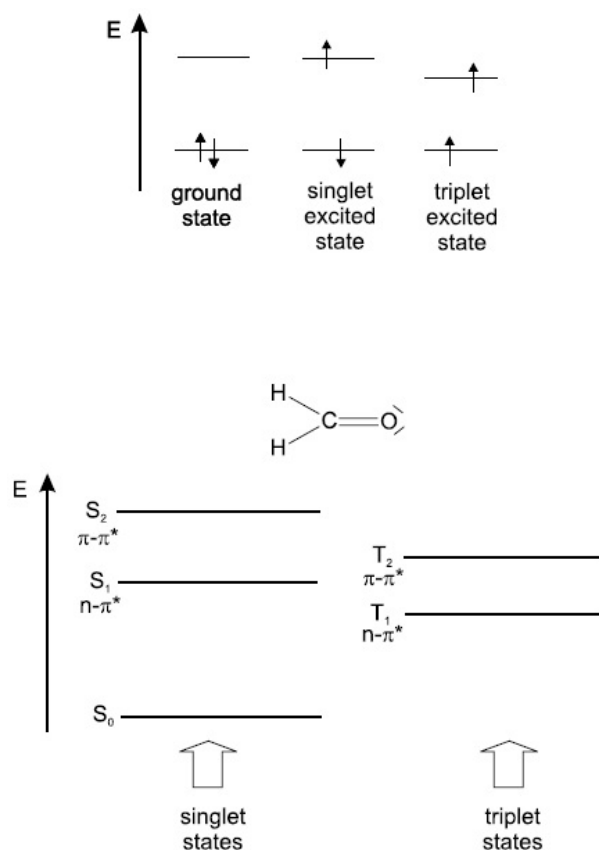


Figure 4: Difference between singlet and triplet states for formaldehyde [12a]

The bonding and non-bonding orbitals are localized between pairs of atoms. This is valid for formaldehyde, but it is no longer adequate in the case of alternating single and double carbon-carbon bonds (conjugated system). Overlapping of  $\pi$  orbitals allow the electrons to be delocalized over the whole system (resonance effect). This applies for butadiene and benzene, two simple conjugated systems.

In this case the  $\pi$  electron system can be considered as independent, because there is no interaction between the  $\sigma$  and the  $\pi$  orbitals. The greater the propagation of the  $\pi$  electron system, the lower the energy of the low lying  $\pi \rightarrow \pi^*$  transition. The corresponding absorption band increases, due to its wavelength dependency. This is valid for linear conjugated systems as well as cyclic conjugated systems. [14]

## 2.3 Selection rules [12a]

There are two major rules for absorption transitions.

### 2.3.1 Spin-forbidden transitions

Transitions between states of different multiplicities are forbidden. That means no singlet-triplet or triplet-singlet transitions are allowed. However a weak interaction between the wave-functions of different multiplicities exists via spin-orbit coupling. This can be understood by considering the motion of an electron in a Bohr-like orbit. The rotation around the nucleus generates a magnetic moment. The electron spins at its own axis which generates another magnetic moment. Spin-orbit coupling results from the interaction between these two magnets. [12a]

Due to the effect of spin-orbit coupling an important procedure is possible. Intersystem crossing is the crossing from the first singlet excited state  $S_1$  to the first triplet state  $T_1$ . It is favored by heavy atoms because this coupling varies with the fourth power of the atomic number.

### 2.3.2 Symmetry-forbidden transitions

A transition can be forbidden for symmetric reasons. Nevertheless they can be observed, because the molecular vibrations cause some deviation from perfect symmetry (vibronic coupling). [12a]

## 2.4 The Frank-Condon principle [12a]

The motions of electrons are much faster than those of the nuclei (Born-Oppenheimer approximation). Promotion of an electron to an antibonding molecular orbital upon excitation takes about  $10^{-15}$  s, which is very fast compared to the characteristic time for molecular vibrations ( $10^{-10} - 10^{-12}$  s). An electronic transition is preferred, if there are no changes in the positions of the nuclei in the molecular entity and its environment. The resulting state is called Frank-Condon state and the transition is called vertical-transition. This is illustrated by the following Figure. The energy function is a function of the nuclear configuration and it's represented by a Morse function.

According to the Boltzmann distribution most of the molecules are in ground state at room temperature. In addition to the 0-0 transition there are several vibronic transitions, whose entities depend on the relative position and shape of the potential energy curves. [12a]

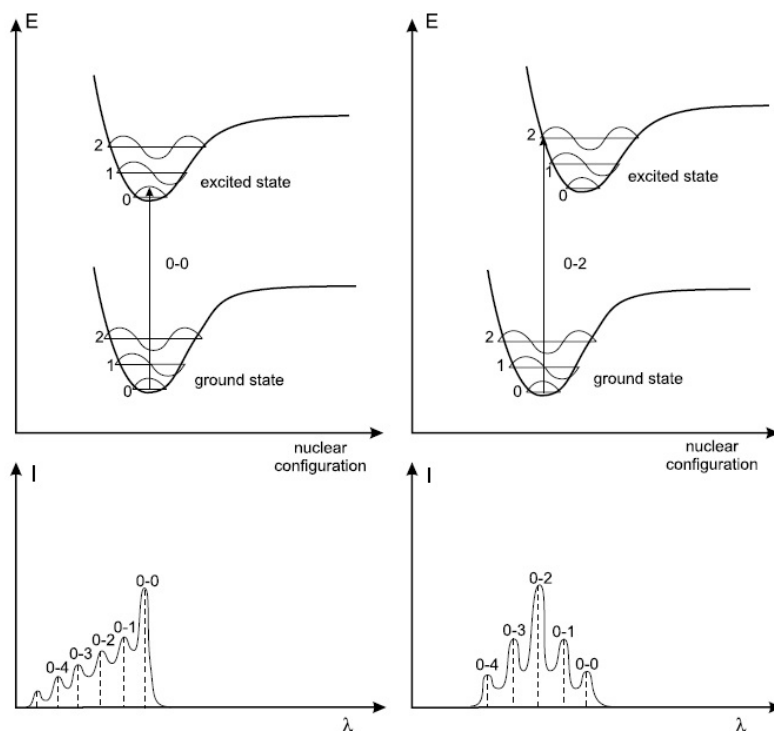


Figure 5 Top: potential energy diagrams with vertical transition. Bottom: shape of the absorption bands; dashed lines represent the absorption lines in vapor [12a]

The width of a band in an absorption spectrum is a result of two effects called homogeneous and inhomogeneous broadening. Homogeneous broadening assumes the existence of a continuous set of vibrational sublevels in each electronic state. Inhomogeneous broadening is due to the results of the structure of the solvation shell. Such effects exist for emission bands in fluorescence as well.

Shifts in the spectra according to the effect of substitution will be discussed later. A shift to longer wavelength is called bathochromic shift or red-shift and a shift to shorter wavelength is called a hypsochromic shift or blue-shift. [12a]

## 2.5 Characteristics of fluorescence emission [12a]

### 2.5.1 Radiative and non-radiative transitions

The Perrin-Jablonski diagram is suitable for visualizing the following processes.

- Photon absorption
- Internal conversion (IC)
- Intersystem crossing (ISC)
- Fluorescence
- Phosphorescence

The singlet electronic states are marked  $S_0$  (fundamental electronic state)  $S_1 \dots S_n$  and the triplet states  $T_1 \dots T_n$ . Vibrational levels are assigned with each electronic state. One important fact is that absorption is very fast (approximately  $10^{-15}$  s) with respect to all other processes. [12a]

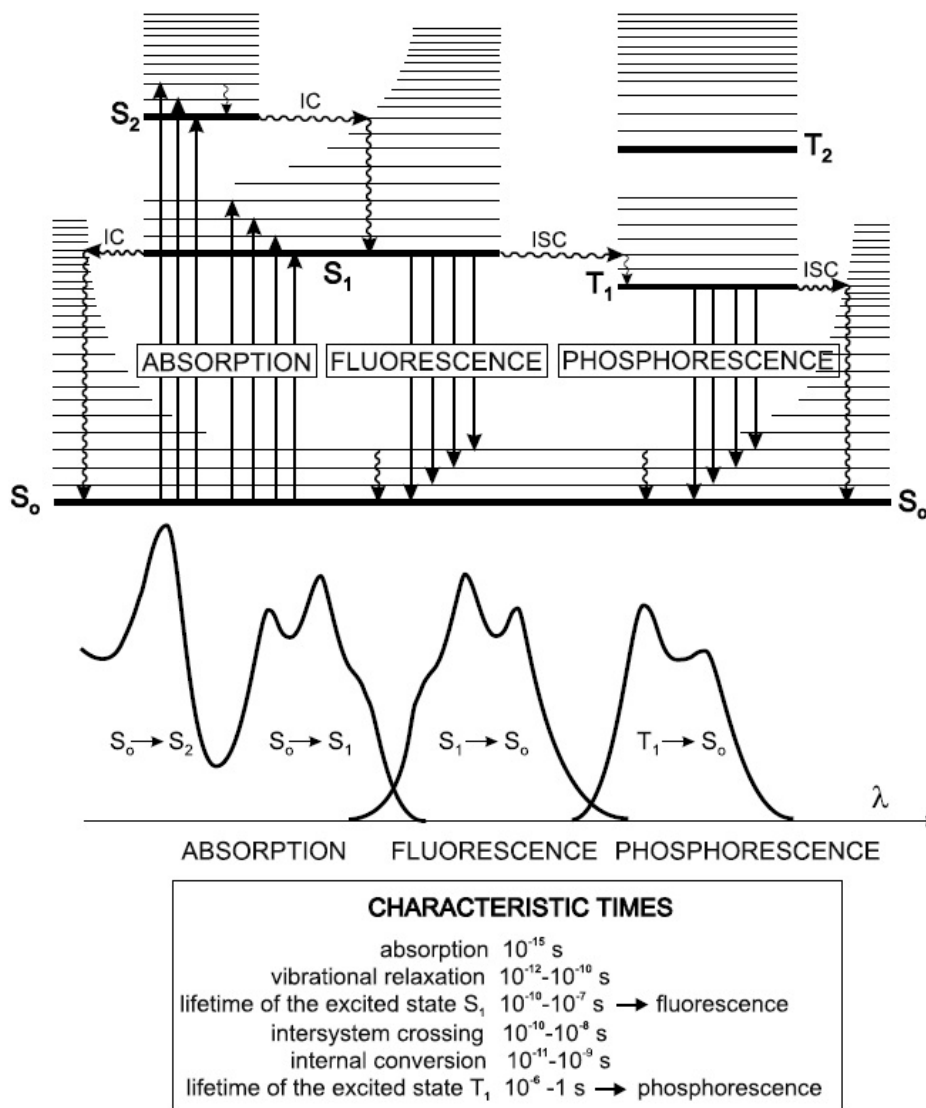


Figure 6: Perrin-Jablonski diagram and illustration of the relative positions of absorption, fluorescence and phosphorescence spectra [12a]

The vertical arrows corresponding to absorption start from the lowest vibrational energy level. Absorption of a photon can promote a molecule to one of the vibrational levels of  $S_1 \dots S_n$ .

### 2.5.2 Internal conversion (IC) [12a]

A non-radiative transition between two electronic states of the same spin multiplicity is called internal conversion. If a molecule is excited to an energy level higher than the lowest vibrational level of the first electronic state, vibrational relaxation (and internal conversion if the singlet excited state is higher than  $S_1$ ) leads the excited molecule towards the zero vibrational level of the  $S_1$  singlet state. An internal conversion to  $S_0$  is possible, but it is less efficient than conversion from  $S_2$  to  $S_1$ , because of the larger energy gap between  $S_1$  and the ground state. The rule of thumb here is that the smaller the energy gap between the initial and the final electronic state, the larger the efficiency of the internal conversion. Therefore, internal conversion from  $S_1$  to  $S_0$  can compete with emission of photons and intersystem crossing.

### 2.5.3 Intersystem crossing (ISC) [12a]

A non-radiative transition between two isoenergetic vibrational levels, which belong to the electronic state of different multiplicities, is called intersystem crossing. An excited molecule in the zero vibrational level of the  $S_1$  state can move to the isoenergetic level of the  $T_n$  state. The transport to the lowest vibrational level of  $T_1$  happens via vibrational relaxation. Intersystem crossing is fast enough to challenge with other pathways of de-excitation from  $S_1$  (fluorescence and internal conversion).

The possibility of intersystem crossing depends on the singlet and on the triplet states. Intersystem crossing is often very efficient, when the transition  $S_0 \rightarrow S_1$  is of the type  $n \rightarrow \pi^*$ .

In appearance of heavy atoms (atoms whose atomic number is large e.g. Br, Pb) spin-orbit coupling takes place and this favors intersystem crossing.

### 2.5.4 Fluorescence [12a]

Fluorescence is characterized by the emission of photons according to the  $S_1 \rightarrow S_0$  relaxation. If only one species exists in ground state, fluorescence does not depend on the excitation wavelength, because emission only occurs from  $S_1 \rightarrow S_0$ . The 0-0 transition is usually the same for absorption and fluorescence. Due to vibrational relaxation an energy loss in the excited state happens and that's the reason why the fluorescence spectrum is located at higher wavelength (lower energy) than the absorption spectrum. This observation corresponds with the Stokes Rule. It is also possible, that the absorption spectrum partially overlaps the emission spectrum. At room temperature, a small fraction of molecules is in a vibrational level higher than zero in the ground state as well as in the excited state.

The differences between the vibrational levels are similar in ground state and excited state. This declares that the fluorescence spectrum often resembles the first absorption band. The Stokes-shift is the gap between the first absorption band and the fluorescence maximum. It is important to know, that the emission of a photon is as fast as absorption of a photon. Excited molecules stay in the  $S_1$  state for a certain time before emitting a photon or undergo another de-excitation process. The decay of fluorescence intensity is characteristic and is quite similar to the radioactive decay.

The emission of fluorescence photons is described as a spontaneous process, but under certain conditions stimulated emission is possible.

#### 2.5.4.1 Spontaneous and stimulated emissions [12a][15][16]

The probability of transition of a molecule between two energy levels  $E_1$  and  $E_2$  is described by the Einstein coefficients.

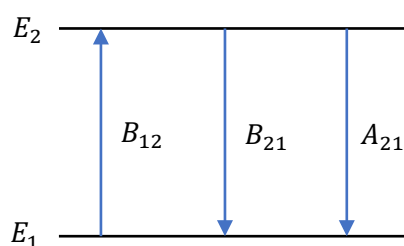


Figure 7: Energy levels and Einstein coefficients

$B_{12}$  is the induced absorption coefficient,  $B_{21}$  is the induced emission coefficient and  $A_{21}$  is the spontaneous emission coefficient. The rate of the emission-induced process  $E_2 \rightarrow E_1$  is equal to the rate of the absorption-induced process  $E_1 \rightarrow E_2 \Rightarrow B_{12} = B_{21}$ .

$N_1$  and  $N_2$  are the numbers of molecules in the states 1 and 2. These numbers must satisfy the Boltzmann Law, where  $h$  is Planck's constant ( $h = 6.626 \cdot 10^{-34} \text{ J} \cdot \text{s}$ ) and  $k$  is Boltzmann's constant ( $k = 1.380 \cdot 10^{-23} \frac{\text{J}}{\text{K}}$ ).

$$\frac{N_1}{N_2} = e^{\left(\frac{-E_1-E_2}{kT}\right)} = e^{\left(\frac{h \cdot \nu}{kT}\right)} \quad \text{Equ. (2.2)}$$

The absorption-rate from state 1 to state 2 is  $N_1 B_{12} \rho(\nu)$ , where  $\rho(\nu)$  the energy density depending on the frequency is  $\nu$ . The emission-rate from state 2 to state 1 is  $N_2 \cdot A_{21} + B_{21} \rho(\nu)$ . These two states are equal, when the system is in equilibrium.

$$\frac{N_1}{N_2} = \frac{B_{21} \rho(\nu) + A_{21}}{B_{12} \rho(\nu)} = 1 + \frac{A_{21}}{B_{12} \rho(\nu)} \quad \text{Equ. (2.3)}$$

The radiation density  $\rho(\nu)$  distributes from the Planck's black body radiation law.

$$\rho(\nu) = \frac{8\pi h \nu^3}{c^3 e^{\left(\frac{h\nu}{kT}\right)} - 1} \quad \text{Equ. (2.4)}$$

The combination of these three equations leads to:

$$A_{21} = \frac{8\pi h \nu^3}{c^3} B_{21} \quad \text{Equ. (2.5)}$$

It is very important to know that the ratio  $\frac{A_{21}}{B_{21}}$  is proportional to the cube of the frequency and that's the reason why in visible regions essentially all emissions are spontaneous for the common radiation levels. At longer wavelengths (e.g. radiofrequencies) spontaneous emission is insubstantial. To observe induced emission the population of the first singlet state  $S_1$  has to be larger than that of  $S_0$ . By looking at the Boltzmann distribution it is easy to see that this condition is far away from the case at room temperature. So an inversion of the population is required (e.g.  $N_{S_1} > N_{S_0}$ ). Inversion of a four level system can be achieved by using optical pumping by an intense light source (flash lamps or lasers) or via electrical discharge in a gas. [12a]

In opposition to spontaneous emission, induced emission (also known as stimulated emission) is coherent. This means that all the emitted photons have the same physical characteristics. Which is the same direction, the same phase and the same polarization. These are the characteristics of laser emission (L.A.S.E.R. = Light Amplification by Stimulated Emission of Radiation). De-excitation is triggered by the interaction of an incident photon with an excited atom or molecule, which induces emission of photons having the same characteristics as those of the incident photon and that's why it's called induced emission. [12a]

### 2.5.5 Phosphorescence

Phosphorescence is the de-excitation process from the triplet state  $T_1$  to the ground state  $S_0$ . Although this transition is forbidden, it can be observed because of the spin-orbit coupling. The lifetime of the triplet state may be long enough to observe phosphorescence on a time scale up to seconds or even minutes. The energy of the lowest vibrational level of the triplet state  $T_1$  is lower than that of the singlet  $S_1$  and that's the reason why the phosphorescence spectrum is located at wavelength higher than the fluorescence spectrum. [12a]

## 2.6 Emission and excitation spectra [12a]

### 2.6.1 Emission spectra

The emission spectrum is characteristic for a given compound. The following formula describes the formation of the spectrum.

$$\int_0^{\infty} F_{\lambda}(\lambda_F) d\lambda_F = \Phi_F \quad \text{Equ. (2.6)}$$

Where  $F_{\lambda}(\lambda_F)$  is the term of fluorescence intensity per absorbed photon as a function of the wavelength of the emitted photons. It represents the fluorescence spectrum and it mainly describes the distribution of the probability of the various transitions from the lowest vibrational level of  $S_1$  to the vibrational levels of  $S_0$ .  $\Phi_F$  is the quantum yield and it is described as the fraction of excited molecules that return to the ground state  $S_0$  with emission of fluorescence photons.

The fluorescence intensity is measured at a fixed wavelength (selected by a monochromator) and it is proportional to the number of photons that are absorbed at the excitation wavelength (selected by a monochromator). Therefore it can be described as the difference of the incident light and the transmitted light.

When the concentration of the fluorescent compound is high, inner filter effects may occur and reduce the fluorescence intensity. The photons emit at wavelengths corresponding to the overlap between the absorption and the emission spectrum. A radiative transfer happens and the photons reabsorb.

### 2.6.2 Excitation spectra

The excitation spectrum results as a function of the variations of the fluorescence intensity and the excitation wavelength  $\lambda_E$  for a fixed observation wavelength  $\lambda_F$ . If there is a single species in the ground state the shape of the absorption spectrum and the corrected excitation spectrum is the same. Whenever different forms (aggregates, tautomeric forms) exist in the ground state, the excitation and the absorption spectra are no longer in identical shape.

### 2.6.3 Stokes-shift

The gap between the first absorption maximum and the maximum of the fluorescence spectrum is called Stokes-shift. It is expressed in wavenumbers  $\Delta\bar{\nu} = \bar{\nu}_a - \bar{\nu}_f$ .

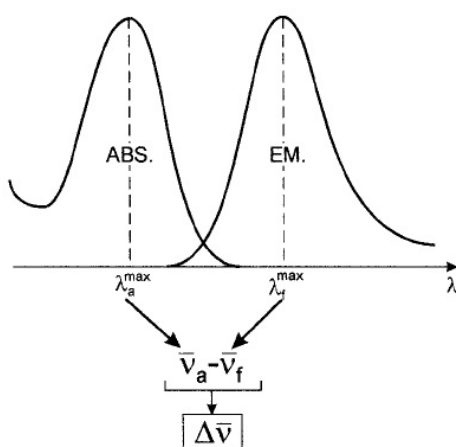


Figure 8: Definition of the Stokes shift [12a]

The Stokes-shift can provide information on the excited states.

## 2.7 Impact of the molecular structure on fluorescence [17]

### 2.7.1 Extent of $\pi$ -electron system

A few highly unsaturated aliphatic compounds show fluorescent behavior, but most fluorescent compounds are aromatic. An increase of the degree of conjugation (enlargement of the  $\pi$  electron system) leads to a shift of the absorption and fluorescence spectra to longer wavelength.

In these case the lowest lying transition is the  $\pi \rightarrow \pi^*$  type, which is characterized by a high fluorescent quantum yield. When a heteroatom is involved in the  $\pi$ -system, a  $n \rightarrow \pi^*$  transition may be the lowest lying transition. These transitions have a 100 times longer radiative lifetime, than that of the  $\pi \rightarrow \pi^*$  transition. This provides a reference point, why the fluorescence quantum yields of many molecules, in which the  $n \rightarrow \pi^*$  transition is the lowest excited state, is so low. This happens mainly at nitrogen heterocycles (pyridine-type nitrogen's). [17]

### 2.7.2 Heterocyclic compounds [12a]

One or more heterocyclic nitrogen atoms (e.g. pyridine, quinoline) are called azarenes and they have a low lying  $n \rightarrow \pi^*$  transition, which explains their low fluorescence quantum yields compared with the hydrocarbons. This is valid for measurements in solid state. [17]

The fluorescence characteristics strongly depend on the nature of the solvent. In protic solvents (e.g. alcohols) hydrogen bonds can be formed between the solvents and the molecule. As a result of this, inversion between the  $\pi \rightarrow \pi^*$  and the  $n \rightarrow \pi^*$  transition happens and this increases the fluorescence quantum yield. Due to the formation of hydrogen bonds the electron density of the nitrogen atom is reduced in excited state. As a consequence, a red-shift of the spectra going from non-polar to polar solvents, takes place. [17]

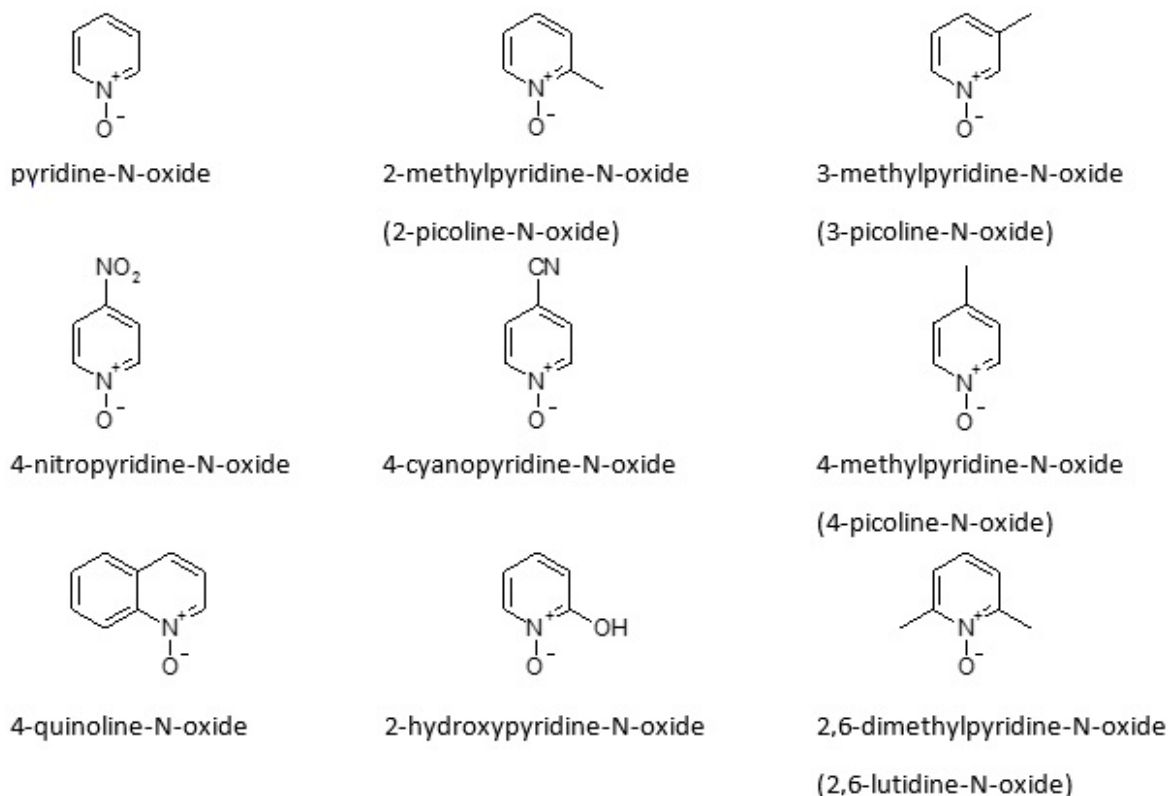


Figure 9: Various types of heterocyclic nitrogen compounds

### 2.7.3 Electron-donating substituents [12a]

Substitution with electron donating groups lead to a shift in both absorption and emission spectra. The presence of lone pairs of electrons from oxygen or nitrogen, does not change the  $\pi \rightarrow \pi^*$  nature of the transitions of the unsubstituted molecule. In opposition to the lone pairs of electrons from carbonyl substituents, the lone pairs from the heteroatoms are involved in the aromatic system.

For steric reasons, the  $-\text{NH}_2$  group is twisted out of the plane of the aromatic system and so the degree of conjugation is decreased. Coplanarity with the aromatic ring is also pronounced with  $-\text{OR}$  substituents. The  $-\text{OH}$  group is nearly coplanar.

Famous electron-donating substituents:  $-\text{OH}$ ,  $-\text{OR}$ ,  $-\text{NH}_2$ ,  $-\text{NHR}$  and  $\text{NR}_2$

### 2.7.4 Electron-withdrawing substituents [12a]

The fluorescence of  $-\text{NO}_2$  substituted aromatic hydrocarbons is not detectable. Intersystem crossing is favored, because these systems have a low lying  $n \rightarrow \pi^*$  transition. Many nitro-aromatic substances show phosphorescence, although their quantum yield for intersystem crossing is significantly under one. The absence of detectable fluorescence is due to a high rate of  $S_1 \rightarrow S_0$  internal conversion, which may be related to a charge-transfer character of the excited state. This can be attributed to the strong electron-withdrawing power of the  $-\text{NO}_2$  group.

Famous electron-withdrawing substituent:  $-\text{CO}$  and  $-\text{NO}_2$

## 2.8 Data analysis and quality parameters [12a]

The first criterion for a good fit is the reduced chi squared ( $\chi_r^2$ ) parameter, whose value should be close to 1. Values in the range from 0.8 to 1.2 provide significant results. Lower values indicate, that the data set is too small and higher values indicate a wrong fitting model.

In Addition to the first criterion graphical tests are useful. The following Figure shows a practical example with the original measured signal (Signal 1) and the fitted curve (Gauss Fit), as well as some useful parameters.

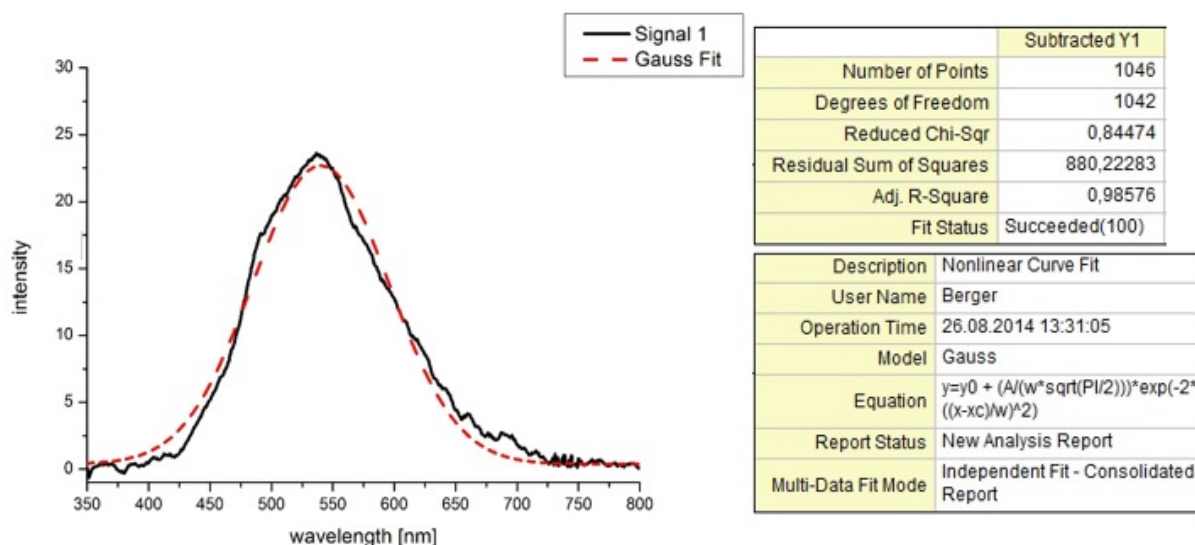


Figure 10: Measured signal and fitted signal

## 2.9 Charge-transfer mechanisms [18]

Charge-transfer effects often take place in coordination chemistry of inorganic solids. There are two different ways depending on the direction of the charge-transfer. The main difference compared to the simple d-d transitions is that charge-transfer transitions are never forbidden. That's the reason why the absorption in the visible region is more distinct.

### 2.9.1 Ligand to metal charge-transfer (LMCT) [18]

By binding of oxidizable ligands to reducible metals (metals in higher oxidation states), transitions in the visible regions are possible.

Halides perform ligand to metal charge-transfer bands in the sequence of  $I^- < Br^- < Cl^- < F^-$  according to the ease of oxidation of these ions. Substituting an organic ligand with electron donating groups, should lead to a charge transfer from the ligand at lower energies, while using electron withdrawing groups should shift the transition to higher energies. There is a correlation between the ionization potential of the substituted ligands as well as the metal ions and the energy of the ligand to metal charge-transfer bands.

The ligand to metal charge-transfer transition energy will decrease from left to the right of the periodic table as the nuclear charge on the metal increases.

### 2.9.2 Metal to ligand charge-transfer (MLCT) [18]

The charge transfer bands move to lower energy as the oxidation state of the metal decreases and the ligand becomes more electronegative and should move to higher energies as the coordination number decreases. There is a connection between the energy of a metal to ligand transition and the affinity of the ligand to accept an electron. Ligands with empty orbitals, adequate energy and symmetry give rise to charge transfer in the visible region. These are less common than ligand to metal charge-transfer processes. In general oxidizing ligands, such as the pyridine-N-oxide exhibit this kind of charge transfer via their  $\pi$  antibonding levels.

The metal to ligand charge-transfer bands are in general weaker than the ligand to metal charge-transfer ones. [18]

### 2.9.3 Effect on the emission spectra

"The observation of large Stokes shifts and broad bands is expected for charge transfer transitions. Often, the charge transfer transition is described as the transfer of an electron from the ligands to the central metal ion. In reality, the transition will not involve the transfer of one electron, but it certainly involves a considerable reorganization of the charge density distribution around the metal ion. This reorganization is accompanied by an expansion of the metal-ligand bonds in the excited state, which gives rise to the observation of large Stokes shifts and broad bands." taken from [48a] [48b]

A large blue-shift in the emission spectra is due to LMCT [19], while MLCT [20] shows a red-shift in the emission spectra. [21]

## 2.10 Chemistry of pyridine-N-oxides [22a]

It was first described in the year 1926 by J. Meisenheimer and since 1954 it is fully commercial available. Up to now more than 19.000 one step reactions are listed in the SciFinder database. [23] Pyridine-N-oxide is very popular, because it is an important part in many drugs and standard aromatic reactions (e.g. Sandmeyer-reaction). It differs in four points compared to the pyridine.

First of all it is more nucleophilic and electrophilic than the pyridine. It is characterized by a higher dipole-moment and from a chemical view it is a much weaker base ( $pK_a$  (pyridine-N-oxide) = 0.79,  $pK_a$  (pyridine) = 5.2)

Several mesomeric forms of pyridine-N-oxide are shown in the next Figure.

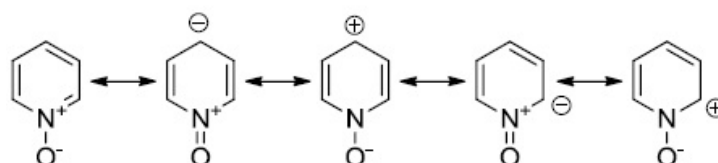


Figure 11: Mesomeric forms of pyridine-N-oxide [22b]

The preferred attack for both nucleophile as well as electrophile is either at the oxygen or on the 2- or the 4-position. Oxygen protonated species react like deactivated pyridines and nucleophilic aromatic substitutions are faster than with pyridine.

## 2.11 Pseudohalides [22c]

Pseudohalides are the anions of the corresponding pseudohalogen groups such as azides, thiocyanates and cyanides. The chemical properties and the behavior of pseudohalides are identical to true halide ions. Internal bonding situations do not affect their chemical behavior, so they can react with metals to form compounds like MX (e.g. NaCl vs.  $\text{NaN}_3$ ).

### 2.11.1 Azides [22c]

Azide  $\text{N}_3^-$  is a linear anion, which can be described in several resonance structures. The most important one is shown in the next Figure.



Figure 12: Azide resonance structure

One of the important fields of application is propelling charge in an airbag. [24] Most of the organic and inorganic azides [25] are prepared directly from sodium azide in an aqueous solution. Azides are explosive and toxic materials and should be handled with care.

### 2.11.2 Thiocyanates [26]

Thiocyanate  $\text{SCN}^-$  is also a linear molecule. It's most important resonance structure is shown in the next Figure.



Figure 13: Thiocyanate resonance structure

It is an ambidentate ligand, because it can act as a nucleophile either on the sulfur or nitrogen.

If  $\text{SCN}^-$  is added to a solution, which contains  $\text{Fe}^{3+}$ -ions, a blood red solution is formed. It's due to the formation of  $[\text{Fe}(\text{NCS})(\text{H}_2\text{O})_5]^{2+}$ . This compound plays an important role in the proof of iron(III) ions.

### 3) Experimental

#### 3.1 Preparation

It is possible, that sodium azide could react with organic molecules on a highly exothermic way. Therefore working with azides has to be done with great care and very carefully. Most of the used chemicals are toxic and harmful for the environment, so working with safety equipment and in fume hoods was absolutely required. Furthermore it was important to use small amounts of our chemicals for the preparations, to reduce damage in the case of an accident. The metal complexes were prepared in 100 mL flasks. They have a screw cap to prevent the uncontrolled evaporation of solvents. A wide range of the pyridine-N-oxide complexes were synthesized at room temperature, but in some cases heating was necessary. To permit this task a heating plate with a water bath was utilized. In order to ensure a slow and continuous crystallization a drying cabinet was used. (40°C) It was often the case that crystallization could not be observed at room temperature. Thus it was possible to store the flasks at 4°C in a refrigerator.

To remove the solid crystals from its liquid phase a special filtering technique was used. Nutsch-type filters were used to collect and dry the crystals. The remaining mother liquor was either used to recrystallize the samples or it was stored in the refrigerator to slowly generate more and purer crystals. Last but not least the collected crystals were stored in wetted glasses with snap on lids and examined with a light microscope.

##### 3.1.1 Preparation of $\text{HN}_3$ saturated water

An azide-generator was used to prepare the  $\text{HN}_3$  saturated water. Therefore an aqueous solution of sulfuric acid in the ratio 1:4 was mixed with sodium azide. The resulting gaseous  $\text{HN}_3$  was sucked in a 200 mL reaction flask (D) which was filled with distilled water. After applying the vacuum the reaction took about 10 minutes and the saturation was successful, if the pH value was between three and four.

$\text{HN}_3$  should always be prepared freshly according to the following chemical equation.

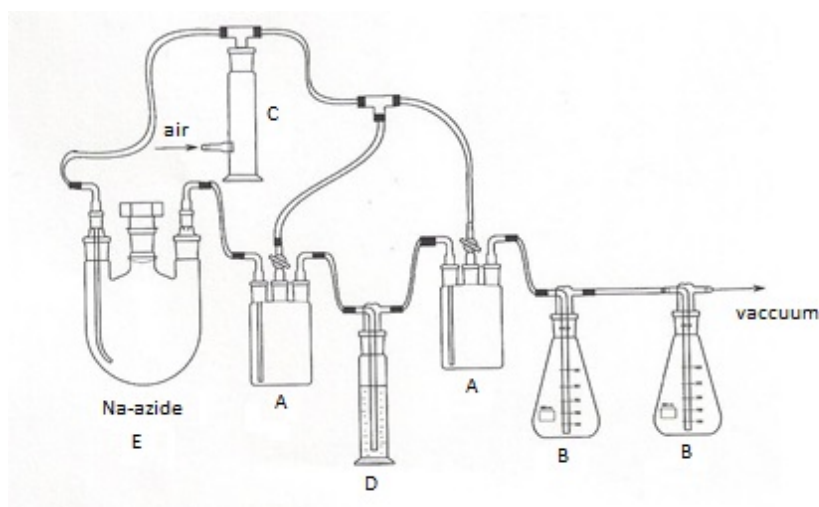


Figure 14: Azide-generator [27]

A...safety-flask

B...concentrated KOH for absorption

C...drying tower for dust absorption

D... reaction flask

E... $\text{NaN}_3$  in diluted  $\text{H}_2\text{SO}_4$  (ratio 1:4)

## 3.2 Used devices

### 3.2.1 Single crystal diffraction

X-ray measurements for single crystals are done using two different devices:

First, a Bruker, and APEX II CCD diffractometer (MoK $\alpha$  radiation  $\lambda = 0.71073 \text{ \AA}$ ) with  $\omega$ -scan mode and graphite-monochromator at 100K. APEX and SAINT [28] software packages were used for data collection and processing. Corrections were applied to all data (for absorption through Laue symmetry requirements) [29]. Structure solution (direct methods) and structure refinement (least-squares) were done by SHELXTL/PC [30] program package. PLATON [31] (a program for automated calculation of derived geometrical data) was used for supporting the structure solution process.

Second, a Bruker-AXS SMART APEX CCD diffractometer at 100K with Mo-radiation ( $\lambda = 0.7107 \text{ \AA}$ ) and graphite monochromator was used.

Data collection was done by Ao. Univ.-Prof. Dr. Franz A. Mautner and Ao. Univ.-Prof. Dr. Christoph Marschner.

### 3.2.2 Luminescence spectroscopy

The LS 55, distributed by the company Perkin Elmer, is a luminescent spectrometer with a pulsed light source. It is possible to measure emission spectra with a fixed excitation wavelength and vice versa. The supplied software called BL studio, allows the complete control of gate and delay functions at long decay time, as well as the automation of 3D plots. [32]

#### Technical data:

- Excitation from 200 to 800 nm with a Xe-flashbulb
- Emission measurements from 200 to 900 nm and detection with a photomultiplier tube R955 Hamamatsu
- Cut off filter at: 290 nm, 350nm, 390nm, 430nm and 515 nm
- Method dependent parameters
  - Emission slit
  - Excitation slit
  - Potential of the photomultiplier
  - Calibration of the specimen carrier
  - Emission filters

As a result of the measurements we get the intensity dependent on the wavelength. Those intensities are relative values, which could be directly compared to the other computational data, if the settings don't change.

### 3.2.3 Diffuse reflection spectroscopy

The Lambda950 (L950), distributed by the company Perkin Elmer, is an optical spectrometer, which provides reflection-measurements in the range from 200 to 2500 nm. It is possible to measure solid, liquid and even gaseous samples. [33]

#### Technical data:

- Integrating sphere consisting of spectralon (Teflon)
- D2-lamp (under 320 nm)
- Tungsten-lamp (320-2500 nm)
  - Lamp change at 319.20 nm
- Monochromator/Detector change at 810 nm
- Photomultiplier detector (PMT)
  - Gain: Auto
  - Response: 0.20 s
- Indium-Gallium-Arsenide detector (InGaAs)
  - Gain: 16
  - Response: 0.20 s
- Slits
  - PMT(fixed): 2.00 nm
  - InGaAs(servo): 2.00 nm

#### 3.2.4 Infrared spectroscopy (FT-IR)

A Bruker Alpha P (Platinum-ATR-cap) spectrometer was used, to characterize the synthesized samples and also to check the specific vibrational bands of the azides and the thiocyanates. The measurements were performed at room temperature. For recording of all spectra, OPUS-software [34] was used and they are all listed in the attachment. The specific vibrations are described for each compound with the following shortcuts: w (weak), m (medium), s (strong) vs (very strong), sh (shoulder); referring to the intensity of the peak. They are sorted from highest to lowest value. All peaks which could be located were referred to values in [35].

---

In the following chapters (4 to 7) the synthesis of the different compounds as well as the CHN analysis, selected IR-bands and the description of the crystal structure with perspective views, packing plots and the associated Table with bonding settings are listed in this order. In case of the preliminary compounds **(7)** and **(18)** only a perspective view with the atom numbering scheme is presented.

## 4) Cd(II) complexes

### 4.1 [Cd(2-picoline-N-oxide)(NCS)<sub>2</sub>]<sub>n</sub> (**1**)

Compound (**1**) was obtained by mixing 3CdSO<sub>4</sub>·8H<sub>2</sub>O (0.26 g, 1.00 mmol), 2-methylpyridine-N-oxide (0.11 g, 1.00 mmol) and KSCN (0.19 g, 2.00 mmol) in 33.00 mL distilled water at room temperature. After one day at room temperature yellow crystals appeared (yield: 0.30 g, 89%). *Anal.* Calc. for C<sub>8</sub>H<sub>7</sub>CdN<sub>3</sub>OS<sub>2</sub> (337.69 g/mol): C, 28.5; H, 2.1; N, 12.4. Found: C, 28.4; H, 2.1; N, 12.4%. Selected IR bands (ATR-IR, cm<sup>-1</sup>): 3095 (w), ν<sub>CN</sub>: 2106 (vs), 1617 (w), 1577 (w), 1492 (m), 1458 (m), 1419 (w), 1383 (w), 1270 (w), 1208 (s), 1159 (w), 1113 (m), 1089 (w), 1053 (w), 995 (w), 934 (w), 903 (w), 870 (w), 845 (s), 807 (w), 773 (vs), ν<sub>CS</sub>: 723 (w), 698 (m), 597 (m), 556 (m), 498 (w), δ<sub>NCS</sub>: 461 (s).

Description of the crystal structure:

A part of the crystal structure of [Cd(2-picoline-N-oxide)(NCS)<sub>2</sub>]<sub>n</sub> (**1**) is shown in Figure 15, and selected bond parameters are listed in Table 3. Cd(1) is six-coordinated by N(11), S(11), N(21), S(21) of four μ<sub>(N,S)</sub> bridging isothiocyanato groups and by O(1) and O(1') of μ<sub>(O,O)</sub> bridging 2-picoline-N-oxide molecules in cis-conformation. The bond distances within the distorted CdN<sub>2</sub>O<sub>2</sub>S<sub>2</sub> octahedron are: Cd-N/O from 2.229(6) to 2.326(5) Å, Cd-S are 2.654(2) and 2.655(2) Å. The isothiocyanato groups form di-μ<sub>(N,S)</sub> double bridges to connect the Cd(II) centers to polymeric chains. These polymeric chains are further connected by the centrosymmetrically related μ<sub>(O,O)</sub> bridging 2-picoline-N-oxide molecules to generate a 2D system extended along the a- and b-axis of the unit cell (Figure 16). One of the two centrosymmetric and eight-membered Cd(NCS)<sub>2</sub>Cd rings is almost planar, whereas the other one adopts a "chair-like" arrangement ["chair angle" θ defined as acute angle between plane of the di-μ<sub>(N,S)</sub> thiocyanato bridges and the Cd/N/S plane is 0.7 and 12.2°, respectively]. The torsions angles are: Cd(1'')-N(11'')...S(11)-Cd(1) = ± 2.3°, Cd(1)-N(21)...S(21\*)-Cd(1\*) = ± 36.1°. The four-membered Cd<sub>2</sub>O<sub>2</sub> rings formed by the μ<sub>(O,O)</sub> bridging 2-picoline-N-oxide molecules are planar. The Cd(1)-O(1)-Cd(1') and O(1)-Cd(1)-O(1') bond angles are 111.6(2) and 68.4(2)°. The Cd-O(1)-N(1) bond angles are 121.3(4) and 125.1(4)°; the Cd-O(1)-N(1)-C(1) torsion angle is ± 98.1°. The intra-plane metal-metal distances are: Cd(1)...Cd(1') = 3.8450(10), Cd(1)...Cd(1'') = 5.9516(12), Cd(1)...Cd(1\*) = 5.9435(12) Å, whereas the shortest Cd...Cd inter-planar separation is 7.4808(15) Å.

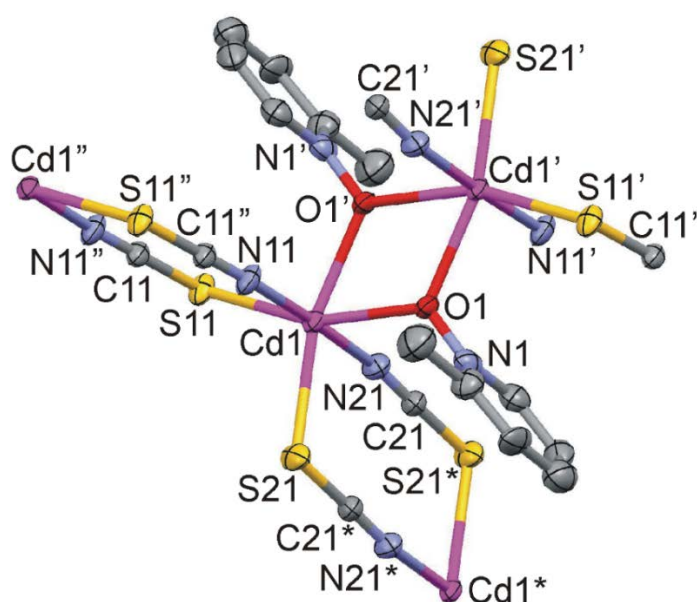


Figure 15: Perspective view of a section of [Cd(2-picoline-N-oxide)(NCS)<sub>2</sub>]<sub>n</sub> (**1**)

Symmetry codes: (') 1-x, 1-y, -z; (') -x, 1-y, -z; (\*) 1-x, 2-y, -z.

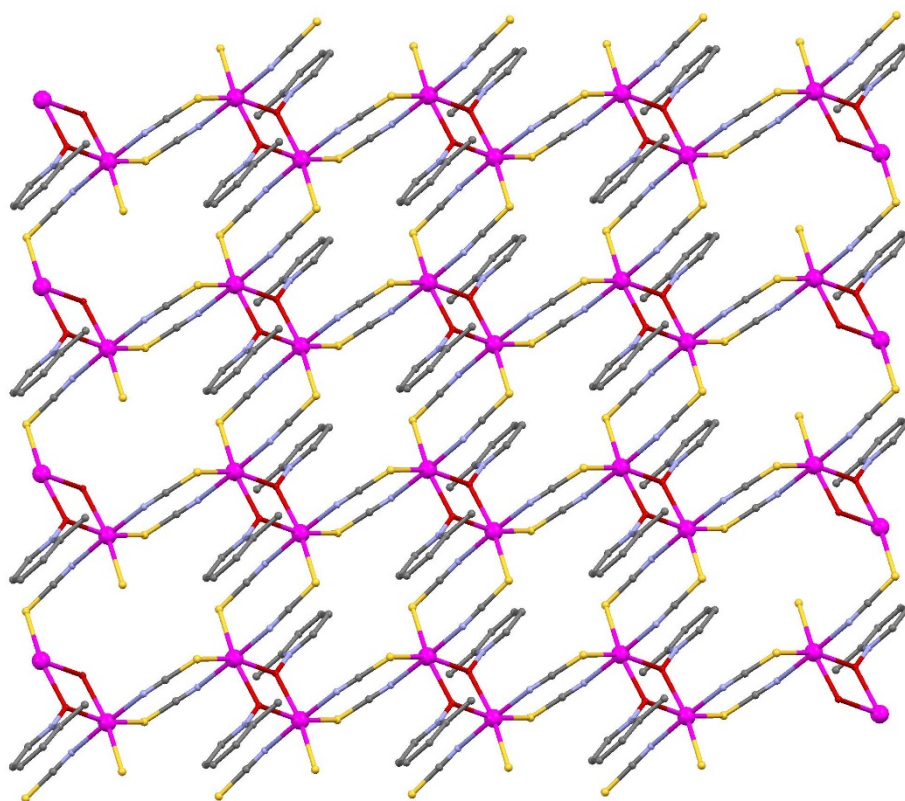


Figure 16: View onto the polymeric layer of  $[\text{Cd}(\text{2-picoline-N-oxide})(\text{NCS})_2]_n$  (**1**)

Table 3: Selected bond parameters of  $[\text{Cd}(\text{2-picoline-N-oxide})(\text{NCS})_2]_n$  (**1**)

Cd(1)-N(11)	2.299(6)	Cd(1)-N(21)	2.314(7)
Cd(1)-O(1)	2.322(5)	Cd(1)-O(1')	2.326(5)
Cd(1)-S(21)	2.654(2)	Cd(1)-S(11)	2.655(2)
S(21*)-C(21)	1.654(7)	O(1)-N(1)	1.323(8)
N(11)-C(11'')	1.141(9)	C(11)-S(11)	1.666(7)
Cd(1)-O(1)-Cd(1')	111.6(2)	S(21)-Cd(1)-S(11)	109.92(7)
O(1)-Cd(1)-O(1')	68.4(2)	O(1)-Cd(1)-S(21)	91.49(14)
O(1)-Cd(1)-S(21')	159.61(13)	O(1)-Cd(1)-S(11)	158.45(14)
O(1)-Cd(1)-S(11')	90.36(13)	N(11)-Cd(1)-N(21)	178.0(2)
N(11)-Cd(1)-O(1)	91.4(2)	N(21)-Cd(1)-O(1)	90.0(2)
N(11)-Cd(1)-O(1')	91.1(2)	N(21)-Cd(1)-O(1')	90.8(2)
N(11)-Cd(1)-S(21)	86.09(18)	N(21)-Cd(1)-S(21)	92.39(17)
N(11)-Cd(1)-S(11)	92.53(16)	N(21)-Cd(1)-S(11)	86.71(17)
N(11'')-C(11)-S(11)	178.9(7)	N(21)-C(21)-S(21*)	177.9(7)
N(1)-O(1)-Cd(1)	125.1(4)	N(1)-O(1)-Cd(1')	121.3(4)
C(11'')-N(11)-Cd(1)	163.9(6)	C(11)-S(11)-Cd(1)	102.4(3)
C(21)-N(21)-Cd(1)	159.5(6)	C(21*)-S(21)-Cd(1)	102.6(3)

Symmetry codes: (') 1-x, 1-y, -z; (') -x, 1-y, -z; (\*) 1-x, 2-y, -z.

## 4.2 [Cd(3-picoline-N-oxide)(NCS)<sub>2</sub>]<sub>n</sub> (**2**)

3CdSO<sub>4</sub>·8H<sub>2</sub>O (0.52 g, 2.00 mmol), 3-methylpyridine-N-oxide (0.22 g, 2.00 mmol) and KSCN (0.37 g, 3.89 mmol) were dissolved in 28.00 mL distilled water at room temperature. After three days at room temperature yellow crystals appeared (yield: 0.43 g, 64%). *Anal.* Calc. for C<sub>8</sub>H<sub>7</sub>CdN<sub>3</sub>OS<sub>2</sub> (337.70 g/mol): C, 28.5; H, 2.1; N, 12.4. Found: C, 28.1; H, 2.0; N, 12.3%. Selected IR bands (ATR-IR, cm<sup>-1</sup>): 3096 (w), ν<sub>CN</sub>: 2103 (vs), 1610 (w), 1488 (m), 1443 (m), 1254 (m), 1154 (s), 1097 (w), 1045 (w), 1013 (w), 941 (m), 880 (w), 801 (s), 746 (s), 675 (s), 561 (s), 525 (w), 491 (m), δ<sub>NCS</sub>: 452 (m).

Description of the crystal structure:

A fragment of the crystal structure of [Cd(3-picoline-N-oxide)(NCS)<sub>2</sub>]<sub>n</sub> (**2**) is shown in Figure 17, and selected bond parameters are listed in Table 4. Cd(1) is six-coordinated by N(11), S(11), N(21), S(21) of four μ<sub>(N,S)</sub> bridging isothiocyanato groups and by O(1) and O(1') of μ<sub>(O,O)</sub> bridging 3-picoline-N-oxide molecules in *cis*-conformation. The bond distances within the distorted CdN<sub>2</sub>O<sub>2</sub>S<sub>2</sub> octahedron are: Cd-N/O from 2.273(3) to 2.366(2) Å, Cd-S are 2.6341(9) and 2.6812(9) Å. The isothiocyanato groups form di-μ<sub>(N,S)</sub> double bridges to connect the Cd(II) centers to polymeric chains. These polymeric chains are further connected by the centrosymmetrically related μ<sub>(O,O)</sub> bridging 3-picoline-N-oxide molecules to generate a 2D system extended along the *a*- and *b*-axis of the unit cell (Figure 18). Both of the two centrosymmetric and eight-membered Cd(NCS)<sub>2</sub>Cd rings adopt a "chair-like" arrangement ["chair angle" θ defined as acute angle between plane of the di-μ<sub>(N,S)</sub> thiocyanato bridges and the Cd/N/S plane is 17.9 and 37.1°, respectively]. The torsions angles are: Cd(1'')...N(11'')...S(11)-Cd(1) = ± 48.2°, Cd(1)-N(21)...S(21\*)-Cd(1\*) = ± 74.6°. The four-membered Cd<sub>2</sub>O<sub>2</sub> rings formed by the μ<sub>(O,O)</sub> bridging 3-picoline-N-oxide molecules are planar. The Cd(1)-O(1)-Cd(1') and O(1)-Cd(1)-O(1') bond angles are 108.33(8) and 71.67(8)°. The Cd-O(1)-N(1) bond angles are 118.95(17) and 125.03(18)°; the Cd-O(1)-N(1)-C(1) torsion angle is ± 94.2°. The intra-plane metal-metal distances are: Cd(1)...Cd(1') = 3.8213(7), Cd(1)...Cd(1'') = 5.8115(10), Cd(1)...Cd(1\*) = 5.5347(9) Å, whereas the shortest Cd...Cd inter-planar separation is 7.0573(12) Å

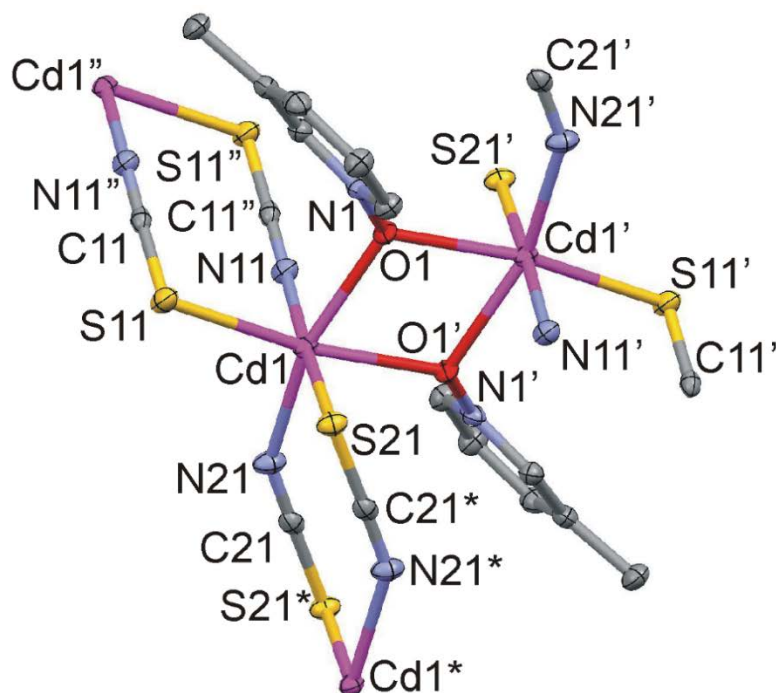


Figure 17: Perspective view of a section of [Cd(3-picoline-N-oxide)(NCS)<sub>2</sub>]<sub>n</sub> (**2**)

Symmetry codes: (') 1-x, 1-y, 1-z; (") 1-x, -y, 1-z; (\*) -x, 1-y, 1-z.

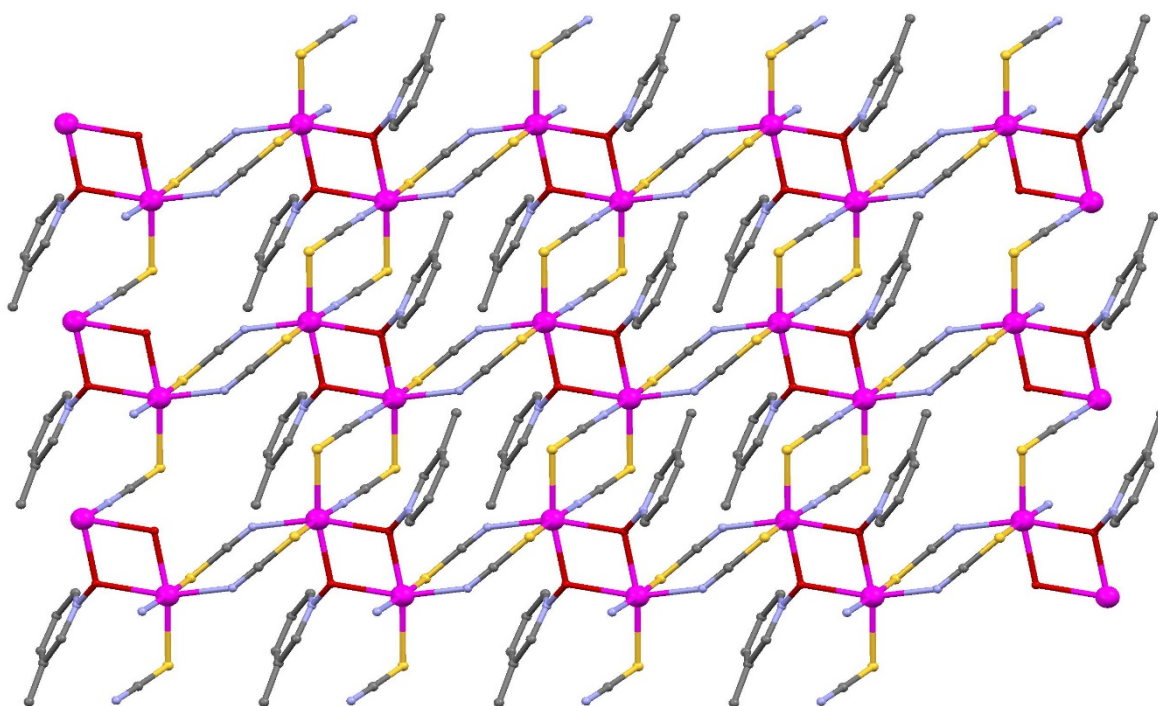


Figure 18: View onto the polymeric layer of  $[Cd(3\text{-picoline-N-oxide})(NCS)_2]_n$  (**2**)

Table 4: Selected bond parameters of  $[Cd(3\text{-picoline-N-oxide})(NCS)_2]_n$  (**2**)

Cd(1)-N(21)	2.273(3)	Cd(1)-N(11)	2.298(3)
Cd(1)-O(1')	2.348(2)	Cd(1)-O(1)	2.366(2)
Cd(1)-S(11)	2.6341(9)	Cd(1)-S(21)	2.6812(9)
S(21)-C(21)	1.654(3)	O(1)-N(1)	1.340(3)
N(11)-C(11'')	1.154(4)	N(21)-C(21)	1.155(4)
C(11)-S(11)	1.655(3)		
Cd(1)-O(1)-Cd(1')	108.33(8)	S(11)-Cd(1)-S(21)	83.94(3)
O(1)-Cd(1)-O(1')	71.67(8)	O(1')-Cd(1)-S(11)	165.31(6)
O(1)-Cd(1)-S(11)	95.82(6)	O(1')-Cd(1)-S(21)	88.55(6)
O(1)-Cd(1)-S(21)	91.25(6)	N(21)-Cd(1)-N(11)	89.46(10)
N(21)-Cd(1)-O(1')	89.36(9)	N(11)-Cd(1)-O(1')	91.91(9)
N(21)-Cd(1)-O(1)	159.71(9)	N(11)-Cd(1)-O(1)	84.19(9)
N(21)-Cd(1)-S(11)	103.90(8)	N(11)-Cd(1)-S(11)	94.50(7)
N(21)-Cd(1)-S(21)	95.51(7)	N(11)-Cd(1)-S(21)	175.02(7)
N(11'')-C(11)-S(11)	178.4(3)	N(21)-C(21)-S(21*)	178.9(3)
N(1)-O(1)-Cd(1')	125.03(18)	N(1)-O(1)-Cd(1)	118.95(17)
C(11'')-N(11)-Cd(1)	157.5(3)	C(11)-S(11)-Cd(1)	100.16(11)
C(21)-N(21)-Cd(1)	147.2(3)	C(21*)-S(21)-Cd(1)	93.24(11)

Symmetry codes: (') 1-x, 1-y, 1-z; (") 1-x, -y, 1-z; (\*) -x, 1-y, 1-z.

### 4.3 [Cd(4-cyanopyridine-N-oxide)<sub>2</sub>(NCS)<sub>2</sub>(H<sub>2</sub>O)]<sub>2</sub> (**3**)

Compound (**3**) was obtained by mixing 3CdSO<sub>4</sub>·8H<sub>2</sub>O (0.51 g, 2.00 mmol), 4-cyanopyridine-N-oxide (0.24 g, 2.00 mmol) and KSCN (0.39 g, 4.00 mmol) in 27.00 mL distilled water at 50°C. Upon slow cooling to room temperature colorless crystals of (**3**) were separated after four days (yield: 0.55 g, 57%). *Anal.* Calc. for C<sub>14</sub>H<sub>10</sub>CdN<sub>6</sub>O<sub>3</sub>S<sub>2</sub> (486.81 g/mol): C, 34.5; H, 2.1; N, 17.3. Found: C, 34.5; H, 2.0; N, 17.3%. Selected IR bands (ATR-IR, cm<sup>-1</sup>): 3354 (m,br), ν<sub>CN</sub>: 2102 (s), 2056 (vs), 1923 (w), 1628 (m), 1551 (w), 1513 (w), 1480 (s), 1436 (m), 1309 (w), 1220 (vs), 1173 (vs), 1102 (m), 1046 (w), 954 (w), 850 (s), ν<sub>CS</sub>: 723 (m), 666 (w), 598 (w), 551 (m), δ<sub>NCS</sub>: 454 (m).

Description of the crystal structure:

A perspective view together with the atom numbering scheme of the crystal structure of [Cd(4-cyanopyridine-N-oxide)<sub>2</sub>(NCS)<sub>2</sub>(H<sub>2</sub>O)]<sub>2</sub> (**3**) is shown in Figure 19, and selected bond parameters are listed in Table 5. The octahedron round Cd(1) is formed by N(11) and S(11) of two μ<sub>(N,S)</sub> bridging isothiocyanato groups, by N(21) of a terminal isothiocyanato group, O(1) and O(2) of two trans-coordinated terminal 4-cyanopyridine-N-oxide molecules and O(3) of a terminal aqua ligand [Cd-N = 2.199(2) and 2.230(2), Cd-S = 2.7797(7), Cd-O from 2.3409(16) to 2.3669(16) Å]. Centrosymmetric dimeric units are built by μ<sub>(N,S)</sub> isothiocyanato double bridges. Their eight-membered Cd(NCS)<sub>2</sub>Cd ring adopt a “chair-like” arrangement [“chair angle” θ defined as acute angle between plane of the di-μ<sub>(N,S)</sub> thiocyanato bridges and the Cd(1)/N(11)/S(11) plane is 10.1°]. The torsion angle: Cd(1)-N(11)...S(11')-Cd(1') = ± 35.7°. The isothiocyanato groups have the following bond parameters: Cd-N-C: 162.30(18) and 162.72(18)°, Cd-S-C: 100.68(8)°, N-C-S: 176.8(2) and 177.6(2)°, N-C: 1.162(3) and 1.169(3) Å, C-S: 1.650(2) and 1.630(2) Å. The terminal 4-cyanopyridine-N-oxide molecules have Cd-O-N bond angles of 112.66(12) and 112.88(12)°; the Cd(1)-O(1)-N(1)-C(1) and Cd(1)-O(2)-N(2)-C(14) torsion angles are 84.3 and 80.5°, respectively. The 4-cyanopyridine-N-oxide molecules form an interplanar angle of 8.9°. The Cd(1)...Cd(1') distance within the Cd(NCS)<sub>2</sub>Cd ring is 5.9712(7) Å, the shortest Cd...Cd inter-dimer separation is 5.6422(7) Å. The aqua ligand forms hydrogen bonds of type O-H...O to O atoms of adjacent 4-cyanopyridine-N-oxide molecules to generate a supramolecular 2D system oriented along the a- and b-axis of the unit cell (Figure 20) [O(3)...O(1)(1-x,-y,1-z) = 3.014(2) Å, O(3)-H(31)...O(1) = 174(2)°; O(3)...O(2)(2-x,-y,1-z) = 2.883(2) Å, O(3)-H(32)...O(2) = 176(2)°].

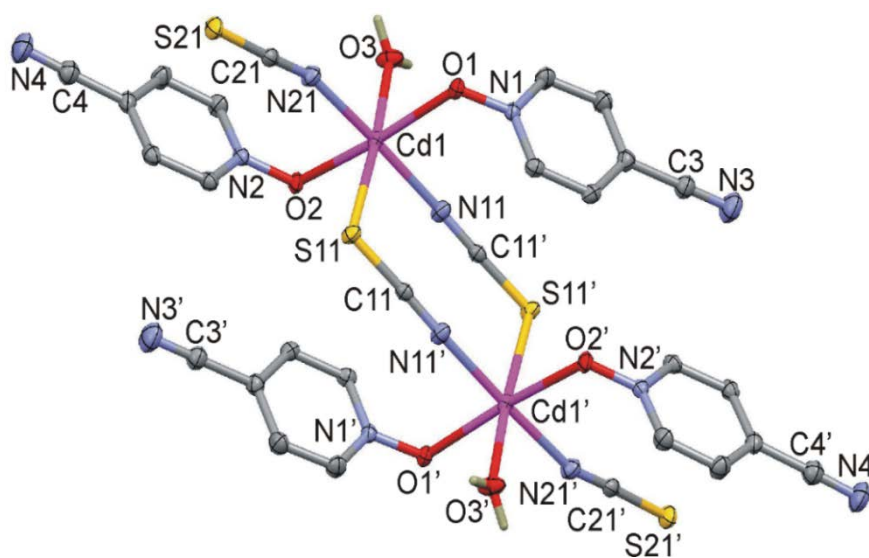


Figure 19: Perspective view of a section of [Cd(4-cyanopyridine-N-oxide)<sub>2</sub>(NCS)<sub>2</sub>(H<sub>2</sub>O)]<sub>2</sub> (**3**)

Symmetry code: (') 2-x,1-y,1-z.

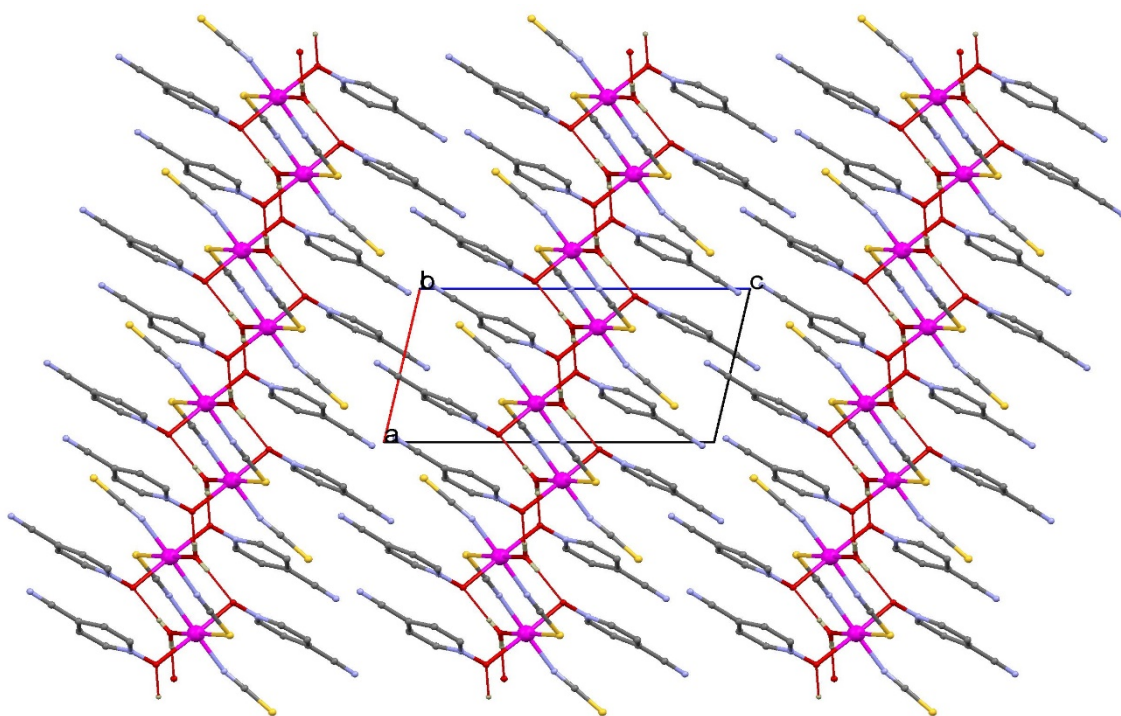


Figure 20: View onto the 1D sheet of  $[Cd(4\text{-cyanopyridine-}N\text{-oxide})_2(NCS)_2(H_2O)_2]_2$  (**3**)

Table 5: Selected bond parameters of  $[Cd(4\text{-cyanopyridine-}N\text{-oxide})_2(NCS)_2(H_2O)_2]_2$  (**3**)

Cd(1)-N(21)	2.199(2)	Cd(1)-N(11)	2.230(2)
Cd(1)-O(1)	2.3409(16)	Cd(1)-O(2)	2.3445(16)
Cd(1)-O(3)	2.3669(16)	Cd(1)-S(11)	2.7797(7)
N(11)-C(11')	1.162(3)	C(11)-N(11')	1.162(3)
C(11)-S(11)	1.650(2)	N(21)-C(21)	1.169(3)
C(21)-S(21)	1.630(2)	O(1)-N(1)	1.336
O(2)-N(2)	1.334(2)		
N(21)-Cd(1)-N(11)	176.23(7)	N(21)-Cd(1)-O(1)	88.01(6)
N(11)-Cd(1)-O(1)	91.97(6)	N(21)-Cd(1)-O(2)	91.93(6)
N(11)-Cd(1)-O(2)	88.54(6)	N(21)-Cd(1)-O(3)	91.80(7)
N(11)-Cd(1)-O(3)	91.96(7)	N(21)-Cd(1)-S(11)	85.11(6)
N(11)-Cd(1)-S(11)	91.13(5)	N(11')-C(11)-S(11)	176.8(2)
N(21)-C(21)-S(21)	177.6(2)	N(1)-O(1)-Cd(1)	112.88(12)
N(1)-O(1)-Cd(1)	112.88(12)	N(2)-O(2)-Cd(1)	112.66(12)
O(1)-Cd(1)-O(2)	173.09(5)	O(1)-Cd(1)-O(3)	87.16(6)
O(2)-Cd(1)-O(3)	85.93(6)	O(1)-Cd(1)-S(11)	94.80(4)
O(2)-Cd(1)-S(11)	92.08(4)	O(3)-Cd(1)-S(11)	176.28(5)
C(11')-N(11)-Cd(1)	162.30(18)	C(11)-S(11)-Cd(1)	100.68(8)
C(21)-N(21)-Cd(1)	162.72(18)		

Symmetry codes: (') 2-x, 1-y, 1-z.

#### 4.4 [Cd(4-nitropyridine-N-oxide)<sub>2</sub>(NCS)<sub>2</sub>]<sub>n</sub> (**4**)

3CdSO<sub>4</sub>·8H<sub>2</sub>O (0.26 g, 1.00 mmol), 4-nitropyridine-N-oxide (0.14 g, 1.00 mmol) and KSCN (0.20 g, 2.11 mmol) were dissolved in 50.00 mL distilled water at room temperature. Upon slow cooling to 4°C yellow crystals of (**4**) were separated after 1 week (yield: 0.35 g, 69%). *Anal.* Calc. for C<sub>12</sub>H<sub>8</sub>CdN<sub>6</sub>O<sub>6</sub>S<sub>2</sub> (508.77 g/mol): C, 28.3; H, 1.6; N, 16.5. Found: C, 28.3; H, 1.6; N, 16.5%. Selected IR bands (ATR-IR, cm<sup>-1</sup>): 3106 (m,br), 3029 (w), 2094 (s), 1597 (m), 1519 (vs), 1472 (m), 1345 (vs), 1223 (vs), 1173 (s), 1122 (s), 1033 (w), 937 (w), 860 (vs), 816 (m), 771 (w), 750 (m), 676 (m), 646 (vs), 539 (w), 510 (w), δ<sub>NCS</sub>: 462 (s).

Description of the crystal structure:

The 1:2 complex crystallizes in the orthorhombic space group Pbcn with Z = 4. The cadmium(II) center is located on a two-fold rotation axis. A fragment of the crystal structure of the [Cd(4-nitropyridine-N-oxide)<sub>2</sub>(NCS)<sub>2</sub>]<sub>n</sub> (**4**) is shown in Figure 21, and selected bond parameters are listed in Table 6. Cd(1) is six-coordinated by N(11), S(11), N(11'), S(11') of four μ<sub>(N,S)</sub> bridging isothiocyanato groups and by O(1) and O(1') of two terminal 4-nitropyridine-N-oxide molecules in cis-conformation. The bond distances within the distorted CdN<sub>2</sub>O<sub>2</sub>S<sub>2</sub> octahedron are: Cd-N/O = 2.2780(17) and 2.3418(14) Å, Cd-S = 2.7218(5) Å. The isothiocyanato groups form di-μ<sub>(N,S)</sub> double bridges to connect the Cd(II) centers to polymeric chains oriented along the c-axis of the unit cell (Figure 22). The eight-membered Cd(NCS)<sub>2</sub>Cd rings adopt a "chair-like" arrangement ["chair angle" θ defined as acute angle between plane of the di-μ<sub>(N,S)</sub> thiocyanato bridges and the Cd/N/S plane is 13.2°]. The torsions angles are: Cd(1)-N(11)...S(11'')-Cd(1'') = ± 46.5°. The polymeric chain is corrugated with Cd...Cd...Cd angles of 128.6° and Cd...Cd intra-chain distance of 5.9531(10) Å and the shortest Cd...Cd inter-chain separation is 7.0709(12) Å. The terminal 4-nitropyridine-N-oxide molecules have a Cd(1)-O(1)-N(1) bond angle of 114.50(10)°; the Cd-O(1)-N(1)-C(1) torsion angle is 91.3°. The nitro-group in position 4 of the pyridine-N-oxide is rotated out of the pyridine plane by 13.5°.

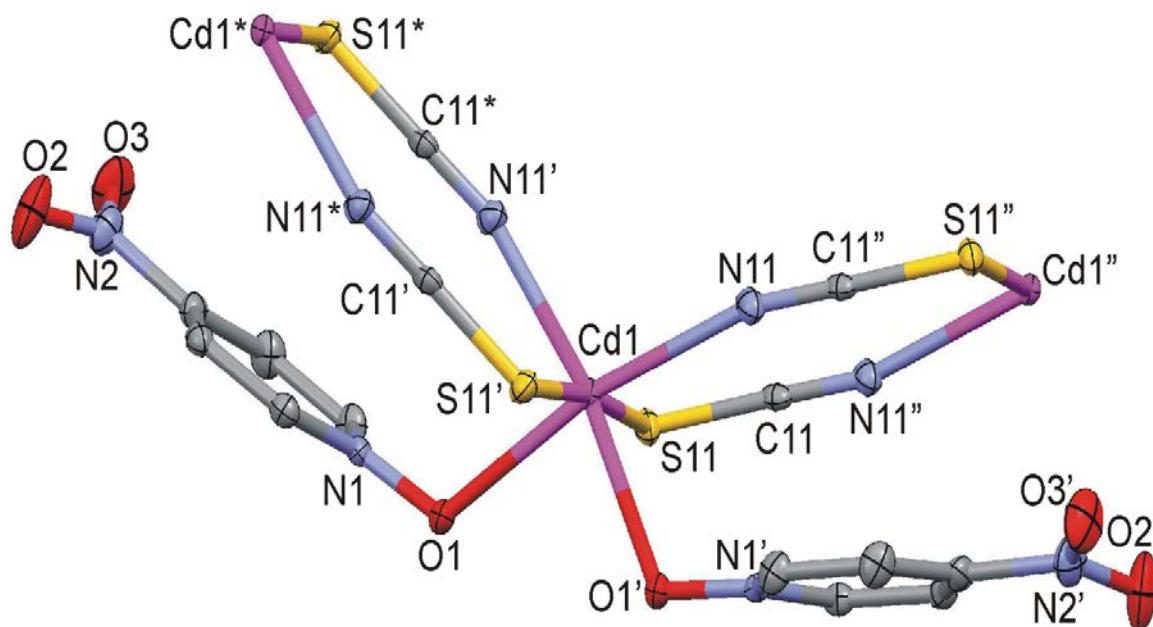


Figure 21: Perspective view of a section of [Cd(4-nitropyridine-N-oxide)<sub>2</sub>(NCS)<sub>2</sub>]<sub>n</sub> (**4**)

Symmetry codes: (') -x, y, 3/2-z; (") -x, -y, 1-z; (\*) x, -y, 1/2+z.

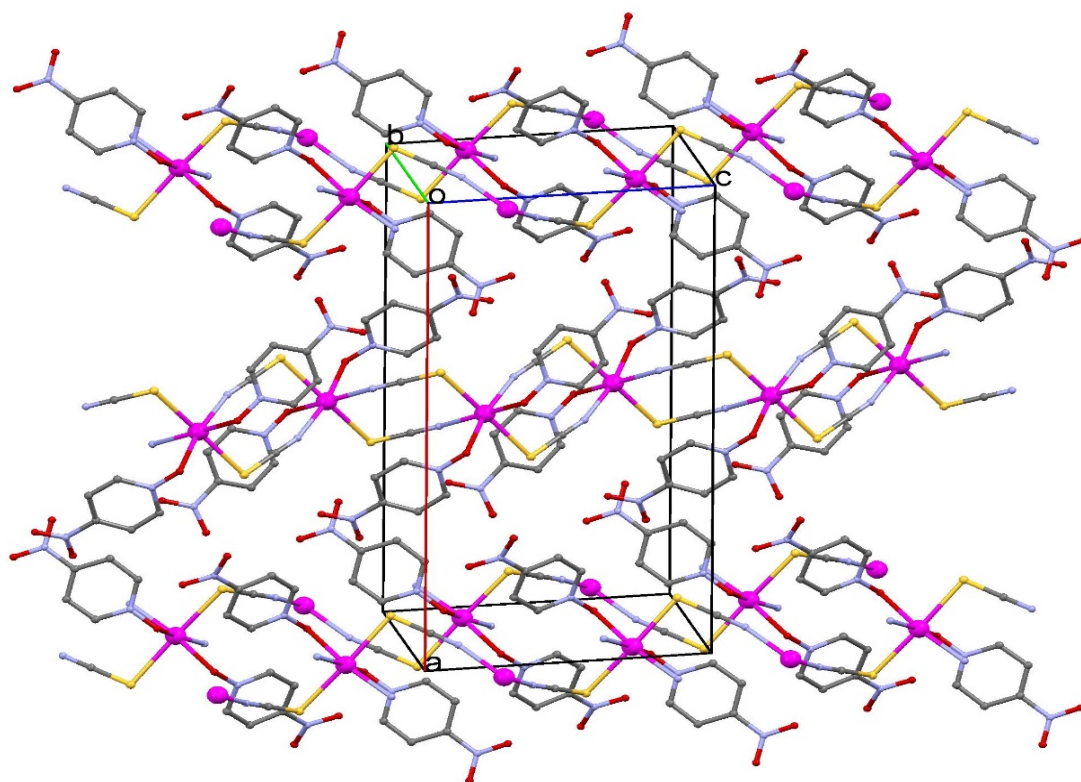


Figure 22: View onto the 1D chain of  $[Cd(4\text{-nitropyridine-}N\text{-oxide})_2(NCS)_2]_n$  (**4**)

Table 6: Selected bond parameters of  $[Cd(4\text{-nitropyridine-}N\text{-oxide})_2(NCS)_2]_n$  (**4**)

Cd(1)-N(11)	2.2780(17)	Cd(1)-O(1)	2.3418(14)
Cd(1)-S(11)	2.7218(5)	O(1)-N(1)	1.324(2)
N(11)-C(11'')	1.158(3)	C(11)-S(11)	1.651(2)
S(11)-Cd(1)-S(11')	174.01(2)	O(1)-Cd(1)-O(1')	82.49(7)
O(1)-Cd(1)-S(11)	83.03(4)	O(1')-Cd(1)-S(11)	92.45(4)
N(11)-Cd(1)-N(11')	100.45(9)	N(11)-Cd(1)-O(1')	88.86(6)
N(11')-Cd(1)-O(1')	169.10(5)	N(11)-Cd(1)-S(11)	90.76(4)
N(11')-Cd(1)-S(11)	93.07(4)	N(11'')-C(11)-S(11)	178.94(17)
N(1)-O(1)-Cd(1)	114.50(10)	C(11'')-N(11)-Cd(1)	162.94(15)

Symmetry codes: (')  $-x, y, 3/2-z$ ; (')  $-x, -y, 1-z$ .

#### 4.5 [Cd(4-quinoline-N-oxide)(NCS)<sub>2</sub>]<sub>n</sub> (**5**)

3CdSO<sub>4</sub>·8H<sub>2</sub>O (0.26 g, 1.00 mmol), 4-quinoline-N-oxide (0.07 g, 0.50 mmol) and KSCN (0.19 g, 2.00 mmol) were dissolved in 45.00 mL distilled water at room temperature. Upon slow cooling to 4°C yellow crystals of **5** were separated after five days (yield: 0.11 g, 58%). *Anal.* Calc. for C<sub>11</sub>H<sub>7</sub>CdN<sub>3</sub>OS<sub>2</sub> (373.73 g/mol): C, 35.4; H, 1.9; N, 11.2. Found: C, 35.5; H, 1.9; N, 11.3%. Selected IR bands (ATR-IR, cm<sup>-1</sup>): 3113 (w), 3077 (w), ν<sub>CN</sub>: 2106 (sh), 2094 (vs), 1579 (m), 1513 (m), 1455 (w), 1392 (8m), 1270 (m), 1229 (m), 1209 (m), 1173 (m), 1142 (m), 1087 (m), 1053 (w), 1016 (w), 961 (w), 924 (w), 877 (m), 805 (s), 768 (s), ν<sub>CS</sub>: 723 (m), 563 (s), 543 (m), 496 (m), δ<sub>NCS</sub>: 456 (m).

Description of the crystal structure:

A section of the crystal structure of [Cd(4-quinoline-N-oxide)(NCS)<sub>2</sub>]<sub>n</sub> (**5**) is shown in Figure 23 and selected bond parameters are listed in Table 7. Cd(1) is six-coordinated by N(11''), S(11), N(21), S(21) of four μ<sub>(N,S)</sub> bridging isothiocyanato groups and by O(1) and O(1') of μ<sub>(O,O)</sub> bridging 4-quinoline-N-oxide molecules in *cis*-conformation. The bond distances within the distorted CdN<sub>2</sub>O<sub>2</sub>S<sub>2</sub> octahedron are: Cd-N/O from 2.256(2) to 2.3480(15) Å, Cd-S are 2.6455(7) and 2.6780(6) Å. The isothiocyanato groups form di-μ<sub>(N,S)</sub> double bridges to connect the Cd(II) centers to polymeric chains. These polymeric chains are further connected by the centrosymmetrically related μ<sub>(O,O)</sub> bridging 4-quinoline-N-oxide molecules to generate a "honeycomb"-like 2D system [38] extended along the *a*- and *b*-axis of the unit cell (Figure 24). Both of the two centrosymmetric and eight-membered Cd(NCS)<sub>2</sub>Cd rings adopt a "chair-like" arrangement ["chair angle" θ defined as acute angle between plane of the di-μ<sub>(N,S)</sub> thiocyanato bridges and the Cd/N/S plane is 42.7 and 48.2°, respectively]. The torsions angles are: Cd(1'')-N(11)...S(11)-Cd(1) = ± 78.9°, Cd(1)-N(21)...S(21\*)-Cd(1\*) = ± 82.7°. The four-membered Cd<sub>2</sub>O<sub>2</sub> rings formed by the μ<sub>(O,O)</sub> bridging 4-quinoline-N-oxide molecules are planar. The Cd(1)-O(1)-Cd(1') and O(1)-Cd(1)-O(1') bond angles are 107.36(6) and 72.64(6)°. The Cd-O(1)-N(1) bond angles are 123.41(12) and 125.14(12)°; the Cd-O(1)-N(1)-C(1) torsion angles are -73.0 and 81.3°. The 4-quinoline-N-oxide molecules and the Cd<sub>2</sub>O<sub>2</sub> rings form intra-planar angles of 87.0°. The intra-plane metal-metal distances are: Cd(1)...Cd(1') = 3.7582(5), Cd(1)...Cd(1'') = 5.6077(7), Cd(1)...Cd(1\*) = 5.4792(7) Å, whereas the shortest Cd...Cd inter-planar separation is 8.2376(11) Å.

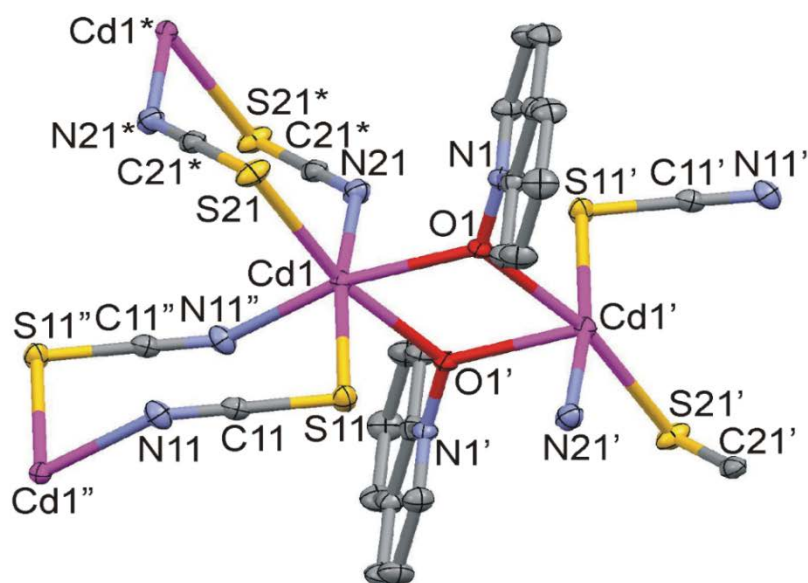


Figure 23: Perspective view of a section of [Cd(4-quinoline-N-oxide)(NCS)<sub>2</sub>]<sub>n</sub> (**5**)

Symmetry codes: (') -x, 1-y, -z; (") -1-x, -y, -z; (\*) -1-x, 1-y, -z.

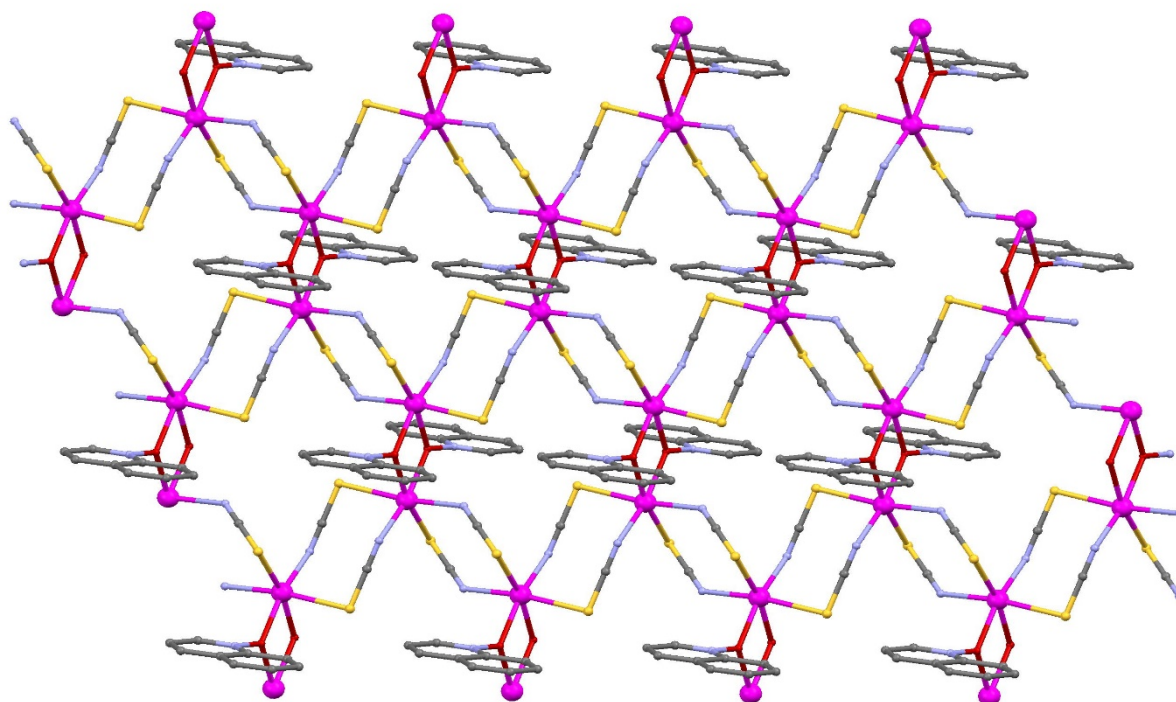


Figure 24: View onto the 2D polymeric layer of  $[Cd(4\text{-quinoline-N-oxide})(NCS)_2]_n$  (**5**)

Table 7: Selected bond parameters of  $[Cd(4\text{-quinoline-N-oxide})(NCS)_2]_n$  (**5**)

Cd(1)-N(11'')	2.256(2)	Cd(1)-O(1*)	2.3163(17)
Cd(1)-N(21)	2.3211(18)	Cd(1)-O(1')	2.3480(15)
Cd(1)-S(21)	2.6455(7)	Cd(1)-S(11)	2.6780(6)
O(1)-N(1)	1.342(2)	N(11)-C(11)	1.165(3)
N(21)-C(21*)	1.156(3)	C(21)-S(21)	1.660(2)
C(11)-S(11)	1.649(2)		
Cd(1)-O(1)-Cd(1')	107.36(6)	S(21)-Cd(1)-S(11)	96.13(2)
O(1)-Cd(1)-N(21)	92.05(6)	O(1)-Cd(1)-O(1')	72.64(6)
O(1)-Cd(1)-S(21)	95.44(4)	O(1)-Cd(1)-S(21)	167.64(4)
O(1)-Cd(1)-S(11)	84.17(4)	O(1')-Cd(1)-S(11)	86.11(4)
N(11'')-Cd(1)-O(1)	166.09(6)	N(11')-Cd(1)-N(21)	89.99(7)
N(11'')-Cd(1)-O(1')	93.89(6)	N(21)-Cd(1)-O(1')	84.36(6)
N(11'')-Cd(1)-S(21)	98.19(6)	N(21)-Cd(1)-S(21)	92.99(5)
N(11)-Cd(1)-S(11)	91.61(5)	N(21)-Cd(1)-S(11)	170.43(5)
N(11)-C(11)-S(11)	178.49(18)	N(21*)-C(21*)-S(21)	179.8(2)
N(1)-O(1)-Cd(1)	125.14(12)	N(1)-O(1)-Cd(1')	123.41(12)
C(11)-N(11)-Cd(1')	139.37(16)	C(11)-S(11)-Cd(1)	96.86(7)
C(21)-N(21)-Cd(1*)	137.56(17)	C(21)-S(21)-Cd(1)	92.68(8)

Symmetry codes: (') -x, 1-y, -z; (') -1-x, -y, -z; (\*) -1-x, 1-y, -z.

#### 4.6 [Cd(2,6-lutidine-N-oxide)(NCS)<sub>2</sub>]<sub>n</sub> (**6**)

3CdSO<sub>4</sub>·8H<sub>2</sub>O (0.52 g, 2.00 mmol), 2,6-dimethylpyridine-N-oxide (0.49 g, 4.00 mmol) and KSCN (0.39 g, 4.11 mmol) were dissolved in 25.50 mL distilled water at room temperature. After 1 week at room temperature yellow crystals appeared (yield: 0.53 g, 76%). *Anal.* Calc. for C<sub>9</sub>H<sub>9</sub>CdN<sub>3</sub>OS<sub>2</sub> (351.72 g/mol): C, 30.7; H, 2.6; N, 11.9. Found: C, 28.9; H, 2.9; N, 11.3%. Selected IR bands (ATR-IR, cm<sup>-1</sup>): ν<sub>CN</sub>: 2105 (vs), 1618 (w), 1581 (m), 1492 (m), 1387 (w), 1186 (s), 1102 (m), 1033 (w), 993 (w), 938 (w), 912 (w), 824 (s), 786 (s), 680 (m), 567 (w), 541 (w), 520 (m), 493 (w), δ<sub>NCS</sub>: 465 (m).

Description of the crystal structure:

A fragment of the crystal structure of [Cd(2,6-lutidine-N-oxide)(NCS)<sub>2</sub>]<sub>n</sub> (**6**) is shown in Figure 25 and selected bond parameters are listed in Table 8. The compound crystallizes in monoclinic space group C2c and the two cadmium(II) centers are located on two-fold-rotation axis. Each Cd(II) center has a distorted octahedral geometry, and is ligated by four μ<sub>(N,S)</sub> bridging isothiocyanato groups and two μ<sub>(O,O)</sub> bridging 2,6-lutidine-N-oxide molecules in *cis*-conformation. Along the *a*-axis a polymeric chain is formed, where the cadmium(II) centers are connected by di-μ<sub>(N,S)</sub> double bridges. Di-μ<sub>(O,O)</sub> bridging 2,6-lutidine-N-oxide molecules in addition connect the polymeric chains along the *b*-axis to generate a “honeycomb”-like layer [38] structure. The Cd-N/O bond distances are in the range from 2.278(7) to 2.349(5) Å; the Cd-S bond lengths are 2.669(2) and 2.687(2) Å. Eight-membered Cd(NCS)<sub>2</sub>Cd rings adopts a “chair-like” arrangement [“chair angle” θ defined as acute angle between plane of the di-μ<sub>(N,S)</sub> thiocyanato bridges and the Cd/N/S plane is 12.1 and 10.7°, for Cd(1) and Cd(2), respectively]. The torsions angles are: Cd(1)-N(21)...S(21)-Cd(2) = -37.6°, Cd(1)-S(11)...N(11)-Cd(2) = 40.2°. The four-membered Cd<sub>2</sub>O<sub>2</sub> rings formed by the μ<sub>(O,O)</sub> bridging 2,6-lutidine-N-oxide molecules have Cd(1)-O(1)-Cd(2), O(1)-Cd(1)-O(a) and O(1)-Cd(2)-O(a) bond angles of 111.0(2), 68.9(3) and 69.1(3)°. The Cd-O(1)-N(1) bond angles are 122.1(4) and 126.9(4)°; the Cd-O(1)-N(1)-C(1) torsion angle is 89.4 and -87.6° for Cd(1) and Cd(2), respectively. The 2,6-lutidine-N-oxide molecules and the Cd<sub>2</sub>O<sub>2</sub> rings form intra-planar angles of 88.8°. The Cd(1)...Cd(2) distances within the Cd<sub>2</sub>O<sub>2</sub> rings is 3.8663(11) Å, the Cd(1)...Cd(2) distances within the Cd(NCS)<sub>2</sub>Cd rings is 5.9410(8) Å, the shortest Cd...Cd inter-planar separation is 8.1278(14) Å

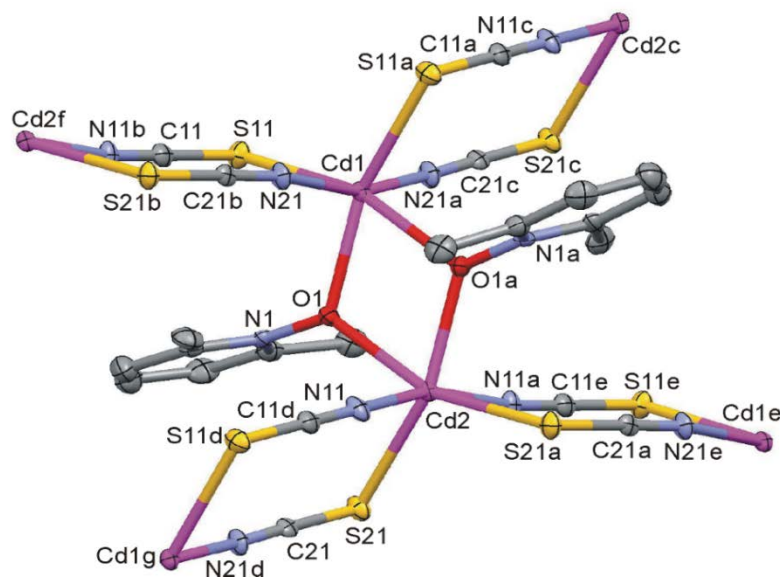


Figure 25: Perspective view of a section of [Cd(2,6-lutidine-N-oxide)(NCS)<sub>2</sub>]<sub>n</sub> (**6**)

Symmetry codes: (a) -x, y, 1/2-z; (b) 1/2-x, -1/2+y, 1/2-z; (c) -1/2+x, -1/2+y, z; (d) 1/2-x, 1/2+y, 1/2-z; (e) -1/2+x, 1/2+y, z; (f) 1/2+x, -1/2+y, z; (g) 1/2+x, -1/2+y, z.

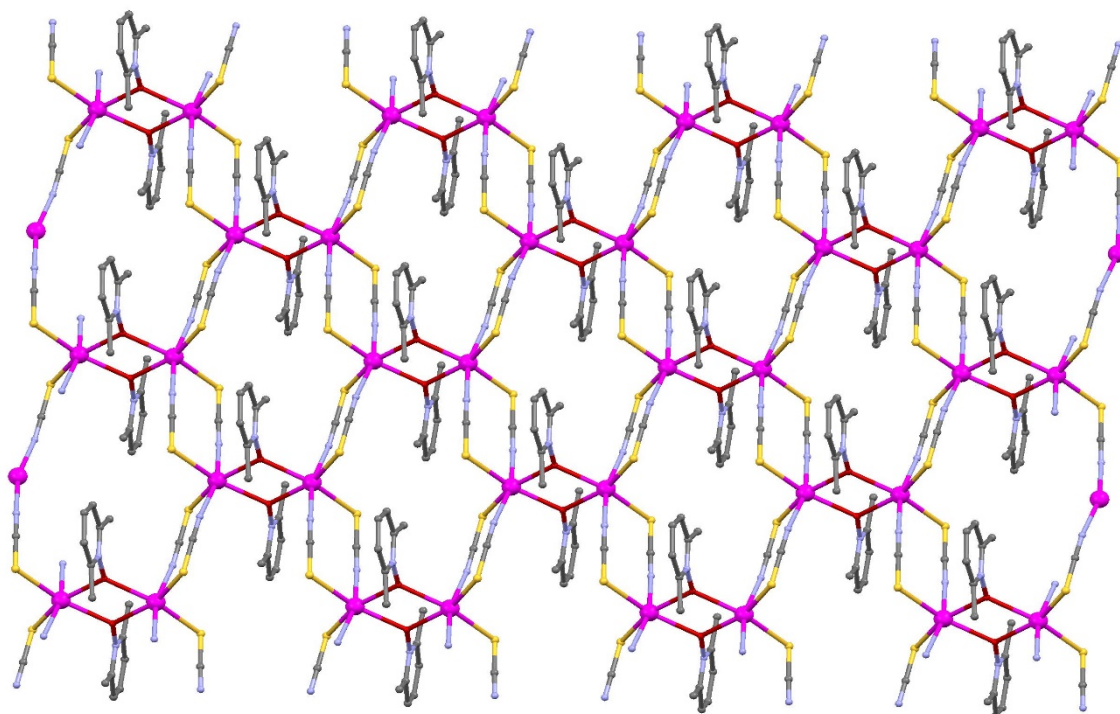


Figure 26: View onto the 2D polymeric layer of  $[Cd(2,6\text{-lutidine-N-oxide})(NCS)_2]_n$  (**6**)

Table 8: Selected bond parameters of  $[Cd(2,6\text{-lutidine-N-oxide})(NCS)_2]_n$  (**6**)

Cd(1)-N(21)	2.308(6)	Cd(1)-O(1)	2.349(5)
Cd(1)-S(11)	2.669(2)	Cd(2)-N(11)	2.278(7)
Cd(2)-O(1)	2.342(5)	Cd(2)-S(21)	2.687(2)
O(1)-N(1)	1.353(8)	N(11)-C(11)	1.157(10)
C(11)-S(11)	1.644(8)	C(21)-N(21b)	1.147(10)
C(21)-S(21)	1.656(8)		
Cd(2)-O(1)-Cd(1)	111.0(2)	S(11)-Cd(1)-S(11a)	111.13(10)
S(21)-Cd(2)-S(21a)	113.35(10)	O(1)-Cd(1)-O(1a)	68.9(3)
O(1a)-Cd(1)-S(11a)	157.67(14)	O(1a)-Cd(1)-S(11a)	90.44(14)
O(1)-Cd(2)-O(1)	69.1(3)	O(1)-Cd(2)-S(21)	156.62(14)
N(21)-Cd(1)-N(21)	164.0(4)	N(21)-Cd(1)-O(1)	98.2(2)
N(21)-Cd(1)-O(1)	95.0(2)	N(21a)-Cd(1)-S(11a)	91.75(18)
N(21a)-Cd(1)-S(11a)	79.18(18)	N(11)-Cd(2)-O(1)	98.9(2)
N(11)-Cd(2)-O(1)	94.0(2)	N(11a)-Cd(2)-S(21a)	91.08(17)
N(11b)-C(11)-S(11)	179.4(8)	N(21)-C(21)-S(21d)	178.5(7)
N(1)-O(1)-Cd(2)	126.9(4)	N(1)-O(1)-Cd(1)	122.1(4)
C(11d)-N(11)-Cd(2)	164.7(6)	C(11)-S(11)-Cd(1)	101.6(3)
C(21b)-N(21)-Cd(1)	162.1(6)	C(21)-S(21)-Cd(2)	101.2(3)

Symmetry codes: (a)  $-x, y, 1/2-z$ , (b)  $1/2-x, -1/2+y, 1/2-z$ ; (c)  $-1/2+x, -1/2+y, z$ ; (d)  $1/2-x, 1/2+y, 1/2-z$ .

#### 4.7 $[\text{Cd}(\text{N}_3)_2(\text{H}_2\text{O})_2]_n(4\text{-quinoline-N-oxide})_{2n}$ (**7**)

$3\text{CdSO}_4 \cdot 8\text{H}_2\text{O}$  (0.27 g, 1.06 mmol), 4-quinoline-N-oxide (0.06 g, 0.40 mmol) and  $\text{NaN}_3$  (0.12 g, 1.85 mmol) were dissolved in 17.00 mL aqueous hydrazoic acid at  $40^\circ\text{C}$ . After slow cooling to room temperature yellow crystals were separated within 10 days. Selected IR bands (ATR-IR,  $\text{cm}^{-1}$ ):  $\nu_{\text{OH}}$ : 3099 (w), 3071 (w), 2068 (sh),  $\nu_{\text{CN}}$ : 2027 (vs), 1831 (w), 1684 (w), 1575 (m), 1446 (w), 1396 (m), 1328 (m), 1266 (m), 1230 (s), 1208 (s), 1179 (m), 1138 (s), 1092 (m), 1058 (m), 879 (s), 798 (s), 774 (s), 736 (m), 647 (m), 611 (m), 579 (m), 552 (s), 495 (m),  $\delta_{\text{NCS}}$ : 461 (w), 419 (m).

Description of the crystal structure:

Preliminary crystal structure investigation reveals that  $[\text{Cd}(\text{N}_3)_2(\text{H}_2\text{O})_2]_n(4\text{-quinoline-N-oxide})_{2n}$  (**7**) is isostructural to the crystal structure of  $[\text{Mn}(\text{N}_3)_2(\text{H}_2\text{O})_2]_n(3\text{-picoline-N-oxide})_{2n}$  (**26**) complex.

A perspective view of together with the atom numbering scheme of the preliminary crystal structure of  $[\text{Cd}(\text{N}_3)_2(\text{H}_2\text{O})_2]_n(4\text{-quinoline-N-oxide})_{2n}$  (**7**) is shown in Figure 27.

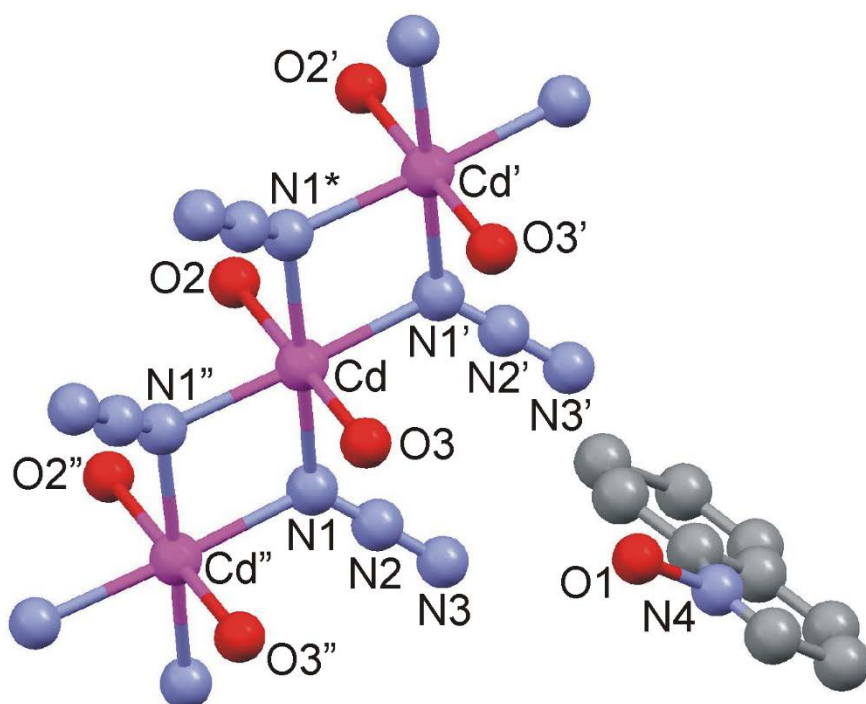


Figure 27: Perspective view of  $[\text{Cd}(\text{N}_3)_2(\text{H}_2\text{O})_2]_n(4\text{-quinoline-N-oxide})_{2n}$  (**7**)

#### 4.8 [Cd(2,6-lutidine-N-oxide)(N<sub>3</sub>)<sub>2</sub>]<sub>n</sub> (**8**)

Compound (**8**) was obtained by mixing 3CdSO<sub>4</sub>·8H<sub>2</sub>O (0.52 g, 1.96 mmol), 2,6-dimethylpyridine-N-oxide (0.31 g, 2.21 mmol) and NaN<sub>3</sub> (0.27 g, 4.15 mmol) in 25.00 mL distilled water at room temperature. Upon slow cooling to 4°C yellow crystals of (**8**) were separated after 2 weeks (yield: 0.32 g, 50%). *Anal.* Calc. for C<sub>7</sub>H<sub>9</sub>CdN<sub>7</sub>O (319.52 g/mol): C, 26.3; H, 2.8; N, 30.7. Found: C, 26.1; H, 2.8; N, 30.8%. Selected IR bands (ATR-IR, cm<sup>-1</sup>): ν<sub>a</sub>: 2086 (vs), 1618 (w), 1574 (w), 1491 (m), 1457 (m), 1419 (m), 1376 (w), ν<sub>s</sub>: 1331 (w), 1304 (m), 1280 (w), 1220 (s), 1162 (w), 1097 (w), 1029 (w), 993 (w), 906 (w), 835 (s), 778 (s), 689 (w), δ<sub>N<sub>3</sub></sub>: 650 (w), 626 (m), 599 (w), 571 (w), 524 (m).

Description of the crystal structure:

The title complex [Cd(2,6-lutidine-N-oxide)(N<sub>3</sub>)<sub>2</sub>]<sub>n</sub> (**8**) crystallizes in the orthorhombic space group Pna21. A fragment of the crystal structure is shown in Figure 28 and selected bond parameters are listed in Table 9. Each cadmium(II) center is octahedrally coordinated by N atoms of five bridging azido groups and O(1) of a terminal 2,6-lutidine-N-oxide molecule. The azido group N(11)-N(12)-N(13) acts as μ<sub>(1,1)</sub> bridge and the azido group N(21)-N(22)-N(23) acts as μ<sub>(1,1,1)</sub> bridge to generate polymeric 1D double chain oriented along the c-axis of the unit cell. The 1D double chain may be described as “ladder of defective cubane” with common faces. The seven corners of each “cubane” unit is built up by three cadmium(II) centers, N(21) atoms of three μ<sub>(1,1,1)</sub> bridges and N(11) atoms of two μ<sub>(1,1)</sub> bridges. The Cd(1)-N bond distances are in the range from 2.296(6) to 2.432(3) Å, the Cd(1)-O(1) bond distance is 2.256(3) Å. The Cd-N(11)-Cd bond angle is 104.18(10)°, the Cd-N(21)-Cd bond angles are 99.82(10), 100.6(2) and 100.7(2)°. Cd-N-N bond angles vary from 109.5(2) to 127.5(6)°. The azido groups have N-N-N bond angles of 178.9(7) and 178.3(6)°. The azido groups are asymmetric with Δ(N-N) of 0.064 and 0.079 Å, for the μ<sub>(1,1)</sub> and μ<sub>(1,1,1)</sub> bridges, respectively. The intra-chain Cd...Cd distances are 3.6691(18) and 3.7180(5) Å, whereas the shortest Cd...Cd inter-chain separation is 6.3834(8) Å. The terminal 2,6-lutidine-N-oxide molecules have a Cd(1)-O(1)-N(1) bond angle of 131.4(3)° and a Cd(1)-O(1)-N(1)-C(1) torsions angle 115.8°. Their pyridine rings form π-π stacking interactions along the c-axis [3.6691(3) Å] (Figure 29).

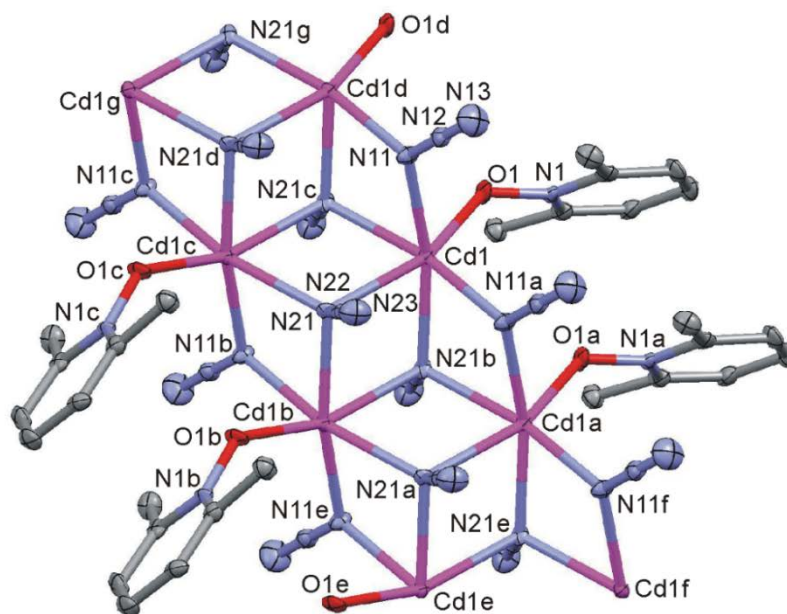


Figure 28: Perspective view of a section of [Cd(2,6-lutidine-N-oxide)(N<sub>3</sub>)<sub>2</sub>]<sub>n</sub> (**8**)

Symmetry codes: (a) x, y, 1+z; (b) 2-x, -y, 1/2+z; (c) 2-x, -y, -1/2+z; (d) x, y, -1+z; (e) 2-x, -y, 3/2+z; (f) x, y, 2+z; (g) 2-x, -y, -5/2+z.

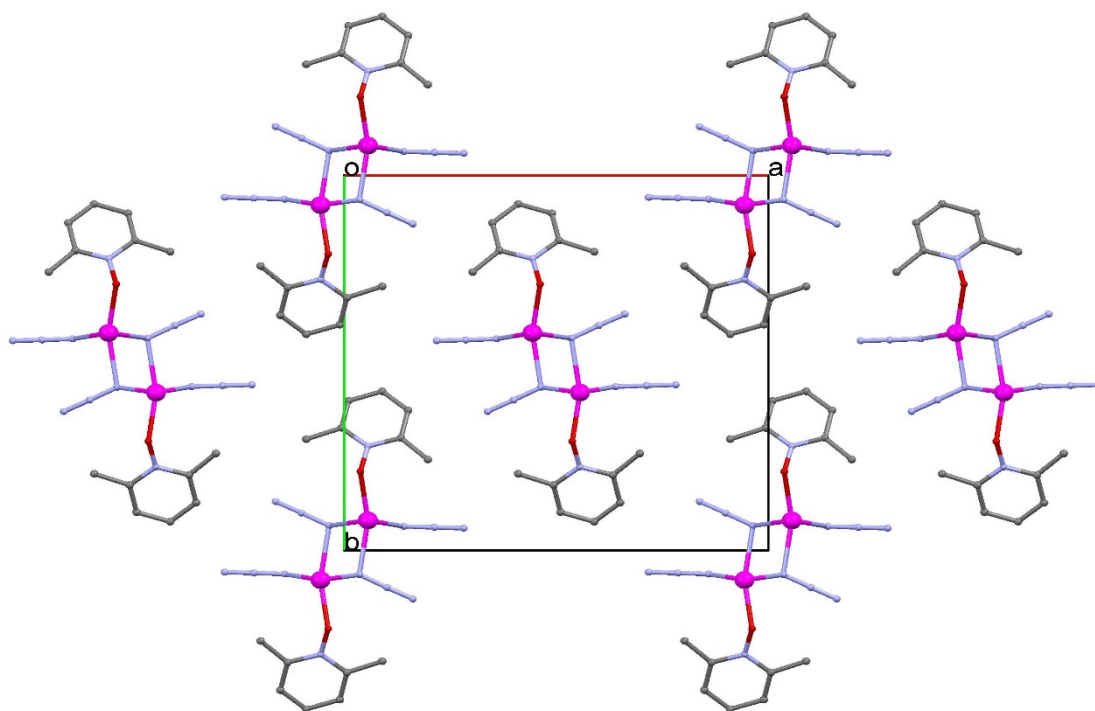


Figure 29: Packing plot of  $[\text{Cd}(2,6\text{-lutidine-}N\text{-oxide})(\text{N}_3)_2]_n$  (**8**) (along the *c*-axis)

Table 9: Selected bond parameters of  $[\text{Cd}(2,6\text{-lutidine-}N\text{-oxide})(\text{N}_3)_2]_n$  (**8**)

Cd(1)-O(1)	2.256(3)	Cd(1)-N(11a)	2.296(6)
Cd(1)-N(11)	2.354(6)	Cd(1)-N(21c)	2.400(7)
Cd(1)-N(21)	2.396(7)	Cd(1)-N(21)	2.432(3)
O(1)-N(1)	1.338(5)	N(11)-N(12)	1.211(4)
N(11)-Cd(1d)	2.296(6)	N(12)-N(13)	1.147(4)
N(21)-N(22)	1.225(4)	N(22)-N(23)	1.146(4)
Cd(1a)-N(11)-Cd(1)	104.18(10)	Cd(1b)-N(21)-Cd(1c)	99.82(10)
Cd(1b)-N(21)-Cd(1)	100.6(2)	Cd(1c)-N(21)-Cd(1)	100.7(2)
O(1)-Cd(1)-N(11a)	112.58(10)	O(1)-Cd(1)-N(11)	89.49(11)
O(1)-Cd(1)-N(21c)	79.69(11)	O(1)-Cd(1)-N(21b)	101.39(10)
O(1)-Cd(1)-N(21)	158.79(16)	N(11)-Cd(1)-N(21b)	167.68(12)
N(11)-Cd(1)-N(21c)	76.1(2)	N(11a)-Cd(1)-N(21b)	77.3(2)
N(11)-Cd(1)-N(21b)	167.61(11)	N(11a)-Cd(1)-N(21)	88.38(18)
N(11)-Cd(1)-N(21c)	88.33(17)	N(21c)-Cd(1)-N(21)	79.31(14)
N(21b)-Cd(1)-N(21)	79.38(16)	N(12)-N(11)-Cd(1)	127.5(6)
N(12)-N(11)-Cd(1d)	127.3(5)	N(13)-N(12)-N(11)	178.9(7)
N(22)-N(21)-Cd(1b)	116.1(5)	N(22)-N(21)-Cd(1c)	126.4(5)
N(22)-N(21)-Cd(1)	109.5(2)	N(23)-N(22)-N(21)	178.3(6)
N(1)-O(1)-Cd(1)	131.4(3)		

Symmetry codes: (a)  $x, y, 1+z$ ; (b)  $2-x, -y, 1/2+z$ ; (c)  $2-x, -y, -1/2+z$ ; (d)  $x, y, -1+z$ .



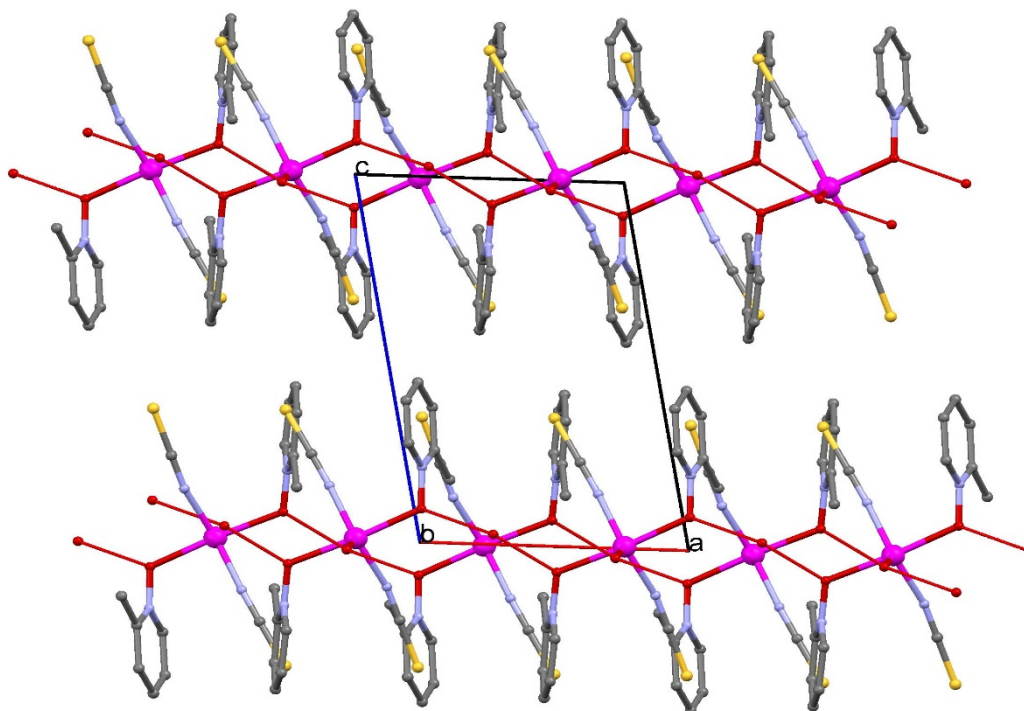


Figure 31: Packing plot of  $[\text{Zn}(\text{2-picoline-N-oxide})_2(\text{NCS})_2(\text{H}_2\text{O})]_n$  (**9**)

Table 10: Selected bond parameters of  $[\text{Zn}(\text{2-picoline-N-oxide})_2(\text{NCS})_2(\text{H}_2\text{O})]_n$  (**9**)

Zn(1)-N(21)	1.9671(15)	Zn(1)-N(11)	1.9712(15)
Zn(1)-O(3)	1.9888(14)	Zn(1)-O(2)	2.1414(12)
Zn(1)-O(1)	2.1551(12)	O(1)-N(1)	1.3464(18)
O(2)-N(2)	1.3466(18)	N(11)-C(11)	1.161(2)
N(21)-C(21)	1.158(2)	C(11)-S(11)	1.6255(18)
C(21)-S(21)	1.6269(18)		
O(3)-Zn(1)-O(2)	91.69(6)	O(2)-Zn(1)-O(1)	176.03(4)
O(3)-Zn(1)-O(1)	90.02(6)	N(21)-Zn(1)-N(11)	135.38(7)
N(21)-Zn(1)-O(3)	108.01(6)	N(11)-Zn(1)-O(3)	116.46(6)
N(21)-Zn(1)-O(2)	90.89(6)	N(11)-Zn(1)-O(2)	91.23(5)
N(21)-Zn(1)-O(1)	91.99(5)	N(11)-Zn(1)-O(1)	84.80(5)
N(11)-C(11)-S(11)	179.39(16)	N(21)-C(21)-S(21)	179.60(18)
N(1)-O(1)-Zn(1)	118.70(9)	N(2)-O(2)-Zn(1)	115.80(10)
C(11)-N(11)-Zn(1)	170.38(15)	C(21)-N(21)-Zn(1)	164.11(15)

## 5.2 $[\text{Zn}(\text{4-quinoline-N-oxide})_6]^{2+}[\text{Zn}(\text{NCS})_4]^{2-}$ (**10**)

Compound (**10**) was obtained by mixing  $\text{ZnSO}_4 \cdot 7\text{H}_2\text{O}$  (0.58 g, 2.00 mmol), 4-quinoline-N-oxide (0.28 g, 2.00 mmol) and KSCN (0.38 g, 4.00 mmol) in 18.00 mL distilled water at 60°C. Upon slow cooling to room temperature colorless crystals of (**10**) were separated after four days (yield: 1.55 g, 63%). *Anal.* Calc. for  $\text{C}_{54}\text{H}_{42}\text{N}_6\text{O}_6\text{Zn}$ ,  $\text{C}_4\text{N}_4\text{S}_4\text{Zn}$  (1234.08 g/mol): C, 56.5; H, 3.4; N, 11.3. Found: C, 56.4; H, 3.4; N, 11.4%. Selected IR bands (ATR-IR,  $\text{cm}^{-1}$ ): 3062 (w), 3018 (w), 2361 (w), 2322 (w),  $\nu_{\text{CN}}$ : 2056 (vs), 1577 (m), 1542 (w), 1515 (m), 1457 (w), 1399 (m), 1314 (w), 1265 (m), 1229 (m), 1207 (m), 1179 (m), 1137 (m), 1090 (s), 1046 (w), 947 (w), 955 (w), 880 (m), 801 (vs), 762 (vs), 624 (w), 563 (s),  $\delta_{\text{NCS}}$ : 481 (m), 425 (w).

Description of the structure:

Crystal structure investigation reveals that the complex exists of  $[\text{Zn}(\text{4-quinoline-N-oxide})_6]^{2+}$  complex cations and  $[\text{Zn}(\text{NCS})_4]^{2-}$  complex anions. The title complex (**10**) crystallizes in the trigonal space group  $R\bar{3}c1$  (no. 164) with  $Z = 4$ . Zn(1) and Zn(2) of complex cations  $[\text{Zn}(\text{4-quinoline-N-oxide})_6]^{2+}$  are located on special positions 1a and 1b, respectively, with site symmetry  $\bar{3}m$ , Zn(3), N(3), C(19), S(3) of  $[\text{Zn}(\text{NCS})_4]^{2-}$  complex anion are located on special position 2d with site symmetry  $3m$ . Zn(1) and Zn(2), respectively, are octahedrally coordinated by O atoms of six 4-quinoline-N-oxide molecules [ $\text{Zn}(1)\text{-O}(1) = 2.1136(10)$ ,  $\text{Zn}(2)\text{-O}(2) = 2.1213(10)$  Å]. Zn(3) is tetrahedrally coordinated by four terminal isothiocyanato groups [ $\text{Zn}(3)\text{-N}(3) = 1.973(3)$ ,  $\text{Zn}(3)\text{-N}(4) = 1.9534(15)$  Å]. The N-Zn(3)-N, Zn(3)-N-C, N-C-S bond angles are  $108.45(5)$  and  $110.47(5)^\circ$ , 180 and  $172.10(15)^\circ$ , 180 and  $179.42(15)^\circ$ , respectively. The terminal 4-quinoline-N-oxide molecules have Zn-O-N bond angles of  $126.59(8)$  and  $126.52(8)^\circ$ . The Zn(1)-O(1)-N(1)-C(1) and Zn(2)-O(2)-N(2)-C(10) torsion angles are  $-44.8$  and  $49.3^\circ$ , respectively.

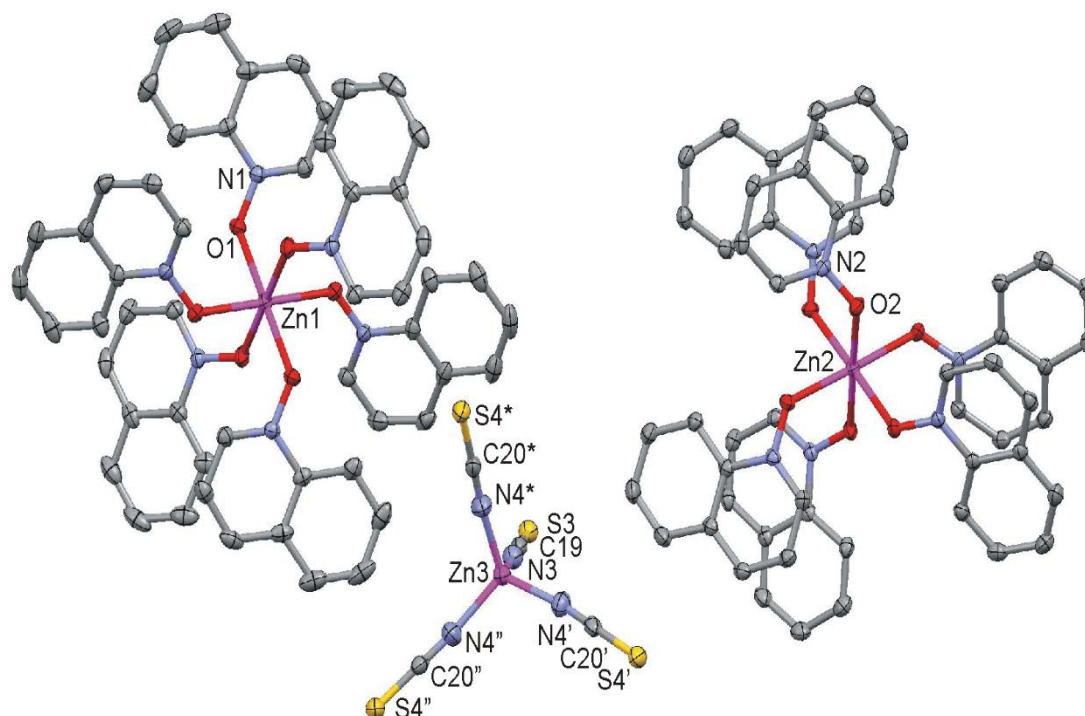


Figure 32: Perspective view of  $[\text{Zn}(\text{4-quinoline-N-oxide})_6]^{2+}[\text{Zn}(\text{NCS})_4]^{2-}$  (**10**)

Symmetry codes: (') 1-y, x-y, z; (") 1-x+y, 1-x, z.

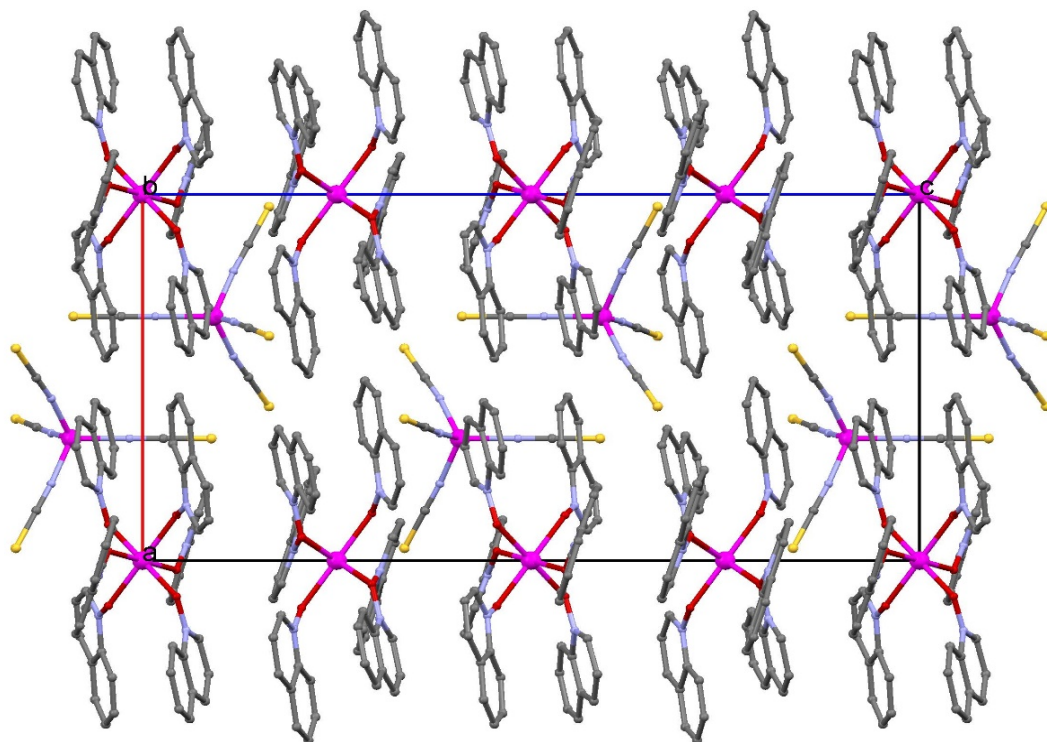


Figure 33: Packing view of  $[Zn(4\text{-quinoline-N-oxide})_6]^{2+}[Zn(NCS)_4]^{2-}$  (**10**) (along *b*-axis)

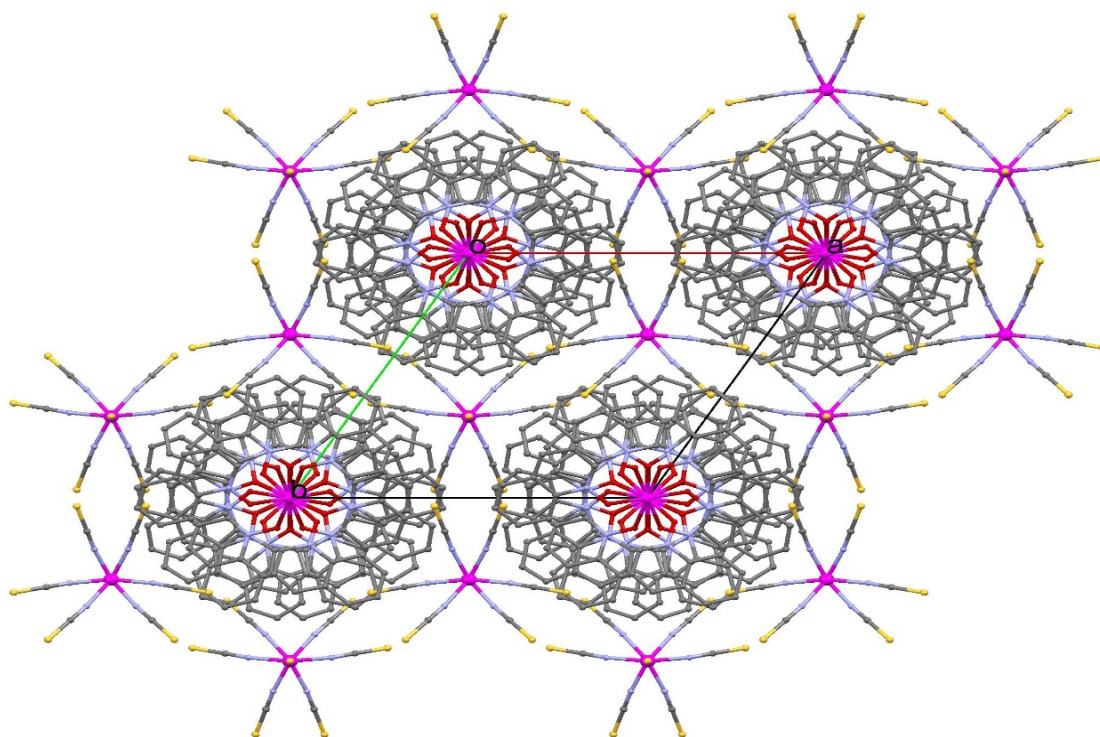


Figure 34: Packing view of  $[Zn(4\text{-quinoline-N-oxide})_6]^{2+}[Zn(NCS)_4]^{2-}$  (**10**) (along *c*-axis)

Table 11: Selected bond parameters of  $[\text{Zn}(\text{4-quinoline-N-oxide})_6]^{2+}[\text{Zn}(\text{NCS})_4]^{2-}$  (10)

Zn(1)-O(1)	2.1136(10)	Zn(2)-O(2)	2.1213(10)
Zn(3)-N(3)	1.973(3)	O(1)-N(1)	1.3342(15)
O(2)-N(2)	1.3323(15)	N(3)-C(19)	1.154(4)
C(19)-S(3)	1.629(4)	N(4)-C(20)	1.157(2)
C(20)-S(4)	1.6208(17)		
O(1)-Zn(1)-O(1*)	92.90(4)	O(1)-Zn(1)-O(1)	87.10(4)
O(1)-Zn(1)-O(1)	180	O(2)-Zn(2)-O(2+)	91.38(4)
O(2)-Zn(2)-O(2)	178.80(5)	O(2)-Zn(2)-O(2)	87.76(6)
N(1)-O(1)-Zn(1)	126.59(8)	N(2)-O(2)-Zn(2)	126.52(8)
N(3)-C(19)-S(3)	180	N(4')-Zn(3)-N(4'')	108.45(5)
N(4)-Zn(3)-N(3)	110.47(5)	N(4)-C(20)-S(4)	179.42(15)
C(19)-N(3)-Zn(3)	180	C(20)-N(4)-Zn(3)	172.10(15)

Symmetry codes: (') 1-y, x-y, z; (") 1-x+y, 1-x, z; (\*) -y, x-y, z; (+) 1-y, -1+x-y, z.

### 5.3 [Zn(4-cyanopyridine-N-oxide)<sub>2</sub>(NCS)<sub>2</sub>(H<sub>2</sub>O)]<sub>2</sub> (**11**)

ZnSO<sub>4</sub>·7H<sub>2</sub>O (2.59 g, 9.00 mmol), 4-cyanopyridine-N-oxide (0.36 g, 3.00 mmol) and KSCN (1.75 g, 18.00 mmol) were dissolved in 18.00 mL distilled water at 50°C. Upon slow cooling to room temperature colorless crystals of (**11**) were separated after two weeks (yield: 1.50 g, 57%). *Anal. Calc.* for C<sub>14</sub>H<sub>10</sub>N<sub>6</sub>O<sub>3</sub>S<sub>2</sub>Zn (439.79 g/mol): C, 38.2; H, 2.3; N, 19.1. Found: C, 37.8; H, 2.2; N, 19.0%. Selected IR bands (ATR-IR, cm<sup>-1</sup>): ν<sub>OH</sub>: 3334 (m,br), ν<sub>CN</sub>: 2079 (vs), 1643 (m), 1553 (w), 1480 (s), 1436 (m), 1219 (s), 1171 (s), 1100 (m), 970 (w), 851 (vs), 725(s), 668 (w), 586 (w), 553 (m), 475 (m), δ<sub>NCS</sub>: 455 (m).

Description of the crystal structure:

The crystal structure of (**11**) (perspective view is shown in Figure 35 and selected bond lengths and bond angles are summarized in Table 12) consists of mononuclear and neutral Zn(II) complexes. Zn(1) is penta-coordinated by N(11) and N(21) of two terminal isothiocyanato anions, by O(1) and O(2) of two neutral 4-cyanopyridine-N-oxide molecules, and O(3) of aqua ligand. The ZnN<sub>2</sub>O<sub>3</sub> polyhedron may be described as a distorted square pyramid (SP) with a τ value of 0.28 [36]. The basal positions are occupied by N(11), N(21), O(1) and O(2) [Zn-N/O from 1.965(3) to 2.161(3) Å] and the apical position by O(3) [Zn(1)-O(3) = 2.088(3) Å]. The Zn(II) center deviates by 0.215 Å from the basal N<sub>2</sub>O<sub>2</sub> plane. The bond parameters of terminal N-coordinated NCS<sup>-</sup> anions are: Zn(1)-N-C = 171.7(3) and 170.5(3)°, N-C-S = 177.6(3) and 177.8(3)°; N-C = 1.171(5) and 1.168(5) Å, C-S = 1.619(4) and 1.615(4) Å. The shortest metal-metal separation is 5.1651(8) Å. The 4-cyanopyridine-N-oxide molecules form Zn-O-N bond angles of 113.89(19) and 114.86(19)°. The torsion angles Zn(1)-O(1)-N(1)-C(7) and Zn(1)-O(2)-N(2)-C(8) are 92.2 and 90.2°, respectively. The aqua ligand forms hydrogen bonds of type O-H...O to O atoms of 4-cyanopyridine -N-oxide molecules to generate a supramolecular 1D system oriented along the a-axis of the unit cell (Figure 36) [O(3)...O(1')(-x,1-y,1-z) = 2.833(4) Å, O(3)-H(31)...O(1') = 176(3)°; O(3)...O(2'')(1-x,1-y,1-z) = 2.846(4) Å, O(3)-H(32)...O(2'') = 172(3)°].

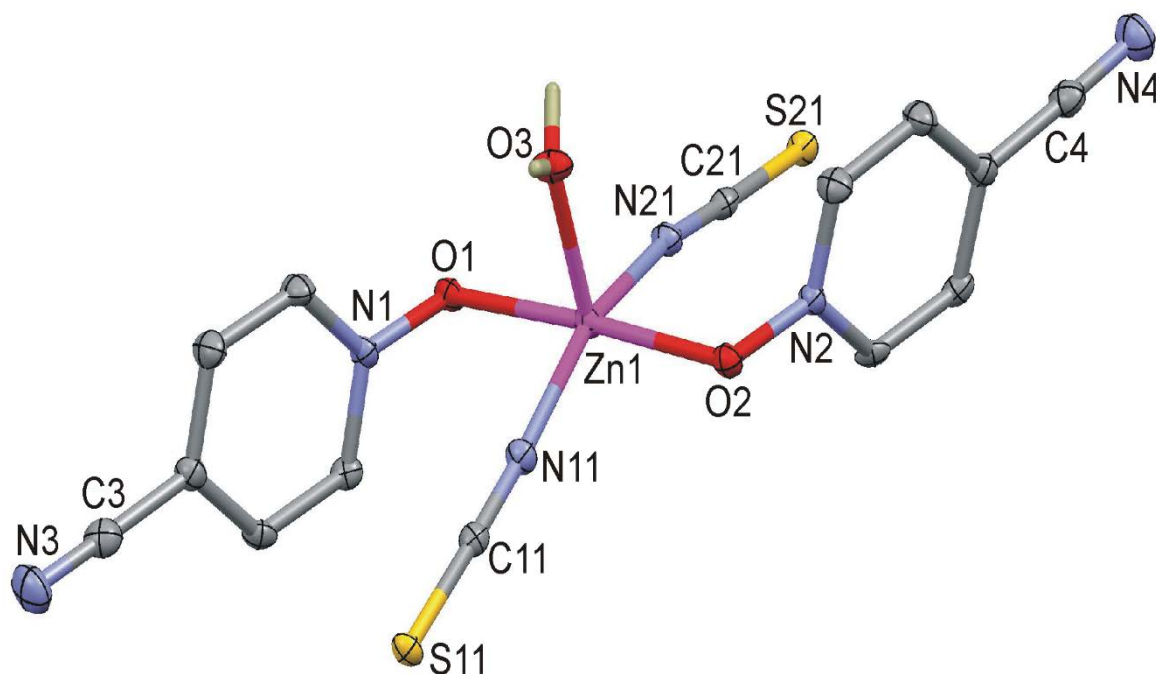


Figure 35: Perspective view of [Zn(4-cyanopyridine-N-oxide)<sub>2</sub>(NCS)<sub>2</sub>(H<sub>2</sub>O)]<sub>2</sub> (**11**)

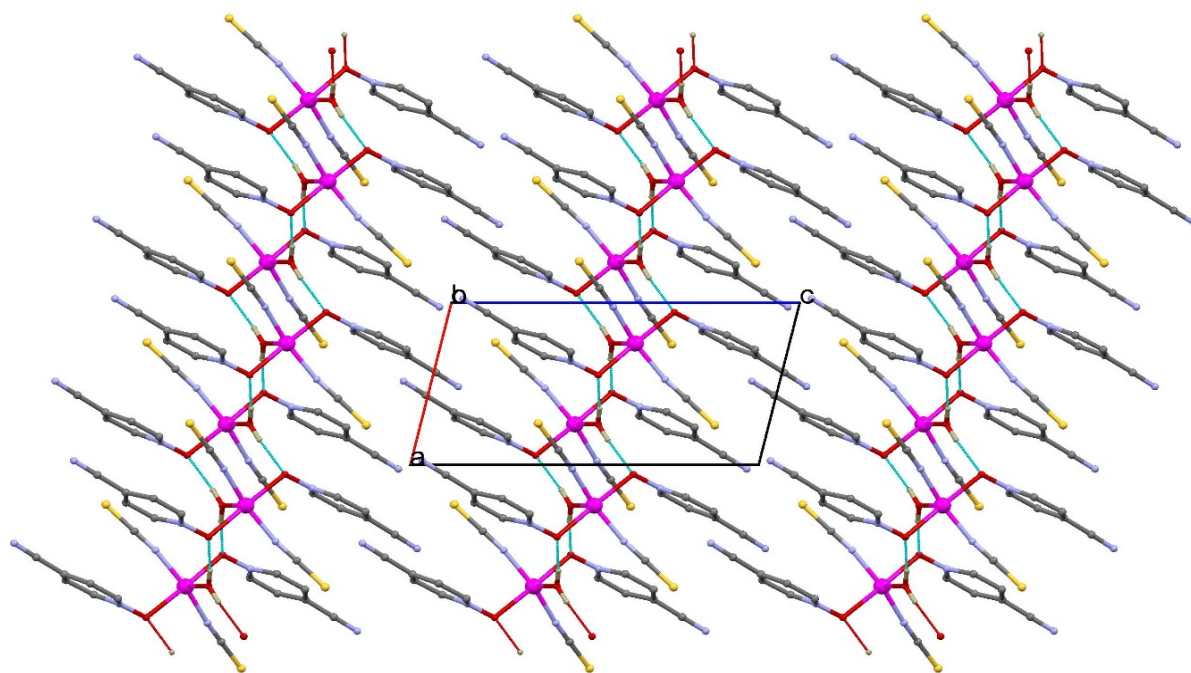


Figure 36: Packing plot of  $[\text{Zn}(\text{4-cyanopyridine-N-oxide})_2(\text{NCS})_2(\text{H}_2\text{O})]_2$  (**11**) (along *b*-axis)

Table 12: Selected bond parameters of  $[\text{Zn}(\text{4-cyanopyridine-N-oxide})_2(\text{NCS})_2(\text{H}_2\text{O})]_2$  (**11**)

Zn(1)-N(11)	1.965(3)	Zn(1)-N(21)	1.968(3)
Zn(1)-O(3)	2.088(3)	Zn(1)-O(2)	2.155(2)
Zn(1)-O(1)	2.161(3)	N(11)-C(11)	1.171(5)
C(11)-S(11)	1.615(4)	N(21)-C(21)	1.168(5)
C(21)-S(21)	1.619(4)	O(1)-N(1)	1.331(4)
O(2)-N(2)	1.333(4)		
N(11)-Zn(1)-N(21)	159.06(13)	N(11)-Zn(1)-O(3)	100.64(12)
N(21)-Zn(1)-O(3)	100.30(12)	N(11)-Zn(1)-O(2)	86.41(11)
N(21)-Zn(1)-O(2)	93.19(11)	N(11)-Zn(1)-O(1)	92.15(11)
N(21)-Zn(1)-O(1)	86.87(11)	N(11)-C(11)-S(11)	177.6(3)
N(21)-C(21)-S(21)	177.8(3)	N(1)-O(1)-Zn(1)	114.86(19)
N(2)-O(2)-Zn(1)	113.89(19)	O(3)-Zn(1)-O(2)	92.02(10)
O(3)-Zn(1)-O(1)	91.79(10)	O(2)-Zn(1)-O(1)	176.12(9)
C(11)-N(11)-Zn(1)	171.7(3)	C(21)-N(21)-Zn(1)	170.5(3)

#### 5.4 [Zn(2,6-lutidine-N-oxide)<sub>2</sub>(NCS)<sub>2</sub>] (**12**)

ZnSO<sub>4</sub>·7H<sub>2</sub>O (2.59 g, 9.00 mmol), 2,6-dimethylpyridine-N-oxide (0.41 g, 3.32 mmol) and KSCN (1.75 g, 18.00 mmol) were dissolved in 28.00 mL distilled water at room temperature. After 11 days at room temperature colorless crystals appeared (yield: 1.414 g, 55%). *Anal.* Calc. for C<sub>16</sub>H<sub>18</sub>N<sub>4</sub>O<sub>2</sub>S<sub>2</sub>Zn (427.85 g/mol): C, 38.2; H, 2.3; N, 19.1. Found: C, 43.5; H, 4.1; N, 12.8%. Selected IR bands (ATR-IR, cm<sup>-1</sup>): 3383 (m,br), 2362 (w), ν<sub>CN</sub>: 2073 (s), 2044 (vs), 1617 (m), 1577 (m), 1519 (w), 1492 (s), 1455 (s), 1420 (m), 1377 (m), 1277 (w), 1197 (s), 1163 (m), 1091 (m), 1034 (m), 992 (m), 963 (w), 922 (w), ν<sub>CS</sub>: 829 (s), 785 (s), 683 (m), 616 (w), 571 (w), 548 (m), 524 (s), δ<sub>NCS</sub>: 482 (m).

Description of the crystal structure:

The crystal structure of (**12**) (perspective view is shown in Figure 37 and selected bond lengths and bond angles are summarized in Table 13) consists of mononuclear and neutral Zn(II) complexes. Zn(1) is tetrahedrally coordinated by N(11) and N(21) of two terminal isothiocyanato anions, further by O(1) and O(2) of two neutral 2,6-lutidine-N-oxide molecules. The Zn(1)-N/O bond distances are in the range from 1.947(2) to 1.9650(16) Å, and the bond angles within the ZnN<sub>2</sub>O<sub>2</sub> tetrahedron vary from 105.20(7) to 112.94(8)°. The bond parameters of terminal N-coordinated NCS<sup>-</sup> anions are: Zn(1)-N-C = 151.32(18) and 171.0(2)°, N-C-S = 177.8(2) and 178.3(2)°; N-C = 1.159(3) and 1.166(3) Å, C-S = 1.612(3) and 1.614(3) Å. The shortest metal-metal separation is 7.6066(6) Å. The 2,6-lutidine-N-oxide molecules form Zn-O-N bond angles of 114.92(12) and 115.29(12)°.

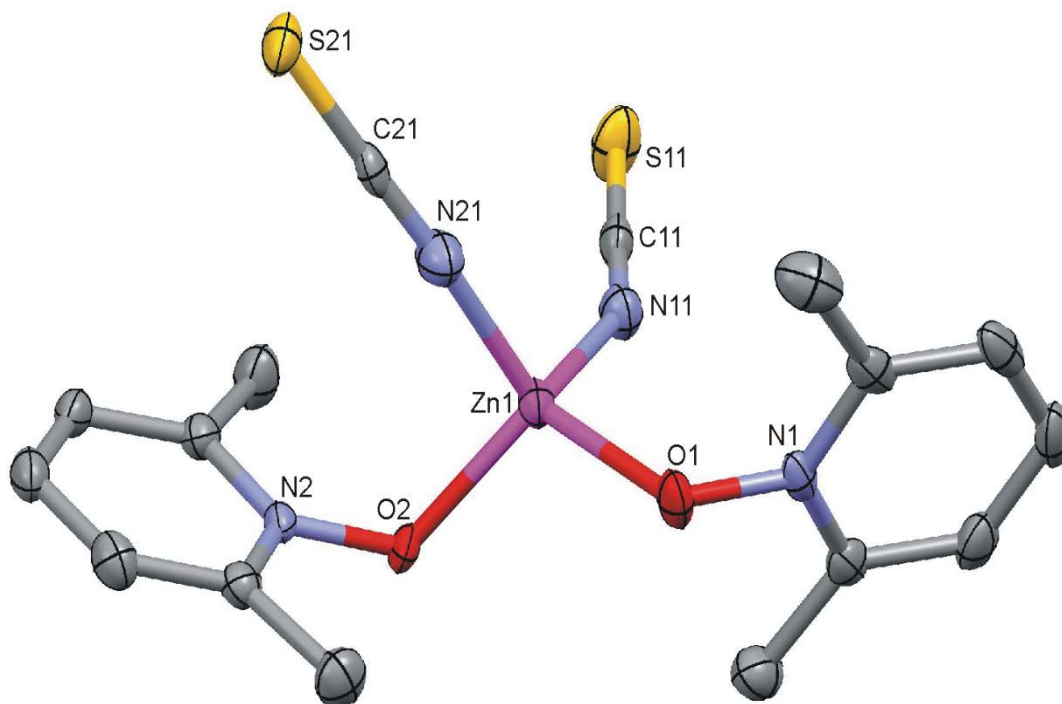


Figure 37: Perspective view of [Zn(2,6-lutidine-N-oxide)<sub>2</sub>(NCS)<sub>2</sub>] (**12**)

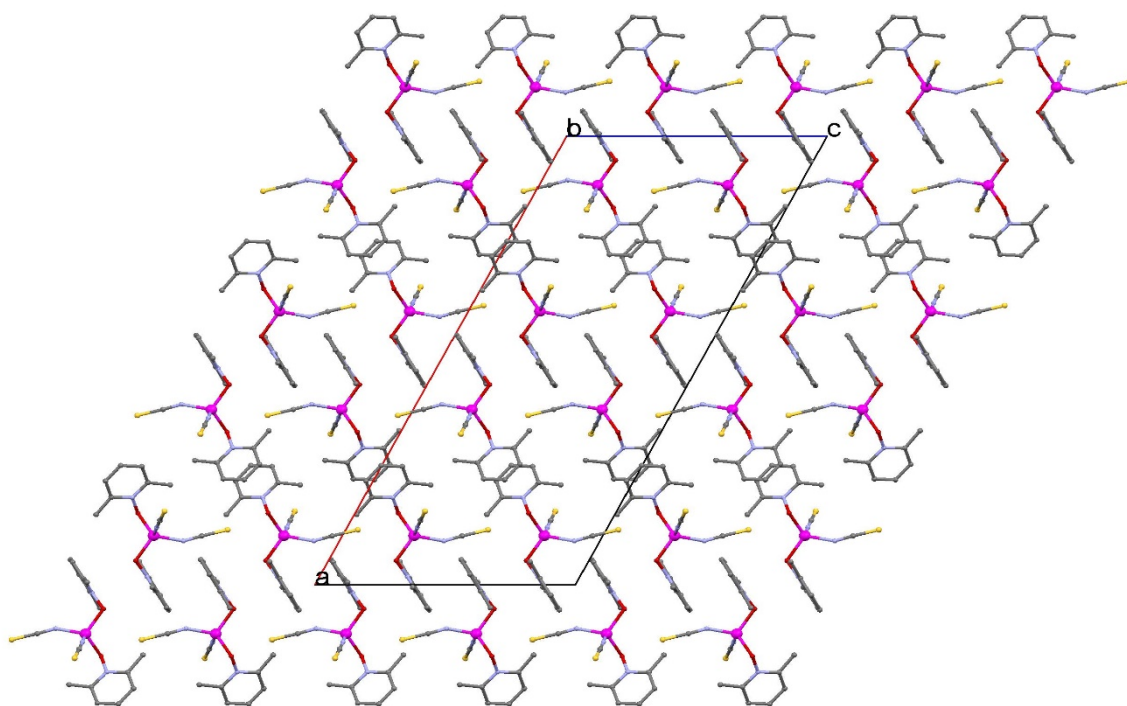


Figure 38: Packing plot of  $[\text{Zn}(\text{2,6-lutidine-N-oxide})_2(\text{NCS})_2]$  (**12**)

Table 13: Selected bond parameters of  $[\text{Zn}(\text{2,6-lutidine-N-oxide})_2(\text{NCS})_2]$  (**12**)

Zn(1)-N(21)	1.947(2)	Zn(1)-N(11)	1.953(2)
Zn(1)-O(2)	1.9547(15)	Zn(1)-O(1)	1.9650(16)
N(11)-C(11)	1.166(3)	N(21)-C(21)	1.159(3)
N(2)-O(2)	1.350(2)	N(1)-O(1)	1.348(2)
C(21)-S(21)	1.614(3)	C(11)-S(11)	1.612(3)
O(2)-Zn(1)-O(1)	108.90(7)	N(21)-Zn(1)-N(11)	109.63(9)
N(21)-Zn(1)-O(2)	105.20(7)	N(11)-Zn(1)-O(2)	112.94(8)
N(21)-Zn(1)-O(1)	112.84(8)	N(11)-Zn(1)-O(1)	107.43(7)
N(21)-C(21)-S(21)	178.3(2)	N(11)-C(11)-S(11)	177.8(2)
C(11)-N(11)-Zn(1)	151.32(18)	C(21)-N(21)-Zn(1)	171.0(2)

## 5.5 [Zn(4-quinoline-N-oxide)(N<sub>3</sub>)<sub>2</sub>]<sub>n</sub> (**13**)

ZnSO<sub>4</sub>·7H<sub>2</sub>O (0.58 g, 2.00 mmol), 4-quinoline-N-oxide (0.14 g, 2.93 mmol) and NaN<sub>3</sub> (0.26 g, 4.00 mmol) were dissolved in 20.00 mL aqueous hydrazoic acid at 40°C. After slow cooling to room temperature colorless crystals were separated within two days (yield: 0.39 g, 66%). *Anal.* Calc. for C<sub>9</sub>H<sub>7</sub>N<sub>7</sub>O<sub>1</sub>Zn (294.61 g/mol): C, 36.7; H, 2.4; N, 33.3. Found: C, 36.0; H, 2.3; N, 32.7%. Selected IR bands (ATR-IR, cm<sup>-1</sup>): 3354 (m,br), ν<sub>a</sub>: 2086 (vs), 2062 (vs), 1647 (w), 1581 (m), 1516 (m), 1455 (w), 1393 (m), ν<sub>s</sub>: 1350 (w), 1292 (m), 1267 (m), 1214 (m), 1178 (w), 1139 (m), 1088 (s), 1052 (m), 879 (m), 799 (s), 770 (s), 724 (m), 665 (m), 625 (w), 583 (m), 566 (s), 500 (m), 478 (w), 435 (w).

Description of the crystal structure:

A section of the crystal structure of [Zn(4-quinoline-N-oxide)(N<sub>3</sub>)<sub>2</sub>]<sub>n</sub> (**13**) is shown in Figure 39 and selected bond parameters are listed in Table 14. Both Zn(II) centers are penta-coordinated by four μ<sub>(1,1)</sub> bridging azido groups and a terminal 4-quinoline-N-oxide molecule. Their ZnN<sub>4</sub>O chromophores have similar distorted trigonal bipyramidal geometry (TBP) with a τ = 0.75 and 0.71, for Zn(1) and Zn(2), respectively [36]. The axial sites are occupied by N(11) and N(31'), respectively N(21) and N(41'') [Zn-N(ax) from 2.099(11) to 2.281(10) Å, N(11)-Zn(1)-N(31') = 172.5(3)°, N(21)-Zn(2)-N(41'') = 168.0(4)°]. The equatorial sites are occupied by N(21), N(31), O(1), respectively N(11), N(41) and O(2) [Zn-N(eq) from 1.945(8) to 2.065(8) Å]. Along the a-axis of the monoclinic unit cell the Zn (II) centers are connected by di-EO azido bridges [EO = end-on, μ<sub>(1,1)</sub>] to zig-zag polymeric chains (Zn...Zn...Zn = 139.3 and 142.6°). The di-μ<sub>(1,1)</sub> azido double bridges have the following bond parameters: Zn-N-Zn from 96.9(3) to 104.5(4)°; N-Zn-N from 77.5(4) to 79.5(4)°; Zn-N-N from 117.1(8) to 135.5(9)°; N-N-N from 172.8(11) to 179.7(12)°. The "out-of-plane" angles N...N-N vary from and 159.4 to 177.8°. [37] The intra-chain Zn(1)...Zn(2), Zn(1)...Zn(1'), Zn(2)...Zn(2'') distances are 3.2559(13), 3.2231(13) and 3.2298(13) Å, the shortest Zn...Zn inter-chain separation is 6.0744(15) Å. The terminal 4-quinoline-N-oxide molecule have a Zn-O-N bond angles of 119.9(6) and 122.6(6)° and the torsions angles are: Zn(1)-O(1)-N(1)-C(1) = 69.9°, Zn(2)-O(2)-N(2)-C(18) = 85.1°.

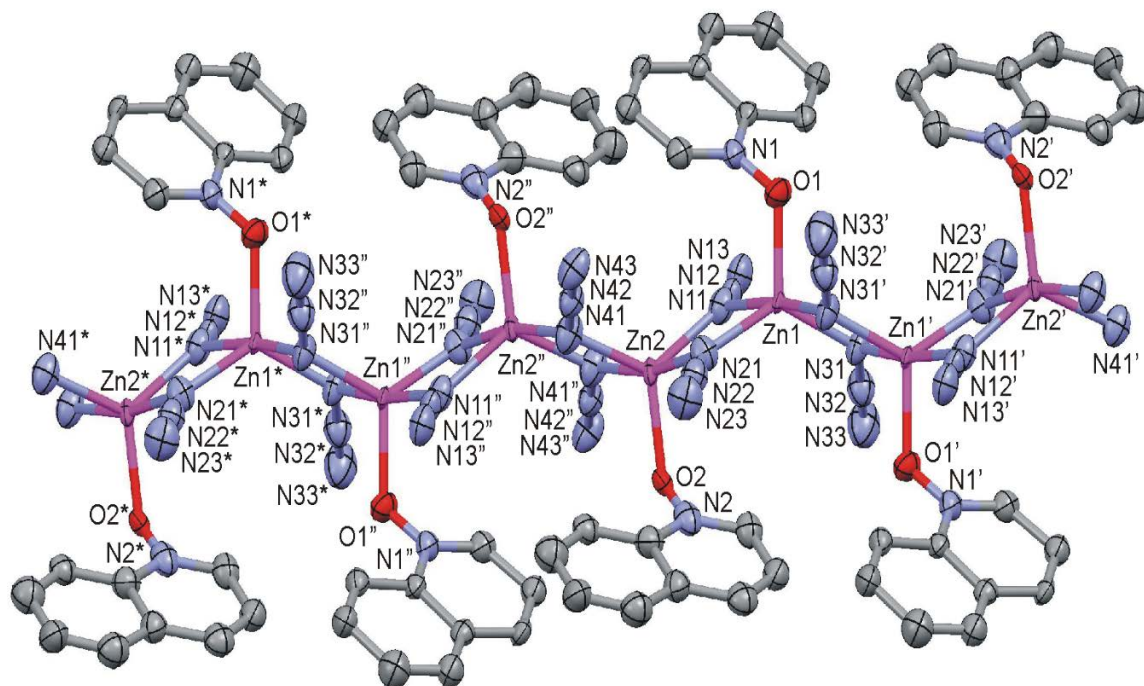


Figure 39: Perspective view of a section of the 1D system of [Zn(4-quinoline-N-oxide)(N<sub>3</sub>)<sub>2</sub>]<sub>n</sub> (**13**)

Symmetry codes: (') -x, 2-y, -z; (") 1-x, 2-y, -z; (\*) 1+x, y, z.

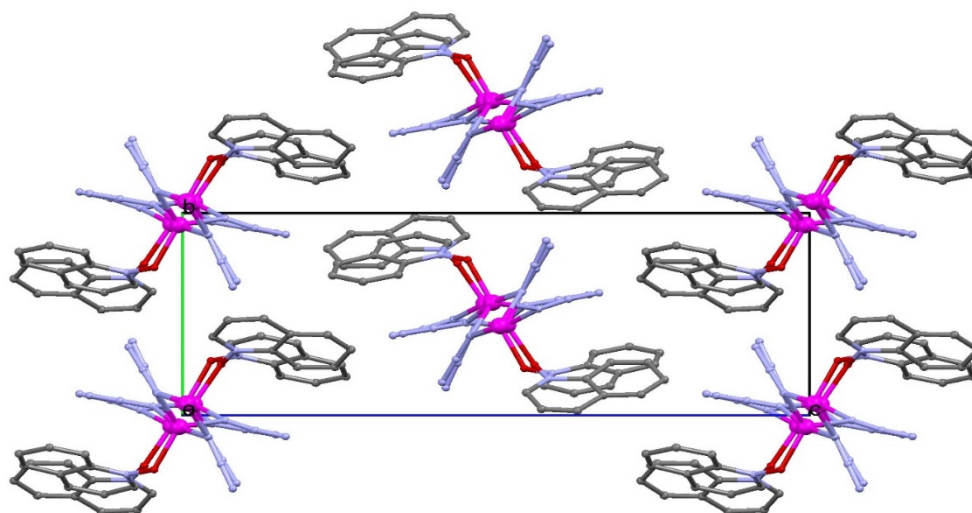


Figure 40: Packing plot of  $[Zn(4\text{-quinoline-N-oxide})(N_3)_2]_n$  (**13**)

Table 14: Selected bond parameters of  $[Zn(4\text{-quinoline-N-oxide})(N_3)_2]_n$  (**13**)

Zn(1)-N(21)	1.945(8)	Zn(1)-O(1)	1.949(7)
Zn(1)-N(31)	1.988(9)	Zn(1)-N(31')	2.200(9)
Zn(1)-N(11)	2.281(10)	Zn(2)-O(2)	1.998(7)
Zn(2)-N(41'')	2.043(10)	Zn(2)-N(11)	2.065(8)
Zn(2)-N(41)	2.099(11)	Zn(2)-N(21)	2.169(10)
N(11)-N(12)	1.161(12)	N(12)-N(13)	1.150(13)
N(21)-N(22)	1.216(12)	N(22)-N(23)	1.125(13)
N(31)-N(32)	1.250(14)	N(41)-N(42)	1.224(14)
N(32)-N(33)	1.161(17)	O(1)-N(1)	1.272(12)
N(42)-N(43)	1.181(14)	O(2)-N(2)	1.297(12)
Zn(1)-N(21)-Zn(2)	104.5(4)	N(33)-N(32)-N(31)	179.7(12)
Zn(2)-N(11)-Zn(1)	96.9(3)	Zn(1)-N(31)-Zn(1')	100.5(4)
O(1)-Zn(1)-N(31)	114.8(3)	Zn(2)-N(41)-Zn(2'')	102.5(4)
O(1)-Zn(1)-N(11)	93.3(3)	O(1)-Zn(1)-N(31')	93.3(3)
O(2)-Zn(2)-N(11)	116.5(3)	O(2)-Zn(2)-N(41)	118.2(3)
N(1)-O(1)-Zn(1)	122.6(6)	O(2)-Zn(2)-N(21)	97.8(3)
N(21)-Zn(1)-O(1)	117.5(4)	N(2)-O(2)-Zn(2)	119.9(6)
N(21)-Zn(1)-N(31')	94.9(3)	N(21)-Zn(1)-N(31)	127.6(4)
N(21)-Zn(1)-N(11)	78.8(3)	N(31)-Zn(1)-N(31')	79.5(4)
N(31')-Zn(1)-N(11)	172.5(3)	N(31)-Zn(1)-N(11)	101.0(4)
N(41)-Zn(2)-N(41'')	77.5(4)	N(41)-Zn(2)-N(11)	125.2(4)
N(41)-Zn(2)-N(21)	95.1(4)	N(11)-Zn(2)-N(41'')	97.3(4)
N(41'')-Zn(2)-N(21)	168.0(4)	N(11)-Zn(2)-N(21)	79.0(3)
N(12)-N(11)-Zn(1)	135.5(7)	N(12)-N(11)-Zn(2)	125.2(7)
N(22)-N(21)-Zn(1)	125.9(8)	N(13)-N(12)-N(11)	172.8(11)
N(23)-N(22)-N(21)	179.1(11)	N(22)-N(21)-Zn(2)	129.1(7)
N(42)-N(41)-Zn(2'')	135.5(9)	N(42)-N(41)-Zn(2)	117.1(8)
N(32)-N(31)-Zn(1)	122.0(7)	N(43)-N(42)-N(41)	179.5(11)
O(2)-Zn(2)-N(41'')	94.1(4)	N(32)-N(31)-Zn(1')	129.6(8)

Symmetrie codes: (')  $x, 3/2-y, 1/2+z$ ; (')'  $x, 3/2-y, -1/2+z$ .

## 5.6 [Zn(2,6-lutidine-N-oxide)(N<sub>3</sub>)<sub>2</sub>]<sub>n</sub> (**14**)

ZnSO<sub>4</sub>·7H<sub>2</sub>O (2.59 g, 9.01 mmol), 2,6-dimethylpyridine-N-oxide (0.37 g, 3.00 mmol) and NaN<sub>3</sub> (1.22 g, 18.77 mmol) were dissolved in 20.00 mL aqueous hydrazoic acid at room temperature. After one day at room temperature colorless crystals appeared (yield: 0.47 g, 57%). *Anal.* Calc. for C<sub>7</sub>H<sub>9</sub>N<sub>7</sub>OZn (272.58 g/mol): C, 30.8; H, 3.3; N, 36.0. Found: C, 30.7; H, 3.2; N, 36.1%. Selected IR bands (ATR-IR, cm<sup>-1</sup>): 3351 (w), 3065 (w), 2639 (w), ν<sub>a</sub>: 2088 (vs), 2055 (vs), 1619 (w), 1581 (w), 1496 (m), 1454 (m), 1427 (w), 1384 (w), 1355 (m), ν<sub>s</sub>: 1294 (s), 1202 (s), 1102 (m), 1029 (m), 990 (m), 926 (w), 834 (s), 784 (s), 718 (w), 668 (m), 600 (m), 573 (w), 532 (s).

Description of the crystal structure:

A part of the crystal structure of [Zn(2,6-lutidine-N-oxide)(N<sub>3</sub>)<sub>2</sub>]<sub>n</sub> (**14**) is shown in Figure 41, and selected bond parameters are listed in Table 15. Zn(1) is penta-coordinated by four μ<sub>(1,1)</sub> bridging azido groups and a terminal 2,6-lutidine-N-oxide molecule. The ZnN<sub>4</sub>O chromophore has a distorted trigonal bipyramidal geometry (TBP) with a τ = 0.82 [36], with N(11') and N(21'') in the axial sites [Zn(1)-N(11') = 2.1936(15), Zn(1)-N(21'') = 2.1631(15) Å, N(11')-Zn(1)-N(21'') = 170.42(5)°], and N(21), N(11) and O(1) in equatorial sites [Zn-N/O from 1.9738(12) to 2.0449(14) Å]. Zn(1) deviates by 0.013 Å from the equatorial N<sub>2</sub>O plane. Along the a-axis of the monoclinic unit cell the Zn(II) centers are connected by di-EO azido bridges [EO = end-on, μ<sub>(1,1)</sub>] to corrugated polymeric chains (Zn...Zn...Zn = 137.6°). The four-membered Zn<sub>2</sub>N<sub>2</sub> rings formed by the di-EO azido bridges are planar. The μ<sub>(1,1)</sub> azido bridges have the following bond parameters: Zn(1)-N(11)-Zn(1') = 100.91(6)°, Zn(1)-N(21)-Zn(1'') = 101.98(6)°; N(11)-Zn(1)-N(11') = 79.09(6)°, N(21)-Zn(1)-N(21'') = 78.02(6)°. The “out-of-plane” angles N(11')...N(11)-N(12) and N(21'')...N(21)-N(22) are 174.0 and 175.0°, respectively. [37] The intra-chain Zn(1)...Zn(1') and Zn(1)...Zn(1'') distances are 3.2629(7) and 3.2707(7) Å, the shortest Zn...Zn inter-chain separation is 6.0915(12) Å. The terminal 2,6-lutidine-N-oxide molecule has a Zn(1)-O(1)-N(1) bond angle of 125.50(10)° and the Zn-O(1)-N(1)-C(1) torsion angle is 78.1°.

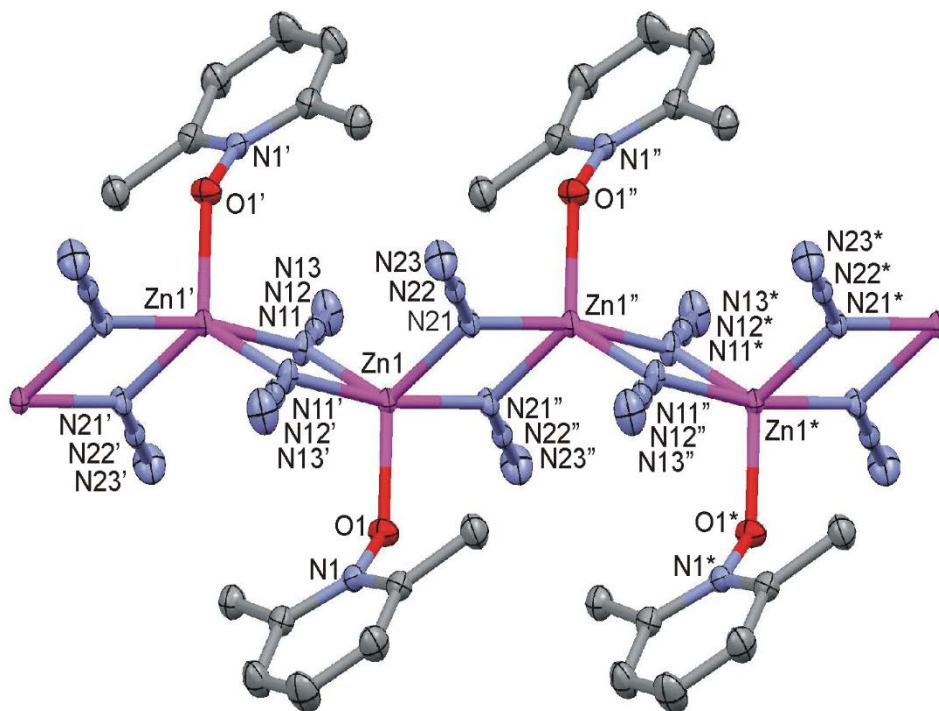


Figure 41: Perspective view of a section of the 1D system of [Zn(2,6-lutidine-N-oxide)(N<sub>3</sub>)<sub>2</sub>]<sub>n</sub> (**14**)

Symmetry codes: (') 1-x, 2-y, 1-z; (") -x, 2-y, 1-z; (\*) -1+x, y, z.

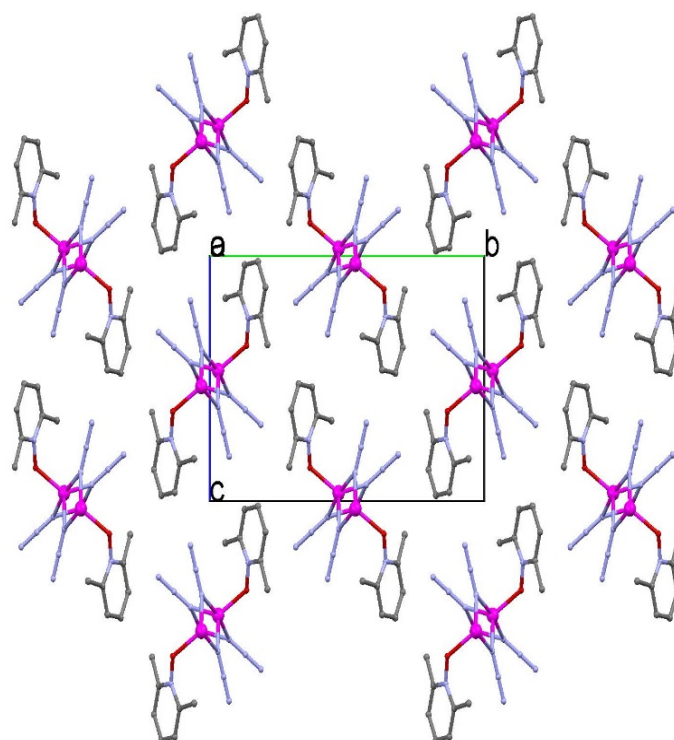


Figure 42: Packing plot of  $[\text{Zn}(\text{2,6-lutidine-N-oxide})(\text{N}_3)_2]_n$  (**14**)

Table 15: Selected bond parameters of  $[\text{Zn}(\text{2,6-lutidine-N-oxide})(\text{N}_3)_2]_n$  (**14**)

Zn(1)-O(1)	1.9738(12)	Zn(1)-N(11)	2.0356(16)
Zn(1)-N(21)	2.0449(14)	Zn(1)-N(21'')	2.1631(15)
Zn(1)-N(11')	2.1936(15)	N(11)-N(12)	1.208(2)
N(12)-N(13)	1.150(2)	N(21)-N(22)	1.210(2)
N(21)-Zn(1)	2.1631(15)	N(22)-N(23)	1.148(2)
O(1)-N(1)	1.3448(18)		
Zn(1)-N(11)-Zn(1')	100.91(6)	Zn(1)-N(21)-Zn(1'')	101.98(6)
O(1)-Zn(1)-N(11)	114.95(6)	O(1)-Zn(1)-N(21)	123.90(6)
O(1)-Zn(1)-N(21'')	93.73(5)	O(1)-Zn(1)-N(11')	95.75(6)
N(1)-O(1)-Zn(1)	125.50(10)	N(11)-Zn(1)-N(21)	121.13(6)
N(11)-Zn(1)-N(21'')	98.09(6)	N(11)-Zn(1)-N(11')	79.09(6)
N(12)-N(11)-Zn(1)	124.09(12)	N(12)-N(11)-Zn(1')	134.58(12)
N(13)-N(12)-N(11)	179.89(16)	N(21)-Zn(1)-N(21)	78.02(6)
N(21)-Zn(1)-N(11')	95.51(6)	N(21'')-Zn(1)-N(11')	170.42(5)
N(22)-N(21)-Zn(1)	122.12(11)	N(22)-N(21)-Zn(1'')	135.87(11)
N(23)-N(22)-N(21)	178.76(17)		

Symmetrie codes: (') 1-x, 2-y, 1-z; (') -x, 2-y, 1-z.

## 5.7 [Zn(4-picoline-N-oxide)(N<sub>3</sub>)<sub>2</sub>]<sub>n</sub> (**15**)

Compound (**15**) was obtained by mixing ZnSO<sub>4</sub>·7H<sub>2</sub>O (2.59 g, 9.01 mmol), 4-methylpyridine-N-oxide (0.43 g, 3.91 mmol) and NaN<sub>3</sub> (1.22 g, 18.77 mmol) in 4.2 mL aqueous hydrazoic acid at room temperature. After 2 weeks clear colorless crystals were separated (yield: 0.65 g, 64%). *Anal.* Calc. for C<sub>6</sub>H<sub>7</sub>N<sub>7</sub>OZn (258.58 g/mol): C, 27.9; H, 2.7; N, 37.9. Found: C, 27.6; H, 2.6; N, 37.7%. Selected IR bands (ATR-IR, cm<sup>-1</sup>): 3404 (w), 3351 (m), 3105 (w), 2141 (s), 2054 (vs), 1626 (w), 1498 (s), 1352 (m), 1290 (s), 1206 (s), 1185 (m), 1089 (m), 855 (m), 831 (s), 759 (s), 695 (w), 664 (m), 620 (w), 601 (m), 528 (w), 487 (m), 457 (w).

Description of the crystal structure:

A fragment of the crystal structure of [Zn(4-picoline-N-oxide)(N<sub>3</sub>)<sub>2</sub>]<sub>n</sub> (**15**) is shown in Figure 43 and selected bond parameters are listed in Table 16. Zn(1) is penta-coordinated by four μ<sub>(1,1)</sub> bridging azido groups and a terminal 4-picoline-N-oxide molecule. The ZnN<sub>4</sub>O polyhedron has a distorted square planar geometry (SP), τ = 0.27 [36], with O(1) in apical position [Zn(1)-O(1) = 1.9800(12) Å] and N(11), N(21), N(11') and N(21') in the basal sites [Zn-N from 2.0182(12) to 2.1884(13) Å]. Zn(1) deviates by 0.505 Å from the basal N<sub>4</sub> plane. Along the c-axis of the monoclinic unit cell the Zn(II) centers are connected by asymmetric di-EO azido bridges [EO = end-on, μ<sub>(1,1)</sub>] to zig-zag polymeric chains (Zn...Zn...Zn = 143.9°). The four-membered Zn<sub>2</sub>N<sub>2</sub> rings formed by the di-EO azido bridges are planar. The μ<sub>(1,1)</sub> azido bridges have the following bond parameters: Zn(1)-N(11)-Zn(1') = 100.79(5)°, Zn(1)-N(21)-Zn(1'') = 102.16(5)°; N(11)-Zn(1)-N(21) = 78.52(5)°, N(11)-Zn(1)-N(21') = 78.47(5)°. The "out-of-plane" angles N(11)...N(21)-N(22) and N(21)...N(11)-N(12) are 167.0 and 156.0°, respectively. [37] The intra-chain Zn(1)...Zn(1') distance is 3.2583(5) Å, the shortest Zn...Zn inter-chain separation is 6.1961(9) Å. The terminal 4-picoline-N-oxide molecule have a Zn(1)-O(1)-N(1) bond angle of 115.49(8)°; and the Zn-O(1)-N(1)-C(1) torsion angle is 88.8°.

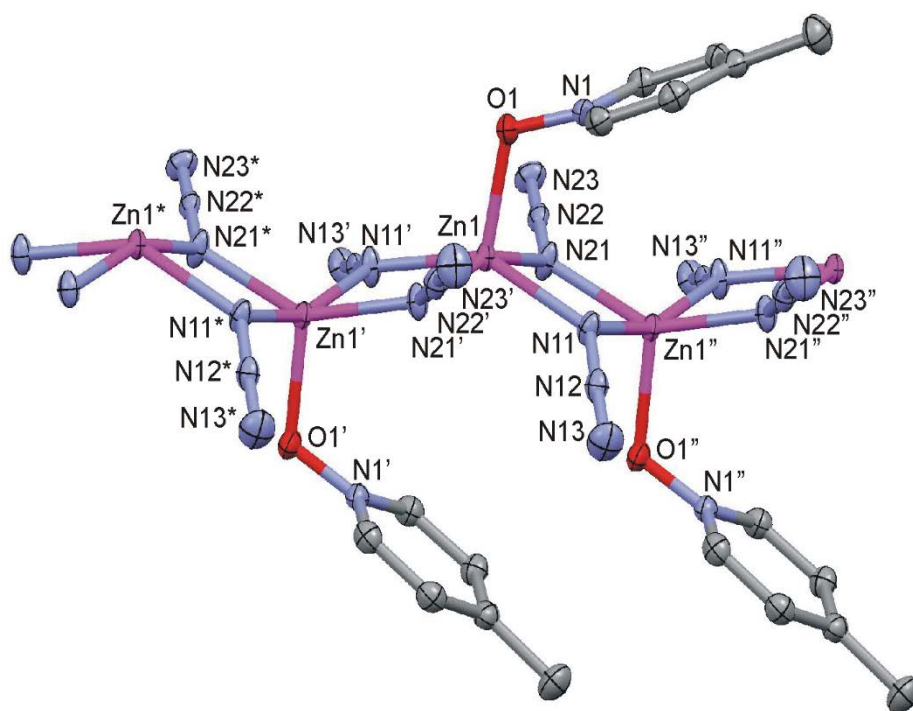


Figure 43: Perspective view of a section of the 1D system of [Zn(4-picoline-N-oxide)(N<sub>3</sub>)<sub>2</sub>]<sub>n</sub> (**15**)

Symmetry codes: (') x, 3/2-y, 1/2+z; (") x, 3/2-y, -1/2+z; (\*) x, y, 1+z.

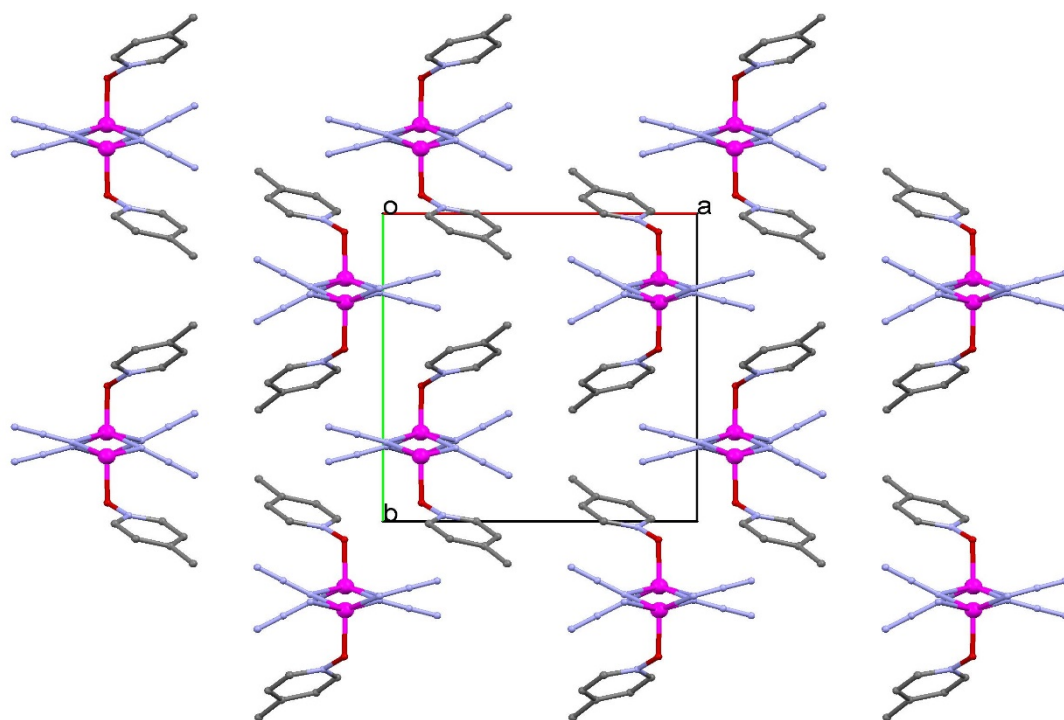


Figure 44: Packing plot of  $[\text{Zn}(\text{4-picoline-N-oxide})(\text{N}_3)_2]_n$  (**15**)

Table 16: Selected bond parameters of  $[\text{Zn}(\text{4-picoline-N-oxide})(\text{N}_3)_2]_n$  (**15**)

Zn(1)-O(1)	1.9800(12)	Zn(1)-N(21')	2.0182(12)
Zn(1)-N(11)	2.0387(13)	Zn(1)-N(21)	2.1680(13)
Zn(1)-N(11')	2.1884(13)	O(1)-N(1)	1.3536(15)
N(11)-N(12)	1.2088(19)	N(11)-Zn(1')	2.1884(13)
N(12)-N(13)	1.1469(19)	N(21)-N(22)	1.211(2)
N(22)-N(23)	1.144(2)		
Zn(1)-N(11)-Zn(1'')	100.79(5)	Zn(1)-N(21)-Zn(1'')	102.16(5)
O(1)-Zn(1)-N(21')	109.36(5)	O(1)-Zn(1)-N(11)	106.87(5)
O(1)-Zn(1)-N(21)	99.96(5)	O(1)-Zn(1)-N(11')	100.05(5)
N(1)-O(1)-Zn(1)	115.49(8)	N(11')-Zn(1)-N(21')	78.52(5)
N(11)-Zn(1)-N(11')	94.85(5)	N(12)-N(11)-Zn(1)	127.22(10)
N(12)-N(11)-Zn(1'')	125.07(10)	N(13)-N(12)-N(11)	178.44(15)
N(21')-Zn(1)-N(11)	143.76(6)	N(21')-Zn(1)-N(21)	95.63(5)
N(21)-Zn(1)-N(11)	78.47(5)	N(21)-Zn(1)-N(11')	159.98(6)
N(22)-N(21)-Zn(1'')	122.17(10)	N(22)-N(21)-Zn(1)	132.87(11)
N(23)-N(22)-N(21)	178.94(16)		

Symmetry codes: (')  $x, 3/2-y, 1/2+z$ ; (')  $x, 3/2-y, -1/2+z$ .

## 5.8 [Zn(2-O-pyridine-N-oxide)(N<sub>3</sub>)(H<sub>2</sub>O)]<sub>n</sub> (**16**)

ZnSO<sub>4</sub>·7H<sub>2</sub>O (2.59 g, 9.01 mmol), 2-hydroxypyridine-N-oxide (0.33 g, 3.00 mmol) and NaN<sub>3</sub> (1.17 g, 18.00 mmol) were dissolved in 13.50 mL aqueous hydrazoic acid at room temperature. After one day at room temperature colorless crystals appeared (yield: 0.45 g, 64%). *Anal.* Calc. for C<sub>5</sub>H<sub>6</sub>N<sub>4</sub>O<sub>3</sub>Zn (235.53 g/mol): C, 25.5; H, 2.6; N, 23.8. Found: C, 25.3; H, 2.5; N, 23.7%. Selected IR bands (ATR-IR, cm<sup>-1</sup>): ν<sub>OH</sub>: 3213 (s,br), 2563 (w), ν<sub>a</sub>: 2112 (s), 2064 (s), 1621 (s), 1549 (w), 1512 (vs), 1446 (m), 1363 (m), 1285 (m), 1230 (w), 1180 (s), 1148 (w), 1109 (m), 924 (w), 884 (m), 846 (w), 783 (w), 741 (m), 690 (w), 609 (m), 545 (m), 497 (w), 448 (w).

Description of the crystal structure:

A fragment of the crystal structure of [Zn(2-O-pyridine-N-oxide)(N<sub>3</sub>)(H<sub>2</sub>O)]<sub>n</sub> (**16**) is shown in Figure 45 and selected bond parameters are listed in Table 17. Zn(1) is penta-coordinated by N(11), N(11') of end-on bridging azido groups, O(3) of a terminal aqua ligand, O(1) and O(2) of a chelating deprotonated 2-O-pyridine-N-oxide molecule. The ZnN<sub>2</sub>O<sub>3</sub> polyhedron has an intermediate geometry between square pyramide (SP) and distorted trigonal bipyramide (TBP) with a τ = 0.49 [36]. The Zn-N/O bond distances are in the range from 2.0332(12) to 2.0684(14) Å. The O(1)-Zn(1)-O(2) chelate angle is 79.24(5)°, Zn(1) and O(3) deviate by 0.044 and 0.245 Å from the mean plane of the 2-O-pyridine-N-oxide molecule. The single end-on azido bridges form polymeric chains along the b-axis of the unit cell (Figure 46). The μ<sub>(1,1)</sub> azido bridges have the following bond parameters: N(11)-N(12) = 1.215(2), N(12)-N(13) = 1.142(2) Å; Zn(1)-N(11)-Zn(1') = 122.57(7)°; N(11)-Zn(1)-N(11') = 111.08(5)°, Zn(1)-N(11)-N(12) = 118.22(11), Zn(1')-N(11)-N(12) = 117.45(11), N(11)-N(12)-N(13) = 179.41(17)°. The intra-chain Zn(1)...Zn(1') and Zn(1)...Zn(1'') distances are 3.6219(7) Å, the shortest Zn...Zn inter-chain separation is 5.1346(9) Å. The chelating 2-O-pyridine-N-oxide molecule has a Zn(1)-O(2)-N(1) bond angle of 111.72(9)°. The aqua ligand forms hydrogen bonds of type O-H...O to O(1) and O(2) atoms of 2-O-pyridine-N-oxide molecules to generate a supramolecular 2D system oriented along the a- and b-axis of the unit cell (Figure 46) [O(3)...O(2)(-x,-1/2+y,1/2-z) = 2.723(2) Å, O(3)-H(31)...O(2) = 167(2)°; O(3)...O(1)(-1/2+x,y,1/2-z) = 2.669(2) Å, O(3)-H(32)...O(1) = 167(3)°].

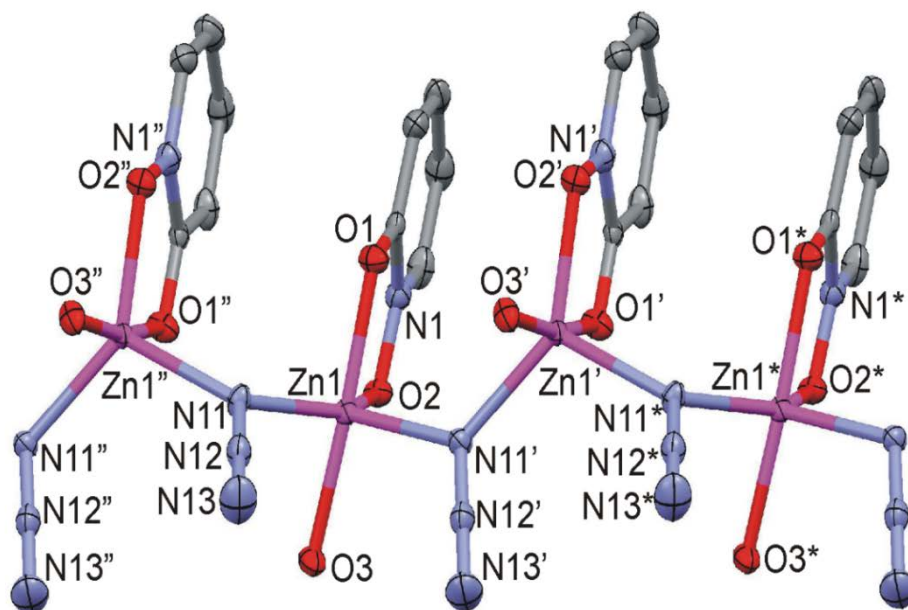


Figure 45: Perspective view of a section of the 1D system of [Zn(2-O-pyridine-N-oxide)(N<sub>3</sub>)(H<sub>2</sub>O)]<sub>n</sub> (**16**)

Symmetry codes: (') 1/2-x, 1/2+y, z; (") 1/2-x, -1/2+y, z; (\*) x, 1+y, z.

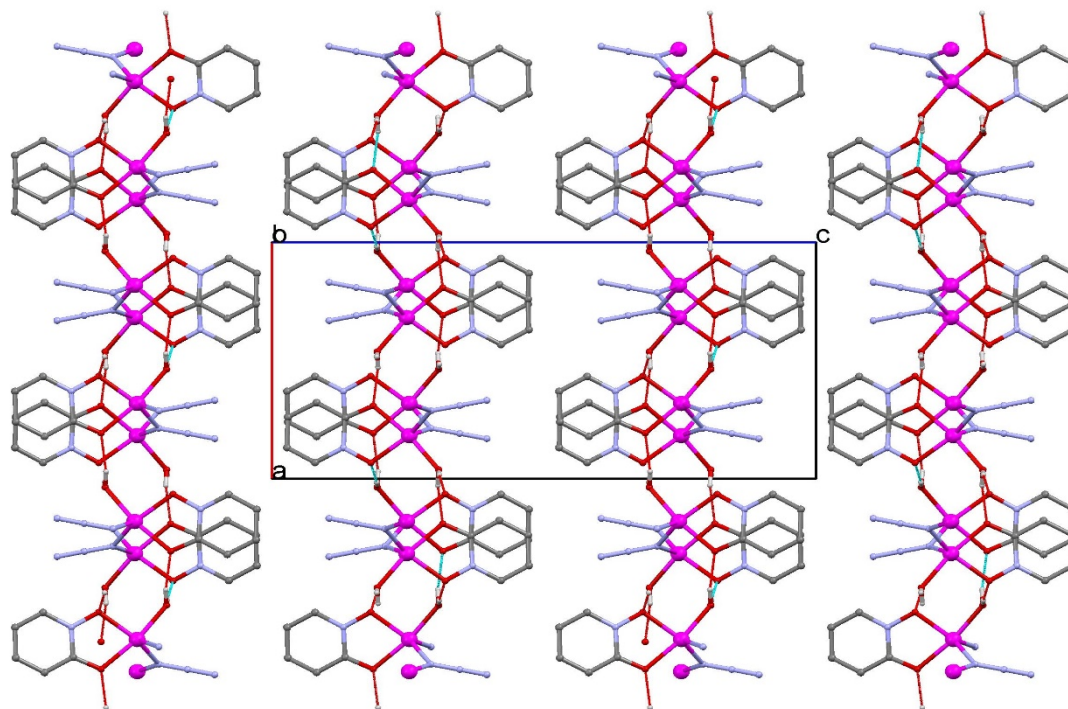


Figure 46: Packing plot of  $[\text{Zn}(\text{2-O-pyridine-N-oxide})(\text{N}_3)(\text{H}_2\text{O})]_n$  (**16**)

Table 17: Selected bond parameters of  $[\text{Zn}(\text{2-O-pyridine-N-oxide})(\text{N}_3)(\text{H}_2\text{O})]_n$  (**16**)

Zn(1)-O(2)	2.0332(12)	Zn(1)-O(3)	2.0500(13)
Zn(1)-O(1)	2.0574(12)	Zn(1)-N(11)	2.0612(15)
Zn(1)-N(11)	2.0684(14)	N(11)-N(12)	1.215(2)
N(11)-Zn(1)	2.0612(15)	N(12)-N(13)	1.142(2)
O(1)-C(1)	1.294(2)	O(2)-N(1)	1.3484(19)
Zn(1)-N(11)-Zn(1'')	122.57(7)	O(1)-Zn(1)-N(11)	95.70(5)
O(1)-Zn(1)-N(11')	91.07(5)	O(2)-Zn(1)-O(3)	91.90(5)
O(2)-Zn(1)-O(1)	79.24(5)	O(2)-Zn(1)-N(11')	108.00(6)
O(2)-Zn(1)-N(11)	140.68(5)	O(3)-Zn(1)-O(1)	170.01(5)
O(3)-Zn(1)-N(11')	96.11(5)	O(3)-Zn(1)-N(11)	88.21(6)
N(1)-O(2)-Zn(1)	111.72(9)	N(11)-Zn(1)-N(11')	111.08(5)
N(12)-N(11)-Zn(1'')	117.45(11)	N(12)-N(11)-Zn(1)	118.22(11)
N(13)-N(12)-N(11)	179.41(17)	C(1)-O(1)-Zn(1)	113.46(10)

Symmetrie codes: (')  $1/2-x, 1/2+y, z$ ; (')  $1/2-x, -1/2+y, z$ .

## 6) Co(II) complexes

### 6.1 [Co(2,6-lutidine-N-oxide)<sub>2</sub>(NCS)<sub>2</sub>]<sub>2</sub> (**17**)

Compound (**17**) was obtained by mixing CoSO<sub>4</sub>·7H<sub>2</sub>O (0.57 g, 2.04 mmol), 2,6-dimethylpyridine-N-oxide (0.48 g, 4.00 mmol) and KSCN (0.39 g, 4.00 mmol) in 12.00 mL distilled water at room temperature. After three days at room temperature orange crystals appeared (yield: 0.58 g, 70%). *Anal.* Calc. for C<sub>16</sub>H<sub>18</sub>CoN<sub>4</sub>O<sub>2</sub>S<sub>2</sub> (421.40 g/mol): C, 45.6; H, 4.23; N, 13.3. Found: C, 45.5; H, 4.2; N, 13.3%. Selected IR bands (ATR-IR, cm<sup>-1</sup>): 2993 (w,br), 2148 (s), ν<sub>CN</sub>: 2079 (vs), 1617 (w), 1577 (m), 1494 (s), 1457 (m), 1420 (m), 1382 (m), 1278 (w), 1192 (vs), 1165 (m), 1091 (m), 1036 (m), 993 (m), 952 (w), 924 (w), ν<sub>CS</sub>: 829 (s), 784 (vs), 686 (m), 573 (w), 549 (m), 529 (m), 495 (w), δ<sub>NCS</sub>: 475 (w), 456 (w).

Description of the crystal structure:

A perspective view of the crystal structure of [Co(2,6-lutidine-N-oxide)<sub>2</sub>(NCS)<sub>2</sub>]<sub>2</sub> (**17**) is shown in Figure 47 and selected bond parameters are listed in Table 18. Co(1) is penta-coordinated by N(11) and S(11) of two μ<sub>(N,S)</sub> bridging isothiocyanato groups, by N(21) of a terminal isothiocyanato group, O(1) and O(2) of two terminal 2,6-lutidine-N-oxide molecules. The CoN<sub>2</sub>O<sub>2</sub>S chromophore has a distorted trigonal bipyramidal geometry (TBP) with a τ = 0.93 [36], with N(11) and N(21) in the axial sites [Co(1)-N(11) = 2.081(7), Co(1)-N(21) = 2.059(7) Å, N(11)-Co(1)-N(21) = 178.2(3)°], and S(11), O(1) and O(2) in equatorial sites [Co-S = 2.420(2), Co-O = 1.978(6) Å]. The di-μ<sub>(N,S)</sub> double bridges form centrosymmetric dimeric units. Their eight-membered Co(NCS)<sub>2</sub>Co ring is almost planar [“chair angle” θ defined as acute angle between plane of the di-μ<sub>(N,S)</sub> thiocyanato bridges and the Co(1)/N(11)/S(11) plane is 3.3°]. The torsion angle: Co(1)-N(11)...S(11')-Co(1') = ± 11.1°. The isothiocyanato group have the following bond parameters: Co-N-C: 164.7(6) and 170.6(6)°, Co-S-C: 102.4(3)°, N-C-S: 179.2(7)°, N-C: 1.160(10) and 1.168(10) Å, C-S: 1.659(8) and 1.628(8) Å. The terminal 2,6-lutidine-N-oxide molecules have Co-O-N bond angles of 119.3(4) and 121.6(4)°; the Co(1)-O(1)-N(1)-C(5) and Co(1)-O(2)-N(2)-C(8) torsion angles are 92.2 and 91.9°, respectively. The 2,6-lutidine-N-oxide molecules form an intra-planar angle of 66.6°. The Co(1)...Co(1') distance within the Co(NCS)<sub>2</sub>Co ring is 5.6293(15) Å, the shortest Co...Co inter-dimer separation is 7.1222(16) Å (Figure 48).

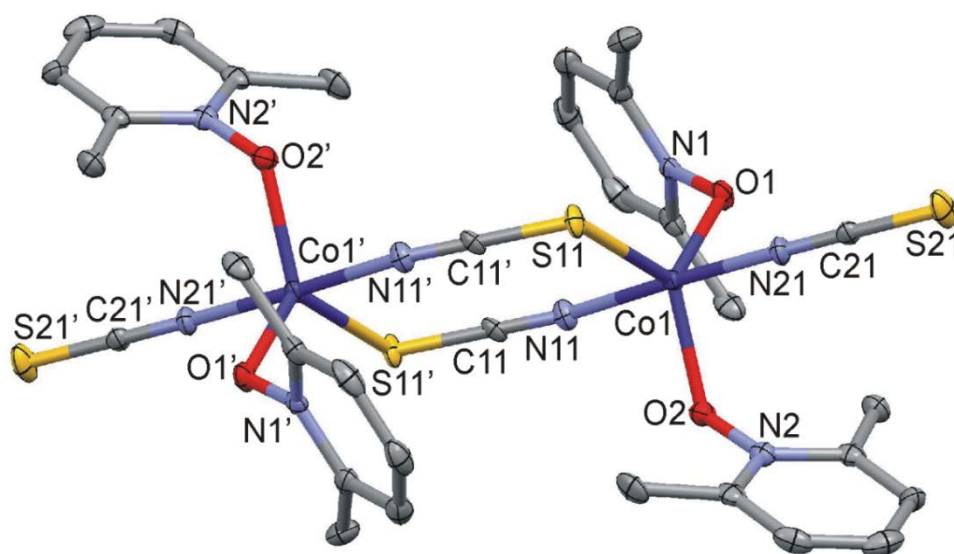


Figure 47: Perspective view of [Co(2,6-lutidine-N-oxide)<sub>2</sub>(NCS)<sub>2</sub>]<sub>2</sub> (**17**)

Symmetry code: (') 1-x, 2-y, -z.

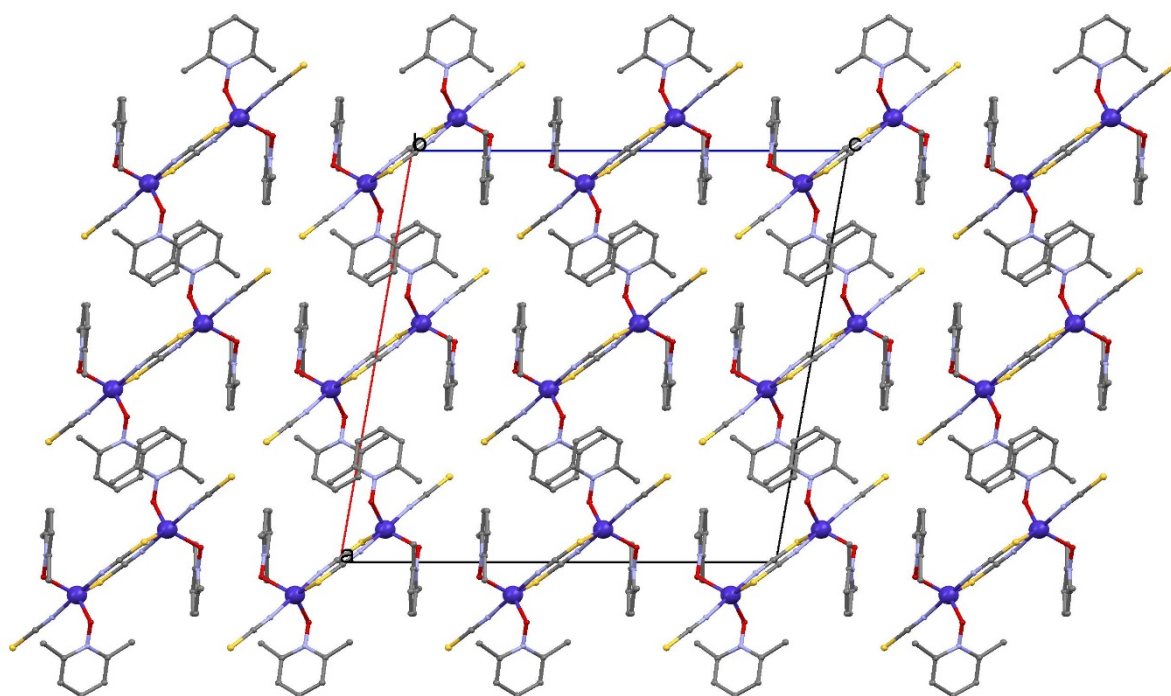


Figure 48: Packing plot of  $[\text{Co}(\text{2,6-lutidine-N-oxide})_2(\text{NCS})_2]_2$  (**17**)

Table 18: Selected bond parameters of  $[\text{Co}(\text{2,6-lutidine-N-oxide})_2(\text{NCS})_2]_2$  (**17**)

Co(1)-O(1)	1.978(5)	Co(1)-O(2)	1.978(6)
Co(1)-N(21)	2.059(7)	Co(1)-N(11)	2.081(7)
Co(1)-S(11)	2.420(2)	O(1)-N(1)	1.362(8)
O(2)-N(2)	1.344(8)	N(11)-C(11')	1.160(10)
N(21)-C(21)	1.168(10)	C(11)-S(11)	1.659(8)
C(21)-S(21)	1.628(8)		
O(1)-Co(1)-O(2)	118.1(2)	O(1)-Co(1)-N(21)	88.9(2)
O(2)-Co(1)-N(21)	94.5(2)	O(1)-Co(1)-N(11)	91.6(2)
O(2)-Co(1)-N(11)	83.8(2)	O(1)-Co(1)-S(11)	119.31(18)
O(2)-Co(1)-S(11)	122.62(18)	N(21)-Co(1)-N(11)	178.2(3)
N(21)-Co(1)-S(11)	87.9(2)	N(11)-Co(1)-S(11)	93.32(19)
N(11)-C(11)-S(11')	179.2(7)	N(1)-O(1)-Co(1)	119.3(4)
N(2)-O(2)-Co(1)	121.6(4)	C(11)-N(11)-Co(1')	164.7(6)
C(11)-S(11)-Co(1)	102.4(3)	C(21)-N(21)-Co(1)	170.6(6)

Symmetrie code: (') 1-x, 2-y, -z.

## 6.2 [Co(4-cyanopyridine-N-oxide)<sub>2</sub>(NCS)<sub>2</sub>(H<sub>2</sub>O)]<sub>2</sub> (**18**)

Compound (**18**) was obtained by mixing CoSO<sub>4</sub>·7H<sub>2</sub>O (1.12 g, 4.00 mmol), 4-cyanopyridine-N-oxide (0.24 g, 2.00 mmol) and KSCN (0.78 g, 8.00 mmol) in 13.00 mL distilled water at 50°C. Upon slow cooling to room temperature red crystals of (**18**) were separated after four days. Selected IR bands (ATR-IR, cm<sup>-1</sup>): ν<sub>OH</sub>: 3364 (m,br), 2102 (s), ν<sub>CN</sub>: 2073 (vs), 1929 (w), 1696 (w), 1633 (m), 1555 (w), 1481 (s), 1436 (m), 1308 (w), 1210 (s), 1171 (s), 1101 (m), 972 (w), 848 (s), 781 (w), 723 (m), 668 (w), 607 (w), 546 (m), δ<sub>NCS</sub>: 481 (m), 457 (m).

Description of the crystal structure:

Preliminary crystal structure investigation reveal that [Co(4-cyanopyridine-N-oxide)<sub>2</sub>(NCS)<sub>2</sub>(H<sub>2</sub>O)]<sub>2</sub> (**18**) is isostructural to the crystal structures of their corresponding Mn(II) and Cd(II) complexes.

A perspective view of together with the atom numbering scheme of the preliminary crystal structure of [Co(4-cyanopyridine-N-oxide)<sub>2</sub>(NCS)<sub>2</sub>(H<sub>2</sub>O)]<sub>2</sub> (**18**) is shown in Figure 49.

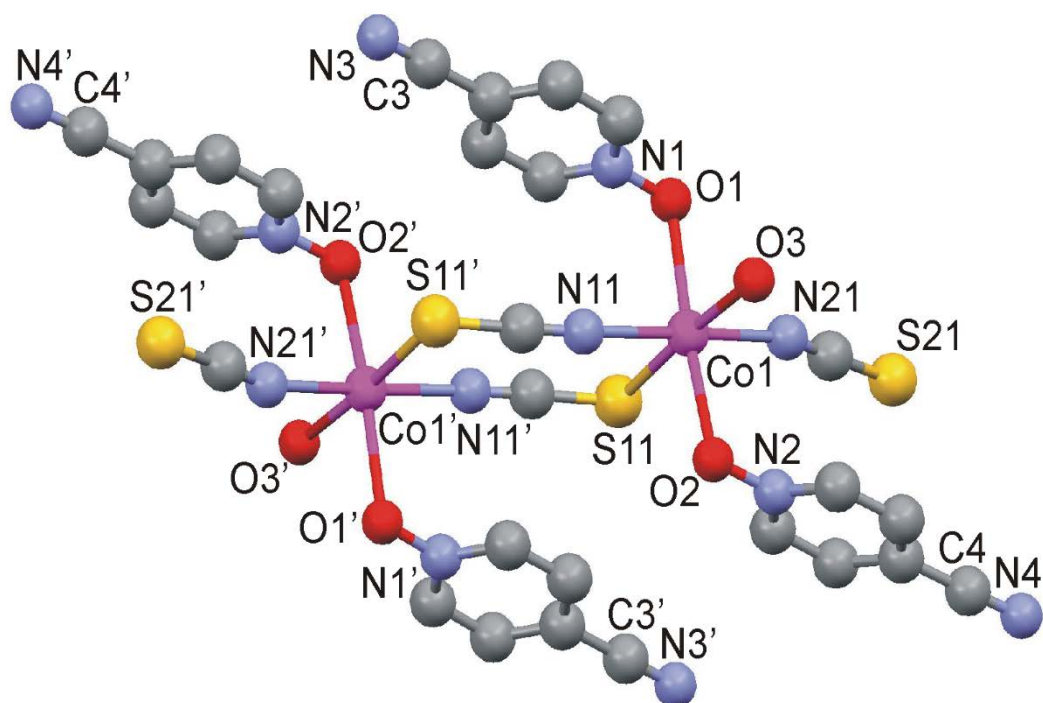


Figure 49: Perspective view of [Co(4-cyanopyridine-N-oxide)<sub>2</sub>(NCS)<sub>2</sub>(H<sub>2</sub>O)]<sub>2</sub> (**18**)

### 6.3 [Co(N<sub>3</sub>)<sub>2</sub>(H<sub>2</sub>O)<sub>2</sub>]<sub>n</sub>(3-picoline-N-oxide)<sub>2n</sub> (**19**)

Compound (**19**) was obtained by mixing CoCl<sub>2</sub>·6H<sub>2</sub>O (0.48 g, 2.00 mmol), 3-methylpyridine-N-oxide (0.43 g, 4.00 mmol) and NaN<sub>3</sub> (0.26 g, 4.00 mmol) in 14.00 mL aqueous hydrazoic acid at room temperature. After five days at room temperature blue crystals appeared (yield: 0.53 g, 67%). *Anal.* Calc. for C<sub>12</sub>H<sub>18</sub>CoN<sub>8</sub>O<sub>4</sub> (397.27 g/mol): C, 36.3; H, 4.6; N, 28.2. Found: C, 36.1; H, 4.5; N, 28.2%. Selected IR bands (ATR-IR, cm<sup>-1</sup>): ν<sub>OH</sub>: 3148 (s,br), 3052 (w), 2359 (w), ν<sub>a</sub>: 2042 (vs), 1801 (w), 1654 (w), 1608 (w), 1577 (w), 1492 (w), 1454 (m), 1416 (m), 1332 (m), 1285 (w), ν<sub>s</sub>: 1260 (m), 1162 (s), 1090 (m), 1015 (m), 942 (m), 918 (w), 883 (w), 801 (m), 745 (w), 673 (m), 653 (w), 591 (w), 563 (s), 496 (m), 434 (s).

Description of the crystal structure:

“A fragment of the crystal structure of [Co(N<sub>3</sub>)<sub>2</sub>(H<sub>2</sub>O)<sub>2</sub>]<sub>n</sub>(3-picoline-N-oxide)<sub>2n</sub> (**19**) is shown in Figure 50, a packing plot is given in Figure 51. Selected bond parameters are listed in Table 19. All non-hydrogen atoms are located at special positions of space group Ibam (no. 72): Co(1) at 4b with site symmetry 222, aqua oxygen atom O(1) at 8g with site symmetry 2, azido group and 3-picoline-N-oxide at 8j with site symmetry m. The single crystal structure determination revealed that complex (**19**) should be formulated as [Co(N<sub>3</sub>)<sub>2</sub>(H<sub>2</sub>O)<sub>2</sub>]<sub>n</sub>(3-picoline-N-oxide)<sub>2n</sub> in which the 3-picoline-N-oxide molecules are non-coordinated and serve as stabilizers of the lattice. The structure of (**19**) consists of a 1D [Co(N<sub>3</sub>)<sub>2</sub>(H<sub>2</sub>O)<sub>2</sub>]<sub>n</sub> chain running along the c-axis. Each cobalt atom in the chain is linked to the two of each neighboring symmetry related counter parts by two azido ligands, i.e. each Co(II) is ligated with four bridging azido ligands [Co-N = 2.1568(8) Å] forming a cyclic four-membered Co<sub>2</sub>N<sub>2</sub> unit. The remaining two coordination sites are occupied by atoms of two trans aqua molecules [Co-O = 2.0760(11) Å]. The coordination environment of each Co(II) is best described as a distorted octahedron with CoN<sub>4</sub>O<sub>2</sub> chromophore. The azido groups function in the μ<sub>(1,1)</sub> bridging fashion and are asymmetric [N(11)-N(12) = 1.2060(17), N(12)-N(13) = 1.1537(18) Å, Δd = 0.052 Å]. The “out-of-plane” angle [37] of the azido group from the Co<sub>2</sub>N<sub>2</sub> ring = 39.4(2)°. Each non-coordinated 3-picoline-N-oxide molecule forms two hydrogen bonds of type O...H-O with oxygen atoms of two adjacent aqua molecules in the chain [O(2)..O(1) = 2.6900(11) Å, O(2)..H(92)-O(1) = 172.5(13)°](Figure 50 and 51). The intra-chain Co...Co distance is 3.2381(2) Å, whereas the shortest inter-chain metal-metal separation is 6.4762(4) Å. The present complex (**19**) is isomorphic to the corresponding Zn(II) complex.” adopted from [38]

Table 19: Selected bond parameters of [Co(N<sub>3</sub>)<sub>2</sub>(H<sub>2</sub>O)<sub>2</sub>]<sub>n</sub>(3-picoline-N-oxide)<sub>2n</sub> (**19**)

Co(1)-O(2)	2.0760(11)	Co(1)-N(11)	2.1568(8)
N(11)-N(12)	1.2060(17)	N(12)-N(13)	1.1537(18)
N(5)-O(1)	1.3334(14)		
O(2)-Co(1)-O(2a)	180	N(11b)-Co(1)-N(11d)	177.07(6)
O(2a)-Co(1)-N(11c)	91.46(3)	N(11)-Co(1)-N(11d)	97.38(5)
N(12)-N(11)-Co(1)	120.68(5)	N(13)-N(12)-N(11)	178.64(15)

Symmetry codes: (a) -x, -y, z; (b) -x, -y, -z; (c) -x, -y, 1/2-z; (d) x, -y, 1/2+z.

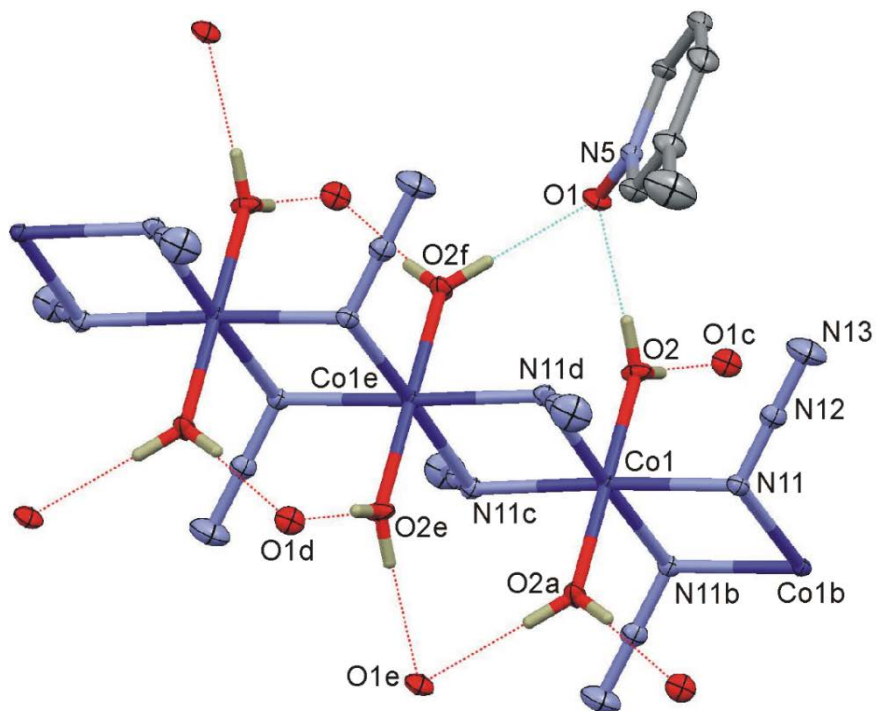


Figure 50: Perspective view of a section of  $[\text{Co}(\text{N}_3)_2(\text{H}_2\text{O})_2]_n(3\text{-picoline-N-oxide})_{2n}$  (**19**)

Symmetry code: (a)  $-x, -y, z$ ; (b)  $-x, -y, -z$ ; (c)  $-x, -y, 1/2-z$ ; (d)  $x, -y, 1/2+z$ ; (e)  $-x, -y, 1-z$ ; (f)  $x, y, 1-z$ .

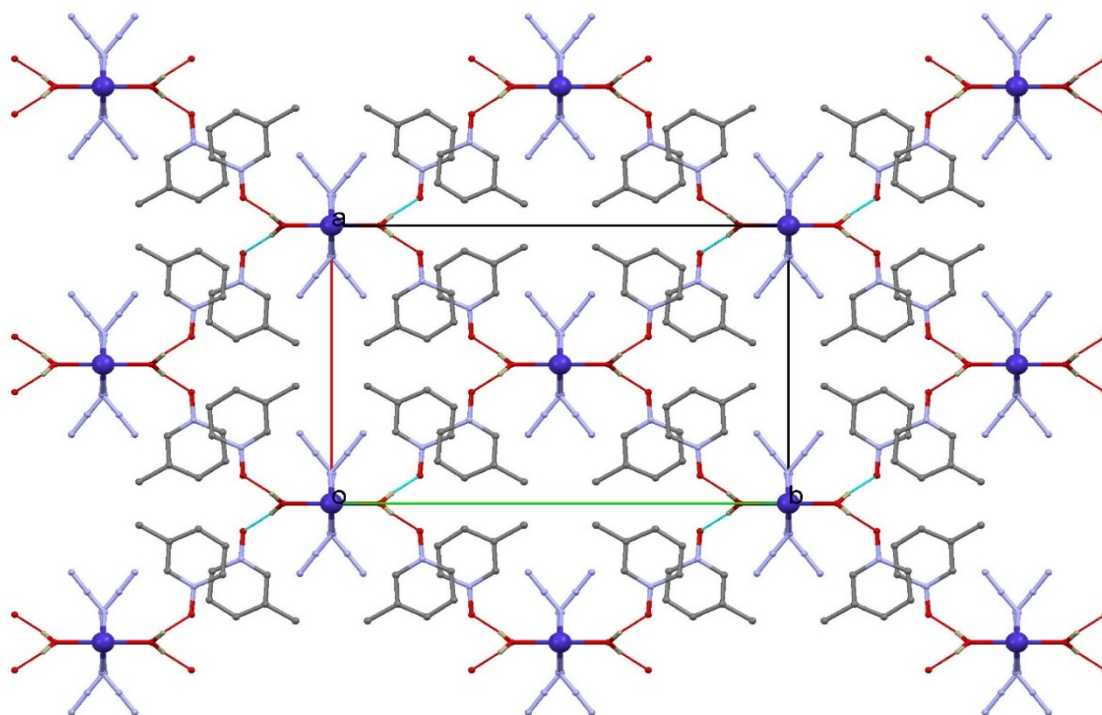


Figure 51: Packing plot of  $[\text{Co}(\text{N}_3)_2(\text{H}_2\text{O})_2]_n(3\text{-picoline-N-oxide})_{2n}$  (**19**)

#### 6.4 [Co(2,6-lutidine-N-oxide)(N<sub>3</sub>)<sub>2</sub>]<sub>n</sub> (**20**)

CoCl<sub>2</sub>·6H<sub>2</sub>O (0.48 g, 2.00 mmol), 2,6-dimethylpyridine-N-oxide (0.48 g, 4.00 mmol) and NaN<sub>3</sub> (0.26 g, 4.00 mmol) were dissolved in 13.00 mL distilled water at room temperature. After two days at room temperature orange crystals appeared (yield: 0.27 g, 51%). *Anal.* Calc. for C<sub>7</sub>H<sub>9</sub>CoN<sub>7</sub>O (266.14 g/mol): C, 31.6; H, 3.4; N, 36.8. Found: C, 31.0; H, 3.3; N, 36.7%. Selected IR bands (ATR-IR, cm<sup>-1</sup>): 3322 (w), 3075 (w), 2628 (w), 2572 (w), 2368 (w), ν<sub>a</sub>: 2081 (vs), 2034 (vs), 1617 (w), 1575 (w), 1493 (m), 1459 (m), 1426 (w), 1388 (w), 1355 (w), ν<sub>s</sub>: 1289 (s), 1194 (s), 1164 (w), 1095 (m), 1035 (w), 997 (w), 926 (w), 831 (s), 793 (s), 725 (w), 667 (m), 596 (m), 572 (w), 550 (m), 529 (m), 493 (w).

Description of the crystal structure:

A part of the crystal structure of [Co(2,6-lutidine-N-oxide)(N<sub>3</sub>)<sub>2</sub>]<sub>n</sub> (**20**) is shown in Figure 52 and selected bond parameters are listed in Table 20. Co(1) is penta-coordinated by four μ<sub>(1,1)</sub> bridging azido groups and a terminal 2,6-lutidine-N-oxide molecule. The CoN<sub>4</sub>O chromophore has a distorted trigonal bipyramidal geometry (TBP) with a τ = 0.782 [36], with N(11) and N(21'') in the axial sites [Co(1)-N(11) = 2.0237(16), Co(1)-N(21'') = 2.1291(16) Å, N(11)-Co(1)-N(21'') = 171.22(6)°], and N(21), N(11') and O(1) in equatorial sites [Co-N/O from 1.9532(14) to 2.0237(16) Å]. Along the b-axis of the monoclinic unit cell the Co(II) centers are connected by di-EO azido bridges [EO = end-on, μ<sub>(1,1)</sub>] to corrugated polymeric chains (Co...Co...Co = 139.6°). The four-membered Co<sub>2</sub>N<sub>2</sub> rings formed by the di-EO azido bridges are planar. The μ<sub>(1,1)</sub> azido bridges have the following bond parameters: Co(1)-N(11)-Co(1') = 101.48(7)°, Co(1)-N(21)-Co(1'') = 99.81(7)°; N(11)-Co(1)-N(11') = 78.52(7)°, N(21)-Co(1)-N(21'') = 80.19(7)°. The "out-of-plane" angles N(11')...N(11)-N(12) and N(21'')...N(21)-N(22) are 177.6 and 173.2°, respectively. [37] The intra-chain Co(1)...Co(1') and Co(1)...Co(1'') distances are 3.2420(7) and 3.1742(7) Å, the shortest Co...Co inter-chain separation is 6.0221(12) Å. The terminal 2,6-lutidine-N-oxide molecule have a Co(1)-O(1)-N(1) bond angle of 123.33(11)°; and the Co-O(1)-N(1)-C(1) torsion angle is 93.3°.

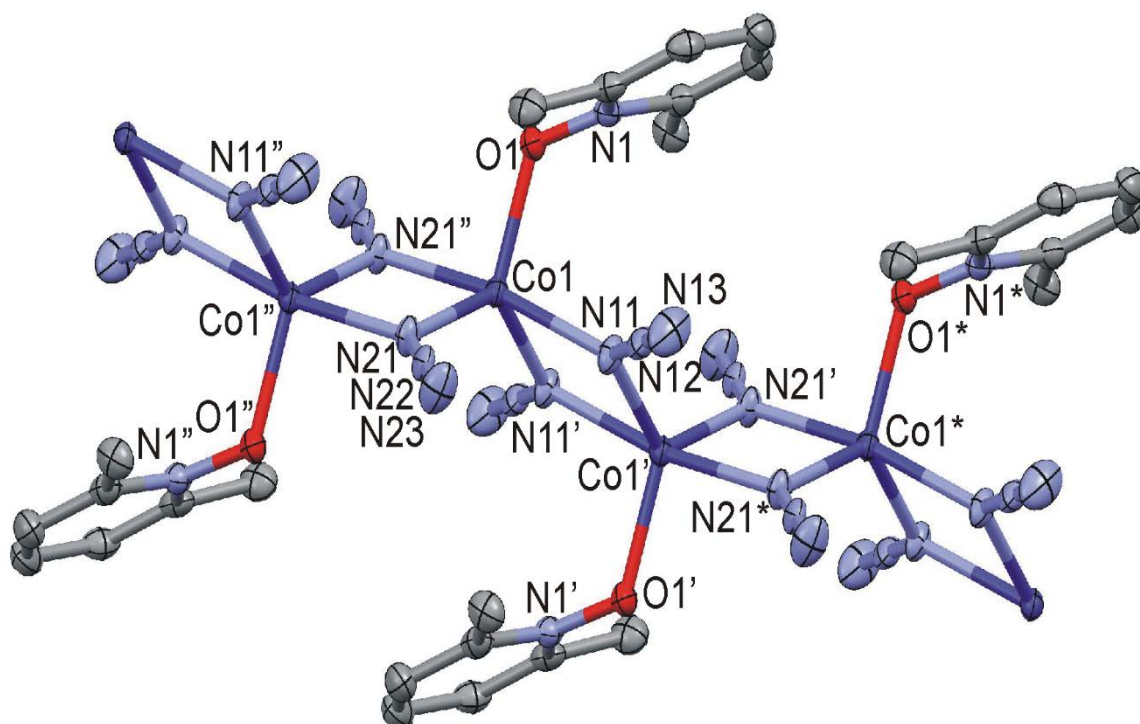


Figure 52: Perspective view of a section of the 1D system of [Co(2,6-lutidine-N-oxide)(N<sub>3</sub>)<sub>2</sub>]<sub>n</sub> (**20**)

Symmetry codes: (') -x, -y, -z; (") -x, 1-y, -z; (\*) x, -1+y, +z.

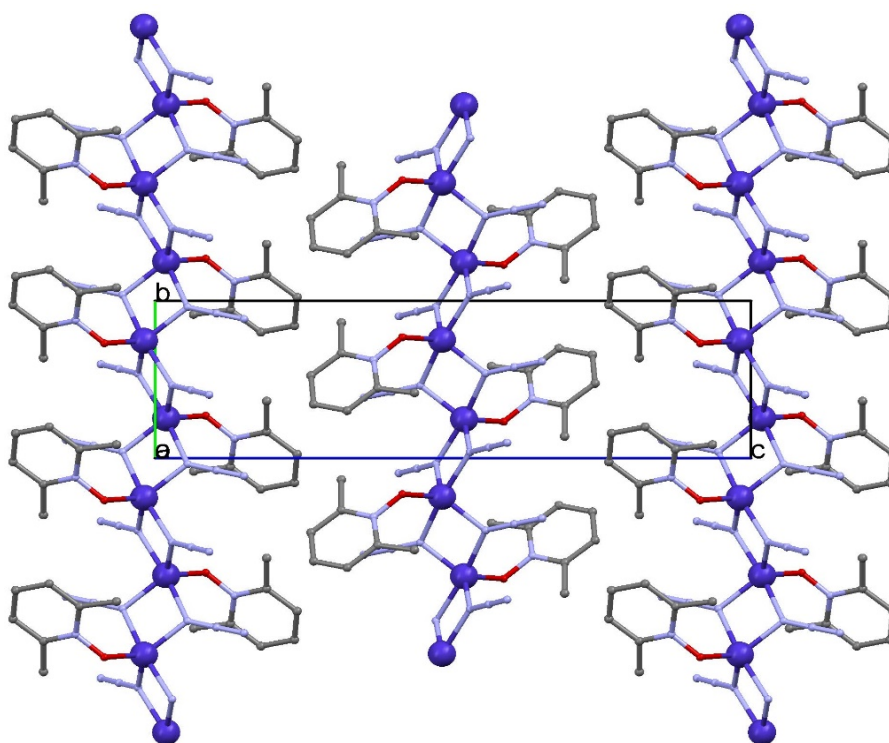


Figure 53: Packing plot of  $[\text{Co}(2,6\text{-lutidine-}N\text{-oxide})(\text{N}_3)_2]_n$  (**20**)

Table 20: Selected bond parameters of  $[\text{Co}(2,6\text{-lutidine-}N\text{-oxide})(\text{N}_3)_2]_n$  (**20**)

Co(1)-O(1)	1.9532(14)	Co(1)-N(21)	2.0192(16)
Co(1)-N(11')	2.0237(16)	Co(1)-N(21'')	2.1291(16)
Co(1)-N(11)	2.1618(16)	O(1)-N(1)	1.3449(19)
N(11)-N(12)	1.212(2)	N(11)-Co(1')	2.0237(16)
N(12)-N(13)	1.146(2)	N(21)-N(22)	1.216(2)
N(21)-Co(1'')	2.1291(16)	N(22)-N(23)	1.148(2)
Co(1')-N(11)-Co(1)	101.48(7)	Co(1)-N(21)-Co(1'')	99.81(7)
O(1)-Co(1)-N(21)	115.59(6)	O(1)-Co(1)-N(11')	120.07(6)
O(1)-Co(1)-N(21'')	92.32(6)	O(1)-Co(1)-N(11)	96.44(6)
N(11')-Co(1)-N(21'')	96.61(6)	N(11)-Co(1)-N(11')	78.52(7)
N(12)-N(11)-Co(1')	124.93(13)	N(12)-N(11)-Co(1)	133.56(13)
N(13)-N(12)-N(11)	179.3(2)	N(21)-Co(1)-N(11')	124.34(7)
N(21)-Co(1)-N(21'')	80.19(7)	N(21)-Co(1)-N(11)	96.45(6)
N(21'')-Co(1)-N(11)	171.22(6)	N(22)-N(21)-Co(1)	126.66(13)
N(22)-N(21)-Co(1)	132.88(13)	N(23)-N(22)-N(21)	179.56(18)

Symmetry codes: (') -x, -y, -z; (') -x, 1-y, -z.

## 7) Mn(II) complexes

### 7.1 [Mn(2-picoline-N-oxide)(NCS)<sub>2</sub>]<sub>n</sub> (**21**)

Mn(NO<sub>3</sub>)<sub>2</sub>·4H<sub>2</sub>O (1.00 g, 4.00 mmol), 2-methylpyridine-N-oxide (0.22 g, 2.00 mmol) and KSCN (0.78 g, 8.00 mmol) were dissolved in 4.5 mL distilled water at room temperature. After four days at room temperature yellow crystals appeared (yield: 0.34 g, 61%). *Anal.* Calc. for C<sub>8</sub>H<sub>7</sub>MnN<sub>3</sub>OS<sub>2</sub> (280.23 g/mol): C, 34.3; H, 2.5; N, 15.0. Found: C, 34.0; H, 2.4; N, 15.0%. Selected IR bands (ATR-IR, cm<sup>-1</sup>): 3431 (w,br), ν<sub>CN</sub>: 2096 (vs), 1826 (w), 1648 (w), 1617 (w), 1575 (w), 1493 (m), 1460 (s), 1419 (w), 1384 (w), 1208 (s), 1160 (m), 1114 (m), 1038 (w), 1000 (m), 953 (w), 929 (w), 873 (w), 847 (s), 777 (s), 696 (m), 599 (m), 559 (m), δ<sub>NCS</sub>: 471 (s).

Description of the crystal structure:

A fragment of the crystal structure of [Mn(2-picoline-N-oxide)(NCS)<sub>2</sub>]<sub>n</sub> (**21**) is presented in Figure 54 and selected bond parameters are summarized in Table 21. Mn(1) is six-coordinated by N(11), S(11), N(21''), S(21) of four μ<sub>(N,S)</sub> bridging isothiocyanato groups and by O(1) and O(1') of μ<sub>(O,O)</sub> bridging 2-picoline-N-oxide molecules in cis-conformation. The bond distances within the distorted MnN<sub>2</sub>O<sub>2</sub>S<sub>2</sub> octahedron are: Mn-N/O from 2.1562(2) to 2.195(2) Å, Mn-S are 2.6631(9) and 2.6685(10) Å. The isothiocyanato groups form di-μ<sub>(N,S)</sub> double bridges to connect the Mn(II) centers to corrugated polymeric chains. These polymeric chains are further connected by the centrosymmetrically related μ<sub>(O,O)</sub> bridging 2-picoline-N-oxide molecules to generate a "honeycomb"-like 2D system [38] extended along the a- and b-axis of the unit cell (Figure 55). Both centrosymmetric and eight-membered Mn(NCS)<sub>2</sub>Mn rings adopt a "chair-like" arrangement ["chair angle" θ defined as acute angle between plane of the di-μ<sub>(N,S)</sub> thiocyanato bridges and the Mn/N/S plane is 7.8 and 11.4°, respectively]. The torsions angles are: Mn(1)-N(11)...S(11'')-Mn(1'') = ± 28.9°, Mn(1)-N(21'')...S(21\*)-Mn(1\*) = ± 39.3°. The four-membered Mn<sub>2</sub>O<sub>2</sub> rings formed by the μ<sub>(O,O)</sub> bridging 2-picoline-N-oxide molecules are planar. The Mn(1)-O(1)-Mn(1') and O(1)-Mn(1)-O(1') bond angles are 109.12(8) and 70.88(8)°. The Mn-O(1)-N(1) bond angles are 123.28(15) and 125.51(16)°; the Mn-O(1)-N(1)-C(1) torsion angle is ± 80.5°. The intra-plane metal-metal distances are: Mn(1)...Mn(1') = 3.5724(7), Mn(1)...Mn(1'') = 5.9206(9), Mn(1)...Mn(1\*) = 5.9175(9) Å, whereas the shortest Mn...Mn inter-planar separation is 7.5702(10) Å. The Mn(1\*)...Mn(1)...Mn(1'') is 140.5°.

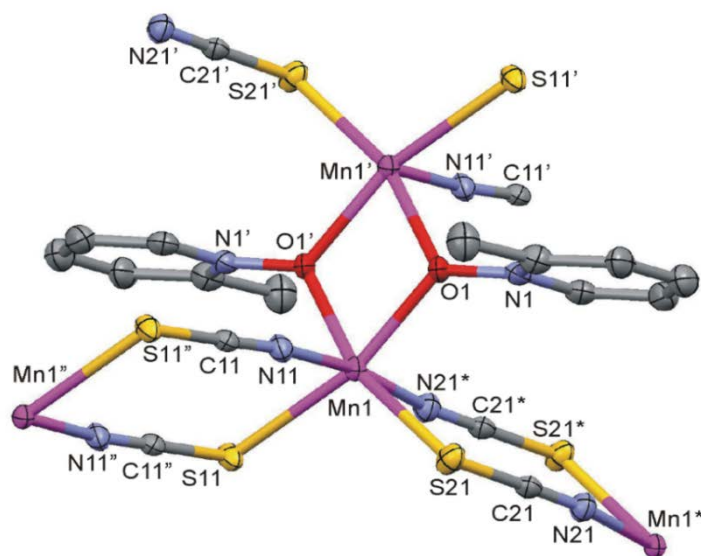


Figure 54: Perspective view of a section of [Mn(2-picoline-N-oxide)(NCS)<sub>2</sub>]<sub>n</sub> (**21**)

Symmetry codes: (') 1-x, 1-y, -z; (") 1-x, -y, -z; (\*) -x,1-y,-z.

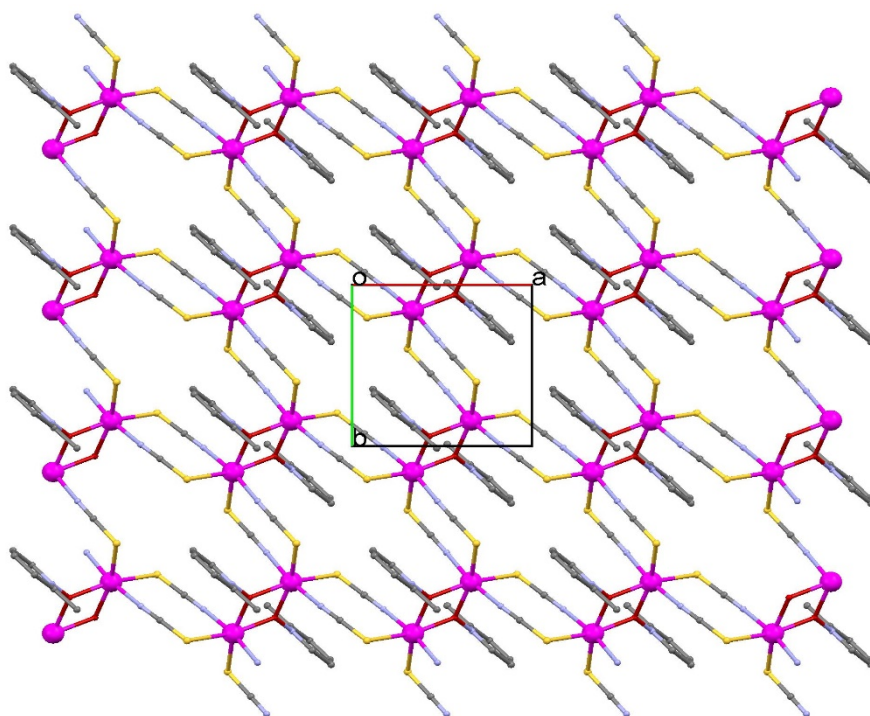


Figure 55: Packing plot of  $[Mn(2\text{-picoline-N-oxide})(NCS)_2]_n$  (**21**)

Table 21: Selected bond parameters of  $[Mn(2\text{-picoline-N-oxide})(NCS)_2]_n$  (**21**)

Mn(1)-N(11)	2.156(2)	Mn(1)-N(21'')	2.162(2)
Mn(1)-O(1)	2.1894(19)	Mn(1)-O(1')	2.195(2)
Mn(1)-S(21)	2.6631(9)	Mn(1)-S(11)	2.6685(10)
N(11)-C(11)	1.154(4)	C(11)-S(11'')	1.651(3)
N(21)-C(21)	1.153(4)	C(21)-S(21)	1.650(3)
O(1)-N(1)	1.338(3)		
N(11)-Mn(1)-N(21)	171.22(9)	N(11)-Mn(1)-O(1')	93.73(8)
N(21)-Mn(1)-O(1)	93.34(8)	N(11)-Mn(1)-O(1)	93.56(9)
N(21)-Mn(1)-O(1)	93.67(8)	N(11)-Mn(1)-S(21)	85.47(7)
N(21)-Mn(1)-S(21)	89.21(7)	N(11)-Mn(1)-S(11)	89.39(6)
N(21)-Mn(1)-S(11)	85.50(7)	N(11)-C(11)-S(11)	179.3(3)
N(21)-C(21)-S(21)	179.0(2)	N(1)-O(1)-Mn(1)	125.51(16)
Mn(1)-O(1)-Mn(1)	109.12(8)	N(1)-O(1)-Mn(1)	123.28(15)
O(1)-Mn(1)-O(1')	70.88(8)	O(1)-Mn(1)-S(21)	91.03(5)
O(1)-Mn(1)-S(21)	161.80(5)	O(1)-Mn(1)-S(11)	161.74(6)
O(1)-Mn(1)-S(11)	90.98(5)	S(21)-Mn(1)-S(11)	107.17(3)
C(11)-N(11)-Mn(1)	164.7(2)	C(11)-S(11)-Mn(1)	103.81(10)
C(21)-N(21)-Mn(1)	162.7(2)	C(21)-S(21)-Mn(1)	103.72(10)

Symmetry codes: (') 1-x, 1-y, -z; (') -x, 1-y, -z.

## 7.2 $[\text{Mn}(\text{3-picoline-N-oxide})_2(\text{NCS})_2]_n$ (**22**)

$\text{Mn}(\text{NO}_3)_2 \cdot 4\text{H}_2\text{O}$  (1.00 g, 4.00 mmol), 3-methylpyridine-N-oxide (0.22 g, 2.00 mmol) and KSCN (0.78 g, 8.00 mmol) were dissolved in 4.0 mL distilled water at room temperature. After four days at room temperature yellow crystals appeared (yield: 0.47 g, 61%). *Anal.* Calc. for  $\text{C}_{14}\text{H}_{14}\text{MnN}_4\text{O}_2\text{S}_2$  (389.35 g/mol): C, 43.2; H, 3.6; N, 14.4. Found: C, 43.0; H, 3.5; N, 14.5%. Selected IR bands (ATR-IR,  $\text{cm}^{-1}$ ):  $\nu_{\text{CN}}$ : 2096 (s), 2069 (vs), 1607 (w), 1580 (w), 1488 (m), 1453 (m), 1382 (w), 1315 (w), 1263 (m), 1160 (s), 1094 (w), 1049 (w), 1018 (m), 946 (m), 882 (m), 795 (s), 750 (m), 676 (s), 566 (s), 529 (w), 487 (s), 445 (w).

Description of the structure:

A section of the crystal structure of the 1:2 complex  $[\text{Mn}(\text{3-picoline-N-oxide})_2(\text{NCS})_2]_n$  (**22**) is presented in Figure 56 and selected bond parameters are summarized in Table 22. Mn(1) is six-coordinated by N(11), S(11) of two  $\mu_{(\text{N,S})}$  bridging isothiocyanato groups, N(21) of a terminal isothiocyanato group, by O(1) and O(1') of  $\mu_{(\text{O,O})}$  bridging 3-picoline-N-oxide molecules and O(2) of a terminal 3-picoline-N-oxide molecule. The bond distances within the distorted  $\text{MnN}_2\text{O}_3\text{S}$  octahedron are: Mn-N/O from 2.1890(14) to 2.3233(12) Å, Mn(1)-S(11) is 2.7470(7) Å. Along the a-axis of the triclinic unit cell the Mn(II) centers are alternatively connected by centrosymmetric di- $\mu_{(\text{N,S})}$  double isothiocyanato bridges and centrosymmetric  $\mu_{(\text{O,O})}$  bridging 3-picoline-N-oxides in cis-conformation. The polymeric chains are not linear  $[\text{Mn}(1') \dots \text{Mn}(1) \dots \text{Mn}(1^*) = 112.6^\circ]$  (Figure 57). The eight-membered  $\text{Mn}(\text{NCS})_2\text{Mn}$  ring adopts a "chair-like" arrangement ["chair angle"  $\theta$  defined as acute angle between plane of the di- $\mu_{(\text{N,S})}$  thiocyanato bridges and the Mn/N/S plane is  $10.0^\circ$ ]. The torsions angles are:  $\text{Mn}(1)\text{-N}(11) \dots \text{S}(11')\text{-Mn}(1'') = \pm 39.8^\circ$ ;  $\text{Mn}(1'')\text{-S}(11')\text{-C}(11'')\text{-N}(11) = \pm 109.3^\circ$ ;  $\text{Mn}(1'')\text{-N}(11'')\text{-C}(11'')\text{-S}(11) = \pm 150.6^\circ$ . The four-membered  $\text{Mn}_2\text{O}_2$  ring formed by the  $\mu_{(\text{O,O})}$  bridging 3-picoline-N-oxide molecules is planar. The Mn(1)-O(1)-Mn(1') and O(1)-Mn(1)-O(1') bond angles are  $105.77(5)$  and  $74.23(5)^\circ$ . The intra-chain metal-metal distances are:  $\text{Mn}(1) \dots \text{Mn}(1') = 3.6104(5)$ ,  $\text{Mn}(1) \dots \text{Mn}(1'') = 5.9306(7)$  Å, whereas the shortest Mn...Mn inter-chain separation is  $8.0423(10)$  Å. The bond parameters of the  $\mu_{(\text{O,O})}$  bridging 3-picoline-N-oxide are:  $\text{Mn-O}(1)\text{-N}(1) = 122.99(8)$  and  $124.39(8)^\circ$ ; the Mn-O(1)-N(1)-C(1) torsion angle is  $\pm 61.0^\circ$ . The bond parameters of the terminal 3-picoline-N-oxide molecule are:  $\text{Mn-O}(2)\text{-N}(2) = 117.08(9)^\circ$ ; Mn-O(2)-N(2)-C(13) torsion angle =  $78.2^\circ$ . The Mn(1)-N(21)-C(21) angle and Mn(1)-N(21)-C(21)-S(21) torsion angle of the terminal isothiocyanato ligand is  $165.64(13)$  and  $-85.7^\circ$ , respectively.

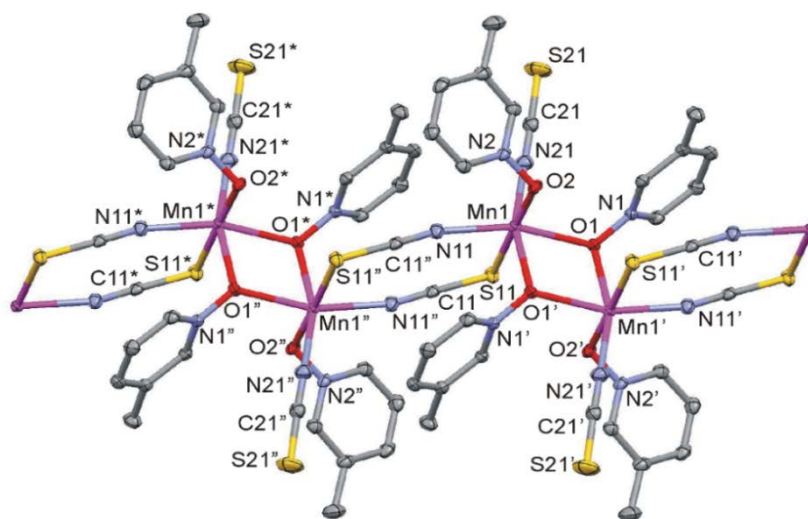


Figure 56: Perspective view of a section of  $[\text{Mn}(\text{3-picoline-N-oxide})_2(\text{NCS})_2]_n$  (**22**)

Symmetry codes: (') -x, 2-y, -z; (") 1-x, 2-y, -z; (\*) 1+x, y, z.

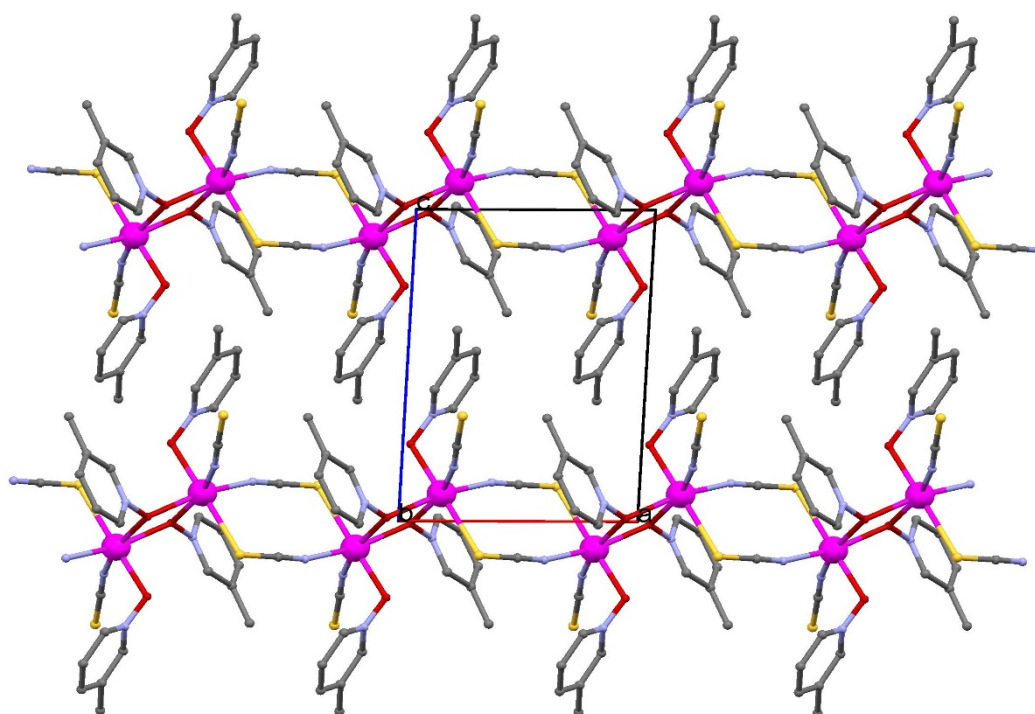


Figure 57: Packing plot of  $[Mn(3\text{-picoline-N-oxide})_2(NCS)_2]_n$  (**22**)

Table 22: Selected bond parameters of  $[Mn(3\text{-picoline-N-oxide})_2(NCS)_2]_n$  (**22**)

Mn(1)-N(11)	2.1890(14)	Mn(1)-O(2)	2.1942(12)
Mn(1)-O(1)	2.2037(11)	Mn(1)-N(21)	2.2657(15)
Mn(1)-O(1')	2.3233(12)	Mn(1)-S(11)	2.7470(7)
N(11)-C(11'')	1.185(2)	C(11)-S(11)	1.6838(17)
N(21)-C(21)	1.207(2)	C(21)-S(21)	1.7059(18)
O(1)-N(1)	1.4010(17)	O(2)-N(1)	1.3315(17)
N(11)-Mn(1)-O(2)	90.32(5)	N(11)-Mn(1)-O(1)	160.82(5)
N(11)-Mn(1)-N(21)	109.71(6)	N(11)-Mn(1)-O(1')	87.25(5)
N(21)-Mn(1)-O(1')	162.86(5)	N(11)-Mn(1)-S(11)	91.15(4)
N(21)-Mn(1)-S(11)	89.32(4)	N(11)-C(11)-S(11)	178.62(14)
N(21)-C(21)-S(21)	178.59(15)	N(1)-O(1)-Mn(1)	124.39(8)
N(1)-O(1)-Mn(1)	122.99(8)	N(2)-O(2)-Mn(1)	117.08(9)
Mn(1)-O(1)-Mn(1)	105.77(5)	O(2)-Mn(1)-O(1)	93.70(4)
O(2)-Mn(1)-N(21)	89.97(5)	O(1)-Mn(1)-N(21)	89.06(5)
O(2)-Mn(1)-O(1')	87.37(5)	O(1)-Mn(1)-O(1')	74.23(5)
O(2)-Mn(1)-S(11)	178.51(3)	O(1)-Mn(1)-S(11)	84.97(3)
O(1)-Mn(1)-S(11)	92.91(3)	C(11'')-N(11)-Mn(1)	165.23(12)
C(11)-S(11)-Mn(1)	99.54(6)	C(21)-N(21)-Mn(1)	165.64(13)

Symmetry codes: (') -x, 2-y, -z; (') 1-x, 2-y, -z.

### 7.3 $[\text{Mn}(\text{4-picoline-N-oxide})_2(\text{NCS})_2(\text{H}_2\text{O})_2]_n$ (**23**)

$\text{Mn}(\text{NO}_3)_2 \cdot 4\text{H}_2\text{O}$  (1.00 g, 4.00 mmol), 4-methylpyridine-N-oxide (0.22 g, 2.00 mmol) and KSCN (0.78 g, 8.00 mmol) were dissolved in 4.5 mL distilled water at room temperature. After four days at room temperature yellow crystals appeared (yield: 0.67 g, 79%). *Anal.* Calc. for  $\text{C}_{14}\text{H}_{18}\text{MnN}_4\text{O}_4\text{S}_2$  (425.38 g/mol): C, 39.5; H, 4.3; N, 13.2%. Selected IR bands (ATR-IR,  $\text{cm}^{-1}$ ):  $\nu_{\text{OH}}$ : 3336 (s,br),  $\nu_{\text{CN}}$ : 2072 (s), 2041 (s), 1654 (m), 1628 (m), 1497 (s), 1458 (m), 1365 (m), 1244 (w), 1209 (m), 1181 (s), 1121 (m), 1045 (w), 968 (w), 944 (w), 852 (m),  $\nu_{\text{CS}}$ : 826 (s), 758 (m), 690 (w), 618 (m), 513 (m),  $\delta_{\text{NCS}}$ : 472 (m).

Description of the crystal structure:

A perspective view of the crystal structure of the monomeric complex  $[\text{Mn}(\text{4-picoline-N-oxide})_2(\text{NCS})_2(\text{H}_2\text{O})_2]_n$  (**23**) together with the atom numbering scheme is presented in Figure 58 and selected bond parameters are given in Table 23. Mn(1) is six-coordinated by N(11), N(21) of two terminal isothiocyanato groups, by O(1) and O(2) of two terminal 4-picoline-N-oxide molecules, and O(3) and O(4) of two terminal aqua ligands. The bond distances within the distorted  $\text{MnN}_2\text{O}_4$  octahedron are: Mn-N is 2.134(2) and 2.156(2) Å, Mn-O from 2.2078(18) to 2.2745(17) Å. The trans-coordinated terminal isothiocyanato ligands have Mn-N-C, N-C-S angles and Mn-N-C-S torsions angles of 158.1(2) and 167.4(2)°, 178.8(2) and 177.9(2)°, -25.0 and 151.5°, respectively. The cis-coordinated terminal 4-picoline-N-oxide molecules form Mn-O-N angles and Mn-O-N-C torsions angles of 111.78(12) and 117.34(13)°, -99.0 and 109.2°, respectively; their mean planes form an inter-planar angle of 72.7°. The aqua ligand forms hydrogen bonds of type O-H...O and O-H...S to generate a supramolecular 1D system along the a-axis of the triclinic unit cell (Figure 59):

$\text{O}(3)\dots\text{O}(2)(1+x,y,z) = 2.758(2)$  Å,  $\text{O}(3)\text{-H}(31)\dots\text{O}(2) = 175(3)^\circ$ ;

$\text{O}(3)\dots\text{S}(11)(1+x,y,z) = 3.461(2)$  Å,  $\text{O}(3)\text{-H}(32)\dots\text{S}(11) = 161(2)^\circ$ ;

$\text{O}(4)\dots\text{O}(1)(2-x,1-y,1-z) = 2.823(2)$  Å,  $\text{O}(4)\text{-H}(41)\dots\text{O}(1) = 169(2)^\circ$ ;

$\text{O}(4)\dots\text{O}(1)(1+x,y,z) = 2.783(2)$  Å,  $\text{O}(4)\text{-H}(42)\dots\text{O}(1) = 174(3)^\circ$ .

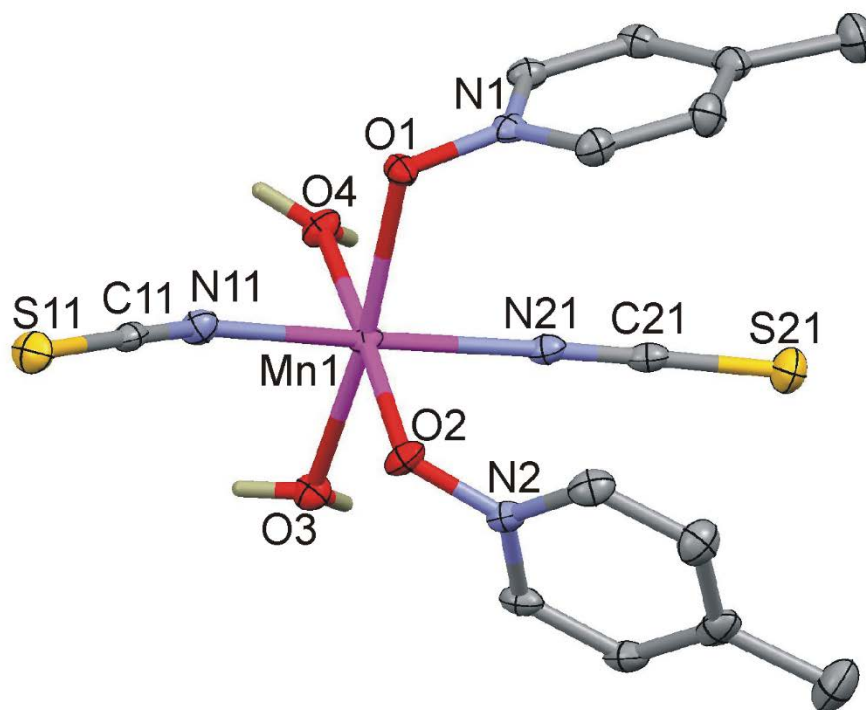


Figure 58: Perspective view of  $[\text{Mn}(\text{4-picoline-N-oxide})_2(\text{NCS})_2(\text{H}_2\text{O})_2]_n$  (**23**)

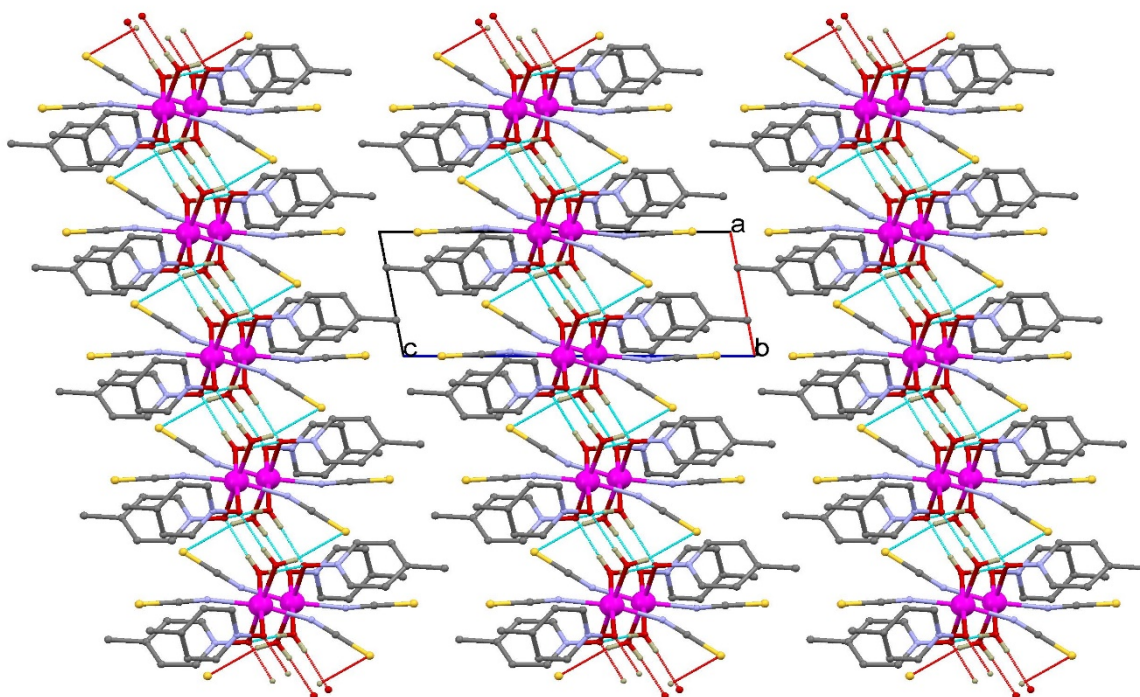


Figure 59: Packing plot of  $[Mn(4\text{-picoline-N-oxide})_2(NCS)_2(H_2O)_2]_n$  (**23**)

Table 23: Selected bond parameters of  $[Mn(4\text{-picoline-N-oxide})_2(NCS)_2(H_2O)_2]_n$  (**23**)

Mn(1)-N(11)	2.134(2)	Mn(1)-N(21)	2.156(2)
Mn(1)-O(4)	2.2078(18)	Mn(1)-O(2)	2.2152(18)
Mn(1)-O(3)	2.2480(19)	Mn(1)-O(1)	2.2745(17)
N(11)-C(11)	1.162(3)	C(11)-S(11)	1.633(3)
N(21)-C(21)	1.172(3)	C(21)-S(21)	1.625(3)
O(1)-N(1)	1.357(3)	O(2)-N(2)	1.342(3)
N(11)-Mn(1)-N(21)	168.94(8)	N(11)-Mn(1)-O(4)	95.77(8)
N(21)-Mn(1)-O(4)	92.66(8)	N(11)-Mn(1)-O(2)	83.61(7)
N(21)-Mn(1)-O(2)	88.31(7)	N(11)-Mn(1)-O(3)	93.25(8)
N(21)-Mn(1)-O(3)	94.33(7)	N(11)-Mn(1)-O(1)	83.73(7)
N(21)-Mn(1)-O(1)	89.84(7)	N(11)-C(11)-S(11)	178.8(2)
N(21)-C(21)-S(21)	177.9(2)	N(1)-O(1)-Mn(1)	111.78(12)
N(2)-O(2)-Mn(1)	117.34(13)	O(4)-Mn(1)-O(2)	177.21(7)
O(4)-Mn(1)-O(3)	86.97(7)	O(2)-Mn(1)-O(3)	90.35(7)
O(4)-Mn(1)-O(1)	85.44(7)	O(2)-Mn(1)-O(1)	97.19(6)
O(3)-Mn(1)-O(1)	171.50(6)	C(11)-N(11)-Mn(1)	158.1(2)
C(21)-N(21)-Mn(1)	167.4(2)		

#### 7.4 [Mn(4-cyanopyridine-N-oxide)<sub>2</sub>(NCS)<sub>2</sub>(H<sub>2</sub>O)]<sub>2</sub> (**24**)

Mn(NO<sub>3</sub>)<sub>2</sub>·4H<sub>2</sub>O (1.00 g, 4.00 mmol), 4-cyanopyridine-N-oxide (0.24 g, 2.00 mmol) and KSCN (0.78 g, 8.00 mmol) were dissolved in 5.1 mL distilled water at 50°C. Upon slow cooling to room temperature yellow crystals of **24** were separated after four days (yield: 0.59 g, 69%). *Anal.* Calc. for C<sub>14</sub>H<sub>10</sub>MnN<sub>6</sub>O<sub>3</sub>S<sub>2</sub> (429.34 g/mol): C, 39.2; H, 2.3; N, 19.6. Found: C, 39.2; H, 2.3; N, 19.4%. Selected IR bands (ATR-IR, cm<sup>-1</sup>): ν<sub>OH</sub>: 3364 (s,br), 2086 (s), ν<sub>CN</sub>: 2055 (vs), 1635 (m), 1552 (w), 1514 (w), 1482 (s), 1436 (m), 1392 (w), 1219 (s), 1172 (s), 1103 (w), 1046 (w), 971 (w), 948 (w), 850 (s), 723 (m), 668 (w), 611 (w), 551 (m), 454 (m).

Description of the crystal structure:

A perspective view together with the atom numbering scheme of the crystal structure of [Mn(4-cyanopyridine-N-oxide)<sub>2</sub>(NCS)<sub>2</sub>(H<sub>2</sub>O)]<sub>2</sub> (**24**) is shown in Figure 60 and selected bond parameters are listed in Table 24. The octahedron round Mn(1) is formed by N(11') and S(11) of two μ<sub>(N,S)</sub> bridging isothiocyanato groups, by N(21) of a terminal isothiocyanato group, O(1) and O(2) of two trans-coordinated terminal 4-cyanopyridine-N-oxide molecules and O(3) of a terminal aqua ligand [Mn-N = 2.1000(17) and 2.1229(17), Mn-S = 2.8185(7), Mn-O from 2.2064(14) to 2.2214(14) Å]. Centrosymmetric dimeric units are built by μ<sub>(N,S)</sub> isothiocyanato double bridges. Their eight-membered Mn(NCS)<sub>2</sub>Mn ring adopt a "chair-like" arrangement ["chair angle" θ defined as angle between plane of the di-μ<sub>(N,S)</sub> thiocyanato bridges and the Mn(1)/N(11')/S(11) plane is 170.7°]. The torsion angle: Mn(1)-S(11)...N(11)-Mn(1') = ± 37.4°. The isothiocyanato group have the following bond parameters: Mn-N-C: 164.39(15) and 167.08(15)°, Mn-S-C: 103.13(7)°, N-C-S: 177.60(17) and 177.67(16)°, N-C: 1.165(2) and 1.171(2) Å, C-S: 1.6251(19) and 1.6383(19) Å. The terminal 4-cyanopyridine-N-oxide molecules have Mn-O-N bond angles of 114.38(10) and 115.38(10)°; the Mn(1)-O(1)-N(1)-C(7) and Mn(1)-O(2)-N(2)-C(8) torsion angles are 93.5 and 96.6°, respectively. The 4-cyanopyridine-N-oxide molecules form an inter-planar angle of 9.3°. The Mn(1)...Mn(1') distance within the Mn(NCS)<sub>2</sub>Mn ring is 6.0149(8) Å, the shortest Mn...Mn inter-dimer separation is 5.4108(7) Å. The aqua ligand forms hydrogen bonds of type O-H...O to O atoms of adjacent 4-cyanopyridine-N-oxide molecules to generate a supramolecular 2D system oriented along the a- and b-axis of the unit cell (Figure 61) [O(3)...O(1)(1-x,2-y,-z) = 2.954(2) Å, O(3)-H(31)...O(1) = 178(2)°; O(3)...O(2)(-x,2-y,-z) = 2.8821(19) Å, O(3)-H(32)...O(2) = 176(2)°].

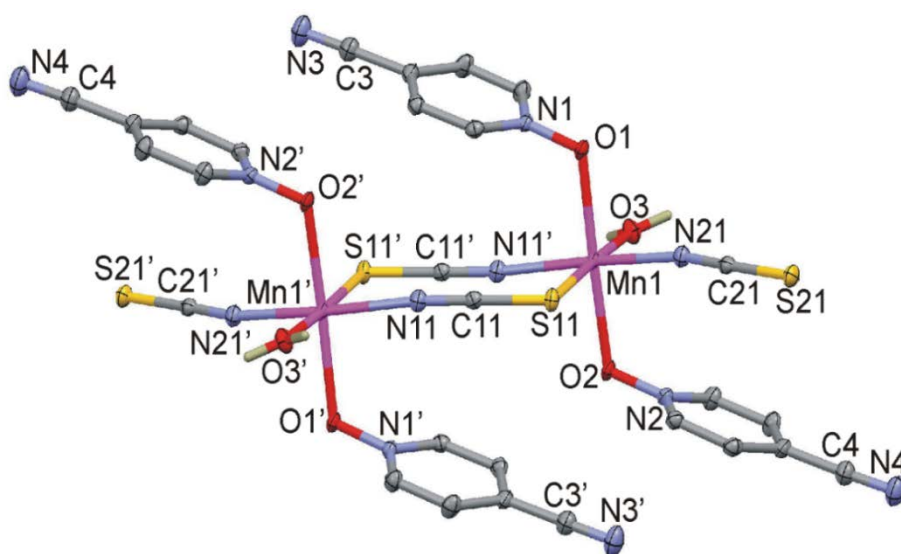


Figure 60: Perspective view of [Mn(4-cyanopyridine-N-oxide)<sub>2</sub>(NCS)<sub>2</sub>(H<sub>2</sub>O)]<sub>2</sub> (**24**)

Symmetry code: (') 1-x, -y, 1-z.

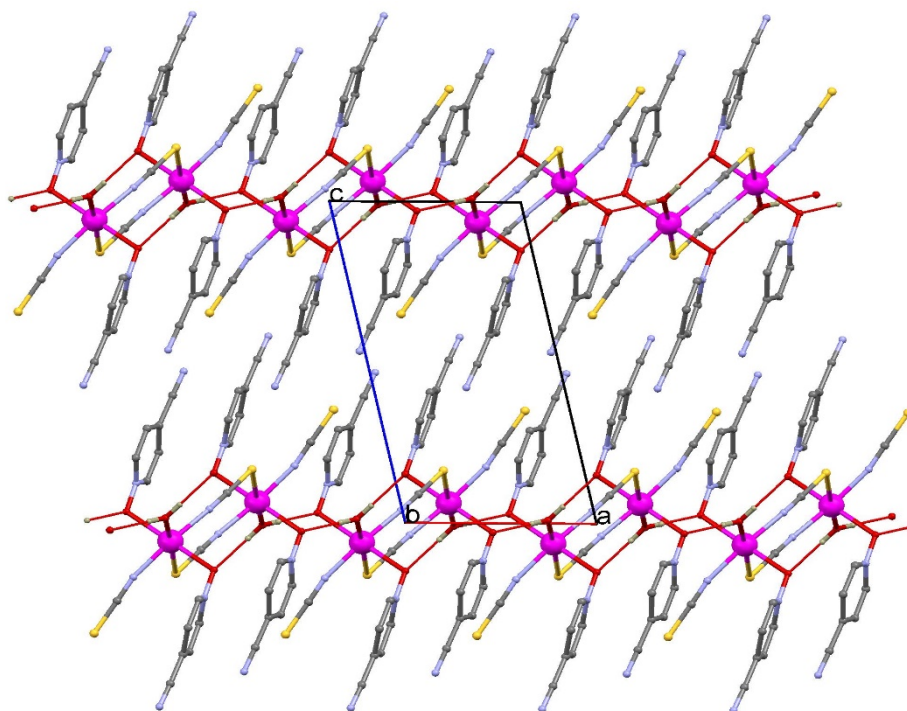


Figure 61: Packing plot of  $[\text{Mn}(\text{4-cyanopyridine-N-oxide})_2(\text{NCS})_2(\text{H}_2\text{O})]_2$  (**24**)

Table 24: Selected bond parameters of  $[\text{Mn}(\text{4-cyanopyridine-N-oxide})_2(\text{NCS})_2(\text{H}_2\text{O})]_2$  (**24**)

Mn(1)-N(21)	2.1000(17)	Mn(1)-N(11')	2.1229(17)
Mn(1)-O(1)	2.2064(14)	Mn(1)-O(2)	2.2090(14)
Mn(1)-O(3)	2.2214(14)	Mn(1)-S(11)	2.8185(7)
N(11)-C(11)	1.165(2)	C(11)-S(11)	1.6383(19)
N(21)-C(21)	1.171(2)	C(21)-S(21)	1.6251(19)
O(1)-N(1)	1.3402(19)	O(2)-N(2)	1.3342(19)
N(21)-Mn(1)-N(11')	169.17(6)	N(21)-Mn(1)-O(1)	87.49(6)
N(11')-Mn(1)-O(1)	93.09(6)	N(21)-Mn(1)-O(1)	92.01(6)
N(11')-Mn(1)-O(2)	87.97(6)	N(21)-Mn(1)-O(3)	95.67(6)
N(11')-Mn(1)-O(3)	95.15(6)	N(21)-Mn(1)-S(11)	81.61(5)
N(11')-Mn(1)-S(11)	87.56(5)	N(11)-C(11)-S(11)	177.67(16)
N(21)-C(21)-S(21)	177.60(17)	N(1)-O(1)-Mn(1)	114.38(10)
N(2)-O(2)-Mn(1)	115.38(10)	O(1)-Mn(1)-O(2)	176.99(5)
O(1)-Mn(1)-O(3)	89.04(5)	O(2)-Mn(1)-O(3)	88.06(5)
O(1)-Mn(1)-S(11)	91.91(4)	O(2)-Mn(1)-S(11)	90.96(4)
O(3)-Mn(1)-S(11)	177.08(4)	O(1)-N(1)-C(7)	119.15(15)
C(11)-N(11)-Mn(1')	164.39(15)	C(11)-S(11)-Mn(1)	103.13(7)
C(21)-N(21)-Mn(1)	167.08(15)		

Symmetry codes: (') -x, 1-y, -z.



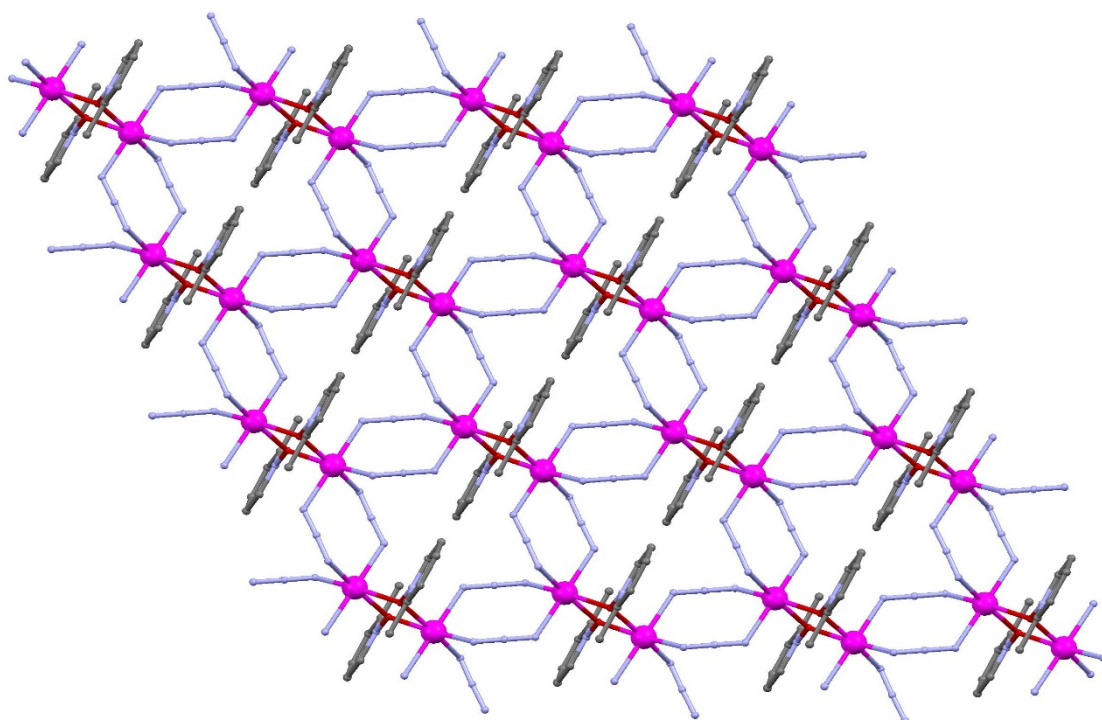


Figure 63: Packing plot of  $[Mn(2\text{-picoline-N-oxide})(N_3)_2]_n$  (**25**)

Table 25: Selected bond parameters of  $[Mn(2\text{-picoline-N-oxide})(N_3)_2]_n$  (**25**)

Mn(1)-O(1)	2.171(4)	Mn(1)-N(21)	2.185(5)
Mn(1)-N(13)	2.186(6)	Mn(1)-N(11)	2.226(4)
Mn(1)-N(23)	2.237(4)	O(1)-N(1)	1.350(5)
N(11)-N(12)	1.185(7)	N(12)-N(13)	1.189(7)
N(21)-N(22'')	1.175(7)	N(22)-N(23*)	1.173(7)
Mn(1)-O(1')	2.174(4)		
Mn(1)-O(1)-Mn(1')	106.55(15)	O(1)-Mn(1)-N(21)	94.49(18)
O(1')-Mn(1)-N(21)	167.89(19)	O(1)-Mn(1)-N(13)	169.01(16)
O(1')-Mn(1)-N(13)	95.66(17)	O(1)-Mn(1)-N(11)	90.64(18)
O(1')-Mn(1)-N(11)	89.94(16)	O(1)-Mn(1)-N(23)	89.54(18)
O(1')-Mn(1)-N(23)	90.07(16)	O(1)-Mn(1)-O(1')	73.45(15)
N(1)-O(1)-Mn(1)	124.2(3)	N(1)-O(1)-Mn(1')	125.3(3)
N(21)-Mn(1)-N(13)	96.4(2)	N(21)-Mn(1)-N(11)	89.08(17)
N(13)-Mn(1)-N(11)	90.76(18)	N(21)-Mn(1)-N(23)	90.94(16)
N(13)-Mn(1)-N(23)	89.06(19)	N(11)-Mn(1)-N(23)	179.8(2)
N(12'')-N(11)-Mn(1)	125.7(4)	N(11'')-N(12)-N(13)	177.8(6)
N(12)-N(13)-Mn(1)	120.2(4)	N(22)-N(21)-Mn(1)	122.6(4)
N(23*)-N(22)-N(21)	177.8(5)	N(22*)-N(23)-Mn(1)	126.1(4)

Symmetry codes: (') -x, -y, 2-z; (') -x, 1-y, 2-z; (\*) 1-x, -y, 2-z-

## 7.6 $[\text{Mn}(\text{N}_3)_2(\text{H}_2\text{O})_2]_n(3\text{-picoline-N-oxide})_{2n}$ (**26**)

$\text{Mn}(\text{NO}_3)_2 \cdot 4\text{H}_2\text{O}$  (1.06 g, 4.24 mmol), 3-methylpyridine-N-oxide (0.23 g, 2.09 mmol) and  $\text{NaN}_3$  (0.53 g, 8.15 mmol) were dissolved in 6 mL distilled water at room temperature. After one day at room temperature yellow crystals appeared (yield: 0.42 g, 54%). *Anal.* Calc. for  $\text{C}_{12}\text{H}_{18}\text{MnN}_8\text{O}_4$  (393.28 g/mol): C, 36.7; H, 4.6; N, 28.5. Found: C, 34.6; H, 4.5; N, 27.5%. Selected IR bands (ATR-IR,  $\text{cm}^{-1}$ ):  $\nu_{\text{OH}}$ : 3362 (w), 3313 (s,br), 3051 (w),  $\nu_a$ : 2044 (vs), 1804 (w), 1655 (w), 1607 (m), 1579 (w), 1492 (m), 1454 (m), 1414 (m), 1323 (s),  $\nu_s$ : 1257 (s), 1160 (s), 1090 (m), 1010 (m), 940 (m), 920 (w), 883 (w), 799 (m), 744 (m), 672 (m),  $\delta_{\text{N}_3}$ : 640 (w), 616 (m), 564 (s), 543 (w), 494 (s), 433 (m).

Description of the crystal structure:

"A fragment of the crystal structure of  $[\text{Mn}(\text{N}_3)_2(\text{H}_2\text{O})_2]_n(3\text{-picoline-N-oxide})_{2n}$  (**26**) is shown in Figure 64, a packing plot is given in Figure 65. Selected bond parameters are listed in Table 26. All non-hydrogen atoms are located at special positions of space group *Ibam* (no. 72): Mn(1) at 4b with site symmetry 222, aqua oxygen atom O(1) at 8g with site symmetry 2, azido group and 3-picoline-N-oxide at 8j with site symmetry *m*. The single crystal structure determination revealed that complex (**26**) should be formulated as  $[\text{Mn}(\text{N}_3)_2(\text{H}_2\text{O})_2]_n(3\text{-picoline-N-oxide})_{2n}$  in which the 3-picoline-N-oxide molecules are non-coordinated and serve as stabilizers of the lattice. The structure of (**26**) consists of a 1D  $[\text{Mn}(\text{N}_3)_2(\text{H}_2\text{O})_2]_n$  chain running along the *c*-axis. Each manganese atom in the chain is linked to the two of each neighboring symmetry related counter parts by two azido ligands, i.e. each Mn(II) is ligated with four bridging azido ligands [ $\text{Mn-N} = 2.2387(11)$  Å] forming a cyclic four-membered  $\text{Mn}_2\text{N}_2$  unit. The remaining two coordination sites are occupied by atoms of two trans aqua molecules [ $\text{Mn-O} = 2.1609(14)$  Å]. The coordination environment of each Mn(II) is best described as a distorted octahedron with  $\text{MnN}_4\text{O}_2$  chromophore. The azido groups function in the  $\mu_{(1,1)}$  bridging fashion and are asymmetric [ $\text{N}(11)\text{-N}(12) = 1.213(2)$ ,  $\text{N}(12)\text{-N}(13) = 1.147(2)$  Å,  $\Delta d = 0.066$  Å]. The "out-of-plane" angle [37] of the azido group from the  $\text{Mn}_2\text{N}_2$  ring =  $39.5(2)^\circ$ . Each non-coordinated 3-picoline-N-oxide molecule forms two hydrogen bonds of type  $\text{O}\cdots\text{H-O}$  with oxygen atoms of two adjacent aqua molecules in the chain [ $\text{O}(2)\cdots\text{O}(1) = 2.6907(13)$  Å,  $\text{O}(2)\cdots\text{H}(92)\text{-O}(1) = 171.2(17)^\circ$ ](Figure 64 and 65). The intra-chain Mn...Mn distance is  $3.3173(3)$  Å, whereas the shortest inter-chain metal-metal separation is  $6.6346(7)$  Å. The present complex (**26**) is isomorphic to the corresponding Zn(II) complex." adopted from [38]

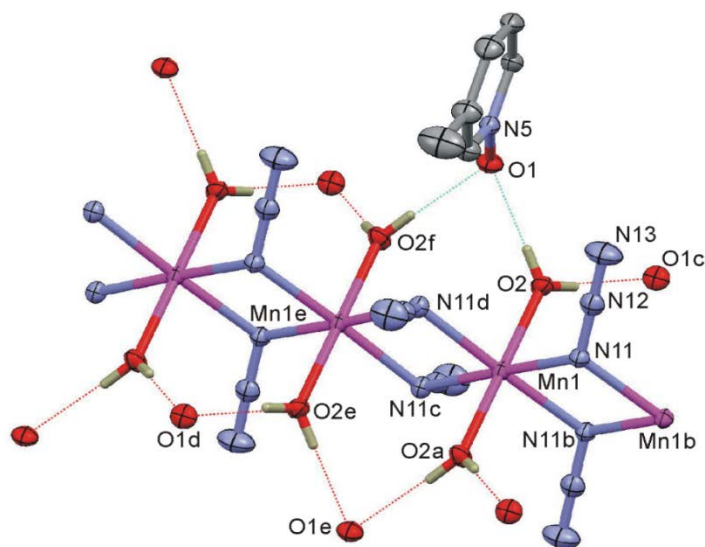


Figure 64: Perspective view of a section of  $[\text{Mn}(\text{N}_3)_2(\text{H}_2\text{O})_2]_n(3\text{-picoline-N-oxide})_{2n}$  (**26**)

Symmetry code: (a)  $-x, -y, z$ ; (b)  $-x, -y, -z$ ; (c)  $-x, -y, 1/2-z$ ; (d)  $x, -y, 1/2+z$ ; (e)  $-x, -y, 1-z$ ; (f)  $x, y, 1-z$ .

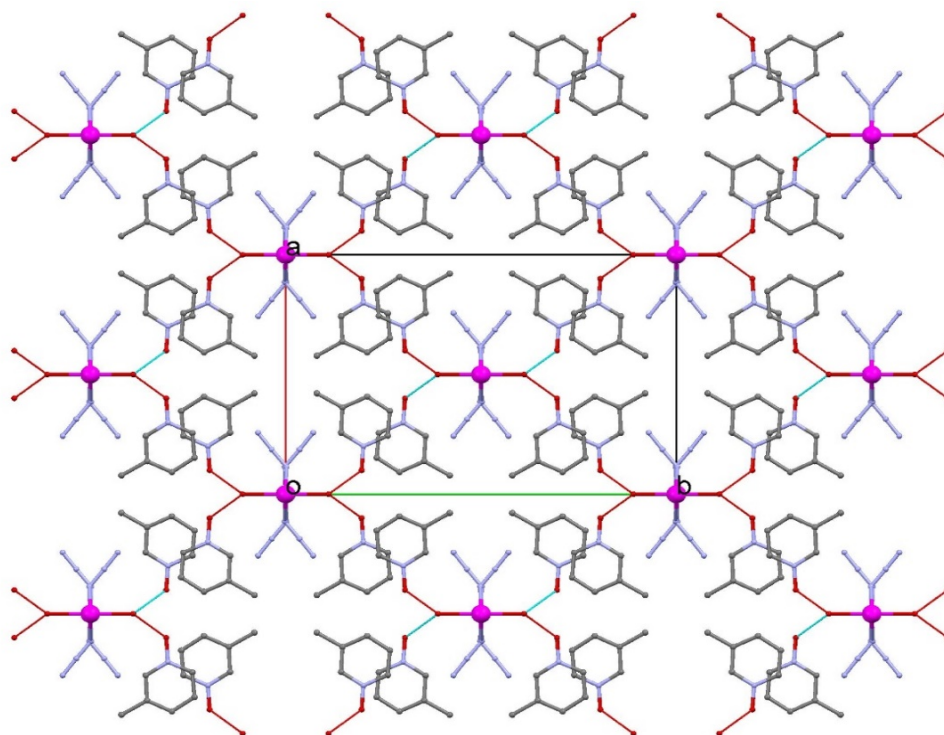


Figure 65: Packing plot of  $[Mn(N_3)_2(H_2O)_2]_n(3\text{-picoline-N-oxide})_{2n}$  (**26**)

Table 26: Selected bond parameters of  $[Mn(N_3)_2(H_2O)_2]_n(3\text{-picoline-N-oxide})_{2n}$  (**26**)

Mn(1)-O(2)	2.1609(14)	Mn(1)-N(11)	2.2387(11)
N(11)-N(12)	1.213(2)	N(12)-N(13)	1.147(2)
N(5)-O(1)	1.3362(19)		
O(2)-Mn(1)-O(2a)	180	N(11b)-Mn(1)-N(11d)	177.88(7)
O(2)-Mn(1)-N(11c)	91.06(3)	N(11)-Mn(1)-N(11d)	95.65(6)
N(12)-N(11)-Mn(1)	121.24(7)	N(13)-N(12)-N(11)	178.6(2)

Symmetry codes: (a)  $-x, -y, z$ ; (b)  $-x, -y, -z$ ; (c)  $-x, -y, 1/2-z$ ; (d)  $x, -y, 1/2+z$ .

## 7.7 [Mn<sub>3</sub>(N<sub>3</sub>)<sub>6</sub>(4-picoline-N-oxide)<sub>2</sub>(H<sub>2</sub>O)<sub>2</sub>]<sub>n</sub> (**27**)

Mn(NO<sub>3</sub>)<sub>2</sub>·4H<sub>2</sub>O (1.04 g, 4.16 mmol), 4-methylpyridine-N-oxide (0.21 g, 1.91 mmol) and NaN<sub>3</sub> (0.52 g, 8.15 mmol) were dissolved in 2.7 mL distilled water at room temperature. After five days at room temperature yellow crystals appeared (yield: 0.81 g, 61%). *Anal.* Calc. for C<sub>12</sub>H<sub>18</sub>Mn<sub>3</sub>N<sub>20</sub>O<sub>4</sub> (671.28 g/mol): C, 21.5; H, 2.7; N, 41.7. Found: C, 21.3; H, 2.7; 41.7%. Selected IR bands (ATR-IR, cm<sup>-1</sup>): ν<sub>OH</sub>: 3397 (s,br), 3109 (m), ν<sub>a</sub>: 2126 (vs), 2082 (vs), 2061 (vs), 1614 (w), 1492 (m), 1455 (w), 1349 (s), 1256 (s), ν<sub>s</sub>: 1199 (s), 1121 (w), 1033 (w), 952 (w), 852 (m), 828 (m), 761 (m), 696 (w), 649 (w), 632 (w), 608 (w), 550 (w), 474 (m).

Description of the crystal structure:

A part of the 3D network structure of [Mn<sub>3</sub>(N<sub>3</sub>)<sub>6</sub>(4-picoline-N-oxide)<sub>2</sub>(H<sub>2</sub>O)<sub>2</sub>]<sub>n</sub> (**27**) is shown in Figure 66, a packing plot is given in Figures 67 and 68, selected bond parameters are listed in Table 27. Complex (**27**) crystallizes in the orthorhombic space group Pccn with Z is 4. The 3D network is built up by trinuclear Mn(1)-Mn(2)-Mn(1a) subunits with the central Mn(2) located on a two-fold rotation axis. Mn(1) is octahedrally coordinated by four azido groups, one aqua ligand and one 4-picoline-N-oxide molecule. The octahedron around Mn(2) is formed by four azido groups and two 4-picoline-N-oxide molecules. Within the trinuclear subunit the central Mn(2) is connected to Mn(1) and Mn(1a) centers via N(11) and N(11a) of end-on azido groups and O(1) and O(1a) of μ<sub>(0,0')</sub> bridging 4-picoline-N-oxide molecules. The trinuclear subunits are connected by eight end-to-end azido bridges to generate the 3D network structure. The Mn-N bond distances are in the range from 2.1563(12) to 2.2248(11) Å, the Mn-O distances are in the range from 2.1861(10) to 2.2348(9) Å. The end-on azido bridge and the μ<sub>(0,0')</sub> bridging 4-picoline-N-oxide molecule have the following bond parameters: Mn(1)-N(11) = 2.2248(11), Mn(2)-N(11) = 2.1970(11), Mn(1)-O(1) = 2.2348(9), Mn(2)-O(1) = 2.2257(9) Å; Mn(1)-N(11)-Mn(2) = 104.96(4), Mn(1)-O(1)-Mn(2) = 103.68(3), N(11)-Mn(1)-O(1) = 73.88(4), N(11)-Mn(2)-O(1) = 74.96(4)°. The Mn(1)...Mn(2) separation is 3.5073(5) Å, the Mn(1)...Mn(2)...Mn(1a) angle is 133.7°. The three end-to-end bridging azido groups form the following torsion angles: Mn(1)-N(23)...N(21b)-Mn(2b) = -123.8°, Mn(1)-N(31)...N(31c)-Mn(1c) = 38.3°, Mn(1)-N(41)...N(41d)-Mn(1d) = 180°. The corresponding metal...metal separations are: Mn(1)...Mn(2b) = 6.1776(8), Mn(1)...Mn(1c) = 5.8156(8), Mn(1)...Mn(1d) = 6.0299(8)°. The Mn-N-N bond angles of the EE azido bridges [EE = end-end, μ<sub>(1,3)</sub>] are in the range from 125.23(7) to 143.43(10)°. The N(11)-N(12) and N(12)-N(13) bond distance of the asymmetric end-on azido group are 1.2020(15) and 1.1521(16) Å, the N-N bond distances of the symmetric end-to-end azido groups are in the range from 1.1630(16) to 1.1798(16) Å; the N-N-N bond angles of the azido groups vary from 175.79(19) to 180°. The μ<sub>(0,0')</sub> bridging 4-picoline-N-oxide forms Mn(2)-O(1)-N(1) and Mn(1)-O(1)-N(1) bond angles of 117.53(7) and 130.39(7)°, the Mn-O(1)-N(1)-C(1) torsions angles are -42.6 and 99.9° for Mn(1) and Mn(2), respectively. The aqua ligand forms hydrogen bonds of type O-H...N to N atoms of adjacent azido groups [O(2)...N(21) = 2.8263(17) Å, O(2)-H(90)...N(21) = 159(2)°; O(2)...N(13')(1/2+x,-y,1/2-z) = 2.8458(17) Å, O(2)-H(90)...N(13') = 179(2)°].

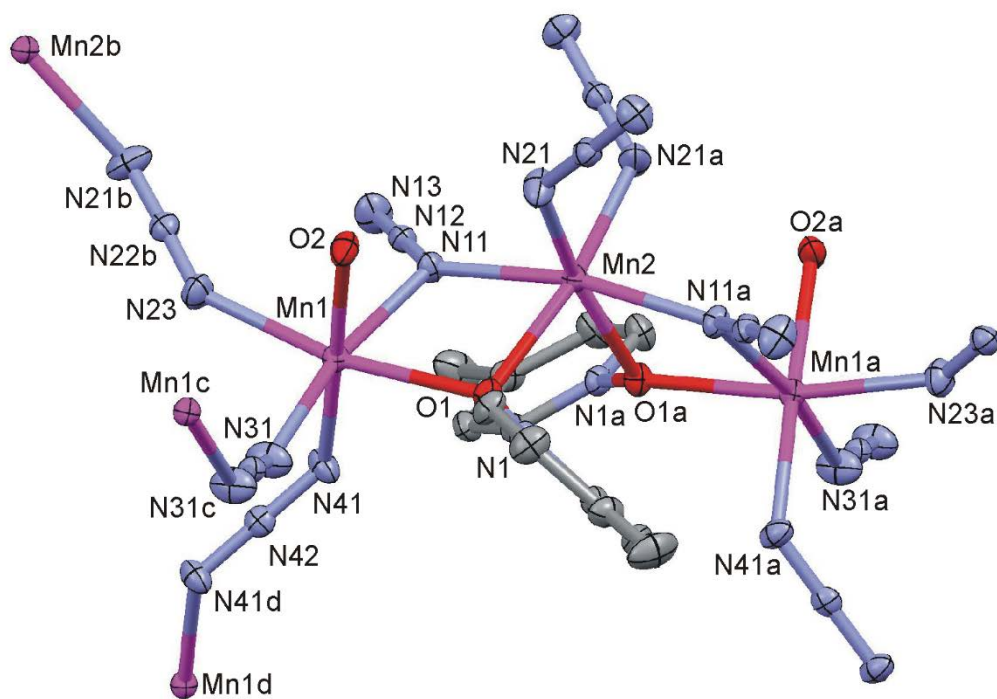


Figure 66: Perspective view with atom numbering scheme for the trinuclear subunit of  $[Mn_3(N_3)_6(4\text{-picoline-N-oxide})_2(H_2O)_2]_n$  (**27**)

Symmetry codes: (a)  $1/2-x, 1/2-y, z$ ; (b)  $2-x, -1/2+y, 1/2-z$ ; (c)  $5/2-x, 1/2-y, z$ ; (d)  $2-x, -y, -z$ ; (e)  $1/2+x, -y, 1/2-z$ ;

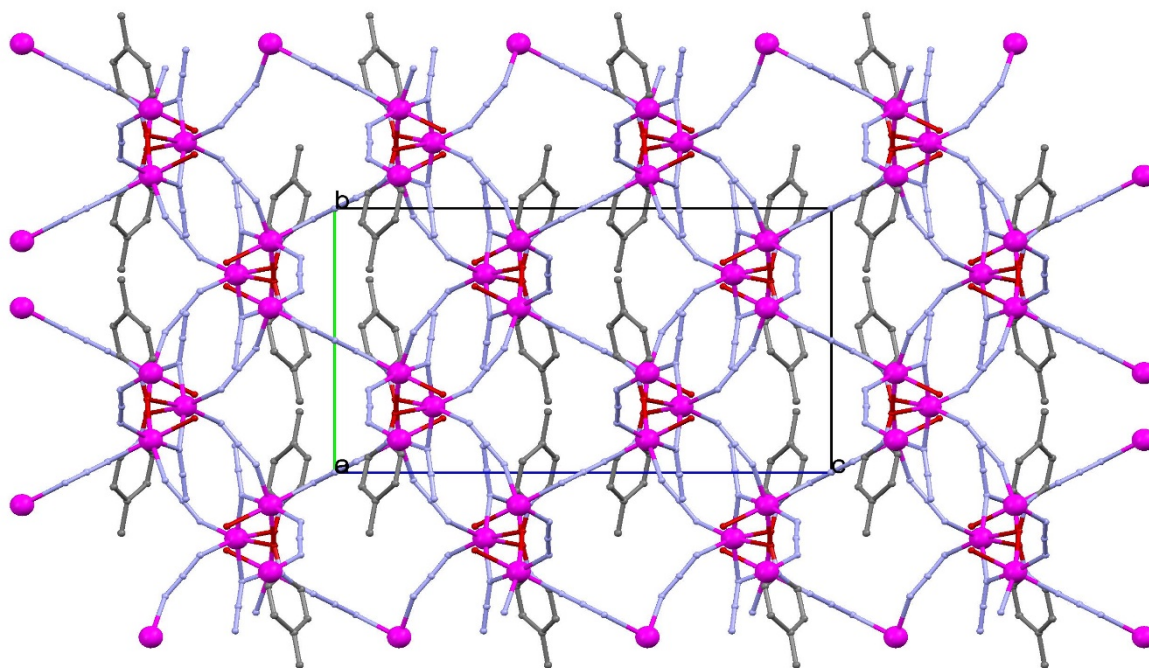


Figure 67: Packing plot of the 3D network of  $[Mn_3(N_3)_6(4\text{-picoline-N-oxide})_2(H_2O)_2]_n$  (**27**)

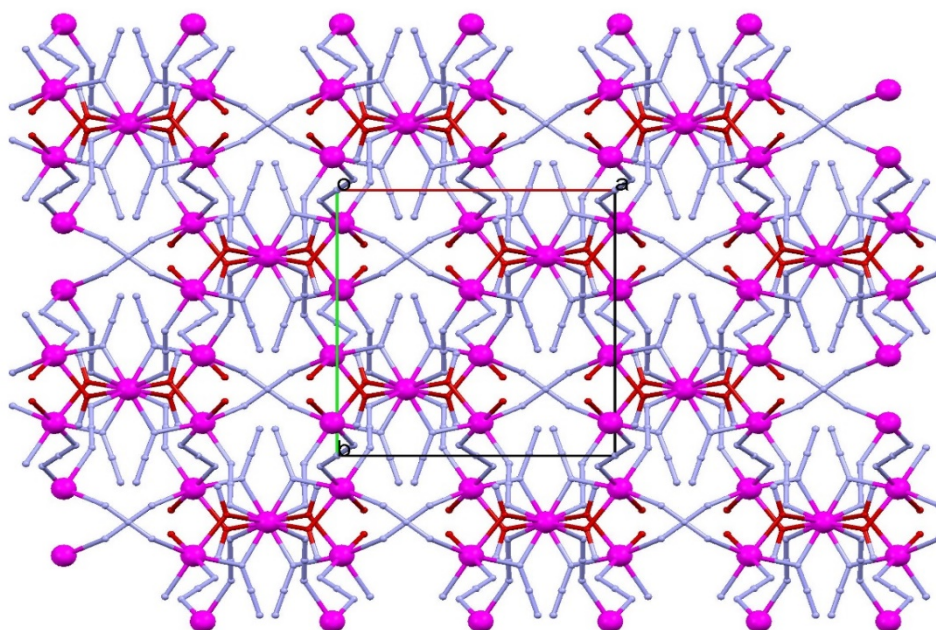


Figure 68: Mn-O-N-sublattice of  $[Mn_3(N_3)_6(4\text{-picoline-N-oxide})_2(H_2O)_2]_n$  (27)

Table 27: Selected bond parameters of  $[Mn_3(N_3)_6(4\text{-picoline-N-oxide})_2(H_2O)_2]_n$  (27)

Mn(1)-N(31)	2.1563(12)	Mn(1)-N(41)	2.1808(11)
Mn(1)-O(2)	2.1861(10)	Mn(1)-N(23)	2.2096(12)
Mn(1)-N(11a)	2.2248(11)	Mn(1)-O(1)	2.2348(9)
Mn(2)-N(11)	2.1970(11)	Mn(2)-N(21)	2.1983(12)
Mn(2)-O(1)	2.2257(9)	O(1)-N(1)	1.3547(13)
N(11)-N(12)	1.2020(15)	N(12)-N(13)	1.1521(16)
N(21)-N(22)	1.1798(16)	N(22)-N(23)	1.1630(16)
N(31a)-N(32)	1.1644(11)	N(41)-N(42)	1.1743(11)
Mn(2)-N(11)-Mn(1)	104.96(4)	Mn(2)-O(1)-Mn(1)	103.68(3)
O(2)-Mn(1)-N(23)	87.89(4)	O(2)-Mn(1)-N(11)	89.57(4)
O(2)-Mn(1)-O(1)	85.26(4)	O(1)-Mn(2)-O(1a)	92.67(5)
N(31)-Mn(1)-N(41)	88.64(4)	N(31)-Mn(1)-O(2)	91.27(4)
N(41)-Mn(1)-O(2)	178.75(4)	N(31)-Mn(1)-N(23)	94.66(5)
N(41)-Mn(1)-N(23)	90.87(5)	N(31)-Mn(1)-N(11)	168.95(5)
N(41)-Mn(1)-N(11)	90.76(4)	N(23)-Mn(1)-N(11)	96.39(4)
N(31)-Mn(1)-O(1)	95.20(4)	N(41)-Mn(1)-O(1)	95.99(4)
N(23)-Mn(1)-O(1)	168.11(4)	N(11)-Mn(1)-O(1)	73.88(4)
N(11)-Mn(2)-N(11a)	167.98(6)	N(11)-Mn(2)-N(21)	94.62(4)
N(11a)-Mn(2)-N(21)	93.43(4)	N(21)-Mn(2)-N(21a)	95.72(7)
N(11)-Mn(2)-O(1a)	96.96(4)	N(21)-Mn(2)-O(1a)	167.91(4)
N(11)-Mn(2)-O(1)	74.60(4)	N(12)-N(11)-Mn(2)	133.08(9)
N(12)-N(11)-Mn(1)	120.39(8)	N(13)-N(12b)-N(11)	178.22(13)
N(22)-N(21)-Mn(2)	132.10(10)	N(23)-N(22b)-N(21b)	178.11(14)
N(22b)-N(23)-Mn(1)	143.43(10)	N(32)-N(31)-Mn(1)	140.57(11)
N(31)-N(32)-N(31c)	175.79(19)	N(42)-N(41)-Mn(1)	125.23(7)
N(41)-N(42)-N(41d)	180	N(1)-O(1)-Mn(2)	117.53(7)
N(1)-O(1)-Mn(1)	130.39(7)		

Symmetrie codes: (a)  $1/2-x, 1/2-y, z$ ; (b)  $2-x, -1/2+y, 1/2-z$ ; (c)  $5/2-x, 1/2-y, z$ ; (d)  $2-x, -y, -z$ .

## 8) Luminescence data

### 8.1 Introduction

The following specimens are pre-investigated with a UV (ultra violet) mercury vapor lamp at two different wavelengths (254 and 366 nm).

All samples were measured using the “phosphorescence” mode of the Perkin Elmer LS 55 spectrophotometer. The specimen carrier was adjusted, by two screws (white rings in Figure 69). To ensure, that the focus is always in the focal plane, the intensity was observed by adjusting the specimen carrier with the aid of a well-known substance. In our case scheelite ( $\text{CaWO}_4$ ) was used, because it is a strong luminophore. [39]

Scheelite shows a strong emission maximum at approximately 420 nm, while excited with a wavelength of 254 nm. An excitation and emission spectrum for every substance was recorded in solid state at 298 K. To achieve the maximum intensity of the emission signal, the incoming light beam had the wavelength of the excitation maximum.

The recorded spectra were manually baseline corrected and normalized.

#### 8.1.1 Adjustment of the specimen carrier

First of all a well-known sample (scheelite) was measured with the following settings. Excitation wavelength of 254 nm and a cut off filter at 290 nm. This should lead to an emission maximum at 420 nm. In the next step the locking screws have to get untightened until they are loose. Then you have to switch to “Manual Control” modus in the software BL Studio. [40] The above mentioned settings should be listed in the software. The signal intensity has to be between 100 und 500 units. If this is not the case the adjusting screws should be rotated to achieve a more intense signal. After achieving this maximum all locking screws should be tightened and the adjustment is finished.

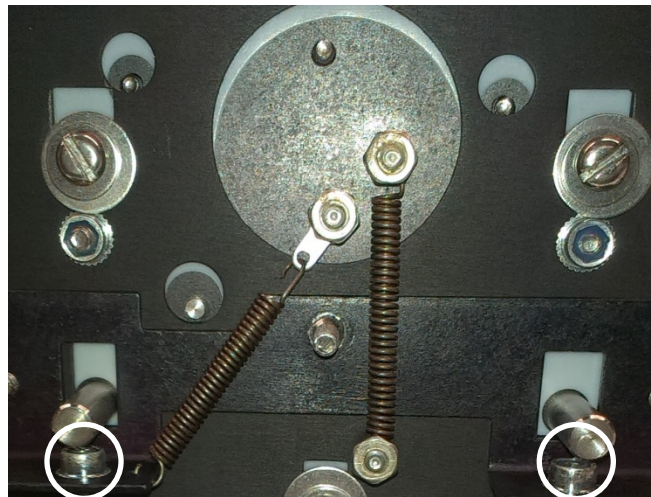


Figure 69: Specimen carrier

### 8.2 The measuring procedure

After the assessment with the UV lamp the respective measurement mode has to be chosen. It is important to keep the physical properties of the pulsing Xe-lamp in mind, while thinking of conclusions and interpretations for the spectra. The following Figure shows the excitation conditions.

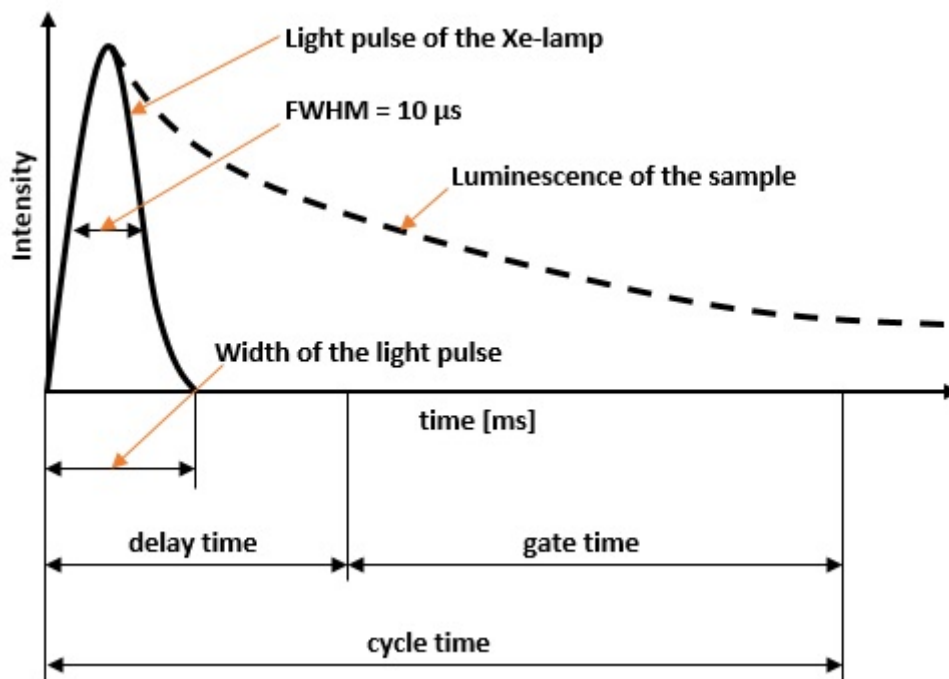


Figure 70: Excitation condition of the LS 55 [41]

There are three different modes provided with the LS 55. [41]

### 1) Fluorescence mode

The luminescence measurement of the sample takes place at the maxima of the excitation impulse. The photomultiplier (PMT) detects the darkcurrent after every completed pulse to reduce fluctuations. In many solid state samples the luminescence is long lasting, therefore this mode is susceptible to some errors.

### 2) Phosphorescence mode

The luminescence measurement of the sample starts after a defined time of the excitation signal (delay time) and lasts a defined time (gate time). This is the best way to measure solid samples and reduce darkcurrent effects. Table 28 shows the standard measurement parameters for this method.

### 3) Chemoluminescence mode

This mode is quite similar to the phosphorescence mode with the main difference, that there is no excitation. It is useful to measure different lamp spectra.

Table 28: Standard parameters for the phosphorescence mode

	Exc. 254 nm	Exc. 266 nm	Exc. 355 nm	Exc. 366 nm
<b>Em. Slit [nm]</b>	8	8	20	20
<b>Ex. Slit [nm]</b>	10	10	10	10
<b>U(PMT) [V]</b>	775	775	775	775
<b>Em. Filter [nm]</b>	290	290	390	390
<b>Delay [ms]</b>	0.10	0.10	0.10	0.10
<b>Gate [ms]</b>	3.00	3.00	3.00	3.00
<b>Cycle time [ms]</b>	20	20	20	20

### 8.3 Measurement settings

#### Explanation of the setting parameters:

Start... Scanning wavelength start

End... Scanning wavelength end

Ex. WL... Excitation wavelength

Ex. Slit... Width of the excitation slit (max. value 15)

Em. Slit... Width of the emission slit (max. value 20)

Em. Filter... Cut off filter on the emission monochromator

Gain... Sensitivity of the detector (Low, Medium 775 [V] and High 900 [V])

Delay... Defined time after the excitation-signal

Gate... Lasting of the signal

The following Table shows the measurement settings for the samples.

*Table 29: Measurement settings Ligands/Complexes in phosphorescence mode*

Ligands/Complexes	Start [nm]	End [nm]	Ex. WL [nm]	Ex. Slit [nm]	Em. Slit [nm]	Em. Filter [nm]
2-hydroxypyridine-N-oxide	400	900	390	15	20	430
2,6-dimethylpyridine-N-oxide	390	800	406	15	20	430
2-methylpyridine-N-oxide	400	900	340	15	20	390
3-methylpyridine-N-oxide	350	800	330	15	20	350
4-methylpyridine-N-oxide	350	900	290	15	20	350
4-quinoline-N-oxide	350	700	327	15	20	350
4-Cyanopyridine-N-oxide	300	900	266	15	20	290
[ZnSCN <sub>4</sub> ] <sup>2-</sup>	300	750	259	15	20	290
[Cd(2-picoline-N-oxide)(NCS) <sub>2</sub> ] <sub>n</sub> <b>(1)</b>	300	900	387	15	20	430
[Cd(3-picoline-N-oxide)(NCS) <sub>2</sub> ] <sub>n</sub> <b>(2)</b>	300	900	380	15	20	430
[Cd(4-cyanopyridine-N-oxide) <sub>2</sub> (NCS) <sub>2</sub> (H <sub>2</sub> O)] <sub>2</sub> <b>(3)</b>	300	900	330	15	20	350
[Cd(4-nitropyridine-N-oxide) <sub>2</sub> (NCS) <sub>2</sub> ] <sub>n</sub> <b>(4)</b>	300	900	395	15	20	430
[Cd(4-quinoline-N-oxide)(NCS) <sub>2</sub> ] <sub>n</sub> <b>(5)</b>	300	900	334	15	20	350
[Cd(2,6-lutidine-N-oxide)(NCS) <sub>2</sub> ] <sub>n</sub> <b>(6)</b>	300	900	324	15	20	350
[Cd(2,6-lutidine-N-oxide)(N <sub>3</sub> ) <sub>2</sub> ] <sub>n</sub> <b>(8)</b>	350	900	320	15	20	350
[Zn(2-picoline-N-oxide) <sub>2</sub> (NCS) <sub>2</sub> (H <sub>2</sub> O)] <sub>n</sub> <b>(9)</b>	300	900	325	15	20	350
[Zn(4-quinoline-N-oxide) <sub>6</sub> ] <sup>2+</sup> [Zn(NCS) <sub>4</sub> ] <sup>2-</sup> <b>(10)</b>	300	900	390	15	20	430
[Zn(4-cyanopyridine-N-oxide) <sub>2</sub> (NCS) <sub>2</sub> (H <sub>2</sub> O)] <sub>2</sub> <b>(11)</b>	300	900	335	15	20	350
[Zn(2,6-lutidine-N-oxide) <sub>2</sub> (NCS) <sub>2</sub> ] <b>(12)</b>	350	900	310	15	20	350
[Zn(4-quinoline-N-oxide)(N <sub>3</sub> ) <sub>2</sub> ] <sub>n</sub> <b>(13)</b>	390	900	340	15	20	390
[Zn(2,6-lutidine-N-oxide)(N <sub>3</sub> ) <sub>2</sub> ] <sub>n</sub> <b>(14)</b>	350	900	318	15	20	350
[Zn(4-picoline-N-oxide)(N <sub>3</sub> ) <sub>2</sub> ] <sub>n</sub> <b>(15)</b>	350	900	304	15	20	350
[Zn(2-O-pyridine-N-oxide)(N <sub>3</sub> )(H <sub>2</sub> O)] <sub>n</sub> <b>(16)</b>	390	900	375	15	20	390

The samples 2,6-dimethylpyridine-N-oxide and 3-methylpyridine-N-oxide were measured in quartz cuvettes because those substances are liquid at room temperature. The other samples were measured in a special powder accessory (Figure 71). [41] All samples were measured at a high detector sensitivity (Gain = 900 [V]).

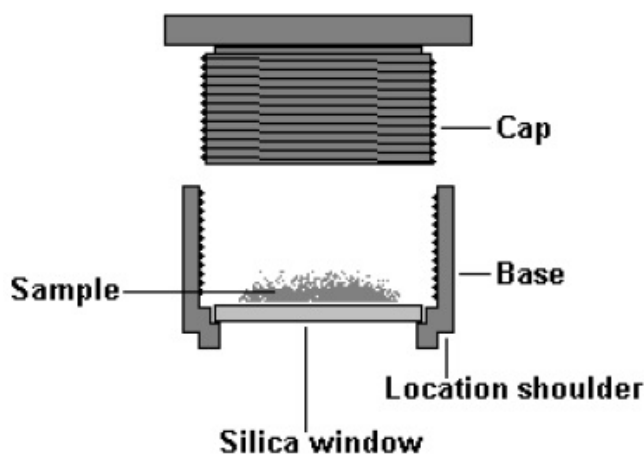


Figure 71: Powder accessory [41]

The samples should be homogeneous and finely powdered to reduce surface structure effects. Additionally the sample had to cover the whole silica window.

## 8.4 Luminescence properties

In the following chapter some physical properties of the luminescent complexes are collected and compared to each other. These parameters are the maximum excitation wavelength ( $\lambda_{ex}$ ) and the maximum emission wavelength ( $\lambda_{em}$ ) as well as the Stokes-shift and the full width at half maximum (FWHM) for each band.

### 8.4.1 Ligands

Table 30: Spectroscopic properties of the ligands

Compounds	$\lambda_{ex}$ [nm]	$\lambda_{em}$ [nm]	$\nu_{ex}$ [cm <sup>-1</sup> ]	$\nu_{em}$ [cm <sup>-1</sup> ]	Stokes-shift [cm <sup>-1</sup> ]	FWHM [cm <sup>-1</sup> ]
2-hydroxypyridine-N-oxide	390	574	25641	17422	8219	3870
2-methylpyridine-N-oxide	340	611	29412	16367	13045	482
3-methylpyridine-N-oxide	330	612	30303	16340	13963	530
4-methylpyridine-N-oxide	290	578	34483	17301	17182	4504
2,6-dimethylpyridine-N-oxide	406	509	24631	19646	4984	4478
4-quinoline-N-oxide	327	584	30581	17123	13458	265
4-cyanopyridine-N-oxide	266	506	37594	19763	17831	6535

All ligands show luminescence behavior in solid state at room temperature. 4-methylpyridine-N-oxide, 4-cyanopyridine-N-oxide and 4-quinoline-N-oxide were dried in a desiccator at 100 mbar pressure and a surrounding temperature of 60°C. The drying agent was silica gel. This was necessary to remove water from the sample. Water shows a strong luminescence quenching effect. [42]

The emission spectra of the ligands are located in the attachment.

## 8.4.2 Cd(II) complexes

Table 31: Spectroscopic properties of the Cd(II) complexes

Compounds	$\lambda_{ex}$ [nm]	$\lambda_{em}$ [nm]	$\nu_{ex}$ [cm <sup>-1</sup> ]	$\nu_{em}$ [cm <sup>-1</sup> ]	Stokes-shift [cm <sup>-1</sup> ]	FWHM [cm <sup>-1</sup> ]
[Cd(2-picoline-N-oxide)(NCS) <sub>2</sub> ] <sub>n</sub> ( <b>1</b> )	354	544	28249	18382	9866	3915
[Cd(3-picoline-N-oxide)(NCS) <sub>2</sub> ] <sub>n</sub> ( <b>2</b> )	380	538	26316	18587	7728	4413
[Cd(4-cyanopyridine-N-oxide) <sub>2</sub> (NCS) <sub>2</sub> (H <sub>2</sub> O)] <sub>2</sub> ( <b>3</b> )	330	518	30303	19305	10998	4318
[Cd(4-nitropyridine-N-oxide) <sub>2</sub> (NCS) <sub>2</sub> ] <sub>n</sub> ( <b>4</b> )	395	573	25316	17452	7864	3250
[Cd(4-quinoline-N-oxide)(NCS) <sub>2</sub> ] <sub>n</sub> ( <b>5</b> )	334	631	29940	15848	14092	4948
[Cd(2,6-lutidine-N-oxide)(NCS) <sub>2</sub> ] <sub>n</sub> ( <b>6</b> )	324	544	30864	18382	12482	4163
[Cd(2,6-lutidine-N-oxide)(N <sub>3</sub> ) <sub>2</sub> ] <sub>n</sub> ( <b>8</b> )	320	538	31250	18587	12663	4316

In the following Figures the emission maxima of the compounds are compared to those of the pure ligands.

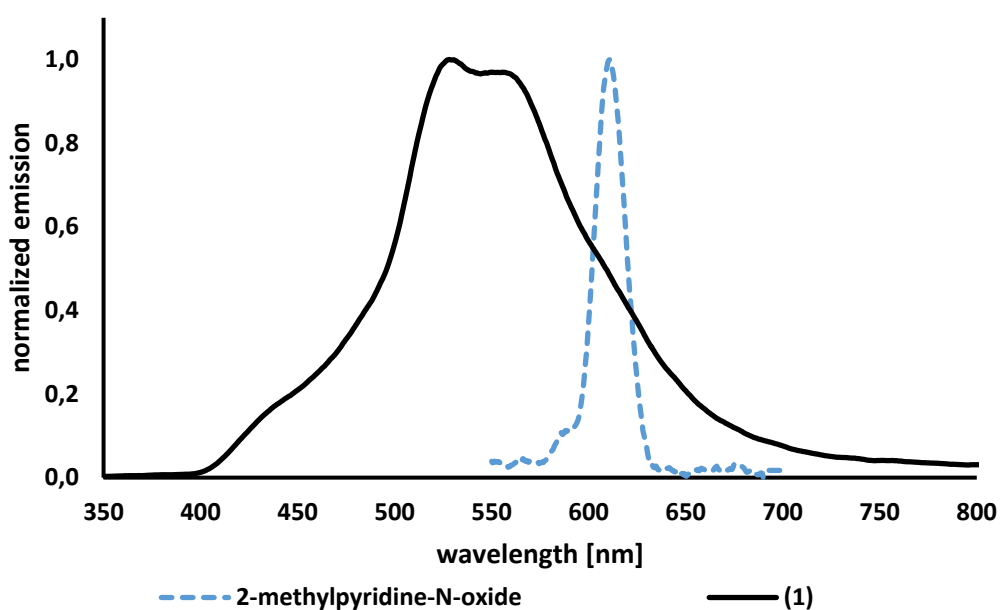


Figure 72: Comparison of the emission maxima of the Cd(II) complexes with 2-methylpyridine-N-oxide

Figure 72 shows a large hypsochromic shift compared to the ligand. The shift to a higher energetic region is referred to a ligand to metal charge-transfer process (LMCT). Another big difference is that compound (**1**) indicates a characteristic broad band, which is assigned to a charge-transfer transition, while the 2-methylpyridine-N-oxide shows its sharp  $\pi \rightarrow \pi^*$  and  $\sigma \rightarrow \sigma^*$  transition. [46]

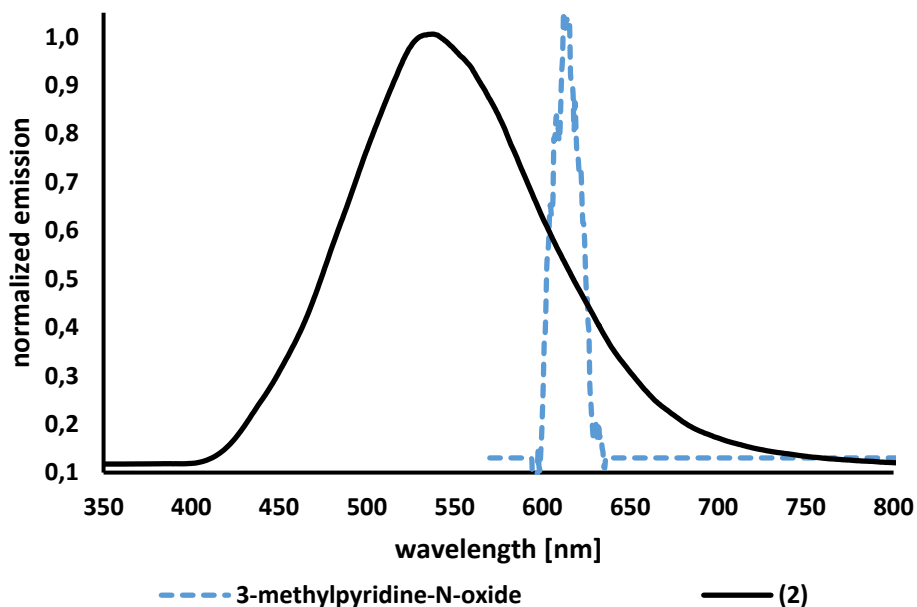


Figure 73: Comparison of the emission maxima of the Cd(II) complex with 3-methylpyridine-N-oxide

In this case the blue-shift of the compound is comparable to the shift in Figure 72. The different substituted methylpyridine-N-oxides demonstrates similar FWHM values and emission maxima. Complex (2) shows the characteristic band form for a charge-transfer transition, which could be expected for chemical similar substances.

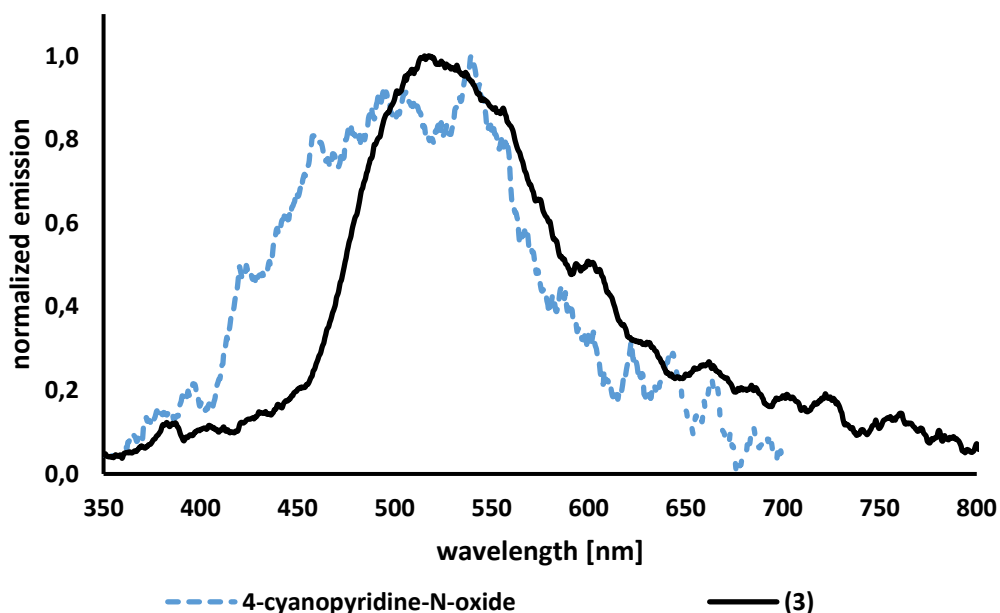


Figure 74: Comparison of the emission maxima of the Cd(II) complex with 4-cyanopyridine-N-oxide

On the basis of the quenching mechanism of the hydrogen bonds, it's notable that the fluorescence quantum efficiency is decreased. [43] Both the 4-cyanopyridine-N-oxide and the complex (3) shows the characteristic charge-transfer properties, while the complex is bathochromically shifted.

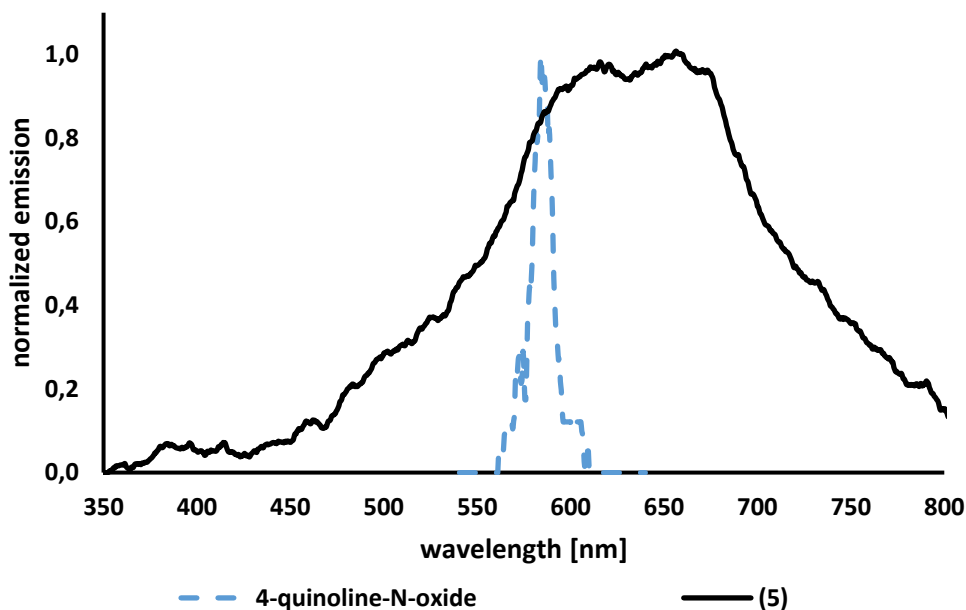


Figure 75: Comparison of the emission maxima of the Cd(II) complex with 4-quinoline-N-oxide

Figure 75 shows the broad, red-shifted (MLCT) thiocyanato complex **(5)** and the sharp emission maxima of the 4-quinoline-N-oxide. It was not possible to detect the luminescence of the azido complex **(7)**, because of the strong quenching effect of the water molecules.

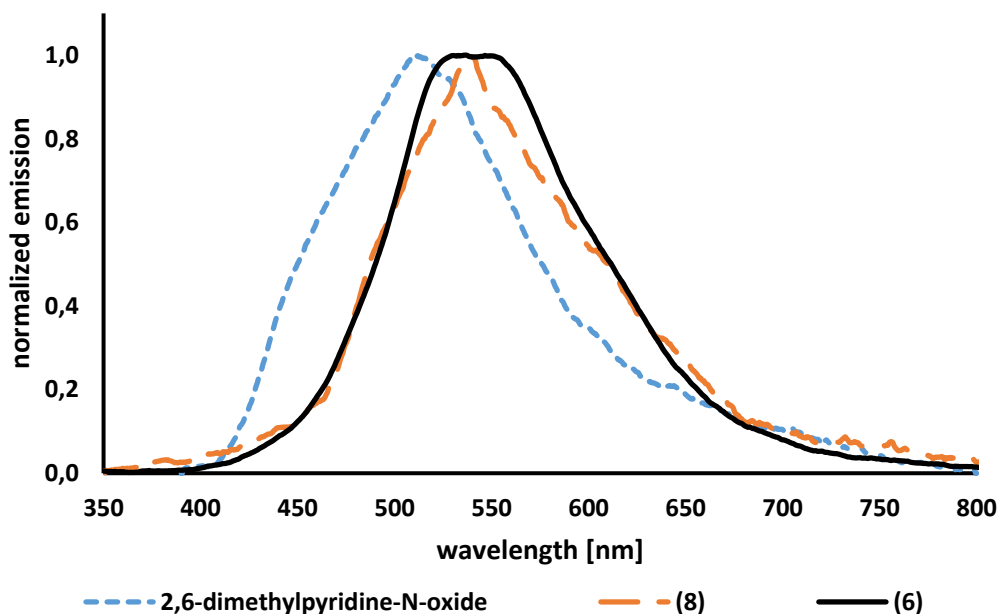


Figure 76: Comparison of the emission maxima of the Cd(II) complexes with 2,6-dimethylpyridine-N-oxide

It is obvious, that both Cd(II) structures are significantly bathochromic shifted compared to the ligand. This shift is an evidence for a charge-transfer transition. As I mentioned in the theoretical part of this work, a shift to lower energy regions is referred to a metal to ligand charge-transfer process (MLCT). The emission maxima of the coordination structures are quite similar.

### 8.4.3 Zn(II) complexes

Table 32: Spectroscopic properties of the Zn(II) complexes

Compounds	$\lambda_{ex}$ [nm]	$\lambda_{em}$ [nm]	$\nu_{ex}$ [cm <sup>-1</sup> ]	$\nu_{em}$ [cm <sup>-1</sup> ]	Stokes-shift [cm <sup>-1</sup> ]	FWHM [cm <sup>-1</sup> ]
[Zn(2-picoline-N-oxide) <sub>2</sub> (NCS) <sub>2</sub> (H <sub>2</sub> O)] <sub>n</sub> ( <b>9</b> )	325	573	30769	17452	13317	3347
[Zn(4-quinoline-N-oxide) <sub>6</sub> ] <sup>2+</sup> [Zn(NCS) <sub>4</sub> ] <sup>2-</sup> ( <b>10</b> )	390	621	25641	16103	9538	4119
[Zn(NCS) <sub>4</sub> ] <sup>2-</sup> ( <b>10a</b> )	259	484	38610	20661	17949	6409
[Zn(4-cyanopyridine-N-oxide) <sub>2</sub> (NCS) <sub>2</sub> (H <sub>2</sub> O)] <sub>2</sub> ( <b>11</b> )	335	530	29851	18868	10983	4011
[Zn(2,6-lutidine-N-oxide) <sub>2</sub> (NCS) <sub>2</sub> ] ( <b>12</b> )	310	528	32258	18939	13319	4042
[Zn(4-quinoline-N-oxide)(N <sub>3</sub> ) <sub>2</sub> ] <sub>n</sub> ( <b>13</b> )	340	614	29412	16287	13125	4155
[Zn(2,6-lutidine-N-oxide)(N <sub>3</sub> ) <sub>2</sub> ] <sub>n</sub> ( <b>14</b> )	318	538	31447	18587	12859	4077
[Zn(4-picoline-N-oxide)(N <sub>3</sub> ) <sub>2</sub> ] <sub>n</sub> ( <b>15</b> )	304	537	32895	18622	14273	4447
[Zn(2-O-pyridine-N-oxide)(N <sub>3</sub> )(H <sub>2</sub> O)] <sub>n</sub> ( <b>16</b> )	375	544	26667	18382	8284	3498

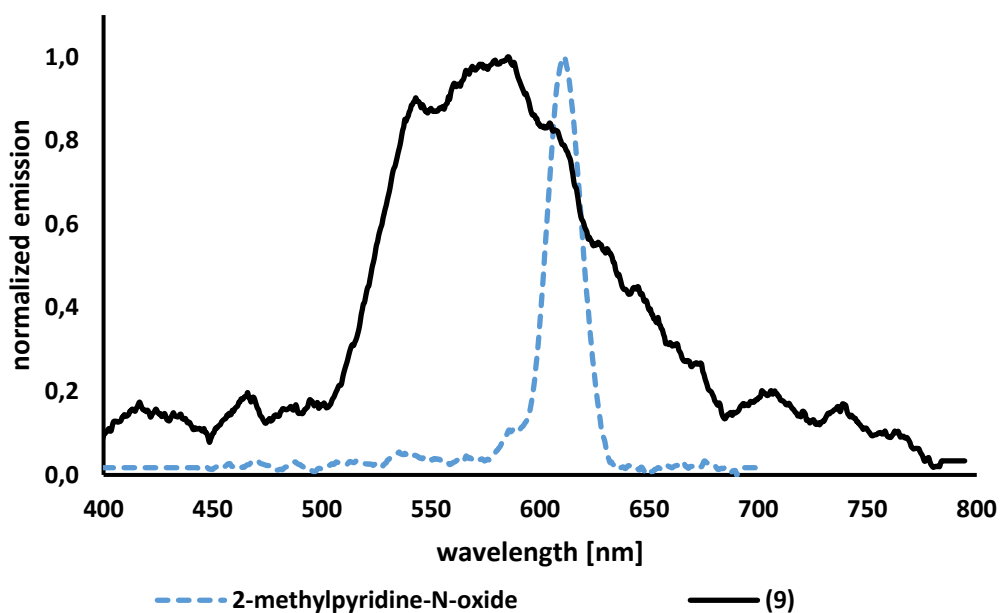


Figure 77: Comparison of the emission maxima of the Zn(II) complex with 2-methylpyridine-N-oxide

Figure 77 shows a large hypsochromic shift compared to the ligand. The shift to a higher energetic region is referred to a ligand to metal charge-transfer process (LMCT). This behavior is quite similar to that in Figure 73. Complex (**9**) indicates a characteristic broad band, which is assigned to a charge-transfer transition, while the 2-methylpyridine-N-oxide shows its sharp  $\pi \rightarrow \pi^*$  and  $\sigma \rightarrow \sigma^*$  transition. [46]

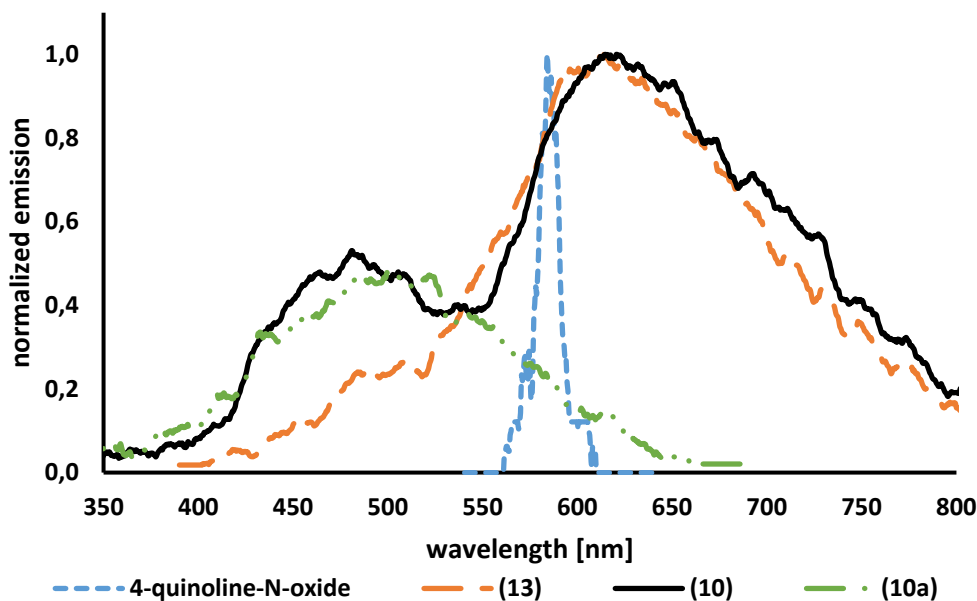


Figure 78: Comparison of the emission maxima of the Zn(II) complexes with 4-quinoline-N-oxide

The azido as well as the thiocyanato structure show a similar emission maximum with a significant bathochromic shift and broad charge-transfer bands. It is worth considering that there is a second band of half of the high and similar FWHM at complex **(10)**. This is due to the circumstance that there exists two motifs in solid state. The smaller band could be identified as complex **(10a)**. [45]

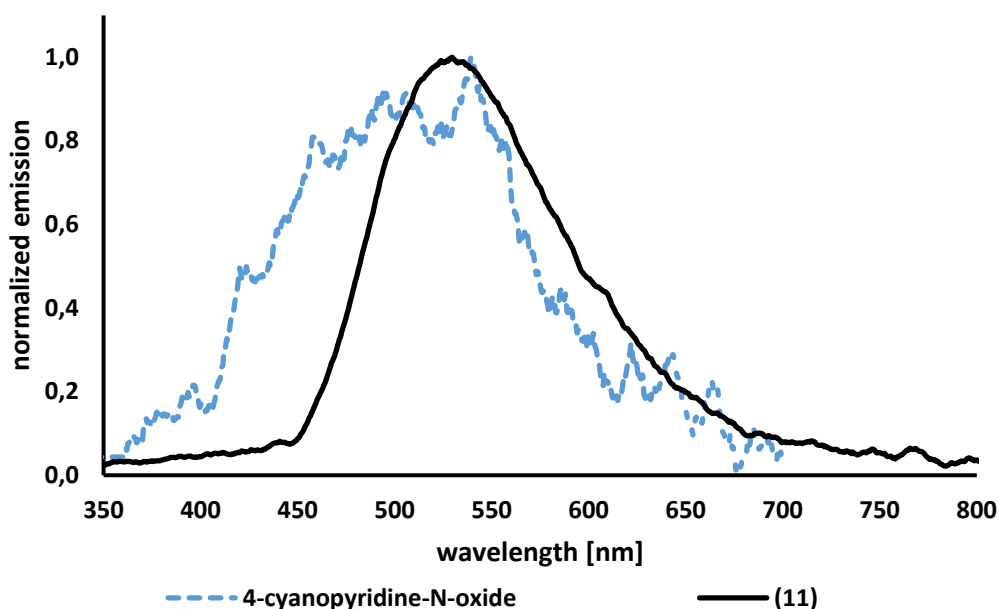


Figure 79: Comparison of the emission maxima of the Zn(II) complex with 4-cyanopyridine-N-oxide

Both the 4-cyanopyridine-N-oxide and the complex **(11)** show the characteristic charge-transfer properties, while the complex is red-shifted. According to the fluorescence quenching theory, the intensity of the ligand has decreased.

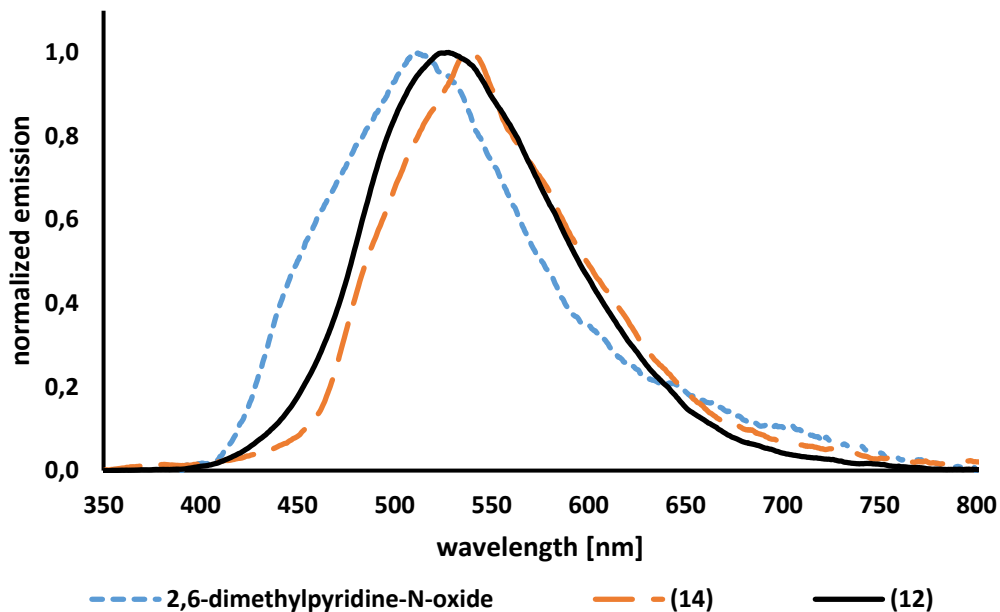


Figure 80: Comparison of the emission maxima of the Zn(II) complexes with 2,6-dimethylpyridine-N-oxide

Both Zn(II) structures are bathochromically shifted and they exhibit a broad band form. This is similar to Figure 76 with the exception that the azido and the thiocyanato structure shows different emission maxima.

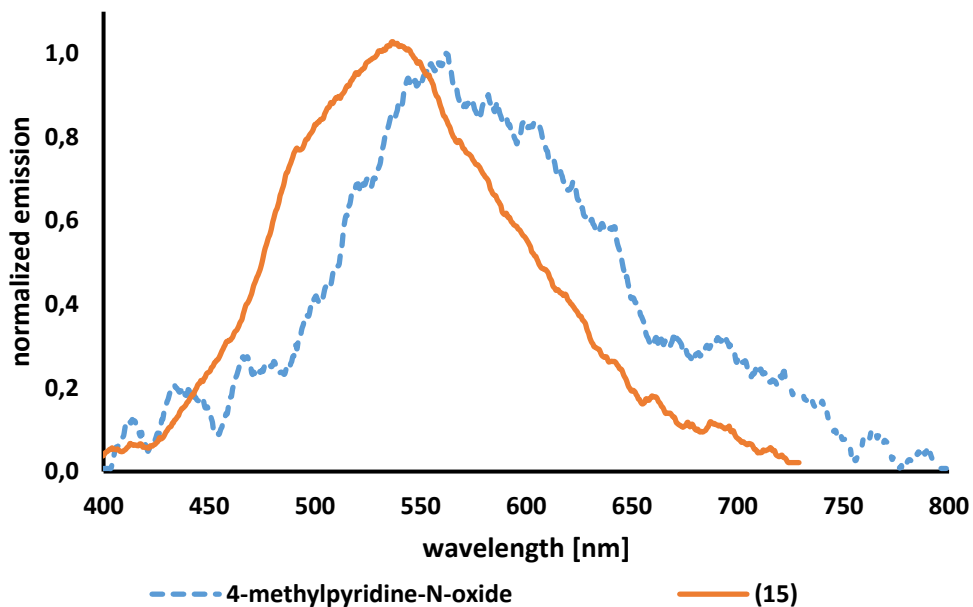


Figure 81: Comparison of the emission maxima of the Zn(II) complex with 4-methylpyridine-N-oxide

The para substituted methylpyridine is a big exception compared to the 2- or 3-Methylpyridine-N-oxide, because it has a broad intramolecular charge-transfer band. [56] The band form and FWHM of the 4-methylpyridine-N-oxide is quite similar to complex (15). A small blue-shift is detectable and this leads to the conclusion that the Zn(II) structure is involved in a charge-transfer transition.

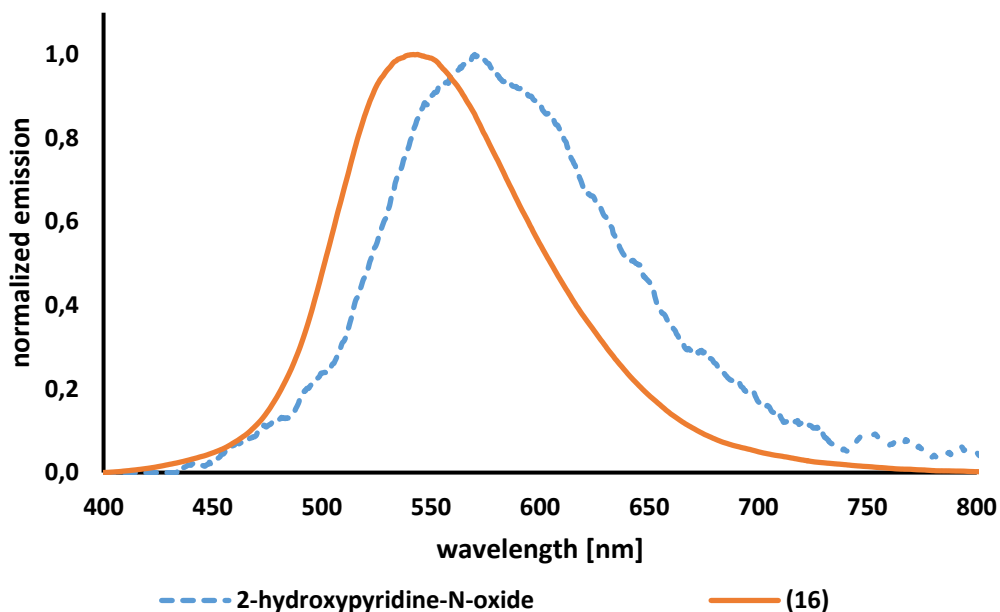


Figure 82: Comparison of the emission maxima of the Zn(II) complex with 2-hydroxypyridine-N-oxide

Figure 82 shows a large blue-shift compared to the ligand. The shift to a higher energetic region is referred to a ligand to metal charge-transfer process (LMCT). A broad band with a high intensity was detectable.

### 8.5 Charge-transfer properties of the Cd(II) and Zn(II) compounds

Table 33: Luminescence properties of the Cd(II) compounds

Structure	shift [nm]	shift [ $\text{cm}^{-1}$ ]	charge-transfer
[Cd(2-picoline-N-oxide)(NCS) <sub>2</sub> ] <sub>n</sub> ( <b>1</b> )	67	2015	LMCT
[Cd(3-picoline-N-oxide)(NCS) <sub>2</sub> ] <sub>n</sub> ( <b>2</b> )	74	2247	LMCT
[Cd(4-cyanopyridine-N-oxide) <sub>2</sub> (NCS) <sub>2</sub> (H <sub>2</sub> O)] <sub>2</sub> ( <b>3</b> )	12	2311	MLCT
[Cd(4-quinoline-N-oxide)(NCS) <sub>2</sub> ] <sub>n</sub> ( <b>5</b> )	47	1275	MLCT
[Cd(2,6-lutidine-N-oxide)(NCS) <sub>2</sub> ] <sub>n</sub> ( <b>6</b> )	35	1081	MLCT
[Cd(2,6-lutidine-N-oxide)(N <sub>3</sub> ) <sub>2</sub> ] <sub>n</sub> ( <b>8</b> )	29	1286	MLCT

Table 34: Luminescence properties of the Zn(II) compounds

Structure	shift [nm]	shift [ $\text{cm}^{-1}$ ]	charge-transfer
[Zn(2-picoline-N-oxide) <sub>2</sub> (NCS) <sub>2</sub> (H <sub>2</sub> O)] <sub>n</sub> ( <b>9</b> )	38	1085	LMCT
[Zn(4-quinoline-N-oxide) <sub>6</sub> ] <sup>2+</sup> [Zn(NCS) <sub>4</sub> ] <sup>2-</sup> ( <b>10</b> )	37	1020	MLCT
[Zn(4-cyanopyridine-N-oxide) <sub>2</sub> (NCS) <sub>2</sub> (H <sub>2</sub> O)] <sub>2</sub> ( <b>11</b> )	24	895	MLCT
[Zn(2,6-lutidine-N-oxide) <sub>2</sub> (NCS) <sub>2</sub> ] ( <b>12</b> )	19	707	MLCT
[Zn(4-quinoline-N-oxide)(N <sub>3</sub> ) <sub>2</sub> ] <sub>n</sub> ( <b>13</b> )	30	836	MLCT
[Zn(2,6-lutidine-N-oxide)(N <sub>3</sub> ) <sub>2</sub> ] <sub>n</sub> ( <b>14</b> )	29	1059	MLCT
[Zn(4-picoline-N-oxide)(N <sub>3</sub> ) <sub>2</sub> ] <sub>n</sub> ( <b>15</b> )	41	1321	LMCT
[Zn(2-O-pyridine-N-oxide)(N <sub>3</sub> )(H <sub>2</sub> O)] <sub>n</sub> ( <b>16</b> )	30	960	LMCT

## 9) Diffuse reflection data

### 9.1 Introduction into the crystal field spectroscopy [57]

Transition metal complexes have the ability to absorb light in the UV/VIS/NIR range of the optical spectrum. Non visible UV light is absorbed by many main group elements. With this kind of spectroscopy it is possible to study electronic transitions as well as structural changes in the complexes.

There are several ways in which light could influence the chemical behavior. First it is possible to raise d-electrons from lower to higher energy levels. This is called d-d- transition. Then there are interactions between the different states of the ligand itself, which is known as inner ligand transition. Last but not least there is a movement between the electrons of the metal and the ligand. This happens in both directions and it is called charge-transfer transition.

### 9.2 Parameters [58]

Several parameters could be identified. The first important parameter is the so called crystal field splitting parameter  $10Dq$ . For large systems (more electrons) a huge crystal field interaction should be considered.

Another resulting parameter is the so called Racah parameter B. The calculation of this parameter could be quite difficult. In this case only two cobalt structures with octahedral geometry are investigated. The following two formulas were used to calculate the parameters.

$$340 Dq^2 + 18 \cdot (v_1 - 2 \cdot v_2) \cdot Dq + v_2^2 - v_2 \cdot v_1 = 0 \quad \text{Equ. (9.1)}$$

$$B = \frac{v_1 - 2 \cdot v_2 + 30 \cdot Dq}{15} \quad \text{Equ. (9.2)}$$

These equations are only valid for  $d^7$  ions in octahedral environment. The Racah parameter B describes the electrostatic repulsion of multi electron systems. This depends on the number of electrons, the spin states and the occupied orbitals.

#### 9.2.1 Tanabe-Sugano diagram [59]

With this method it is possible to plot the energy difference of each excited state against the lowest state of the system. On the x-axis the splitting parameter is plotted and both values are normalized to the Racah parameter B. This is important to determine absorption effects of the metal complexes and the resulting intersection points give both the number and the position of the absorption bands.

### 9.3 Discussion of selected Co(II) compounds

The following Table summarizes the calculated parameters.

Table 35: Spectroscopy parameters of the octahedral Co(II) complexes

	Dq [ $\text{cm}^{-1}$ ]	B [ $\text{cm}^{-1}$ ]
[Co(4-cyanopyridine-N-oxide) <sub>2</sub> (NCS) <sub>2</sub> (H <sub>2</sub> O)] <sub>2</sub> ( <b>18</b> )	1089	617
[Co(N <sub>3</sub> ) <sub>2</sub> (H <sub>2</sub> O) <sub>2</sub> ] <sub>n</sub> (3-picoline-N-oxide) <sub>2n</sub> ( <b>19</b> )	1199	773



## 10) Discussion

The literature research was done by the Cambridge database (CSD version 5.35 with all updates included). [5]

The search routine was a N-N-N and a metal M (M = Cd, Zn, Co, Mn), respectively S-C-N and a metal M (M = Cd, Zn, Co, Mn) fragment. To specify the search procedure a single pyridine-N-oxide ring was created. Substitution on every carbon position of the ring was allowed. All together there were 49 search hits. [5]

### 10.1 Comparison of the published thiocyanato complexes

The following Table contains the published metal thiocyanato complexes with different substituted pyridine-N-oxides as well as their coordination number (CN), the bridging and the REFCODE.

Table 36: Published thiocyanato complexes

<b>Cd(II) compounds</b>	<b>CN</b>	<b>bridging</b>	<b>REFCODE</b>
catena-(bis( $\mu_2$ -Thiocyanato-N,S)-bis(3-methyl-4-nitropyridine-N-oxide-O)-cadmium) [65]	6	di- $\mu_{(N,S)}$ ; 1D	IWENIH
catena-(tetrakis( $\mu_2$ -thiocyanato)-bis( $\mu_2$ -pyridine 1-oxide)-di-cadmium) [66]	6	di- $\mu_{(N,S)}$ ; 2D	SENHUQ
catena-(( $\mu_2$ -4-methylpyridine N-oxide-O,O)-bis( $\mu_2$ -thiocyanato)-cadmium(ii)) [67]	6	di- $\mu_{(N,S)}$ ; two $\mu_2$ 4-methylpyridine-N-oxide; 2D	TEQKAC
catena-(( $\mu_2$ -1,3-bis(4-Pyridyl)propane-N,N'-dioxy-O,O)-( $\mu_2$ -isothiocyanato-N,S)-aqua-isothiocyanato-cadmium(ii)) [68]	6	two $\mu_{(N,S)}$ ; $\mu_{(O,O)}$ ligand 1D; (3D-H-bond)	UMAVEJ
catena-(bis( $\mu_2$ -1,3-bis(4-Pyridyl)propane-N,N'-dioxy-O,O')-bis(thiocyanato)-cadmium(ii)) [68]	6	two NCS <sup>-</sup> ; two end to end coord. ligand; isomorph to Co(II); 2D	UMAWAG
catena-(( $\mu_2$ -3,5-Dimethylpyridine N-oxido)-bis( $\mu_2$ -thiocyanato)-cadmium(ii)) [69]	6	di- $\mu_{(N,S)}$ ; $\mu_2$ 3,5-dimethylpyridine-N-oxide; 3D	XEMLAD
<b>Zn(II) compounds</b>	<b>CN</b>	<b>bridging</b>	<b>REFCODE</b>
catena-(( $\mu_2$ -4,4'-Bipyridine-N,N'-dioxide)-diaqua-bis(isothiocyanato)-zinc(ii) monohydrate) [70]	6	two NCS <sup>-</sup> ; bridging ligand; (1D-H-bond)	LIFXUU
catena-(( $\mu_3$ -1,3-bis(4-Pyridyl)propane-N,N'-dioxy)-aquabis(isothiocyanato)-zinc(ii)) [68]	6	two NCS <sup>-</sup> ; $\mu_3(O,O,O')$ ligand; 2D isomorph to Co(II); (3D-H-bond)	UMAVOT
Diaqua-bis(1,3-bis(4-pyridyl)propane-N,N'-dioxy)-bis(thiocyanato)-zinc(ii) [68]	6	two NCS <sup>-</sup> ; (3D-H-bond)	UMAWIO
<b>Co(II) compounds</b>	<b>CN</b>	<b>bridging</b>	<b>REFCODE</b>
catena-(( $\mu_2$ -N,N'-Ethane-1,2-diylbis(pyridine-4-carboxamide) 1,1'-dioxide)-diaqua-bis(isothiocyanato)-cobalt tetrahydrate) [71]	6	two NCS <sup>-</sup> ; $\mu_2$ bridged ligand; 1D; (2D-H-bond)	FATJAN
catena-(( $\mu_2$ -N,N'-Hexane-1,6-diylbis(pyridine-4-carboxamide) 1,1'-dioxide)-diaqua-bis(isothiocyanato)-cobalt dihydrate) [71]	6	two NCS <sup>-</sup> ; $\mu_2$ bridged ligand; 1D; (2D-H-bond)	FATJER
Diaqua-bis(isothiocyanato-N)-bis(pyridine N-oxide-O)-cobalt(ii) [72]	6	two NCS <sup>-</sup> ; mononuclear Co	FONBIU
Diaqua-bis(3-hydroxypyridine N-oxide)-dithiocyanato-cobalt(ii) [73]	6	two NCS <sup>-</sup> ; mononuclear Co; (3D-H-bond)	IDOYEG
catena-(( $\mu_2$ -4-Methylpyridine N-oxide-O,O)-bis( $\mu_2$ -thiocyanato)-cobalt(ii)) [74]	6	two $\mu_{(1,3)}$ NCS <sup>-</sup> ; $\mu_{(O,O)}$ ligand 2D	MEQKOJ

catena-(( $\mu_2$ -4-Methylpyridine N-oxide-O,O)-( $\mu_2$ -thiocyanato-N,S)-(methanol)-(isothiocyanato-N)-cobalt(ii)) [75]	6	$\mu_{(1,3)}\text{NCS}^-$ ; $\mu_{(0,0)}$ ligand; 1D	REKBUF
catena-(trans-bis( $\mu_2$ -4,4'-Bipyridyl-N,N'-dioxide-O,O')-bis(isothiocyanato)-cobalt(ii) 4,4'-bipyridyl-N,N'-dioxide solvate) [76]	6	two $\text{NCS}^-$ ; four $\mu_{(0,0)}$ ligand; 2D	ROLHUW
catena-(( $\mu_2$ -4,4'-Bipyridyl-N,N'-dioxide-O,O')-diaqua-bis(isothiocyanato)-cobalt(ii) monohydrate) [76]	6	two $\mu_{(1,3)}\text{NCS}^-$ ; 1D	ROLJAE
catena-(( $\mu_2$ -4-Methoxypyridine N-oxide-O,O)-bis( $\mu_2$ -thiocyanato)-cobalt(ii)) [77]	6	$\mu_{(1,3)}\text{NCS}^-$ ; $\mu_{(0,0)}$ ligand; 1D	TERRAK
catena-(bis( $\mu_2$ -thiocyanato)-bis(4-nitropyridine N-oxide)-cobalt(ii)) [78]	6	two $\mu_{(1,3)}$ ; 1D	TILHIG
catena-(( $\mu_3$ -1,3-bis(4-Pyridyl)propane-N,N'-dioxy)-aquabis(isothiocyanato)-cobalt(ii)) [68]	6	two $\text{NCS}^-$ ; $\mu_3(\text{O},\text{O},\text{O}')$ ligand; 2D	UMAVAF
catena-(bis( $\mu_2$ -1,3-bis(4-Pyridyl)propane-N,N'-dioxy-O,O')-bis(thiocyanato)-cobalt(ii)) [68]	6	two $\text{NCS}^-$ ; two ligands end-to-end; 2D	UMAVUZ
bis(Di-isothiocyanato-( $\mu_2$ -(2-pyridinecarboxaldehyde-1-oxido 2'-pyridinylhydrazone-O,O,N,N'))-cobalt(ii)) [79]	6	two $\text{NCS}^-$ ; dimer by the NNN-donor ligand	VAZDAB
Diaqua-bis(8-hydroxyquinoline N-oxide- $\kappa\text{O}^1$ )-bis(isothiocyanato)-cobalt(ii) bis(8-hydroxyquinoline N-oxide) [80]	6	two $\text{NCS}^-$ ; two coord. ligand; one non-coord. ligand; (1D-H-bond)	WIHQOU
<b>Mn(II) compounds</b>	<b>CN</b>	<b>bridging</b>	<b>REFCODE</b>
bis( $\mu_2$ -3,5-Dimethylpyridine-N-oxide)-di-aqua-tetra-isothiocyanato-bis(3,5-dimethylpyridine N-oxide)-di-manganese(ii) [81]	6	four terminal $\text{NCS}^-$ ; dimer $\mu_{(0,0)}$ 3,5-dimethylpyridine-N-oxide	GIWQEJ
catena-(bis( $\mu_2$ -Thiocyanato-N,S)-bis(4-nitropyridine N-oxide-O)-manganese(ii)) [82]	6	di- $\mu_{(N,S)}$ ; 1D	SINKUW
catena-(( $\mu_3$ -1,3-bis(4-Pyridyl)propane-N,N'-dioxy)-aquabis(isothiocyanato)-manganese(ii)) [68]	6	two terminal $\text{NCS}^-$ ; $\mu_3$ -O,O,O' tridentate mode; 2D	UMAVIN
Diaqua-bis(1,3-bis(4-pyridyl)propane-N,N'-dioxy)-bis(thiocyanato)-manganese(ii) [68]	6	two terminal $\text{NCS}^-$ ; $\mu_{(0,0)}$ -substituted pyridine-N-oxide (3D-H-bond); isomorph to Zn(II)	UMAWEK
catena-[tetrakis( $\mu_2$ -Thiocyanato-N,S)-( $\mu_2$ -3-methyl-4-nitropyridine-N-oxide)-manganese(ii)-mercury(ii)] [83]	6	di- $\mu_{(N,S)}$ ; $\mu_{(0,0)}$ ligand; 2D coord. via $\text{Hg}(\text{SCN})_4$	YILVAR

All of the 28 compounds have the coordination number six.

Four Cd(II) compounds have di- $\mu_{(N,S)}$  double bridging thiocyanates, but they differ in their dimensionality. Most of the complexes show a two-dimensional layer. Another  $\mu_{(N,S)}$  isothiocyanato and  $\mu_{(0,0)}$  ligand bridged compound builds a three-dimensional hydrogen bond network. The compound with the end-to-end coordinated ligand and the two  $\text{NCS}^-$  is isomorph to the two-dimensional Co(II) compound. All Zn(II) compounds have two isothiocyanato anions. By now there are only three Zn(II) compounds known and two of them (an one-dimensional and a three-dimensional structure) show hydrogen bonds. The two-dimensional structure is isomorph to the Co(II) ones. The Co(II) complexes connect their metal centers via  $\mu_{(0,0)}$ , respectively  $\mu_3(\text{O},\text{O},\text{O}')$  bridging ligands. Many of them have to isothiocyanate anions as well. Only one compound shows a three-dimensional structure due to the formation of hydrogen bonds, while most of the compounds show an one-dimensional structure. Three Mn(II) compounds are bridged via the oxygen's of their ligands and another one is bridged via  $\text{Hg}(\text{SCN})_4$ . The thiocyanato groups are in terminal position for these compounds. One complex shows the similar di- $\mu_{(N,S)}$  double bridge like the Cd(II) compounds.

## 10.2 Comparison of the published azido complexes

The following Table contains the published metal azido complexes with different substituted pyridine-N-oxides.

Table 37: Published azido complexes

<b>Cd(II) compounds</b>	<b>CN</b>	<b>bridging</b>	<b>REFCODE</b>
catena-(bis( $\mu_3$ -1-oxoisonicotinato)-bis( $\mu_2$ -1,1-azido)-diaqua-dicadmium(ii)) [84]	6	$\mu_{(1,1)}$ ; two bridging 1-oxoisonicotinate ligands 2D; (3D-H-bond)	BIZSAF
catena-(( $\mu_2$ -Azido-N,N)-( $\mu_2$ -azido-N,N'')-( $\mu_2$ -2-picoline N-oxide-O,O)-cadmium(ii)) [85]	6	di- $\mu_{(1,1)}$ ; di- $\mu_{(1,3)}$ ; $\mu_{(O,O)}$ -2-picoline-N-oxide 2D "honeycomb"	FODRUM
catena-(bis( $\mu_2$ -Azido)-diaqua-cadmium(ii) bis(3-methylpyridine-N-oxide)) [38]	6	di- $\mu_{(1,1)}$ ; non-coord. ligand; isomorph to Zn(II); 1D	IZOLIS
<b>Zn(II) compounds</b>	<b>CN</b>	<b>bridging</b>	<b>REFCODE</b>
catena-(( $\mu_3$ -nicotinato N-oxide)-( $\mu_2$ -azido-N,N)-zinc(ii)) [86]	5	$\mu_{(1,1)}$ ; $\mu_3$ -nicotinate N-oxide; 2D	COMDEO
catena-(tetrakis( $\mu_2$ -Azido-N,N)-bis(2-picoline N-oxide-O)-di-zinc(ii)) [85]	5	di- $\mu_{(1,1)}$ ; 1D	FODRIA
catena-(bis( $\mu_2$ -Azido)-diaqua-zinc(ii) pyridine-N-oxide) [38]	6	di- $\mu_{(1,1)}$ ; non-coord. ligand; 1D	IZOLAK
catena-(bis( $\mu_2$ -Azido)-diaqua-zinc(ii) bis(3-methylpyridine-N-oxide)) [38]	6	di- $\mu_{(1,1)}$ ; non-coord. ligand; isomorph to Cd(II); 1D	IZOLEO
<b>Co(II) compounds</b>	<b>CN</b>	<b>bridging</b>	<b>REFCODE</b>
catena-[tetrakis( $\mu_2$ -Azido-N,N)-bis( $\mu_2$ -4-carboxylatopyridine-N-oxide)-tetraaqua-cobalt-di-copper] [87]	6	di- $\mu_{(1,1)}$ Cu; $\mu_{(1,1)}$ Co; $\mu_2$ -ligand; Co-Cu 1D;	GIGCIK
catena-(bis( $\mu_3$ -Pyridine-4-carboxylate N-oxide-O,O',O'')-bis( $\mu_2$ -azido-N,N)-diaqua-di-cobalt) [88]	6	$\mu_{(1,1)}$ ; $\mu_3$ ligand; isomorph to Mn(II); 2D; (3D-H-bond)	NENWUZ
catena-(tetrakis( $\mu_3$ -Nicotinate N-oxide-O,O',O'')-tetrakis( $\mu_2$ -azido-N,N)-tetra-aqua-tetra-cobalt) [88]	6	$\mu_{(1,1)}$ ; $\mu_3$ -nicotinate-N-oxide; 2D	NENXEK
catena-(tetrakis( $\mu_3$ -4-(N-Oxy-4-pyridyl)benzoato)-tetrakis( $\mu_2$ -azido-N,N)-tetra-aqua-tetra-cobalt(II)) [89]	6	$\mu_{(1,1)}$ ; $\mu_3$ ligand; 2D	RALYIO
catena-(bis( $\mu_4$ -N-oxidopyridine-4-carboxylato)-tetrakis( $\mu_2$ -azido-N,N)-bis(methanol)-tri-cobalt(ii)) [90]	6	di- $\mu_{(1,1)}$ ; 2D ; 1D linked by ligands	TAHFEP
catena-(bis( $\mu_2$ -Azido-N,N)-bis( $\mu_2$ -5-(4-pyridyl N-oxide)tetrazolato-N,N')-tetra-aqua-di-cobalt(ii) dihydrate) [91]	6	$\mu_{(1,1)}$ linked by alternating tetrazolato; (2D-H-bond)	TIDYEL
catena-(bis( $\mu_2$ -azido)-diaqua-cobalt(ii) 4,4'-ethane-1,2-diylbis(pyridine) 1,1'-dioxide) [92]	6	di- $\mu_{(1,1)}$ ; 1D chain; (3D-H-bond) via non-coord. ligand	YONMUK

Mn(II) compounds	CN	bridging	REFCODE
catena-(bis(( $\mu_4$ -4-(1-Hydroxy-1 $\lambda^5$ -pyridin-3-yl)benzoato)-( $\mu_2$ -triazido))-di-manganese) [93]	6	$\mu_{(1,1)}$ ; interchain $\mu_4$ bridge 4,3-opybz; 2D	DEHROZ
catena-(bis( $\mu_3$ -Pyridine-4-carboxylate N-oxide-O,O',O''))-bis( $\mu_2$ -azido-N,N)-diaqua-di-manganese) [88]	6	$\mu_{(1,1)}$ ; $\mu_3$ substituted pyridine N-oxide 2D; (3D- H-bond)	NENWOT
catena-(tetrakis( $\mu_3$ -Nicotinate N-oxide-O,O',O''))-tetrakis( $\mu_2$ -azido-N,N)-tetra-aqua-tetra-manganese) [88]	6	$\mu_{(1,1)}$ $\mu_3$ substituted pyridine N-oxide; 2D	NENXAG
catena-(bis( $\mu_2$ -1,3-Azido)-bis(4,4'-bipyridine-N,N'-dioxide)-dichlorotetraaqua-di-manganese(ii) dihydrate) [94]	6	di- $\mu_{(1,3)}$ ; 1D zipped chain; (2D-H-bond)	PALYEH
catena-(bis(( $\mu_4$ -4-(1-oxy-1 $\lambda^5$ -pyridin-4-yl)benzoato)-( $\mu_2$ -4-(1-oxy-1 $\lambda^5$ -pyridin-4-yl)benzoato))-tetrakis( $\mu_2$ -azido)-tetra-aqua-tetra-manganese dihydrate) [95]	6	di- $\mu_{(1,1)}$ ; $\mu_4$ ligand; 3D	WAVXOI
catena-(bis( $\mu_4$ -N-oxidonicotinato-O,O,O',O''))-bis( $\mu_3$ -N-oxidonicotinato-O,O',O''))-bis( $\mu_3$ -formato-O,O,O')-bis( $\mu_2$ -azido-N,N)-tetra-manganese(ii) methanol solvate) [96]	6	$\mu_{(1,1)}$ $\mu_3$ bridged ligand; 3D	WUVYOC
catena-(bis( $\mu_2$ -azido)-diaqua-manganese(ii) 4,4'-ethane-1,2-diylbis(pyridine) 1,1'-dioxide) [92]	6	di- $\mu_{(1,1)}$ ; non-coord. ligand; 1D chain; (3D-H- bond)	YONMOE

All compounds have the coordination number six, apart from two Zn(II) complexes.

The two-dimensional Cd(II) complexes are coordinated via a  $\mu_{(1,1)}$  azido bridge, in the first case, with two ligands as well and a three-dimensional hydrogen bonding network. The second di- $\mu_{(1,1)}$  azido bridged complex has a di- $\mu_{(1,3)}$  azido bridge additionally and a  $\mu_{(0,0)}$  coordinating 2-picoline-N-oxide ligand. This forms a "honeycomb" like layer. Di- $\mu_{(1,1)}$  azido bridges are present in the one-dimensional Cd(II) complex. The one-dimensional compound with the non-coordinating ligand is isomorph to the Zn(II) compound.

Two Zn(II) complexes have the coordination number five. The two-dimensional complex has a  $\mu_{(1,1)}$  azido bridge and a  $\mu_3$ -nicotinate-N-oxide ligand, which builds this two-dimensional layer. All other Zn(II) compounds have di- $\mu_{(1,1)}$  azido bridges and an one-dimensional system and two of them have non-coordinating ligands as well.

The first Co(II) complex has a di- $\mu_{(1,1)}$  azido bridge to a copper metal center, an one-dimensional Co(II)  $\mu_{(1,1)}$  bridged and a  $\mu_3$  coordinated ligand. The last Co(II) compound in Table 37 shows the same behavior like the first one, but it lacks the coordinated ligand, as well as the copper metal center and it forms three-dimensional hydrogen bonded networks via a non-coordinating ligand. A  $\mu_{(1,1)}$  bridged tetrazolato complex forms also two-dimensional layers via hydrogen bonds. The other two-dimensional complexes have  $\mu_{(1,1)}$  or di- $\mu_{(1,1)}$  azido bridges and an extended hydrogen bond network.

Three Mn(II) compounds with two-dimensional structures are known by now. All of them have a  $\mu_{(1,1)}$  azido bridge and different substituted pyridine-N-oxide ligands coordinated. One of these complexes shows a three-dimensional hydrogen bonded network. The first one-dimensional zipped chain has a di- $\mu_{(1,3)}$  azido bridged network and the other one has also a di- $\mu_{(1,3)}$  azido bridged network as well as a three-dimensional hydrogen bonded network. Last but not least there are two Mn(II) complexes with a three-dimensional di- $\mu_{(1,1)}$  azido bridged network or a  $\mu_{(1,1)}$  azido bridged and  $\mu_3$  ligand bridged network.

### 10.3 Comparison of the thiocyanato and azido complexes

The following Table contains the metal thiocyanato and azido complexes from this master thesis with different substituted pyridine-N-oxides.

Table 38: Thiocyanato and azido complexes with their coordination number and bridging

<b>Cd(II) compounds</b>	<b>CN</b>	<b>bridging</b>
[Cd(2-picoline-N-oxide)(NCS) <sub>2</sub> ] <sub>n</sub> ( <b>1</b> )	6	di- $\mu_{(N,S)}$ ; $\mu_{(O,O)}$ bridged 2-picoline-N-oxide; 2D "honeycomb"
[Cd(3-picoline-N-oxide)(NCS) <sub>2</sub> ] <sub>n</sub> ( <b>2</b> )	6	di- $\mu_{(N,S)}$ ; $\mu_{(O,O)}$ bridged 3-picoline-N-oxide; 2D "honeycomb"
[Cd(4-cyanopyridine-N-oxide) <sub>2</sub> (NCS) <sub>2</sub> (H <sub>2</sub> O)] <sub>2</sub> ( <b>3</b> )	6	dimer; two $\mu_{(N,S)}$ ; one terminal NCS <sup>-</sup> ; 1D (2D-H-bond)
[Cd(4-nitropyridine-N-oxide) <sub>2</sub> (NCS) <sub>2</sub> ] <sub>n</sub> ( <b>4</b> )	6	di- $\mu_{(N,S)}$ double bridge; 1D
[Cd(4-quinoline-N-oxide)(NCS) <sub>2</sub> ] <sub>n</sub> ( <b>5</b> )	6	di- $\mu_{(N,S)}$ double bridge; $\mu_{(O,O)}$ 4-quinoline-N-oxide; 2D "honeycomb"
[Cd(2,6-lutidine-N-oxide)(NCS) <sub>2</sub> ] <sub>n</sub> ( <b>6</b> )	6	di- $\mu_{(N,S)}$ double bridge; $\mu_{(O,O)}$ 2,6-lutidine-N-oxide; 2D "honeycomb"
[Cd(N <sub>3</sub> ) <sub>2</sub> (H <sub>2</sub> O) <sub>2</sub> ] <sub>n</sub> (4-quinoline-N-oxide) <sub>2n</sub> ( <b>7</b> )	6	di- $\mu_{(1,1)}$ ; non-coordinated 4-quinoline-N-oxide; 1D
[Cd(2,6-lutidine-N-oxide)(N <sub>3</sub> ) <sub>2</sub> ] <sub>n</sub> ( <b>8</b> )	6	$\mu_{(1,1)}$ , $\mu_{(1,1,1)}$ azido; 1D double chain
<b>Zn(II) compounds</b>	<b>CN</b>	<b>bridging</b>
[Zn(2-picoline-N-oxide) <sub>2</sub> (NCS) <sub>2</sub> (H <sub>2</sub> O)] <sub>n</sub> ( <b>9</b> )	5	two terminal NCS <sup>-</sup> ; mononuclear Zn (1D-H-bond);
[Zn(4-quinoline-N-oxide) <sub>6</sub> ] <sup>2+</sup> [Zn(NCS) <sub>4</sub> ] <sup>2-</sup> ( <b>10</b> )	6/4	six 4-quinoline-N-oxide (complex cation) / four NCS <sup>-</sup> (complex anion)
[Zn(4-cyanopyridine-N-oxide) <sub>2</sub> (NCS) <sub>2</sub> (H <sub>2</sub> O)] <sub>2</sub> ( <b>11</b> )	5	two terminal NCS <sup>-</sup> ; mononuclear Zn (1D-H-bond)
[Zn(2,6-lutidine-N-oxide) <sub>2</sub> (NCS) <sub>2</sub> ] ( <b>12</b> )	4	two terminal NCS <sup>-</sup> ; mononuclear Zn
[Zn(4-quinoline-N-oxide)(N <sub>3</sub> ) <sub>2</sub> ] <sub>n</sub> ( <b>13</b> )	5	di- $\mu_{(1,1)}$ ; 1D
[Zn(2,6-lutidine-N-oxide)(N <sub>3</sub> ) <sub>2</sub> ] <sub>n</sub> ( <b>14</b> )	5	di- $\mu_{(1,1)}$ ; 1D
[Zn(4-picoline-N-oxide)(N <sub>3</sub> ) <sub>2</sub> ] <sub>n</sub> ( <b>15</b> )	5	di- $\mu_{(1,1)}$ ; 1D
[Zn(2-O-pyridine-N-oxide)(N <sub>3</sub> )(H <sub>2</sub> O)] <sub>n</sub> ( <b>16</b> )	5	$\mu_{(1,1)}$ ; 1D (2D-H-bond)
<b>Co(II) compounds</b>	<b>CN</b>	<b>bridging</b>
[Co(2,6-lutidine-N-oxide) <sub>2</sub> (NCS) <sub>2</sub> ] <sub>2</sub> ( <b>17</b> )	5	dimer; two $\mu_{(N,S)}$ ; one terminal NCS <sup>-</sup> ; 1D
[Co(4-cyanopyridine-N-oxide) <sub>2</sub> (NCS) <sub>2</sub> (H <sub>2</sub> O)] <sub>2</sub> ( <b>18</b> )	6	dimer; two $\mu_{(N,S)}$ ; one terminal NCS <sup>-</sup> ; 1D (2D-H-bond)
[Co(N <sub>3</sub> ) <sub>2</sub> (H <sub>2</sub> O) <sub>2</sub> ] <sub>n</sub> (3-picoline-N-oxide) <sub>2n</sub> ( <b>19</b> )	6	di- $\mu_{(1,1)}$ ; non-coordinated 3-picoline-N-oxide; 1D
[Co(2,6-lutidine-N-oxide)(N <sub>3</sub> ) <sub>2</sub> ] <sub>n</sub> ( <b>20</b> )	5	di- $\mu_{(1,1)}$ ; 1D
<b>Mn(II) compounds</b>	<b>CN</b>	<b>bridging</b>
[Mn(2-picoline-N-oxide)(NCS) <sub>2</sub> ] <sub>n</sub> ( <b>21</b> )	6	di- $\mu_{(N,S)}$ ; $\mu_{(O,O)}$ 2-picoline-N-oxide; 2D "honeycomb"
[Mn(3-picoline-N-oxide) <sub>2</sub> (NCS) <sub>2</sub> ] <sub>n</sub> ( <b>22</b> )	6	di- $\mu_{(N,S)}$ ; $\mu_{(O,O)}$ 3-picoline-N-oxide; 1D
[Mn(4-picoline-N-oxide) <sub>2</sub> (NCS) <sub>2</sub> (H <sub>2</sub> O)] <sub>n</sub> ( <b>23</b> )	6	two terminal NCS <sup>-</sup> ; mononuclear Mn (1D-H-bond)
[Mn(4-cyanopyridine-N-oxide) <sub>2</sub> (NCS) <sub>2</sub> (H <sub>2</sub> O)] <sub>2</sub> ( <b>24</b> )	6	dimer; two $\mu_{(N,S)}$ ; one terminal NCS <sup>-</sup> ; 1D (2D-H-bond)
[Mn(2-picoline-N-oxide)(N <sub>3</sub> ) <sub>2</sub> ] <sub>n</sub> ( <b>25</b> )	6	di- $\mu_{(1,3)}$ double bridged; $\mu_{(O,O)}$ 2-picoline-N-oxide; 2D "honeycomb"
[Mn(N <sub>3</sub> ) <sub>2</sub> (H <sub>2</sub> O) <sub>2</sub> ] <sub>n</sub> (3-picoline-N-oxide) <sub>2n</sub> ( <b>26</b> )	6	di- $\mu_{(1,1)}$ non-coordinated 3-picoline-N-oxide; 1D
[Mn <sub>3</sub> (N <sub>3</sub> ) <sub>6</sub> (4-picoline-N-oxide) <sub>2</sub> (H <sub>2</sub> O) <sub>2</sub> ] <sub>n</sub> ( <b>27</b> )	6	8x $\mu_{(1,3)}$ , $\mu_{(1,1)}$ ; $\mu_{(O,O)}$ 4-picoline-N-oxide; 3D

Compounds **(1)** and **(2)** show quite similar properties, both have a di- $\mu_{(N,S)}$  bridging isothiocyanate and  $\mu_{(O,O)}$  bridged ligands as well as a two-dimensional “honeycomb” like layer. This is quite similar to compound **(22)**, with the major difference that it forms an one-dimensional chain. The complexes **(3)**, **(24)** and **(18)** are also quite similar, because both have a two  $\mu_{(N,S)}$  bridged isothiocyanate linkage and one terminal NCS<sup>-</sup>. All of them build an one-dimensional system, which extends to a two-dimensional one via hydrogen bonds. Compound **(4)** has a di- $\mu_{(N,S)}$  double bridge and builds up an one-dimensional system. The complexes **(5)**, **(6)**, **(21)** and **(25)** build a “honeycomb” like two-dimensional layer. This is formed by the thiocyanato/azido bridges and the different ligands. Compound **(7)** builds an one-dimensional chain from a di- $\mu_{(1,1)}$  azido bridge. The complex **(8)** is the only  $\mu_{(1,1)}$  and  $\mu_{(1,1,1)}$  azido bridged, one-dimensional double chain in this work. The compounds **(9)**, **(11)**, **(12)** and **(23)** have two terminal isothiocyanates. So far all metal centers of the compounds have the coordination number six, apart from compound **(9)** and **(11)**, which have coordination number five and compound **(12)**, which is the only compound with coordination number four in this master thesis. The Zn(II) compound **(10)** is also unique in this work, because it has a complex cation (six times 4-quinoline-N-oxide) and a complex anion (four times isothiocyanate). Depending on the metal center of the complex cation the coordination number is six and the metal center of the complex anion has the coordination number four. The compounds **(13)**, **(14)** and **(15)** have an one-dimensional chain with di- $\mu_{(1,1)}$  azido bridges that connect the metal centers. The different ligands are located on terminal positions. Compound **(16)** has a  $\mu_{(1,1)}$  azido bridged one-dimensional chain, with a two-dimensional hydrogen bond network and it is the only compound with a chelating ligand in this work. The complex **(17)** is a  $\mu_{(N,S)}$  bridged dimer. The metal centers of the compounds **(13)**, **(14)**, **(15)**, **(16)** and **(17)** have the coordination number five. Both compounds **(19)** and **(26)** have an one-dimensional chain, which is di- $\mu_{(1,1)}$  azido bridged and both have non-coordinated ligands as well as the coordination number six. The penta-coordinated compound **(20)** is a di- $\mu_{(1,1)}$  azido bridged one-dimensional complex. Compound **(27)** has the only three-dimensional structure in this work. It has eight  $\mu_{(1,3)}$  and  $\mu_{(1,1)}$  azido bridges as well as  $\mu_{(O,O)}$  coordinated 4-picoline-N-oxide that builds a three-dimensional network.

## 10.4 Interpretation of the luminescence data

### 10.4.1 Ligands

2-methylpyridine-N-oxide, 3-methylpyridine-N-oxide and 4-quinoline-N-oxide show similar emission maxima and comparable Stokes-shifts (from 13045 to 13963 cm<sup>-1</sup>) as well as small values for the full width at half maximum compared to the other ligands. One reason for this could be that they show  $\pi \rightarrow \pi^*$  and  $\sigma \rightarrow \sigma^*$  transitions in the UV-visible region. Both the HOMO and the LUMO are the main orbitals for the chemical stability of these ligands. [46] The HOMO has the ability to donate an electron to the LUMO. So this transition implies an electron density transfer from the oxygen atom to the ring and only a small amount of the density was provided by the ring itself. [47]

4-methylpyridine-N-oxide however is an exception to the other methylpyridine-N-oxides. Its emission maximum is quite similar to the 2-hydroxypyridine-N-oxide, but the Stokes-shift is very large and the FWHM is quite similar to the 4-cyanopyridine-N-oxide. Another important fact is, that the 1-hydroxy-2-pyridone tautomer is more common than the 2-hydroxypyridine-N-oxide one. This may be the reason for the chelating effect of this ligand. [44] The large Stokes-shift and the broad FWHM values are also detectable for the 2,6-dimethylpyridine-N-oxide. This leads to the conclusion, that they are involved in charge-transfer transitions and not in  $\pi \rightarrow \pi^*$  or  $\sigma \rightarrow \sigma^*$  transitions. [48a]

#### 10.4.2 Cd(II) complexes

Studies have shown that Cd(II) structures exhibit luminescence properties in solid state at room temperature. [49] The emission spectra of the Cd(II) complexes are located in the attachment.

Since azide and thiocyanate is non-luminescent in the observed region [50] the luminescent properties of the structures are mainly depended on the coordination effects from the ligand to the metal ion. In all cases the emission bands are broad (from 3250 to 4948  $\text{cm}^{-1}$ ) and the Stokes-shifts are large (from 7728 to 14092  $\text{cm}^{-1}$ ). These are two strong indications for charge-transfer transitions. [48a]

The complexes **(1)** and **(6)** have the same emission maximum and also **(2)** and **(8)** show this behavior. Although they have quite similar FWHM values they are not fully comparable because of their different Stokes-shifts. It is notable that the substances **(8)** and **(6)** vary in their structural composition but the Stokes-shifts are quite similar.

Compound **(5)** has the highest emission maximum of 631 nm, the biggest Stokes-shift and the broadest band. No influence from the ligand was detectable in compound **(4)**, so the resulting emission is only due to the charge-transfer effect from the conjugated system of the pyridine-N-oxide ring to the metal center. This effect is amplified to the electron pushing mechanism of the para substituted nitro group. [12a]

Complex **(3)** contains hydrogen bonds, which doesn't disturb the interaction between the ligand and the metal center and therefore no quenching happens. This is documented by the characteristic values for the FWHM and the Stokes-shift. [51]

Due to the electromagnetic spectrum all complexes emit yellow/green light, apart from **(5)** which emits red light.

#### 10.4.3 Zn(II) complexes

Studies have shown that Zn(II) structures exhibit luminescence properties in solid state at room temperature. [52] The emission spectra of the Zn(II) complexes are located in the attachment.

Similar to the Cd(II) complexes the emission bands of the Zn(II) complexes are broad (from 3347 to 4447  $\text{cm}^{-1}$ ) and the Stokes-shifts are large (from 8284 to 14273  $\text{cm}^{-1}$ ). These are two strong indications for charge-transfer transitions as I mentioned above. One interesting fact is, that the emission maximum of compound **(4)** is identical to compound **(9)**, although they have different metal centers and different coordination numbers. Another consensus is the similar FWHM, which indicates in both cases a charge-transfer transition. The biggest difference lies in the values of the Stokes-shift. The compounds **(11)** and **(15)** show similar emission maxima, comparable Stokes-shifts and broad FWHM values. Complex **(12)** and **(14)** differ in their coordination numbers and geometry. Although there are these structural deviations, the location of the emission maxima, the Stokes-shift and the FWHM are in good agreement. Compound **(16)** exhibits the strongest luminescence intensity, because of the strong interaction of the ligand and the metal. This is due to the fact of the increasing rigidity caused by the chelating effect of the 2-hydroxypyridine-N-oxide, which reduces the loss of energy by non-radiative decay. [53][54] Both complexes **(10)** and **(13)** show quite similar emission maxima and resemble FWHM values. The only big difference is the deviation of the Stokes-shift. This can be traced back to fact that complex **(10)** has different moieties. Due to the electromagnetic spectrum all complexes emit yellow/green light, with the only exception of **(10)** and **(13)** which emits red light. This observation corresponds to complex **(5)** and is mainly achieved via MLCT processes. [55]

## 11) Summary

During this master thesis 16 isothiocyanato and 11 azido complexes with divalent cations of cadmium, zinc, cobalt and manganese as metal centres with different substituted pyridine-N-oxides, are synthesized and investigated on their structural properties.

The following substituted pyridine-N-oxides act as neutral, terminal ligands in the different complexes (2-picoline-N-oxide, 3-picoline-N-oxide, 4-picoline-N-oxide, 4-cyanopyridine-N-oxide, 4-nitropyridine-N-oxide, 4-quinoline-N-oxide and 2,6-lutidine-N-oxide). Some of them connect the metal centers via  $\mu_{(O,O)}$  bridging (2-picoline-N-oxide, 3-picoline-N-oxide, 4-quinoline-N-oxide, 4-picoline-N-oxide and 2,6-lutidine-N-oxide). Two already mentioned ligands serve as non-coordinated stabilizers in the lattice (3-picoline-N-oxide and 4-quinoline-N-oxide). 2-hydroxypyridine-N-oxide is the only anionic, chelating ligand in this work.

All reported metal centers from the Cd(II) compounds have the coordination number six. The common bridging is di- $\mu_{(N,S)}$  via the isothiocyanato and  $\mu_{(O,O)}$  with the different substituted pyridine-N-oxides. This results in a usual two-dimensional "honeycomb" like layer structure. An one-dimensional di- $\mu_{(N,S)}$  isothiocyanato bridged dimer with a terminal  $NCS^-$  and an one-dimensional di- $\mu_{(N,S)}$  double bridged compound are also synthesized. In addition to an one-dimensional di- $\mu_{(1,1)}$  azido bridged complex, a  $\mu_{(1,1)}$ ,  $\mu_{(1,3)}$  azido bridged one-dimensional double chain is also present.

The metal center of the Zn(II) compounds have three different coordination numbers. The most common one is five. Two penta-coordinated, one-dimensional compounds with two terminal  $NCS^-$  are equally represented as a mononuclear Zn(II) unit with two terminal  $NCS^-$  and coordination number of four. The complex cation ( $[Zn(4\text{-quinoline-N-oxide})_6]^{2+}$ ) and complex anion ( $[Zn(NCS)_4]^{2-}$ ), which both have the coordination number six and four, respectively, are special cases. Last but not least there are three one-dimensional di- $\mu_{(1,1)}$  azido bridged complexes and a  $\mu_{(1,1)}$  azido bridged compound. All of them have the coordination number five.

The Co(II) compounds have all one-dimensional structures with the coordination numbers five and six, respectively. There are two dimers present, a penta-coordinated  $\mu_{(N,S)}$  isothiocyanato bridged one and a similar one with coordination number six. A penta-coordinated di- $\mu_{(1,1)}$  azido bridged complexes and a di- $\mu_{(1,1)}$  azido bridged complexes with a non-coordinated 3-picoline-N-oxide and the coordination number six are also observed.

All investigated Mn(II) compounds have the coordination number six. Two of them show the well-known "honeycomb" like two-dimensional layers and another one has eight  $\mu_{(1,3)}$  and one  $\mu_{(1,1)}$  azido bridges, as well as one  $\mu_{(O,O')}$  bridged 4-picoline-N-oxide, which builds a three-dimensional network. A mononuclear Mn(II) compound with two terminal  $NCS^-$  and a dimer with di- $\mu_{(N,S)}$  isothiocyanato bridge and one terminal  $NCS^-$  is likewise represented. Similar to the Co(II) compound a di- $\mu_{(1,1)}$  azido bridged, one-dimensional Mn(II) complex with a non-coordinating 3-picoline-N-oxide is also synthesized.

The Racah parameter B and the crystal field splitting parameter are calculated and the spectroscopic transitions are investigated with a Tanabe-Sugano diagram.

The luminescence properties of the Zn(II) and the Cd(II) compounds are investigated by the recording of the excitation and the emission spectrum for the pure ligands and for the compounds, respectively. After the calculation of the Stokes-shift, the FWHM of the band's and the corresponding emission maxima are determined. The charge-transfer properties for the compounds are assigned and compared to each other.

## 12) References

- [1] (a) A.M. Hardy, R.L. La Duca, *Inorg. Chem. Commun.* 12 (2009) 308;  
(b) J.G. Mao, *Coord. Chem. Rev.* 251 (2007) 1493;  
(c) S. Youssif, *Arkivoc part(i)* (2001) 242.
- [2] (a) M. Kumar, M. Srivastava, R.A. Yadav, *Spectrochimica Acta Part A: Molecular and Biomolecular Spectroscopy* 111 (2013) 242;  
(b) R. Sarma, A. Karmakar, J.B. Baruah, *Inorganica Chimica Acta* 361 (2008) 2081;  
(c) A.V. Malkov, M. Bell, F. Castelluzzo, P. Kocovsky, *Org. Lett.* 7 (2005) 3219;  
(d) A. Albini, *Synthesis* (1993) 263;  
(e) J. Monot, M. Petit, S.M. Lane, I. Guisle, J. Léger, C. Tellier, D.R. Talham, B. Bujoli, *J. Am. Chem. Soc.* 130 (2008) 6243;  
(f) J. Umeda, M. Suzuki, M. Kato, M. Moriya, W. Sakamoto, T. Yogo, *J. Power Sources* 195 (2010) 5882.
- [3] (a) C.J. O'Connor, E. Sinn, R.L. Carlin, *Inorg. Chem.* 16 (1977) 3314;  
(b) Z. Hnatejko, D. Kwiatek, G. Dutkiewicz, M. Kubicki, R. Jastrza, S. Lis, *Polyhedron* 81 (2014) 728.
- [4] (a) S.N. Kilényi, *e-EROS Encyclopedia of Reagents for Organic Synthesis*, (2001) Pyridine-N-Oxide;  
(b) RÖMPP Online—Version 3.5 Thieme Chemistry, Stuttgart: Georg Thieme, 2009.
- [5] (a) F.H. Allen, *Acta Cryst.* B58 (2002) 380;  
(b) J. van de Streek, *Acta Cryst.* B62 (2006) 567;  
(c) A.G. Orpen, *Acta Cryst.* B58 (2002) 398;  
(d) F.H. Allen, W.D.S. Motherwell, *Acta Cryst.* B58 (2002) 407;  
(e) R. Taylor, *Acta Cryst.* D58 (2002) 879.
- [6] (a) F.A. Mautner, L. Öhrström, B. Sodin, R. Vicente, *Inorg. Chemistry* 13 (2009) 6280;  
(b) O. Kahn, *Molecular Magnetism*, first edition, Wiley-VCH, New York, 1993;  
(c) J.S. Miller, M. Drillon (Eds.), *Magnetism: Molecules to Materials II; Molecule-Based Magnets*, Wiley-VCH, Weinheim, 2001.
- [7] (a) S. Youngme, J. Phatchimkun, U. Suksangpanya, C. Pakawatchai, G.A. van Albada, M. Quesada, J. Reedijk, *Inorganic Chemistry Communications* 9 (2006) 242;  
(b) A. Escuer, R. Vicente, J. Ribas, X. Solans, *Inorg. Chem.* 34 (1995) 1793;  
(c) R. Cortes, J.I. Ruiz de Larramendi, L. Lezama, T. Rojo, K. Urriaga, M.I. Arriortua, *J. Chem. Soc.*,

- Dalton Trans. 18 (1992) 2723;
- (d) M.G. Barandika, R. Cortes, L. Lezama, M.K. Urriaga, M.I. Arriortua, T. Rojo, J. Chem. Soc., Dalton Trans. 17 (1999) 2971;
- (e) J. Cano, G.D. Munno, F. Lloret, M. Julve, Inorg. Chem. 39 (2000) 1611;
- (f) M.I. Arriortua, R. Cortes, J.L. Mesa, L. Lezama, T. Rojo, G.Villeneuve, Trans. Met. Chem. 13 (1988) 371;
- (g) A. Escuer, I. Castro, F. Mautner, M.S. El Fallah, R. Vicente, Inorg. Chem. 36 (1997) 4633.
- [8] (a) H. Wanga, G. Jiaa, Y. Wanga, Z. Youa, J. Lia, Z. Zhua, F. Yanga, Y. Weia, C. Tua, Optical Materials 12 (2007) 1635;
- (b) M.E. Foglio, G.E. Barberis, J. Phys.[online] 36 (2006) 40.
- [9] Vivian Wing-Wah Yam, Kenneth Kam-Wing Lo, Chem. Soc. Rev. 28 (1999) 323.
- [10] (a) M. Gaft, R. Reisfeld, G. Panczer, Modern Luminescence Spectroscopy of Minerals and Materials, Springer Verlag, Berlin Heidelberg, 2005, p.220;
- (b) G. Boulon, Materials Chemistry and Physics 16 (1987) 301.
- [11] J. Garcia Sole, L.E. Bausa, An Introduction to the Optical Spectroscopy of Inorganic Solids, Wiley-Interscience, England, 2005.
- [12] a) B. Valeur, Molecular Fluorescence Principles and Applications, first edition, Wiley-VCH, Weinheim, 2002.
- b) Dissertation-thesis Javid Shirdal"Photo-Physical Characterisation of Flavin-Pyrene-Phenothiazine Molecular Photonic complexes" Universität Regensburg, 2007.
- [13] G. Herzberg, Molecular Spectra and Molecular Structure. III Electronic Spectra and Electronic Structure of Polyatomic Molecules, Van Nostrand Reinhold Company, New York, 1966.
- [14] H. Jaffé, M. Orchin, Theory and Applications of Ultraviolet Spectroscopy, John Wiley & Sons, New York, 1962.
- [15] J.B. Birks, Photophysics of Aromatic Molecules, Wiley, London, 1969.
- [16] J.B. Birks, Organic Molecular Photophysics, Wiley, London, 1973.
- [17] E.I. Whery, Effects of Molecular Structure on Fluorescence and Phosphorescence, Practical Fluorescence, New York, 1990, pp. 75-125.
- [18] A.B.P. Lever, Journal of Chemical Education, Volume 51 Number 9 (1974) 612.
- [19] A. Lan, L. Han, D. Yuan, F. Jiang, M. Hong, Inorganic Chemistry Communications 10 (2007) 993.
- [20] Antonín Vlcek Jr., Coordination Chemistry Reviews 177 (1998) 219.
- [21] O. Kohle, S. Ruile, M. Grätzel, Inorganic Chemistry 35 (1996) 4779.

- [22] a) A. Albini, S. Pietra, Heterocyclic N-Oxides, CRC Press, New York, 1991;
- b) R.A. Abramovitch, The Chemistry of Heterocyclic Compounds, Pyridine and Its Derivatives, Supplement Part one, John Wiley and Sons, New York London Sydney, Toronto, 1974;
- c) N. Wiberg, E. Wiberg, A.F. Holleman, Lehrbuch der Anorganischen Chemie, 102. Auflage, Walter de Gruyter & Co, Berlin New York, 2007.
- [23] Scifinder, Chemical Abstracts Service, version 2014 (accessed August, 2014).
- [24] U. Rokosch, Airbags und Gurtstraffer, Vogel Buchverlag, Würzburg, 2002.
- [25] Z. Dori, R.F. Ziolo, Chem.Rev. 73 (1973) 247.
- [26] N. Greenwood, A. Earnshaw, Chemistry of the Elements, Oxford Press, England, 1997, p.326.
- [27] Diploma-thesis Beaty Sudy „Synthese und Charakterisierung von Azidokomplexen mit Zn(II) und Co(II)“ TU Graz, 2008
- [28] APEX and SAINT, Area Detector Software package and AXS Area Detector Integration program, Bruker Analytical X-ray, Madison, WI, 1997.
- [29] SADABS, AXS Area Detector Absorption program, Bruker Analytical X-ray, Madison, WI, 1997.
- [30] G. Sheldrick, Acta Cryst. Sect.A. 64 (2008) 112.
- [31] A.L. PLATON, A.L. Spek, A Multipurpose Crystallographic tool, Utrecht University, Utrecht, Netherlands, 2005.
- [32] Perkin Elmer manual „Flexibility Versatility Reliability with LS 55 Luminescence spectrometer“.
- [33] Perkin Elmer manual “100 mm Diffuse Reflectance and Transmission Integrating Sphere Accessory for All High-End LAMBDA Systems“.
- [34] OPUS-software, Vers. 5., Bruker Optics, Billerica, MA, US.
- [35] K. Nakamoto, Infrared and Raman spectra of inorganic and coordination compounds, fourth edition, Wiley interscience, 1986, ( $N_3^-$ : p. 291 Table III-45; for  $SCN^-$ : p.284 Table III-40;  $H_2O$  normal modes page 30).
- [36] A.W. Addison, T. Nageswara Rao, J. Reedijk, J. van Rijn, G.C. Verschoor, J. Chem. Soc., Dalton Trans. 7 (1984) 1349.
- [37] A. Escuer, R. Vicente, M.A.S. Goher, F.A. Mautner, Inorg. Chem. 37 (1998) 782.
- [38] F.A. Mautner, C.Gspan, M.A.S.Goher, M.A.M. Abu-Youssef, Monatsh.Chem. 134 (2003) 1311.
- [39] H.F. Hamerka, C.C. Vlam, Physica Volume 19 Issues 1-12 (1953) 943.
- [40] Software from BioLight Luminescence Systems GmbH, 88690 Uhlidingen-Mühlhofen Germany, Version 2012.

- [41] Perkin Elmer User Guide LS55, Part Number 09934436, Release A, August 2000.
- [42] Yu-Hui Liu, Guang-Jiu Zhao, Guang-Yue Li, Ke-Li Han, *Journal of Photochemistry and Photobiology A: Chemistry* 209 Issues 2–3 (2010) 181.
- [43] Zuo-Qin Liang, Ye-Xin Li, Jia-Xiang Yang, Yan Ren, Xu-Tang Tao, *Tetrahedron Letters* 52 (2011) 1329.
- [44] E. A. Landers, D.J. Phillips, *Inorganica Chimica Acta* 51 (1981) 109.
- [45] L.A. Aslanov, V.M. Ionov, K. Kynev, *Kristallografiya* 21 (1976) 1198.
- [46] S. Gunasekaran, S.A. Balaji, R. Kumaresan, S. Anand, G. Srinivasan, *Canadian Journal of Analytical Sciences and Spectroscopy* 53 Issue 4 (2008) 149.
- [47] D. Shoba, S. Periandi, S. Boomadevi, S. Ramalingam, E. Fereyduni, *Spectrochimica Acta Part A: Molecular and Biomolecular Spectroscopy* 118 (2014) 438.
- [48] a) L. van Pieterse, M. Heeroma, E. de Heer, A. Meijer, *Journal of Luminescence* 91 (2000) 177.
- b) Taken from the internet "opts.phys.msu.ru/ctl", 25.10.2014 at 14.45 o'clock.
- [49] J. Tao, X. Yin, Z.B. Wei, R.B. Huang, L.S. Zheng, *Eur. J. Inorg. Chem.* 1 (2004) 125.
- [50] S. Singh, P. Mayer, A. Pandey, *Indian Journal of Chemistry-A* Volume 49 Issue 10 (2010) 1345.
- [51] Jian-Qiang Liu, Zhen-Bin Jia, Yao-Yu Wang, *Journal of Molecular Structure* 987 (2011) 126.
- [52] L. Croitor, E.B. Coropceanu, A.V. Siminel, M.M. Botoshansky, M.S. Fonari, *Inorganica Chimica Acta* 370 (2011) 411.
- [53] Guo-Ping Yong, Ying-Zhou Li, Yi-Man Zhang, Wen-Long She, *CrystEngComm* 14 (2012) 1439.
- [54] Z.L. Fang, R.M. Yu, J.G. He, Q.S. Zhang, Z.G. Zhao, C.Z. Lu, *Inorg. Chem.* 48 (2009) 7691.
- [55] Xian-yong Wang, Andre Del Guerso, Russell H. Schmehl, *Journal of Photochemistry and Photobiology C: Photochemistry Reviews* 5 (2004) 55.
- [56] I. Deperasinska, A. Makarewicz, A. Szemik-Hojniak, *Acta Physica Polonica A* 112 (2007) 71.
- [57] B. Henderson, G.F. Imbusch, *Optical Spectroscopy of Inorganic Solids*, Oxford Science Publications, 1989.
- [58] G. Racah, *Physical Review* 62 (1942) 438.
- [59] Y. Tanabe, S. Sugano, *Journal of the Physical Society of Japan* 9 (1954) 753.
- [60] C.E. Housecroft, A.G. Sharpe, *Inorganic Chemistry*, 2nd ed., Pearson Publisher, Harlow England, 2004, p.578.
- [61] E. Underhill, E. Billing, *Nature* 5038 (1966) 834.
- [62] Y. Tanabe, S. Sugano *Journal of the Physical Society of Japan* 9 (1954) 766.

- [63] R. Abu-Eittah, G. Arafa, *Journal of Inorg. and Nucl. Chem.* Volume 32 Issue 10 (1970) 3337.
- [64] C.E. Housecroft, A.G. Sharpe, *Inorganic Chemistry*, forth ed., Pearson Publisher, Harlow England, 2012, p.691.
- [65] Xiao-Jun Feng, Jia-Xiang Yang, Wen-Tao Yu, Hoong-Kun Fun, Jie-Ying Wu, Yu-Peng Tian, *Wuji Huaxue Xuebao(Chin.)(Chin.J.Inorg.Chem.)* 20 (2004) 403.
- [66] S. Mondal, A. Guha, E. Suresh, A.D. Jana, A. Banerjee, *J.Mol.Struct.* 1029 (2012) 169.
- [67] J.M. Shi, Z. Liu, C.J. Wu, H.Y. Xu, L.D. Liu, *J.Coord.Chem.* 59 (2006) 1883.
- [68] Lin-Ping Zhang, Wen-Jie Lu, T.C.W. Mak, *Chem.Commun.* 22 (2003) 2830.
- [69] Jing-Min Shi, Feng-Xia Zhang, Jie Huang, Lian-Dong Liu, *Jiegou Huaxue(Chin.J.Struct.Chem.)* 25 (2006) 779.
- [70] S.A. Bourne, L.J. Moitsheki, *Polyhedron* 26 (2007) 2719.
- [71] Wei Cao, Hao-Ling Sun, Zongsheng Li, *Inorg.Chem.Commun.* 19 (2012) 19.
- [72] Jing Min Shi, Liu Zhe, Jian Jun Lu, Lian Dong Liu, *Acta Crystallogr., Sect.E:Struct.Rep.Online* 61 (2005) m1133.
- [73] Jing-Min Shi, Hai-Yan Xu, Lian-Dong Liu, *Acta Crystallogr., Sect.E:Struct.Rep.Online* 62 (2006) m1577.
- [74] Shi-Guo Zhang, Wei-Nan Li, Jing-Min Shi, *Acta Crystallogr., Sect.E:Struct.Rep.Online* 62 (2006) m3506.
- [75] Jing-Min Shi, Zhe Liu, You-Min Sun, Long Yi, Lian-Dong Liu, *Chem.Phys.* 325 (2006) 237.
- [76] A.D. Jana, S.C. Manna, G.M. Rosair, M.G.B. Drew, G. Mostafa, N.R. Chaudhuri, *Cryst.Growth&Des.* 7 (2007) 1365.
- [77] Shi-Guo Zhang, Wei-Nan Li, Jing-Min Shi, *Acta Crystallogr., Sect.E:Struct.Rep.Online* 62 (2006) m3398.
- [78] J.M. Shi, J.N. Chen, C.J. Wu, J.P. Ma, *J.Coord.Chem.* 60 (2007) 2009.
- [79] D.C. Craig, D.J. Phillips, F.M.Z. Kaifi, *Inorg.Chim.Acta* 161 (1989) 247.
- [80] Shi-Guo Zhang, Hai-Yan Xu, Jing-Min Shi, *Acta Crystallogr., Sect.E:Struct.Rep.Online* 63 (2007) m2083.
- [81] J.M. Shi, Z. Liu, W.N. Li, H.Y. Zhao, L.D. Liu, *J.Coord.Chem.* 60 (2007) 1077.
- [82] J.M. Shi, J.N. Chen, L.D. Liu, *Pol.J.Chem.* 80 (2006) 1909.
- [83] Chun-Shang Li, Lin Xue, Yun-Xia Che, Feng Luo, Ji-Min Zheng, T.C.W. Mak, *Inorg.Chim.Acta* 360 (2007) 3569.

- [84] Zhi-Xiang Wang, Xiu-Bing Li, Bai-Wang Sun, *Acta Crystallogr., Sect.E:Struct.Rep.Online* 64 (2008) m792.
- [85] F.A. Mautner, C. Gspan, M.A.S. Goher, M.A.M. Abu-Youssef, *Monatsh.Chem.* 136 (2005) 107.
- [86] Chun-Wei Xin, Fu-Chen Liu, *Acta Crystallogr., Sect.E:Struct.Rep.Online* 64 (2008) m1629.
- [87] Jiong-Peng Zhao, Ran Zhao, Bo-Wen Hu, Qian Yang, Xiao-Feng Zhang, Fu-Chen Liu, *Eur.J.Inorg.Chem.* 13 (2013) 2389.
- [88] Zheng He, Zhe-Ming Wang, Song Gao, Chun-Hua Yan, *Inorg.Chem.* 45 (2006) 6694.
- [89] Xiu-Mei Zhang, Kun Wang, Yan-Qin Wang, En-Qing Gao, *Dalton Trans.* 40 (2011) 12742.
- [90] Fu-Chen Liu, Min Xue, Hai-Chao Wang, Jie Ou-Yang, *Eur.J.Inorg.Chem.* 28 (2010) 4444.
- [91] Zhi-Rong Qu, *Wuji Huaxue Xuebao(Chin.)(Chin.J.Inorg.Chem.)* 23 (2007) 1117.
- [92] Hao-Ling Sun, Zhe-Ming Wang, Song Gao, *Chem.-Eur.J.* 15 (2009) 1757.
- [93] Xiu-Mei Zhang, Wei Gao, Jie-Ping Liu, En-Qing Gao, *Inorg.Chim.Acta* 392 (2012) 311.
- [94] A.K. Ghosh, D. Ghoshal, E. Zangrando, J. Ribas, N.R. Chaudhuri, *Inorg.Chem.* 44 (2005) 1786.
- [95] Xiu-Mei Zhang, Yan-Qin Wang, Xiu-Bing Li, En-Qing Gao, *Dalton Trans.* 41 (2012) 2026.
- [96] Jiong-Peng Zhao, Bo-Wen Hu, Qian Yang, Xiao-Feng Zhang, Tong-Liang Hu, Xian-He Bu, *Dalton Trans.* 39 (2010) 56.

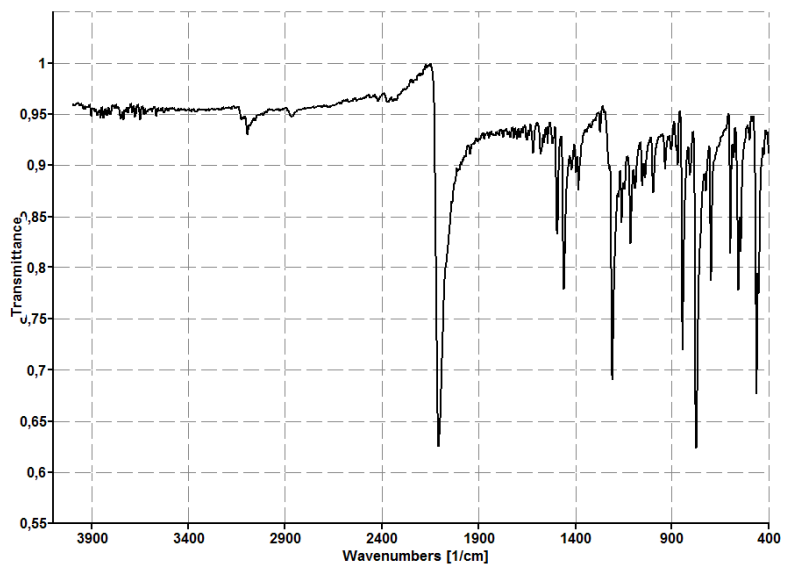
### 13) Attachment

IR-spectra

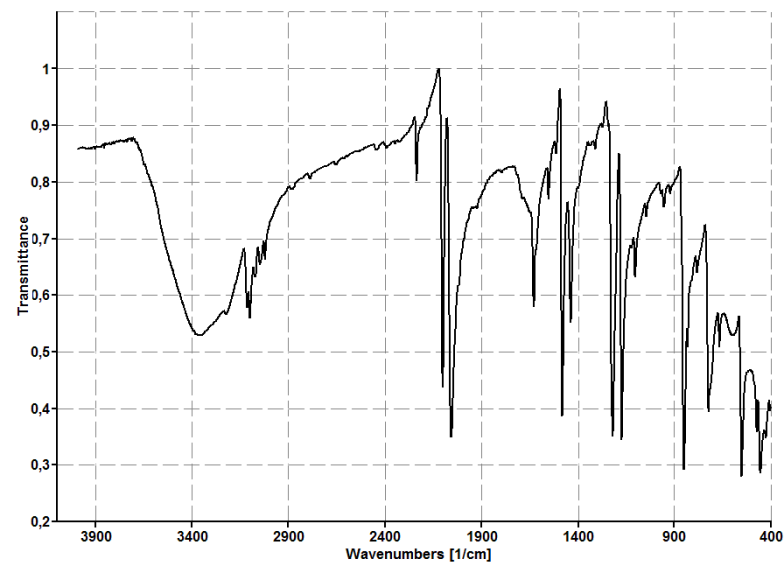
Luminescence-spectra

UV/VIS/NIR-spectra

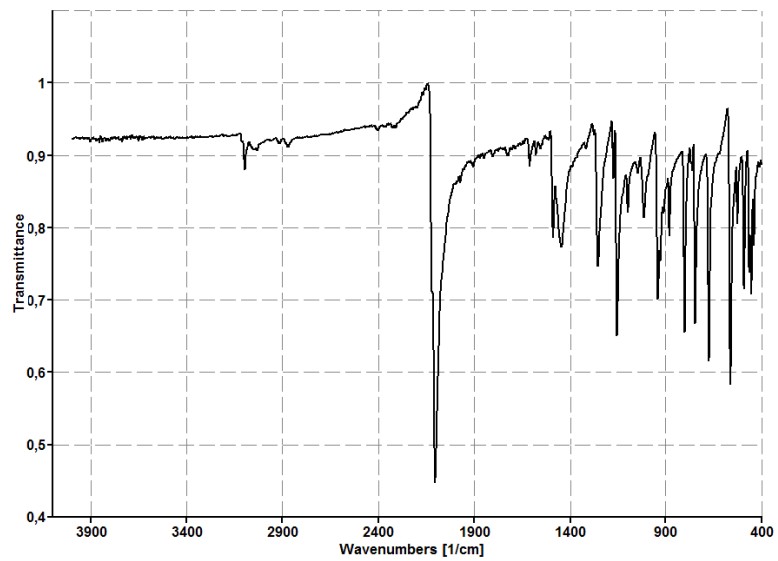
Crystallographic data and processing parameters



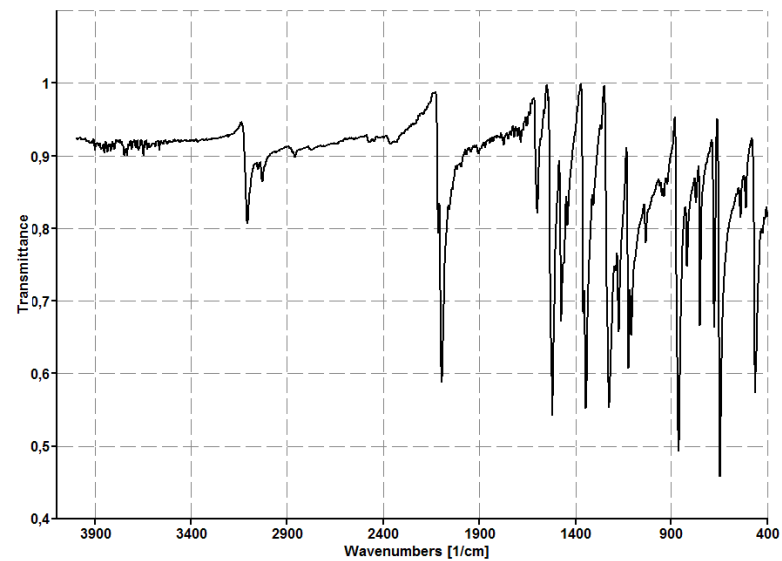
$[\text{Cd}(\text{2-picoline-N-oxide})(\text{NCS})_2]_n$  (**1**)



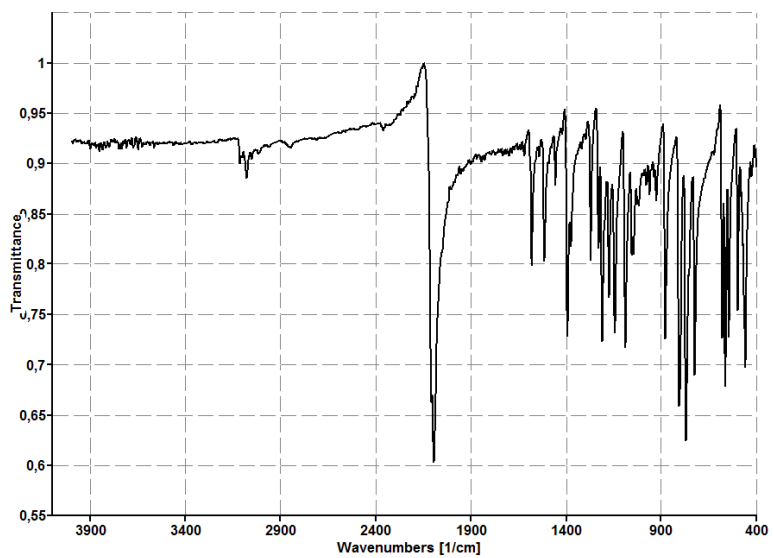
$[\text{Cd}(\text{4-cyanopyridine-N-oxide})_2(\text{NCS})_2(\text{H}_2\text{O})_2]_2$  (**3**)



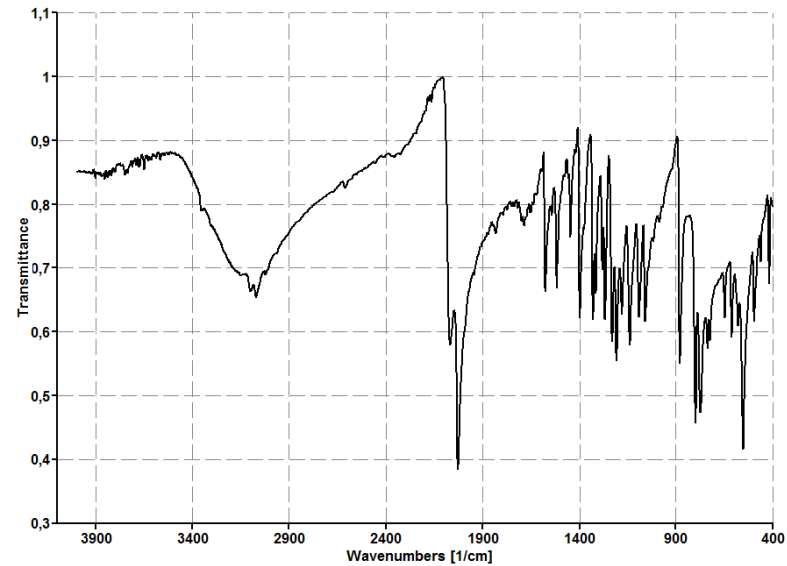
$[\text{Cd}(\text{3-picoline-N-oxide})(\text{NCS})_2]_n$  (**2**)



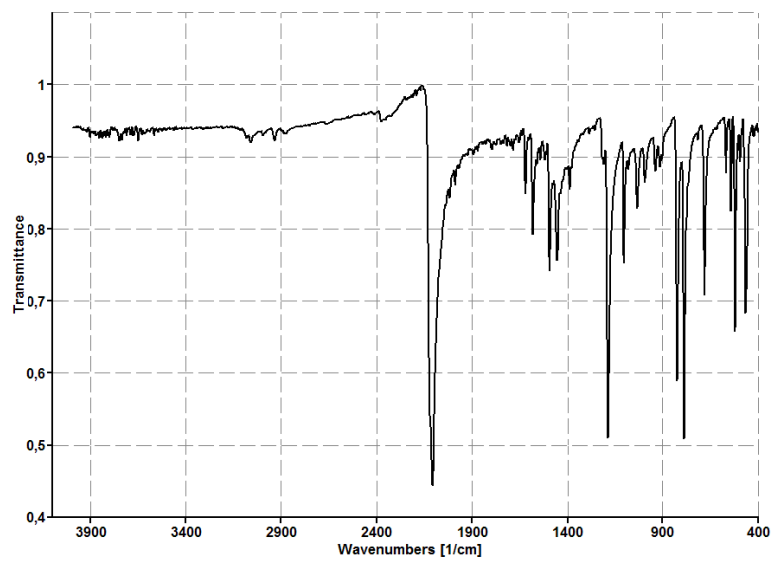
$[\text{Cd}(\text{4-nitropyridine-N-oxide})_2(\text{NCS})_2]_n$  (**4**)



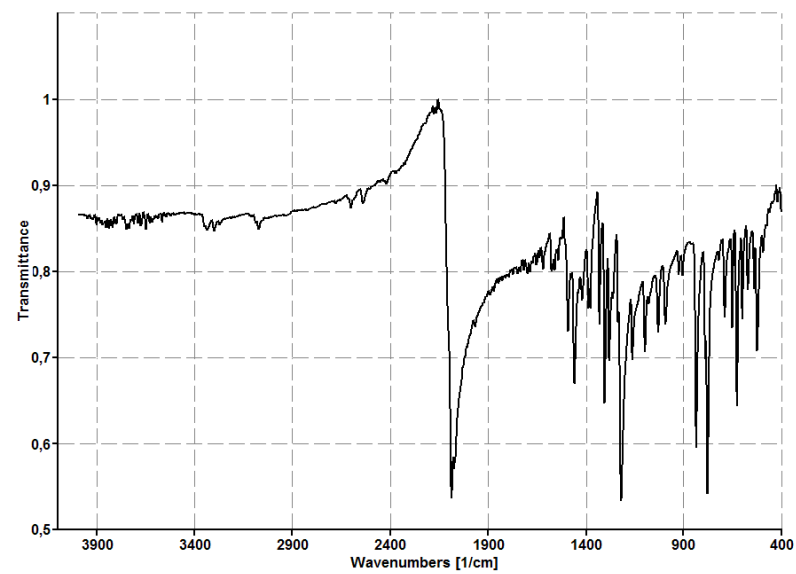
$[Cd(4\text{-quinoline-N-oxide})(NCS)_2]_n$  (5)



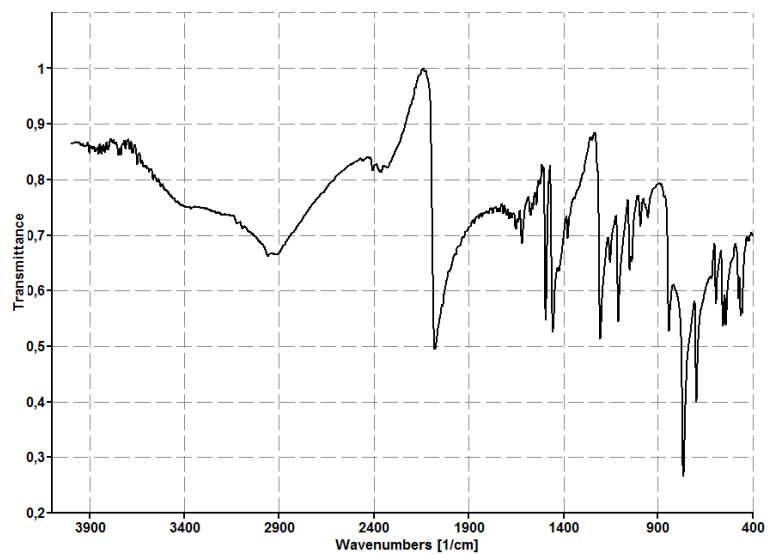
$[Cd(N_3)_2(H_2O)_2]_n(4\text{-quinoline-N-oxide})_{2n}$  (7)



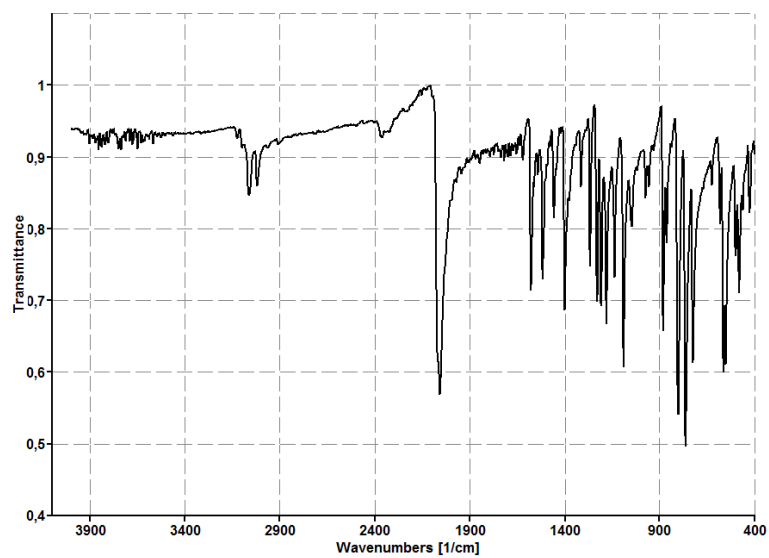
$[Cd(2,6\text{-lutidine-N-oxide})(NCS)_2]_n$  (6)



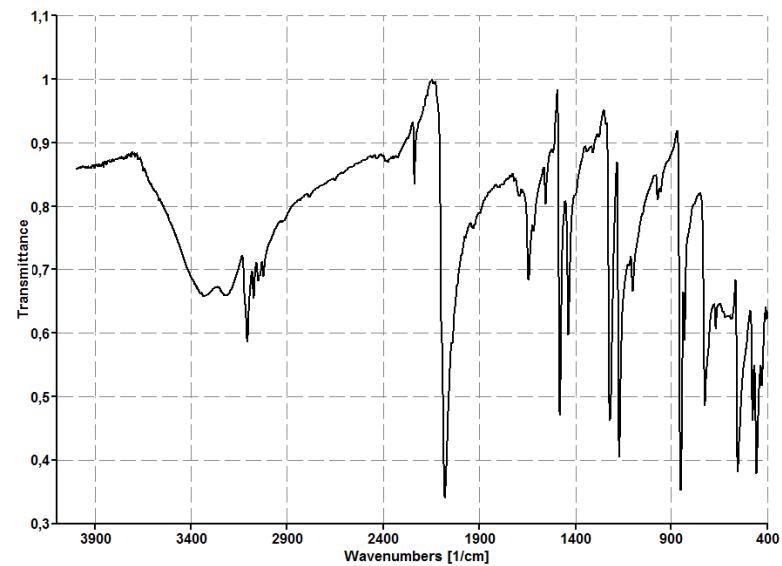
$[Cd(2,6\text{-lutidine-N-oxide})(N_3)_2]_n$  (8)



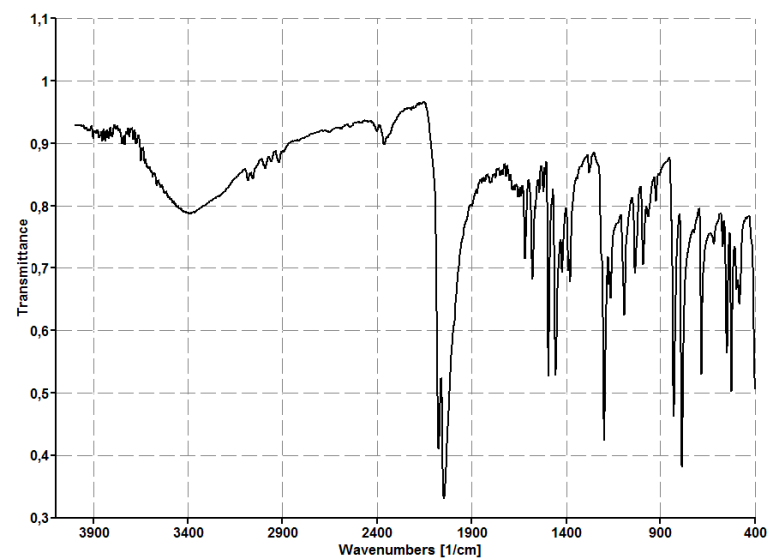
$[\text{Zn}(\text{2-picoline-N-oxide})_2(\text{NCS})_2(\text{H}_2\text{O})]_n$  (**9**)



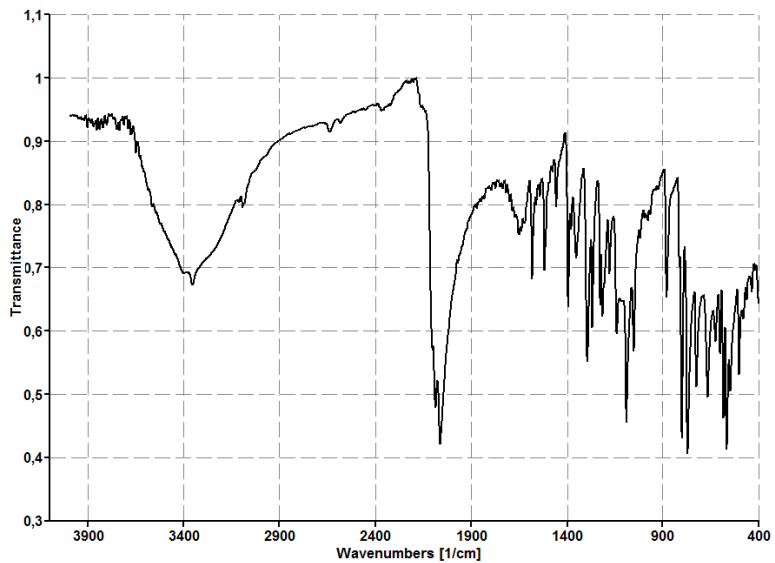
$[\text{Zn}(\text{4-quinoline-N-oxide})_6]^{2+}[\text{Zn}(\text{NCS})_4]^{2-}$  (**10**)



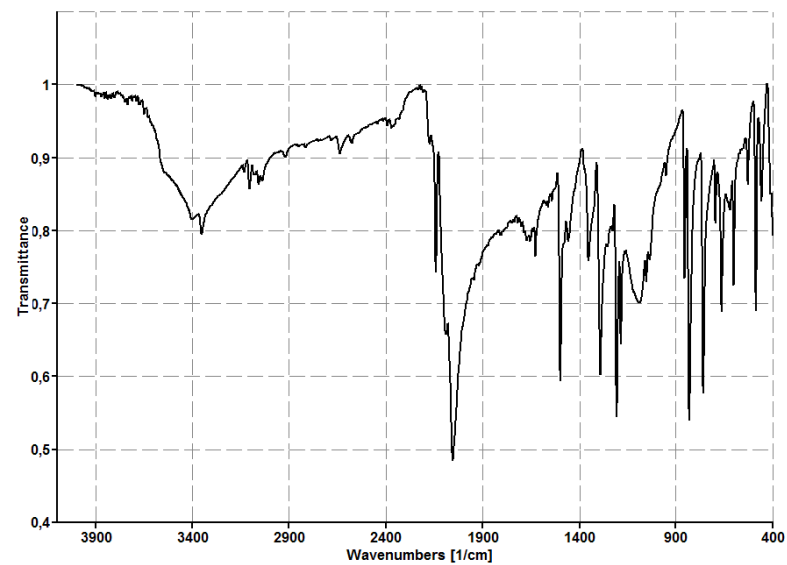
$[\text{Zn}(\text{4-cyanopyridine-N-oxide})_2(\text{NCS})_2(\text{H}_2\text{O})]_2$  (**11**)



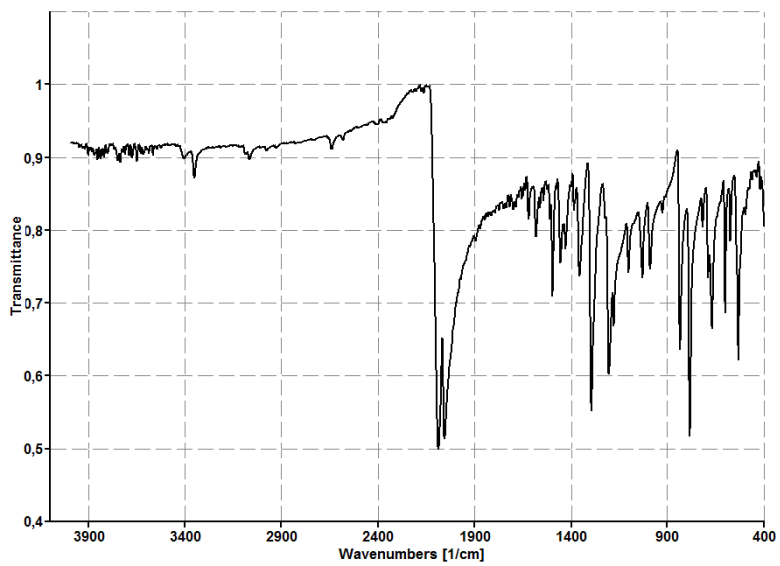
$[\text{Zn}(\text{2,6-lutidine-N-oxide})_2(\text{NCS})_2]$  (**12**)



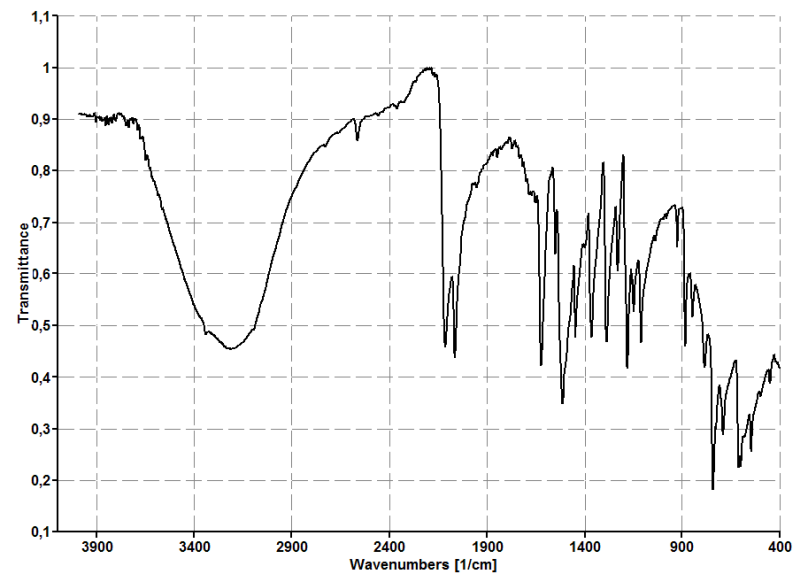
[Zn(4-quinoline-N-oxide)(N<sub>3</sub>)<sub>2</sub>]<sub>n</sub> (13)



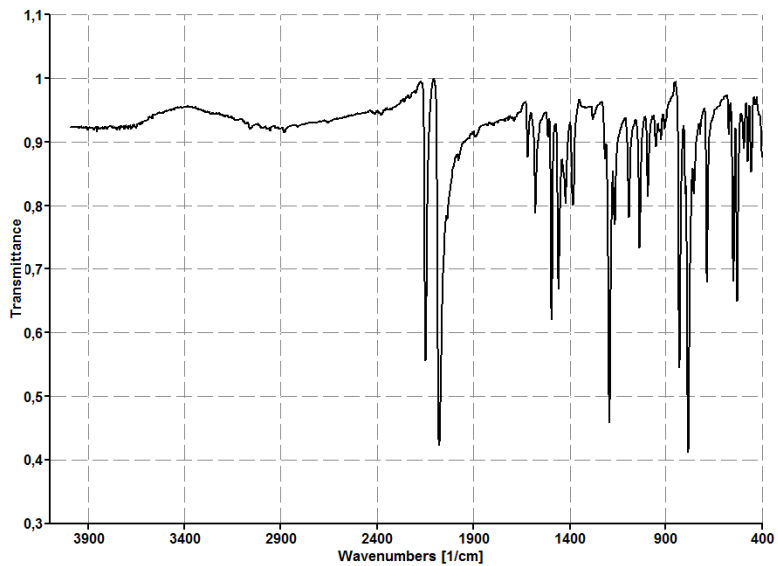
[Zn(4-picoline-N-oxide)(N<sub>3</sub>)<sub>2</sub>]<sub>n</sub> (15)



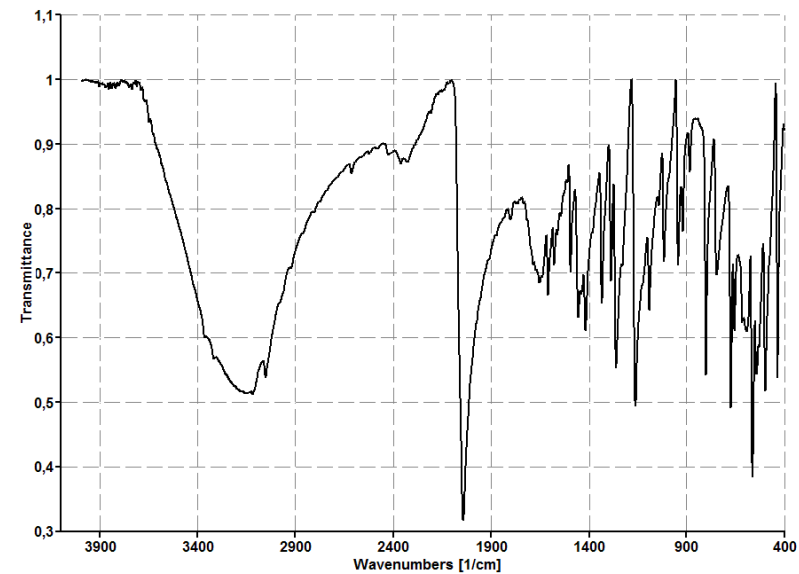
[Zn(2,6-lutidine-N-oxide)(N<sub>3</sub>)<sub>2</sub>]<sub>n</sub> (14)



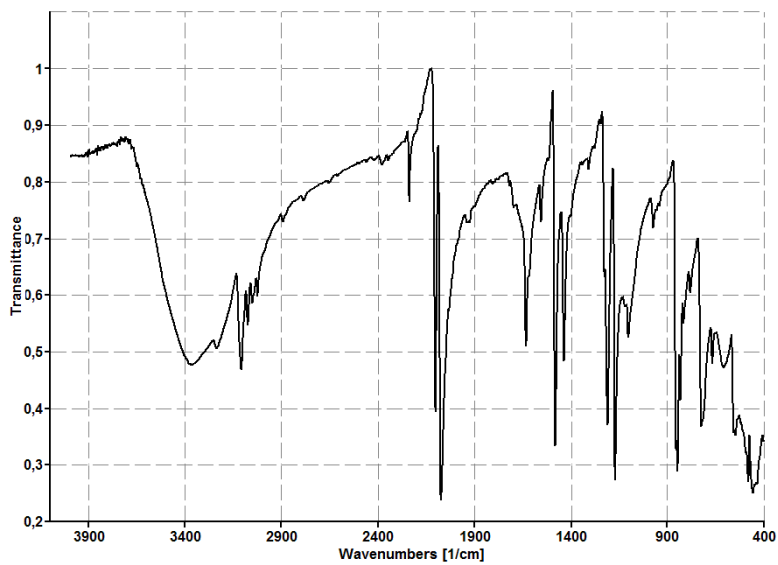
[Zn(2-O-pyridine-N-oxide)(N<sub>3</sub>)(H<sub>2</sub>O)]<sub>n</sub> (16)



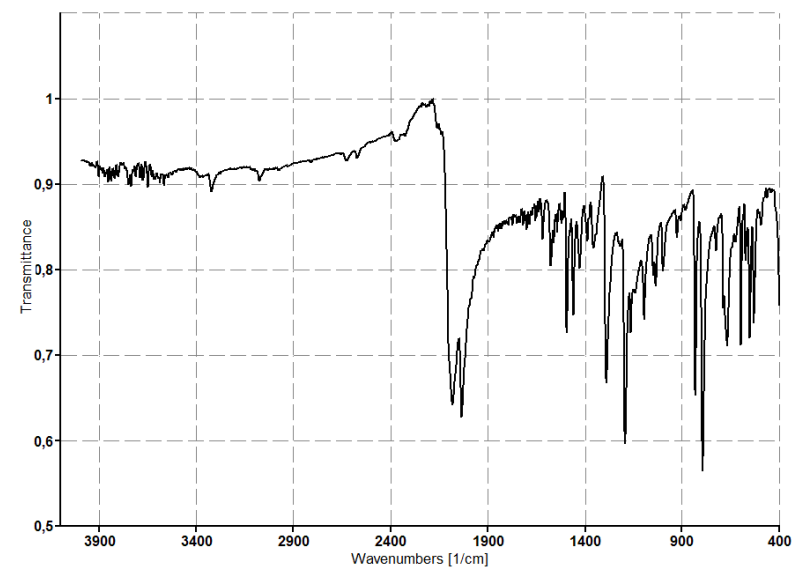
$[\text{Co}(\text{2,6-lutidine-N-oxide})_2(\text{NCS})_2]_2$  (**17**)



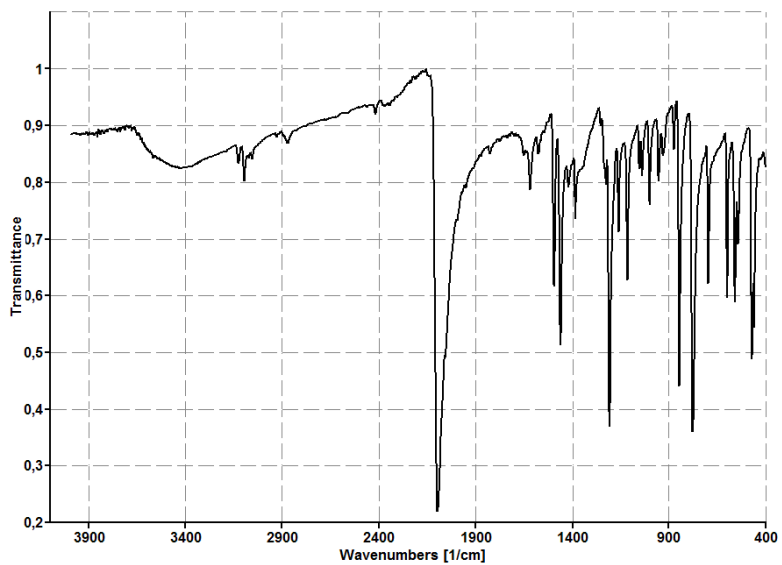
$[\text{Co}(\text{N}_3)_2(\text{H}_2\text{O})_2]_n(\text{3-picoline-N-oxide})_{2n}$  (**19**)



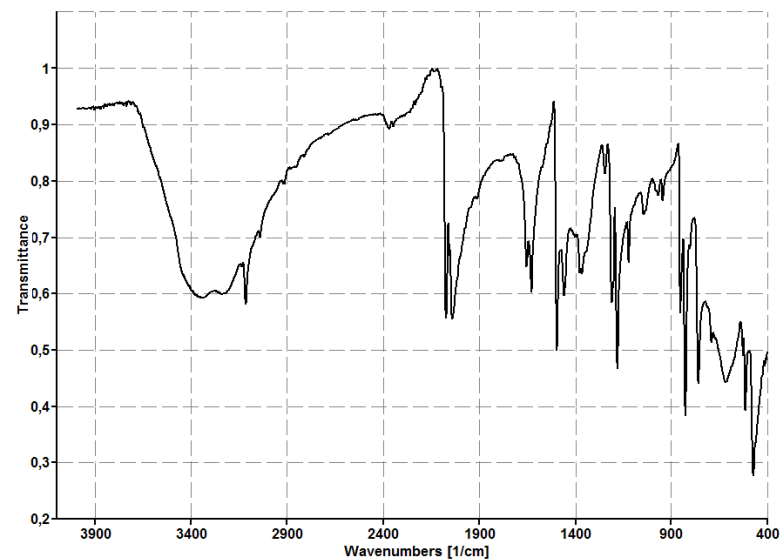
$[\text{Co}(\text{4-cyanopyridine-N-oxide})_2(\text{NCS})_2(\text{H}_2\text{O})]_2$  (**18**)



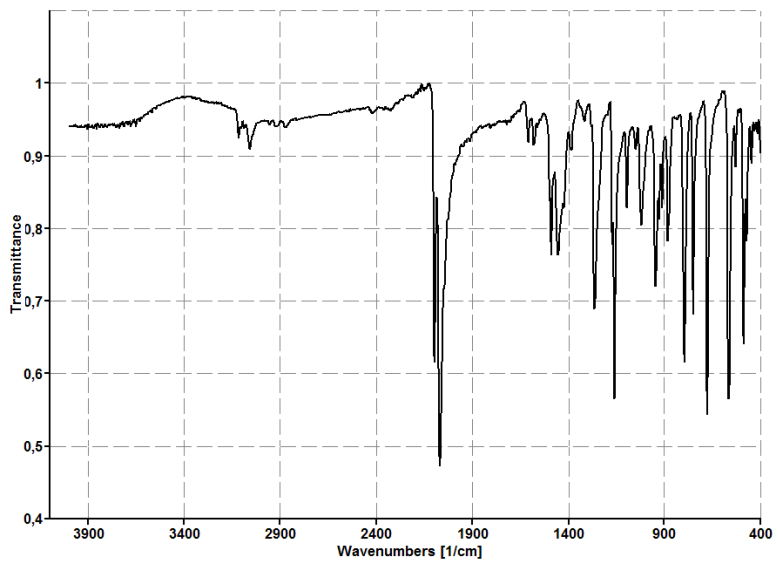
$[\text{Co}(\text{2,6-lutidine-N-oxide})(\text{N}_3)_2]_n$  (**20**)



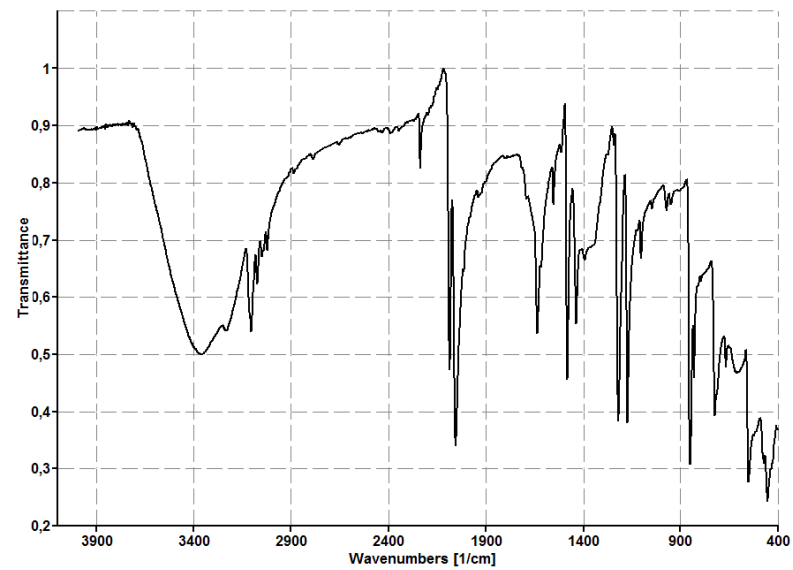
$[\text{Mn}(\text{2-picoline-N-oxide})(\text{NCS})_2]_n$  (21)



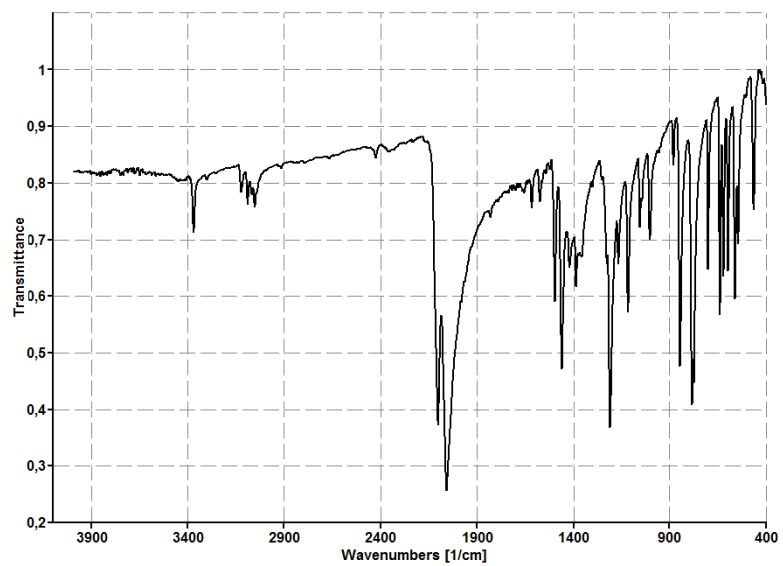
$[\text{Mn}(\text{4-picoline-N-oxide})_2(\text{NCS})_2(\text{H}_2\text{O})_2]_n$  (23)



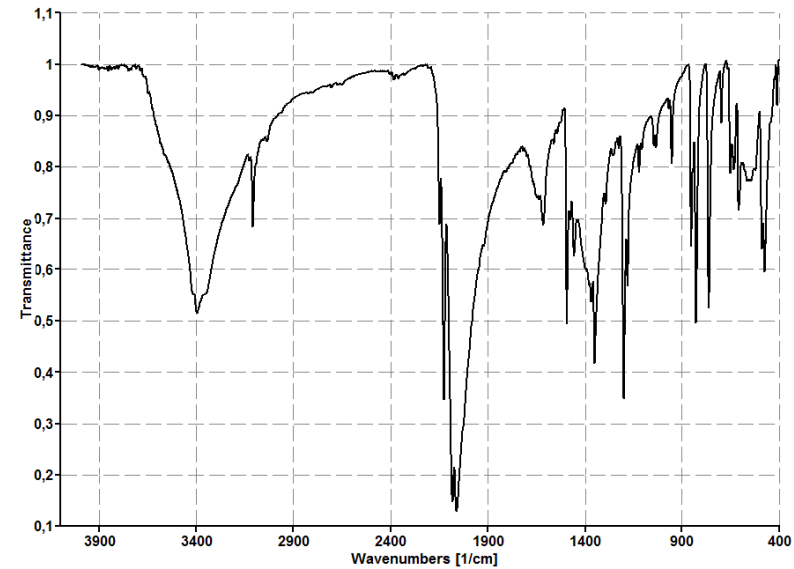
$[\text{Mn}(\text{3-picoline-N-oxide})_2(\text{NCS})_2]_n$  (22)



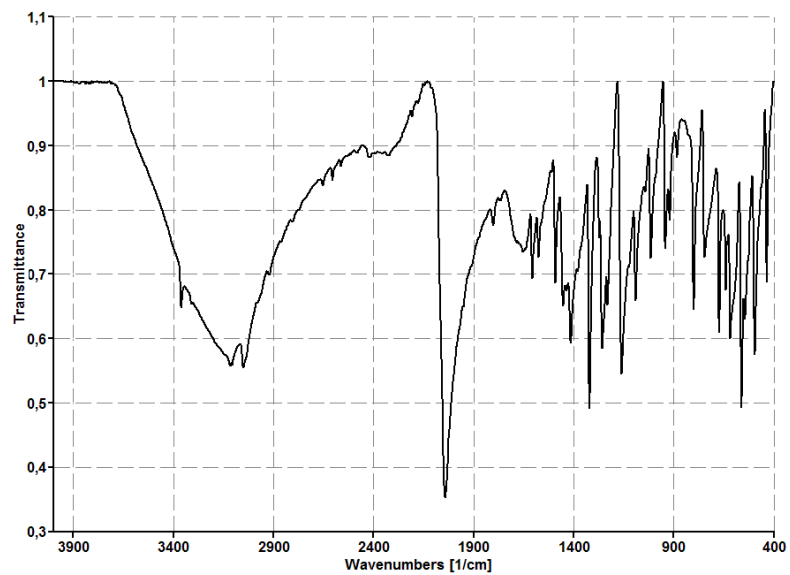
$[\text{Mn}(\text{4-cyanopyridine-N-oxide})_2(\text{NCS})_2(\text{H}_2\text{O})_2]_2$  (24)



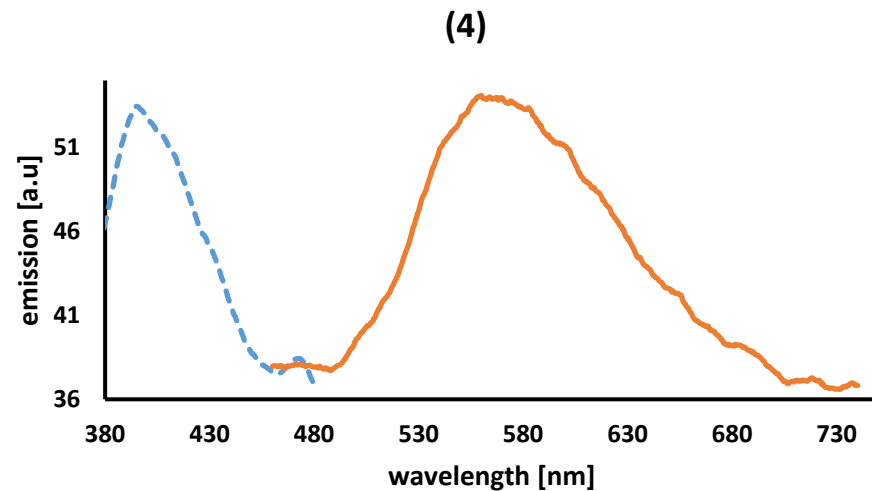
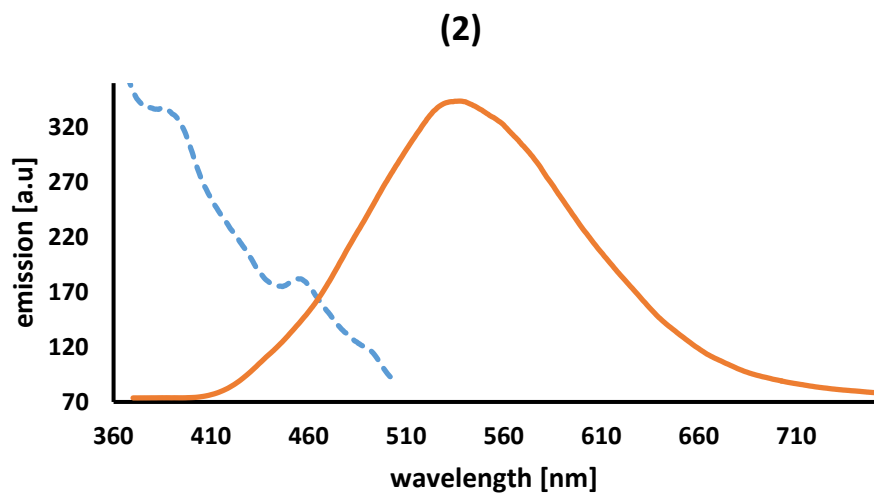
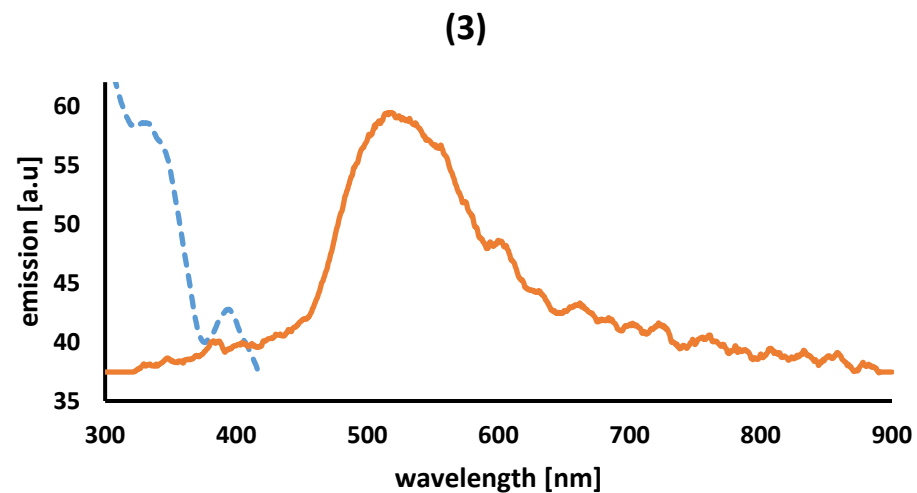
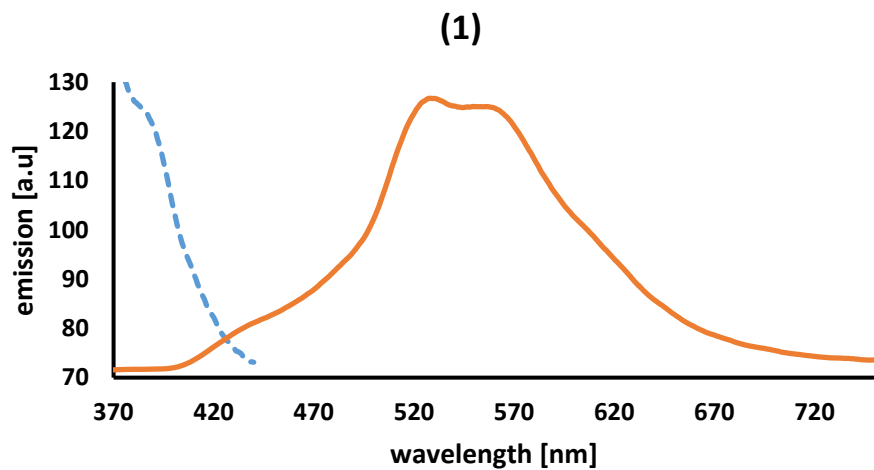
$[\text{Mn}(\text{2-picoline-N-oxide})(\text{N}_3)_2]_n$  (25)



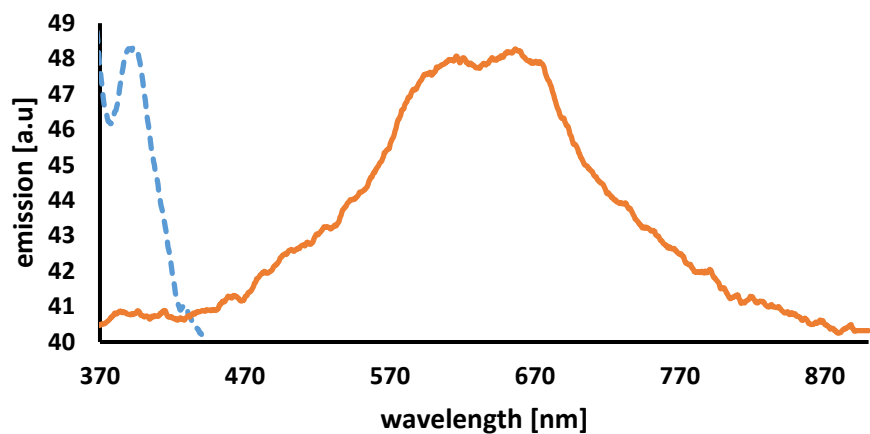
$[\text{Mn}_3(\text{N}_3)_6(\text{4-picoline-N-oxide})_2(\text{H}_2\text{O})_2]_n$  (27)



$[\text{Mn}(\text{N}_3)_2(\text{H}_2\text{O})_2]_n(\text{3-picoline-N-oxide})_{2n}$  (26)

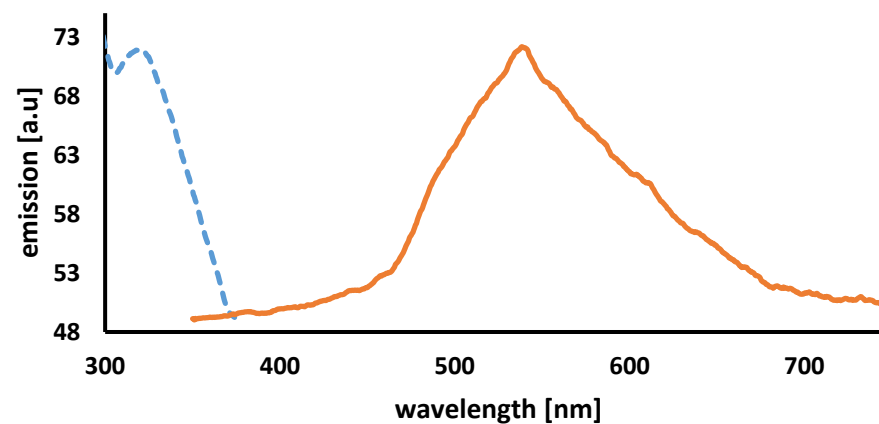


(5)



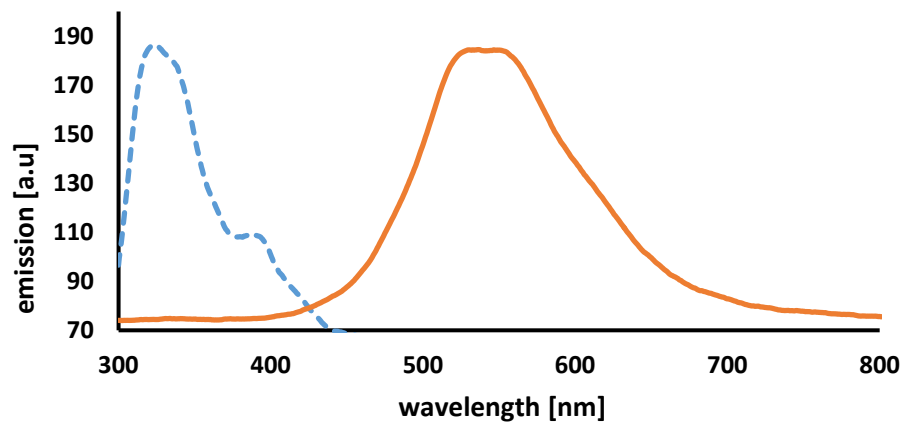
--- Excitation spectrum at 635 nm emission  
— Emission spectrum at 334 nm excitation

(8)



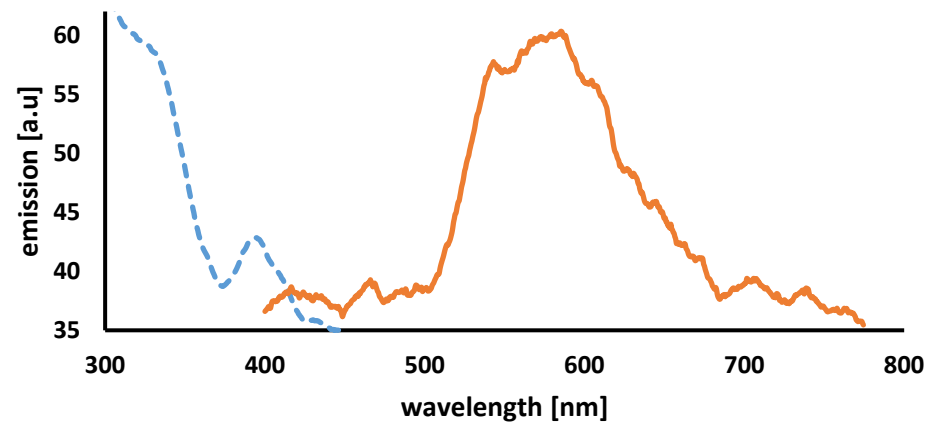
--- Excitation spectrum at 555 nm emission  
— Emission spectrum at 320 nm excitation

(6)



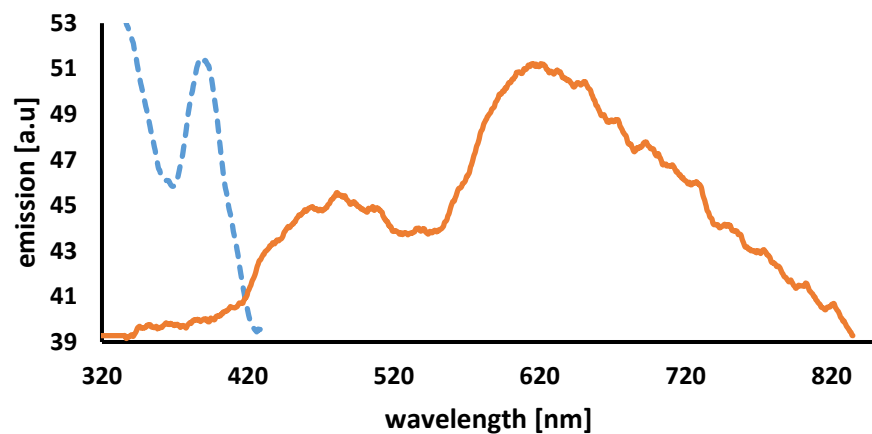
--- Excitation spectrum at 545 nm emission  
— Emission spectrum at 324 nm excitation

(9)



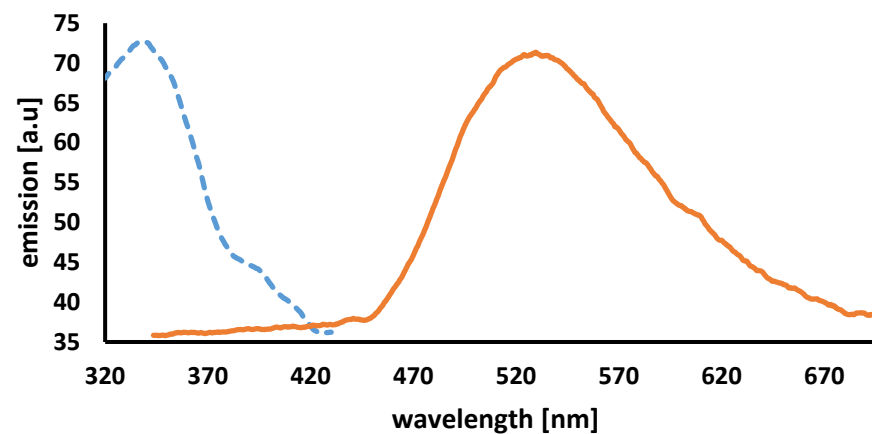
--- Excitation spectrum at 567 nm emission  
— Emission spectrum at 325 nm excitation

(10)



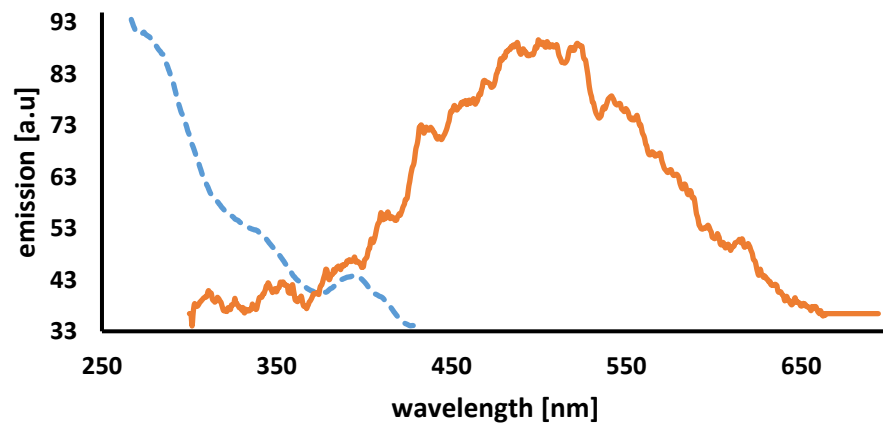
--- Excitation spectrum at 613 nm emission  
— Emission spectrum at 390 nm excitation

(11)



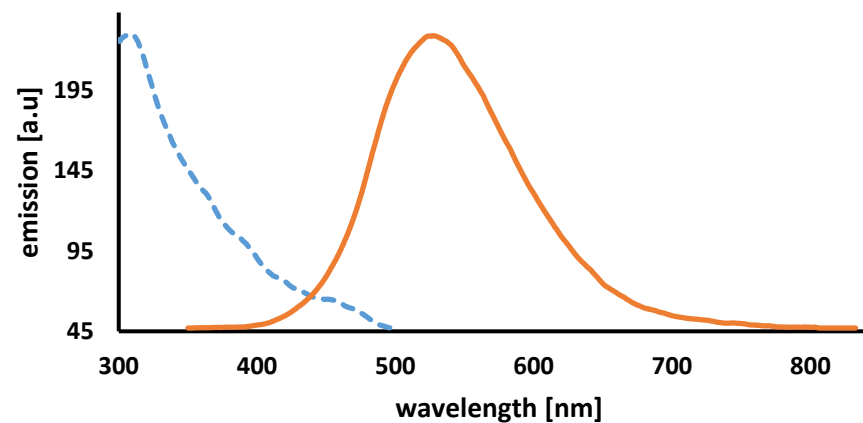
--- Excitation spectrum at 529 nm emission  
— Emission spectrum at 335 nm excitation

(10a)



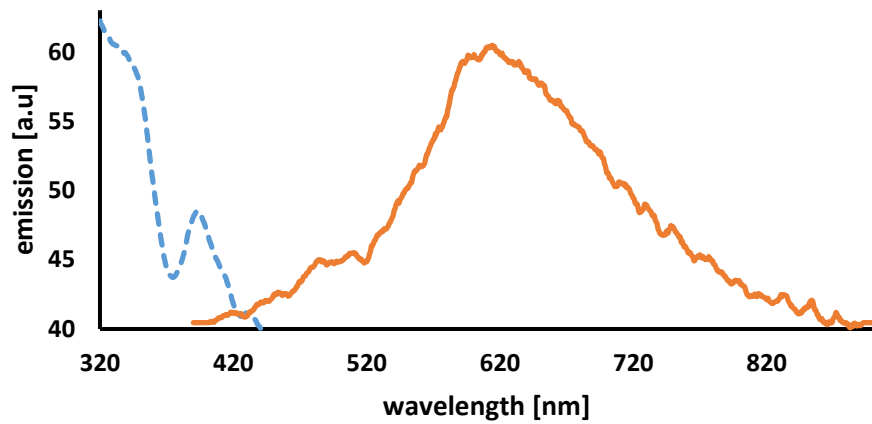
--- Excitation spectrum at 507 nm emission  
— Emission spectrum at 259 nm excitation

(12)



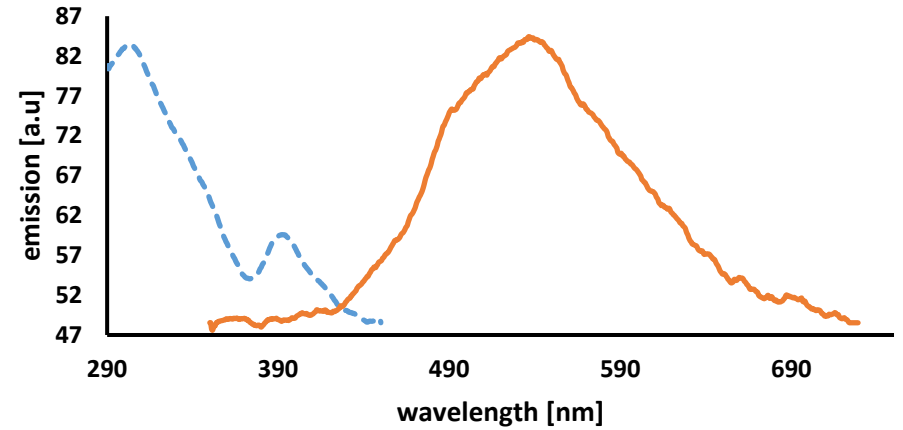
--- Excitation spectrum at 535 nm emission  
— Emission spectrum at 310 nm excitation

(13)



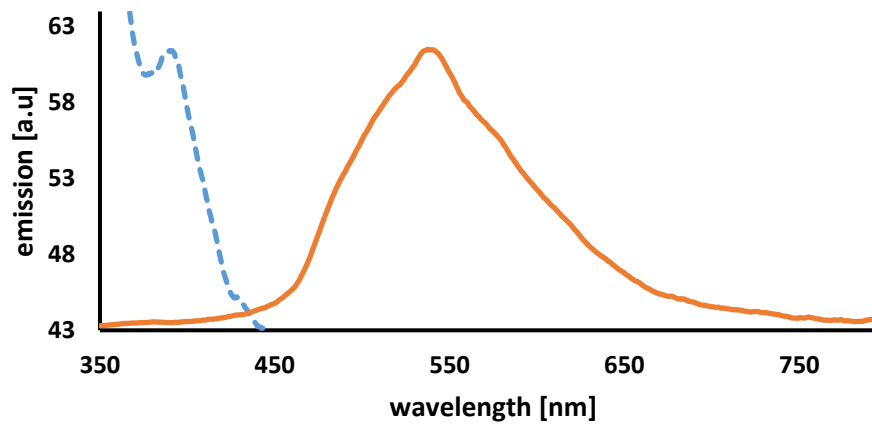
--- Excitation spectrum at 627 nm emission  
— Emission spectrum at 340 nm excitation

(15)



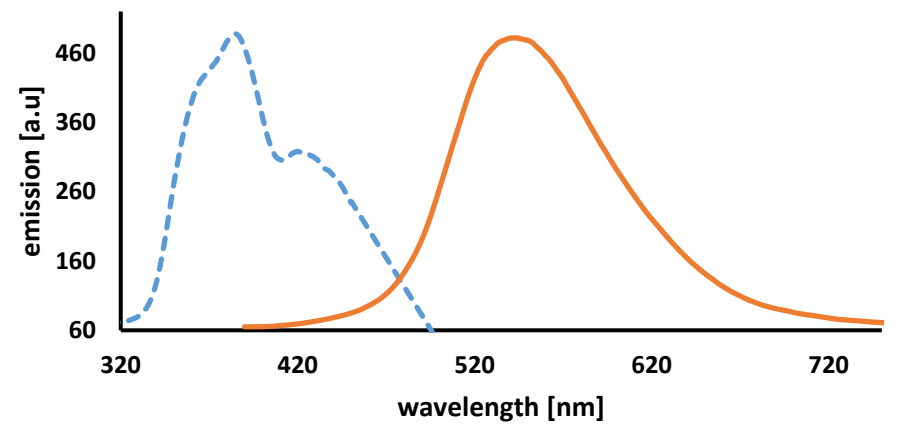
--- Excitation spectrum at 548 nm emission  
— Emission spectrum at 304 nm excitation

(14)



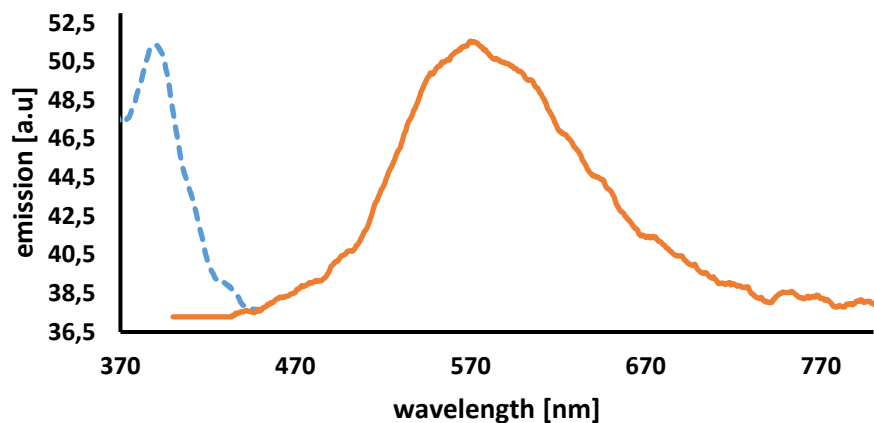
--- Excitation spectrum at 545 nm emission  
— Emission spectrum at 318 nm excitation

(16)



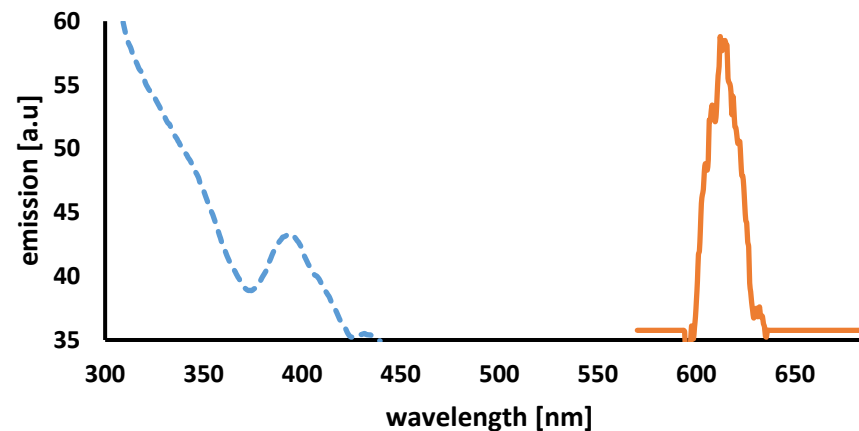
--- Excitation spectrum at 543 nm emission  
— Emission spectrum at 375 nm excitation

### 2-hydroxypyridine-N-oxide



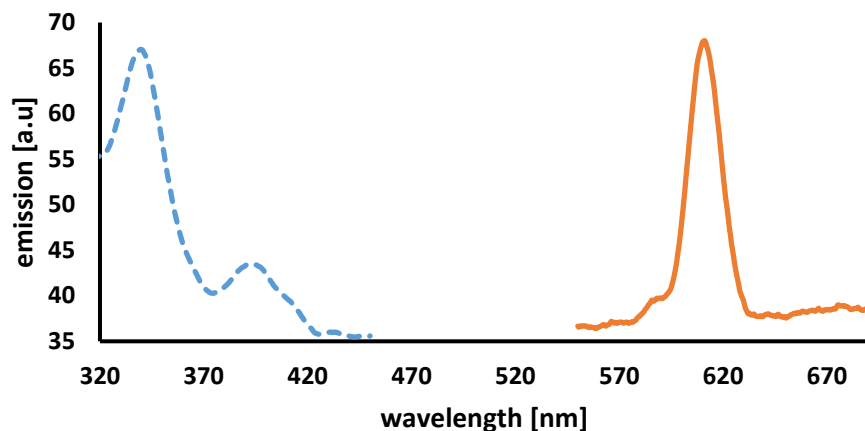
--- Excitation spectrum at 576 nm emission  
— Emission spectrum at 390 nm excitation

### 3-methylpyridine-N-oxide



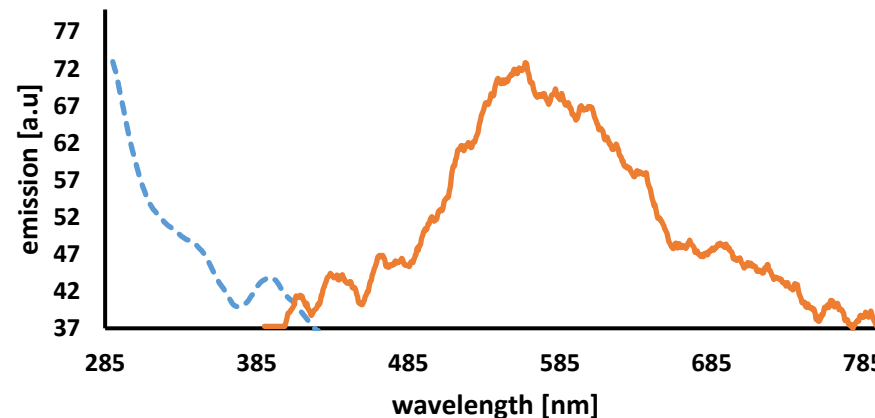
--- Excitation spectrum at 544 nm emission  
— Emission spectrum at 330 nm excitation

### 2-methylpyridine-N-oxide



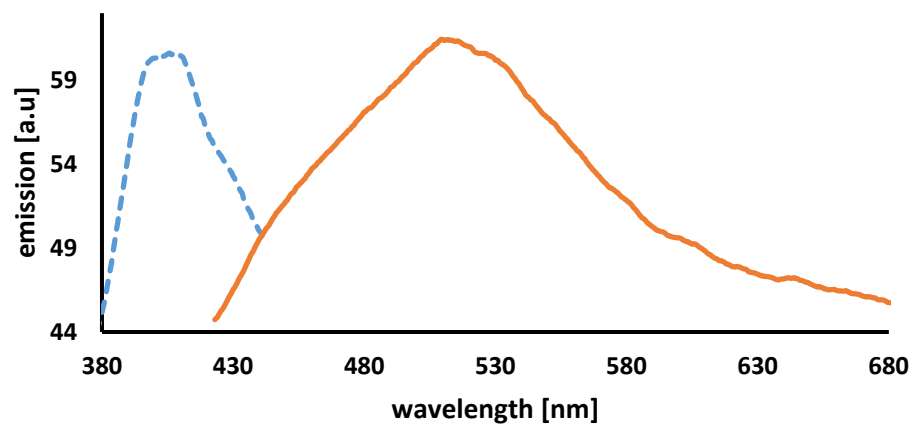
--- Excitation spectrum at 600 nm emission  
— Emission spectrum at 340 nm excitation

### 4-methylpyridine-N-oxide



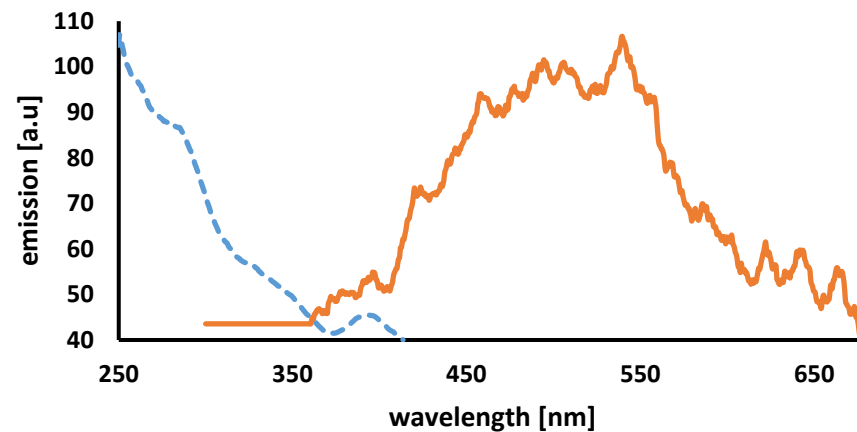
--- Excitation spectrum at 570 nm emission  
— Emission spectrum at 290 nm excitation

**2,6-dimethylpyridine-N-oxide**



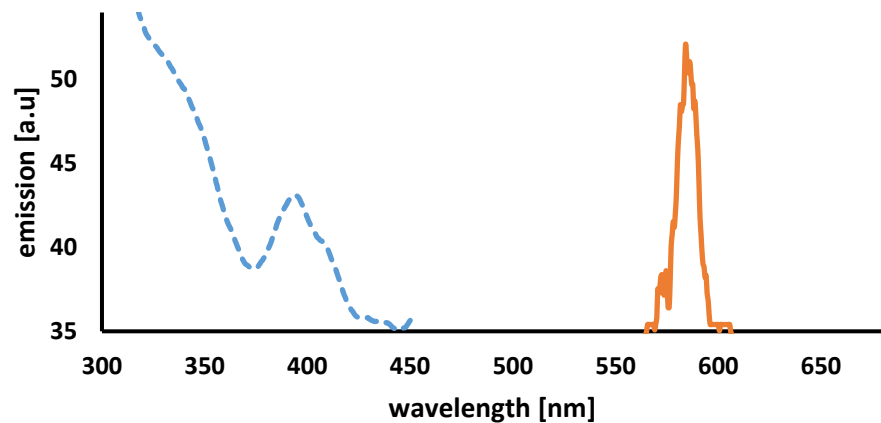
--- Excitation spectrum at 527 nm emission  
— Emission spectrum at 406 nm excitation

**4-cyanopyridine-N-oxide**

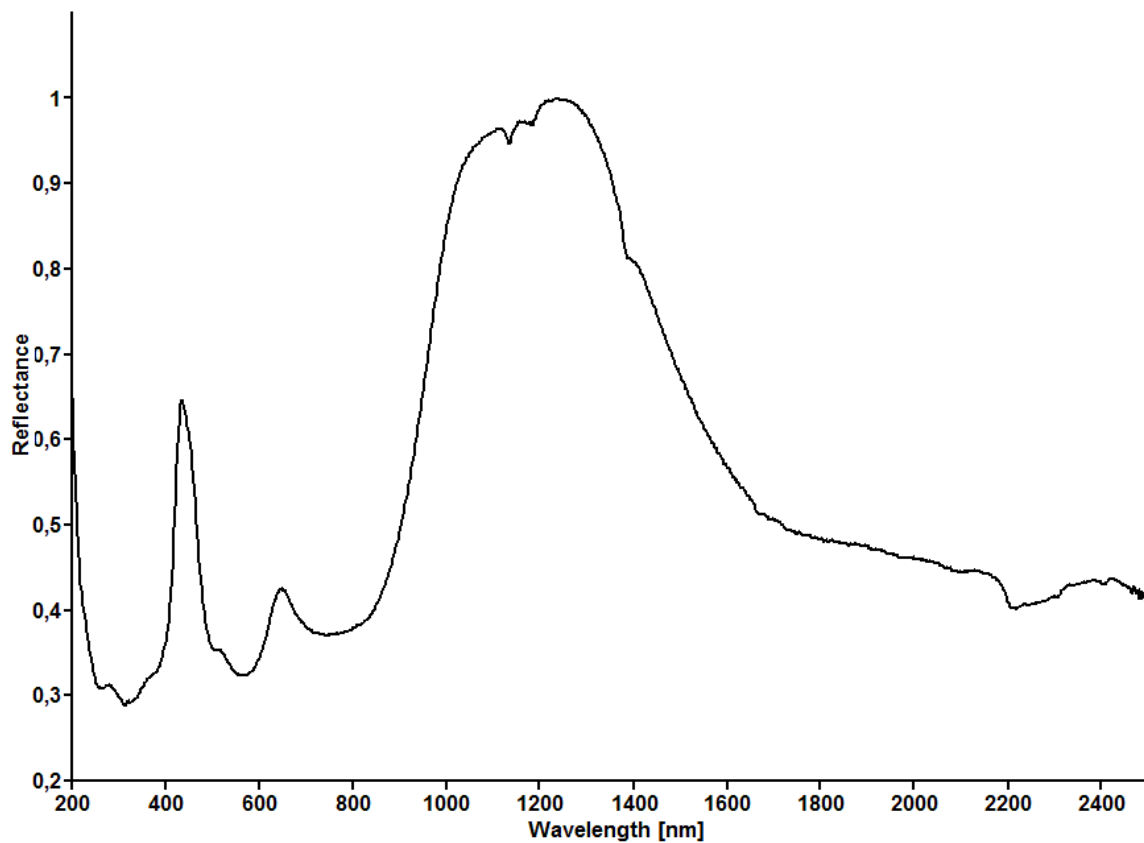


--- Excitation spectrum at 500 nm emission  
— Emission spectrum at 266 nm excitation

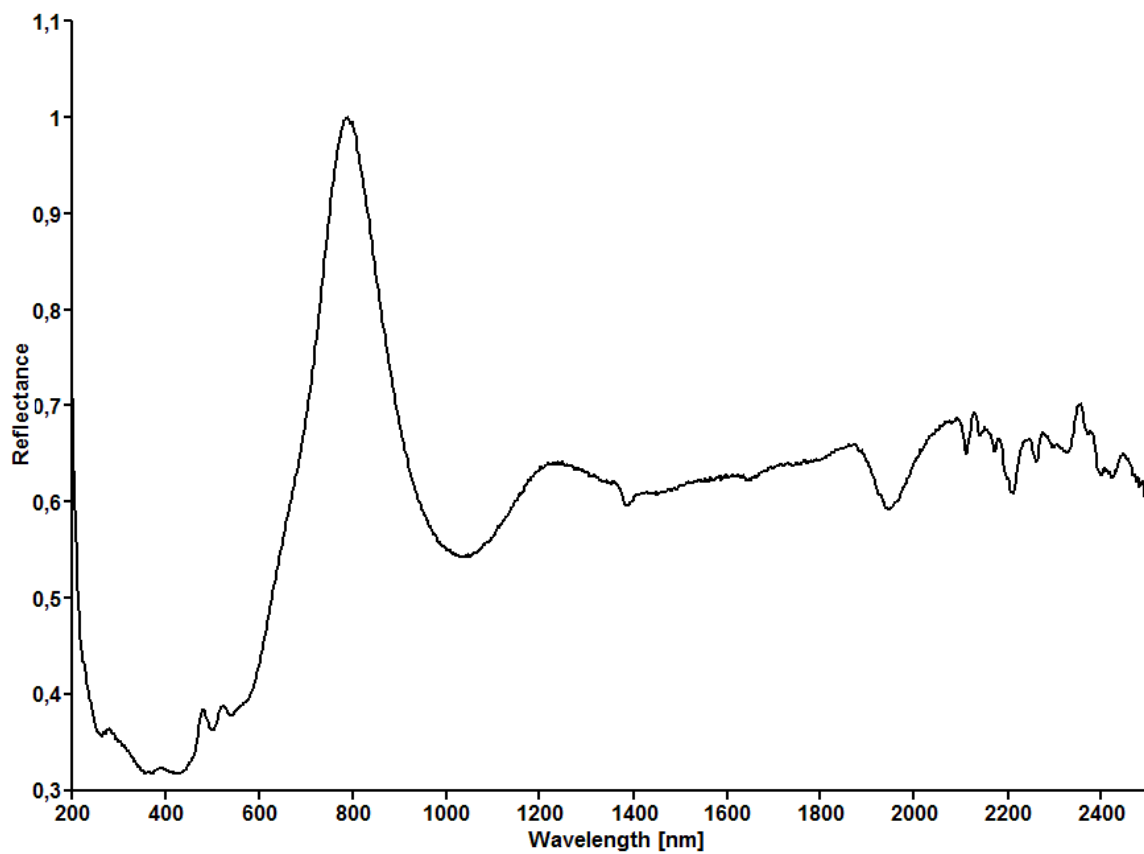
**4-quinoline-N-oxide**



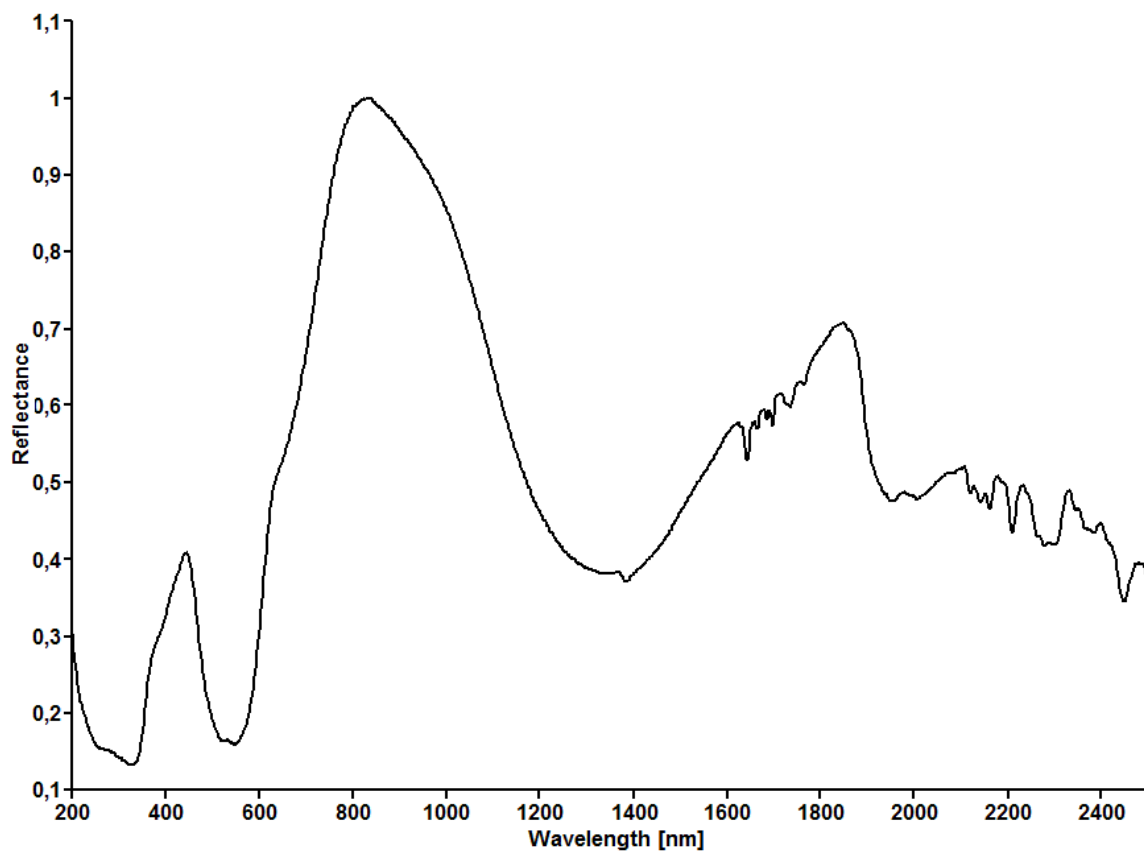
--- Excitation spectrum at 550 nm emission  
— Emission spectrum at 327 nm excitation



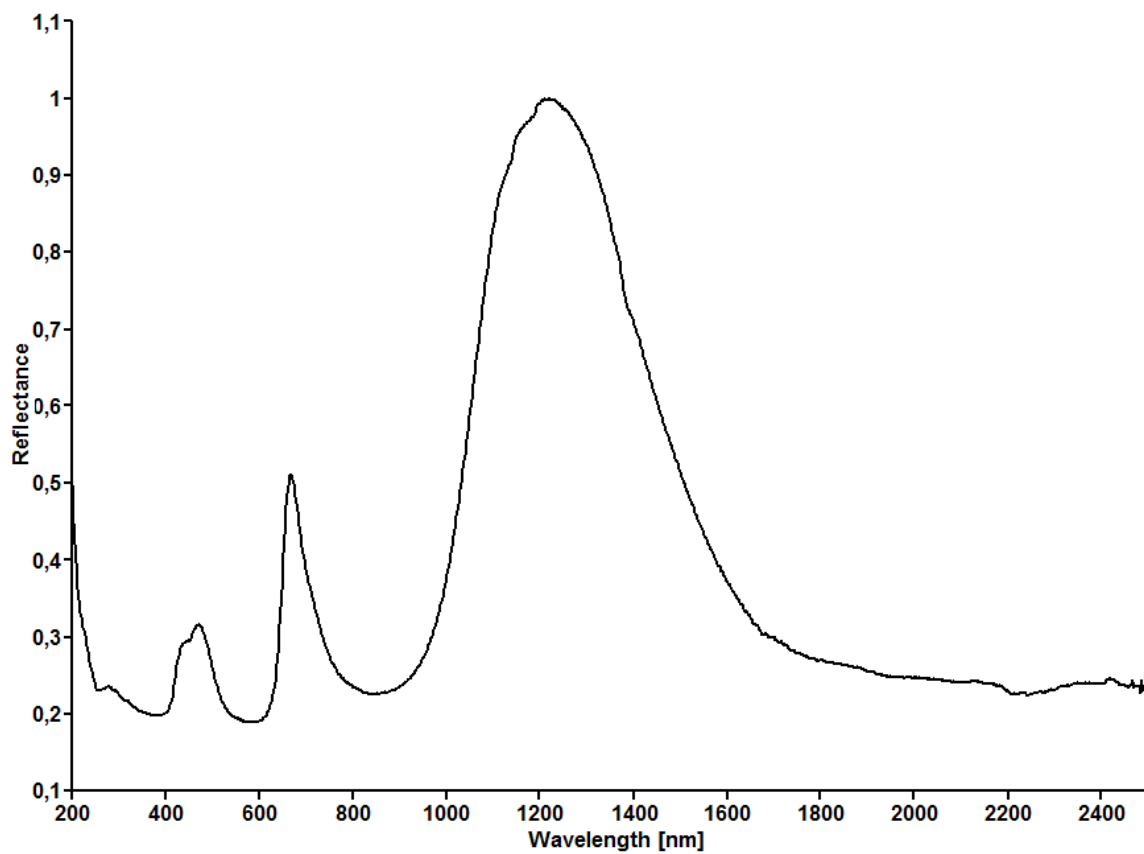
$[\text{Co}(\text{2,6-lutidine-N-oxide})_2(\text{NCS})_2]_2$  (**17**)



$[\text{Co}(\text{4-cyanopyridine-N-oxide})_2(\text{NCS})_2(\text{H}_2\text{O})]_2$  (**18**)



$[\text{Co}(\text{N}_3)_2(\text{H}_2\text{O})_2]_n(3\text{-picoline-N-oxide})_{2n}$  (**19**)



$[\text{Co}(2,6\text{-lutidine-N-oxide})(\text{N}_3)_2]_n$  (**20**)

Crystallographic data and processing parameters of the compounds **(1)-(5)**.

Compounds	(1)	(2)	(3)	(4)	(5)
Empirical formula	C <sub>8</sub> H <sub>7</sub> CdN <sub>3</sub> OS <sub>2</sub>	C <sub>8</sub> H <sub>7</sub> CdN <sub>3</sub> OS <sub>2</sub>	C <sub>28</sub> H <sub>20</sub> Cd <sub>2</sub> N <sub>12</sub> O <sub>6</sub> S <sub>4</sub>	C <sub>12</sub> H <sub>8</sub> CdN <sub>6</sub> O <sub>6</sub> S <sub>2</sub>	C <sub>11</sub> H <sub>7</sub> CdN <sub>3</sub> OS <sub>2</sub>
Formula mass	337.69	337.70	973.62	508.77	373.73
System	Monoclinic	Monoclinic	Triclinic	Orthorhombic	Triclinic
Space group	P2 <sub>1</sub> /c	P2 <sub>1</sub> /c	P-1	Pbcn	P-1
a (Å)	8.1140(14)	7.5021(12)	7.3644(8)	22.111(2)	8.2376(8)
b (Å)	7.8987(13)	7.6905(12)	8.8395(9)	7.1851(12)	8.3425(8)
c (Å)	18.4684(18)	19.9841(19)	14.1100(14)	10.7305(14)	11.1790(14)
α (°)	90	90	99.17(2)	90	107.00(2)
β (°)	94.99(2)	98.60(2)	100.84(2)	90	92.57(2)
γ (°)	90	90	95.45(2)	90	117.25(2)
V (Å <sup>3</sup> )	1179.2(3)	1140.0(3)	883.18(19)	1704.8(4)	638.6(2)
Z	4	4	1	4	2
T (K)	100(2)	100(2)	100(2)	100(2)	100(2)
μ (mm <sup>-1</sup> )	2.182	2.257	1.501	1.572	2.025
D <sub>calc</sub> (Mg/m <sup>3</sup> )	1.902	1.967	1.831	1.982	1.944
Crystal size (mm)	0.37 x 0.32 x 0.23	0.29 x 0.25 x 0.17	0.33 x 0.27 x 0.16	0.34 x 0.21 x 0.16	0.26 x 0.21 x 0.17
θ max (°)	26.31	26.37	26.30	26.30	26.25
Data collected	8897	8525	7002	12282	4407
Unique refl. / R <sub>int</sub>	2375 / 0.0458	2326 / 0.0309	3523 / 0.0204	1727 / 0.0220	2537 / 0.0154
Parameters / Restraints	137 / 0	137 / 0	241 / 2	123 / 0	163 / 0
Goodness-of-Fit on F <sup>2</sup>	1.287	1.152	1.064	1.215	1.118
R1 / wR2 (all data)	0.0610 / 0.1375	0.0286 / 0.0659	0.0233 / 0.0573	0.0212 / 0.0545	0.0181 / 0.0450
Residual extrema (e/Å <sup>3</sup> )	1.40 / -0.89	0.99 / -0.76	0.58 / -0.49	0.28 / -0.61	0.32 / -0.61

Crystallographic data and processing parameters of the compounds **(6)** and **(8)-(11)**.

Compounds	(6)	(8)	(9)	(10)	(11)
Empirical formula	C <sub>9</sub> H <sub>9</sub> CdN <sub>3</sub> OS <sub>2</sub>	C <sub>7</sub> H <sub>9</sub> CdN <sub>7</sub> O	C <sub>14</sub> H <sub>16</sub> N <sub>4</sub> O <sub>3</sub> S <sub>2</sub> Zn	C <sub>58</sub> H <sub>42</sub> N <sub>10</sub> O <sub>6</sub> S <sub>4</sub> Zn <sub>2</sub>	C <sub>14</sub> H <sub>10</sub> N <sub>6</sub> O <sub>3</sub> S <sub>2</sub> Zn
Formula mass	351.72	319.62	417.82	1234.08	439.79
System	Monoclinic	Orthorhombic	Triclinic	Trigonal	Triclinic
Space group	C2/c	Pna2 <sub>1</sub>	P-1	P-3c1	P-1
a (Å)	11.0915(12)	16.6497(13)	7.7916(4)	15.6403(17)	7.2266(8)
b (Å)	11.9941(14)	16.6312(12)	10.2764(5)	15.6403(17)	8.7841(8)
c (Å)	19.4762(19)	3.6691(3)	12.3870(6)	26.407(2)	13.9301(16)
α (°)	90	90	105.748(2)	90	99.427(18)
β (°)	93.45(2)	90	99.078(2)	90	101.759(19)
γ (°)	90	90	95.392(2)	120	96.151(18)
V (Å <sup>3</sup> )	2586.3(5)	1015.99(14)	932.82(8)	5594.2(15)	844.93(18)
Z	8	4	2	4	2
T (K)	100(2)	100(2)	100(2)	100(2)	100(2)
μ (mm <sup>-1</sup> )	1.993	2.140	1.559	1.068	1.729
D <sub>calc</sub> (Mg/m <sup>3</sup> )	1.807	2.090	1.488	1.465	1.729
Crystal size (mm)	0.33 x 0.26 x 0.17	0.29 x 0.24 x 0.18	0.24 x 0.20 x 0.15	0.37 x 0.32 x 0.26	0.38 x 0.27 x 0.15
θ max (°)	26.32	29.00	28.06	26.36	26.35
Data collected	8611	40203	19392	42293	6624
Unique refl. / R <sub>int</sub>	2608 / 0.0568	2661 / 0.0911	4515 / 0.0454	3835 / 0.0300	3392 / 0.0387
Parameters / Restraints	148 / 0	147 / 1	225 / 0	242 / 0	241 / 2
Goodness-of-Fit on F <sup>2</sup>	1.413	1.129	1.162	1.040	1.105
R1 / wR2 (all data)	0.0697 / 0.1459	0.0356 / 0.0990	0.0244 / 0.0843	0.0279 / 0.0772	0.0499 / 0.1490
Residual extrema (e/Å <sup>3</sup> )	1.87 / -1.52	0.96 / -1.24	0.45 / -0.57	0.47 / -0.35	1.44 / -1.80

Crystallographic data and processing parameters of the compounds **(12)**-(**16**).

Compounds	(12)	(13)	(14)	(15)	(16)
Empirical formula	C <sub>16</sub> H <sub>18</sub> N <sub>4</sub> O <sub>2</sub> S <sub>2</sub> Zn	C <sub>18</sub> H <sub>14</sub> N <sub>14</sub> O <sub>2</sub> Zn <sub>2</sub>	C <sub>7</sub> H <sub>9</sub> N <sub>7</sub> OZn	C <sub>6</sub> H <sub>7</sub> N <sub>7</sub> OZn	C <sub>5</sub> H <sub>6</sub> N <sub>4</sub> O <sub>3</sub> Zn
Formula mass	427.85	589.21	272.58	258.58	235.53
System	Monoclinic	Monoclinic	Monoclinic	Monoclinic	Orthorombic
Space group	C2/c	P2 <sub>1</sub> /c	P2 <sub>1</sub> /n	P2 <sub>1</sub> /c	Pbca
a (Å)	33.0436(10)	12.2080(14)	6.0915(12)	12.2116(14)	10.7856(13)
b (Å)	8.3385(3)	8.4721(11)	15.691(3)	13.0588(16)	6.6210(11)
c (Å)	15.4292(5)	23.229(2)	11.049(2)	6.1961(9)	22.4025(19)
α (°)	90	90	90	90	90
β (°)	116.818(2)	105.76(2)	102.77(3)	100.469(18)	90
γ (°)	90	90	90	90	90
V (Å <sup>3</sup> )	3794.0(2)	2312.2(5)	1030.0(4)	971.6(2)	1599.8(4)
Z	8	4	4	4	8
T (K)	100(2)	136(2)	100(2)	100(2)	100(2)
μ (mm <sup>-1</sup> )	1.531	2.124	2.375	2.512	3.049
D <sub>calc</sub> (Mg/m <sup>3</sup> )	1.498	1.692	1.758	1.768	1.956
Crystal size (mm)	0.27 x 0.22 x 0.19	0.38 x 0.15 x 0.15	0.38 x 0.18 x 0.12	0.42 x 0.24 x 0.15	0.34 x 0.30 x 0.20
θ max (°)	26.49	24.990	26.31	26.31	26.29
Data collected	19824	15269	8023	6504	11472
Unique refl. / R <sub>int</sub>	3932 / 0.0418	4050 / 0.0940	2090 / 0.0253	1972 / 0.0253	1624 / 0.0524
Parameters / Restraints	230 / 0	325 / 0	147 / 0	137 / 0	126 / 0
Goodness-of-Fit on F <sup>2</sup>	1.052	1.123	1.053	1.053	1.057
R1 / wR2 (all data)	0.0295 / 0.0691	0.0856 / 0.2459	0.0219 / 0.0576	0.0209 / 0.0566	0.0267 / 0.0729
Residual extrema (e/Å <sup>3</sup> )	0.48 / -0.41	2.10 / -1.50	0.44 / -0.32	0.27 / -0.47	0.65 / -0.88

Crystallographic data and processing parameters of the compounds **(17)** and **(19)-(22)**.

Compounds	(17)	(19)	(20)	(21)	(22)
Empirical formula	C <sub>32</sub> H <sub>36</sub> Co <sub>2</sub> N <sub>8</sub> O <sub>4</sub> S <sub>4</sub>	C <sub>12</sub> H <sub>18</sub> CoN <sub>8</sub> O <sub>4</sub>	C <sub>7</sub> H <sub>9</sub> CoN <sub>7</sub> O	C <sub>8</sub> H <sub>7</sub> MnN <sub>3</sub> OS <sub>2</sub>	C <sub>14</sub> H <sub>14</sub> MnN <sub>4</sub> O <sub>2</sub> S <sub>2</sub>
Formula mass	842.79	397.27	266.14	280.23	389.35
System	Monoclinic	Orthorhombic	Monoclinic	Monoclinic	Triclinic
Space group	C2/c	Ibam	P2 <sub>1</sub> /c	P2 <sub>1</sub> /c	P-1
a (Å)	22.4251(19)	13.1744(9)	8.3254(14)	7.9117(9)	8.0423(8)
b (Å)	7.9767(6)	19.5105(9)	6.0221(12)	7.8460(9)	9.9500(9)
c (Å)	21.1368(17)	6.4762(3)	21.3916(19)	18.5461(19)	11.5610(13)
α (°)	90	90	90	90	82.49(2)
β (°)	98.963(4)	90	99.37(2)	95.26(2)	85.98(2)
γ (°)	90	90	90	90	79.74(2)
V (Å <sup>3</sup> )	3734.8(5)	1664.64(16)	1058.2(3)	1146.4(2)	901.48(17)
Z	4	4	4	4	2
T (K)	100(2)	100(2)	100(2)	100(2)	100(2)
μ (mm <sup>-1</sup> )	1.159	1.068	1.612	1.490	0.976
D <sub>calc</sub> (Mg/m <sup>3</sup> )	1.499	1.585	1.671	1.624	1.434
Crystal size (mm)	0.24 x 0.18 x 0.09	0.34 x 0.17 x 0.09	0.38 x 0.29 x 0.24	0.23 x 0.21 x 0.18	0.28 x 0.24 x 0.18
θ max (°)	27.00	29.28	26.34	26.33	26.36
Data collected	9651	22814	6256	8781	6706
Unique refl. / R <sub>int</sub>	4038 / 0.0596	1234 / 0.0723	2127 / 0.0240	2318 / 0.0257	3652 / 0.0192
Parameters / Restraints	230 / 0	79 / 1	147 / 0	137 / 0	210 / 0
Goodness-of-Fit on F <sup>2</sup>	1.161	1.121	1.058	1.171	1.052
R1 / wR2 (all data)	0.0788 / 0.2493	0.0231 / 0.0680	0.0282 / 0.0708	0.0398 / 0.0893	0.0275 / 0.0730
Residual extrema (e/Å <sup>3</sup> )	1.64 / -1.19	0.48 / -0.52	0.38 / -0.31	0.73 / -0.27	0.72 / -0.53

Crystallographic data and processing parameters of the compounds **(23)**-(**27**).

Compounds	(23)	(24)	(25)	(26)	(27)
Empirical formula	C <sub>14</sub> H <sub>18</sub> MnN <sub>4</sub> O <sub>4</sub> S <sub>2</sub>	C <sub>28</sub> H <sub>20</sub> Mn <sub>2</sub> N <sub>12</sub> O <sub>6</sub> S <sub>4</sub>	C <sub>6</sub> H <sub>7</sub> MnN <sub>7</sub> O	C <sub>12</sub> H <sub>18</sub> MnN <sub>8</sub> O <sub>4</sub>	C <sub>12</sub> H <sub>18</sub> Mn <sub>3</sub> N <sub>20</sub> O <sub>4</sub>
Formula mass	425.38	858.68	248.13	393.28	671.28
System	Triclinic	Triclinic	Triclinic	Orthorhombic	Orthorhombic
Space group	P-1	P-1	P-1	Ibam	Pccn
a (Å)	5.5067(8)	7.2791(8)	7.8894(16)	13.1797(12)	10.6778(12)
b (Å)	12.5168(13)	8.7510(9)	7.9150(16)	19.6646(18)	11.9257(14)
c (Å)	14.0283(14)	13.9870(16)	9.3326(19)	6.6346(7)	20.2105(18)
α (°)	81.832(18)	99.01(2)	71.54(2)	90	90
β (°)	79.64(2)	101.27(2)	75.97(2)	90	90
γ (°)	86.908(19)	95.69(2)	60.26(2)	90	90
V (Å <sup>3</sup> )	941.1(2)	855.22(19)	477.4(2)	1719.5(3)	2573.6(5)
Z	2	1	2	4	4
T (K)	100(2)	100(2)	100(2)	100(2)	100(2)
μ (mm <sup>-1</sup> )	0.949	1.044	1.367	0.804	1.512
D <sub>calc</sub> (Mg/m <sup>3</sup> )	1.501	1.667	1.726	1.519	1.732
Crystal size (mm)	0.41 x 0.17 x 0.08	0.31 x 0.18 x 0.13	0.32 x 0.25 x 0.19	0.42 x 0.11 x 0.08	0.34 x 0.29 x 0.17
θ max (°)	26.33	26.31	24.98	26.280	26.34
Data collected	7394	6751	3311	4799	19112
Unique refl. / R <sub>int</sub>	3767 / 0.0264	3390 / 0.0208	1681 / 0.0258	947 / 0.0249	2625 / 0.0242
Parameters / Restraints	240 / 4	241 / 2	137 / 0	86 / 3	188 / 0
Goodness-of-Fit on F <sup>2</sup>	1.044	1.113	1.148	1.177	1.069
R1 / wR2 (all data)	0.0427 / 0.1071	0.0302 / 0.0750	0.0837 / 0.2107	0.0250 / 0.0787	0.0205 / 0.0544
Residual extrema (e/Å <sup>3</sup> )	0.53 / -0.75	0.50 / -0.34	1.38 / -0.77	0.23 / -0.34	0.28 / -0.23